



CERN-PBC Report-2025-003

# Summary Report of the Physics Beyond Colliders Study at CERN

*R. Alemany Fernández<sup>1</sup>, M. Au<sup>1</sup>, G. Arduini<sup>\*,1</sup>, L. Bandiera<sup>2</sup>, D. Banerjee<sup>1</sup>, H. Bartosik<sup>1</sup>, J. Bernhard<sup>1</sup>, D. Boer<sup>&,3</sup>, J. Boyd<sup>1</sup>, O. Brandt<sup>4</sup>, M. Brugger<sup>1</sup>, O. Buchmüller<sup>5,6</sup>, F. Butin<sup>1</sup>, S. Calatroni<sup>1</sup>, C. Carli<sup>1</sup>, N. Charitonidis<sup>1</sup>, P. Crivelli<sup>7</sup>, D. Curtin<sup>8</sup>, R. T. D'Agnolo<sup>9,10</sup>, G. De Lellis<sup>11,12</sup>, O. Denisov<sup>1,13</sup>, P. Di Nezza<sup>14</sup>, B. Döbrich<sup>15</sup>, Y. Dutheil<sup>1</sup>, J. R. Ellis<sup>1,16</sup>, S. A. R. Ellis<sup>17</sup>, T. Ferber<sup>†,18</sup>, M. Ferro-Luzzi<sup>1</sup>, M. Fraser<sup>1</sup>, T. Galatyuk<sup>&,19</sup>, D. Gamba<sup>1</sup>, C. Gatti<sup>14</sup>, S. Gilardoni<sup>1</sup>, A. Glazov<sup>&,20</sup>, M. Gorshein<sup>21</sup>, E. Granados<sup>1</sup>, E. Gschwendtner<sup>1</sup>, P. Hermes<sup>1</sup>, J. Jaeckel<sup>\*,22</sup>, M. A. Jebramcik<sup>1</sup>, Y. Kadi<sup>1</sup>, F. Kahlhoefer<sup>+,23</sup>, F. Kling<sup>20</sup>, M. Kowalska<sup>1</sup>, M. W. Krasny<sup>1,24</sup>, B. Ketzer<sup>25</sup>, M. Lamont<sup>1</sup>, P. Lenisa<sup>2,26</sup>, A. Lindner<sup>20</sup>, M. Maćkowiak-Pawłowska<sup>27</sup>, A. Martens<sup>28</sup>, F. Martinez Vidal<sup>29</sup>, C. Matteuzzi<sup>30</sup>, N. Neri<sup>31</sup>, L. J. Nevay<sup>1</sup>, M. Ovchinnikov<sup>1</sup>, Y. Papaphilippou<sup>1</sup>, L. L. Pappalardo<sup>2,26</sup>, J. Pawłowski<sup>&,22</sup>, M. Perrin-Terrin<sup>32</sup>, J. Pinfold<sup>33</sup>, L. Ponce<sup>1</sup>, M. Pospelov<sup>+,34,35</sup>, T. Prebibaj<sup>1</sup>, J. Pretz<sup>36,37</sup>, S. Redaelli<sup>1</sup>, J. Rojo<sup>38</sup>, G. Rumolo<sup>1</sup>, A. Rybicki<sup>39</sup>, G. Schnell<sup>\*,40,41</sup>, S. Schuh<sup>1</sup>, I. Schulthess<sup>20</sup>, E. Scomparin<sup>13</sup>, S. Stapnes<sup>1</sup>, P. N. Swallow<sup>4</sup>, F. Terranova<sup>30</sup>, S. Ulmer<sup>42,43</sup>, G. Usai<sup>44</sup>, C. Vallée<sup>32</sup>, M. van Dijk<sup>1</sup>, G. Venanzoni<sup>45,46</sup>, M. Wing<sup>47</sup>, E. D. Zimmerman<sup>48</sup>*

## Abstract

The Physics Beyond Collider (PBC) Study Group was initially mandated by the CERN Management to prepare the previous European Particle Physics Strategy Update for CERN projects other than the high-energy frontier colliders. The main findings were summarized in an PBC Summary Report submitted to the Strategy Update. Following the Update process, the PBC Study Group was confirmed on a permanent basis with an updated mandate taking into account the strategy recommendations. The Study Group is now in charge of supporting the proponents of new ideas to address the technical issues and physics motivation of the projects ahead of their review by the CERN Scientific Committees and decision by the Management. The present document updates the previous PBC summary report to inform the new ongoing European Particle Physics Strategy Update process, taking into account the evolution of the CERN and worldwide landscapes and the new projects under consideration within the Study Group.

Geneva, Switzerland

June 13, 2025

<sup>1</sup>CERN, Geneva, CH  
<sup>2</sup>INFN Ferrara, Ferrara, IT  
<sup>3</sup>Van Swinderen Institute for Particle Physics and Gravity, University of Groningen, Groningen, NL  
<sup>4</sup>Department of Physics, University of Cambridge, Cambridge, UK  
<sup>5</sup>Blackett Laboratory, Imperial College London, London, UK  
<sup>6</sup>University of Oxford, South Parks Road, Oxford, UK  
<sup>7</sup>ETH Zurich, Institute for Particle Physics and Astrophysics, Zurich, CH  
<sup>8</sup>Department of Physics, University of Toronto, Toronto, CAN  
<sup>9</sup>Institut de Physique Théorique, Université Paris Saclay, CNRS, CEA, Gif-sur-Yvette, FR  
<sup>10</sup>Laboratoire de Physique de l’École Normale Supérieure, ENS, Université PSL, CNRS, Sorbonne Université, Université Paris Cité, Paris, FR  
<sup>11</sup>INFN-Sezione di Napoli, Napoli, IT  
<sup>12</sup>Università degli Studi di Napoli Federico II, Napoli, IT  
<sup>13</sup>INFN, Sezione di Torino, Torino, IT  
<sup>14</sup>Laboratori Nazionali di Frascati, INFN, Frascati, IT  
<sup>15</sup>Max-Planck-Institut für Physik (Werner-Heisenberg-Institut), Garching, DE  
<sup>16</sup>King’s College London, Strand, London, UK  
<sup>17</sup>Département de Physique Théorique, Université de Genève, Genève, CH  
<sup>18</sup>Institute of Experimental Particle Physics, Karlsruhe Institute of Technology, Karlsruhe, DE  
<sup>19</sup>Department of Physics, Technische Universität Darmstadt, Darmstadt, DE  
<sup>20</sup>Deutsches Elektronen-Synchrotron DESY, 22603 Hamburg, DE  
<sup>21</sup>Johannes Gutenberg-Universität Mainz, 55128 Mainz, DE  
<sup>22</sup>Institut für Theoretische Physik, Universität Heidelberg, Heidelberg, DE  
<sup>23</sup>Institute for Astroparticle Physics, Karlsruhe Institute of Technology, Karlsruhe, DE  
<sup>24</sup>LPNHE, Sorbonne Université, Université de Paris, CNRS/IN2P3, Paris, FR  
<sup>25</sup>Universität Bonn, Helmholtz-Institut für Strahlen- und Kernphysik, 53115 Bonn, DE  
<sup>26</sup>University of Ferrara, Ferrara, IT  
<sup>27</sup>Warsaw University of Technology, Warsaw, PL  
<sup>28</sup>Université Paris-Saclay, CNRS/IN2P3, IJCLab, Orsay, FR  
<sup>29</sup>Instituto de Física Corpuscular and Universitat de València, Catedrático Jose Beltrán, 2, València, SP  
<sup>30</sup>INFN and Università di Milano Bicocca, Milano, IT  
<sup>31</sup>INFN and Università di Milano, Milano, IT  
<sup>32</sup>Aix Marseille Université, CNRS/IN2P3, CPPM, Marseille, FR  
<sup>33</sup>Centre for Particle Physics Research, Physics Department, University of Alberta, Edmonton, CAN  
<sup>34</sup>William I. Fine Theoretical Physics Institute, School of Physics and Astronomy, University of Minnesota, Minneapolis, US  
<sup>35</sup>School of Physics and Astronomy, University of Minnesota, Minneapolis, US  
<sup>36</sup>RWTH Aachen University, Aachen, DE  
<sup>37</sup>Forschungszentrum Jülich, Jülich, DE  
<sup>38</sup>Nikhef National Institute for Subatomic Physics, Science Park 105, 1098 XG Amsterdam, NL  
<sup>39</sup>Institute of Nuclear Physics, Polish Academy of Sciences, Radzikowskiego 152, 31-342 Krakow, PL  
<sup>40</sup>Department of Physics & EHU Quantum Center, University of the Basque Country UPV/EHU, Bilbao, SP  
<sup>41</sup>IKERBASQUE, Basque Foundation for Science, Bilbao, SP  
<sup>42</sup>Heinrich-Heine Universität, Düsseldorf, DE  
<sup>43</sup>RIKEN, Wako-Saitama, Tokyo, JP  
<sup>44</sup>Università di Cagliari and INFN, Sezione di Cagliari, Monserrato, IT  
<sup>45</sup>University of Liverpool Liverpool, UK  
<sup>46</sup>INFN-Sezione di Pisa, Pisa, IT  
<sup>47</sup>Department of Physics and Astronomy, UCL, London, UK  
<sup>48</sup>University of Colorado, Boulder, Colorado, US

\*Physics Beyond Collider (PBC) coordinator

<sup>+</sup>PBC Feebly Interacting Particle Physics Centre (FPC) convener

<sup>&</sup>PBC QCD Working Group convener

<sup>†</sup>PBC Beyond Standard Model Working Group convener

# Contents

<b>1</b>	<b>Executive summary</b>	<b>5</b>
<b>2</b>	<b>Physics landscape and current open questions targeted by PBC</b>	<b>11</b>
2.1	CERN PBC Experimental landscape . . . . .	11
2.1.1	NA61/SHINE . . . . .	11
2.1.2	NA62 . . . . .	11
2.1.3	NA64 ( $-e, -\mu, -h$ ) – Phase 1 . . . . .	12
2.1.4	NA66/AMBER – Phase 1 . . . . .	12
2.1.5	Fixed-target experiments at the LHC . . . . .	13
2.1.6	FASER . . . . .	14
2.1.7	SND@LHC . . . . .	14
2.2	Theory and phenomenology support and interface . . . . .	15
2.3	Worldwide landscape . . . . .	16
<b>3</b>	<b>Evolution of the CERN accelerator complex and post-LS3 outlook</b>	<b>19</b>
3.1	CERN Accelerator complex after LS2, planned upgrades during LS3 and future perspectives . . . . .	19
3.1.1	LHC Injectors . . . . .	19
3.1.2	Experimental Areas . . . . .	22
3.1.3	AD complex and ELENA . . . . .	27
3.1.4	High Luminosity LHC (HL-LHC) . . . . .	28
3.2	Accelerator Technology developments . . . . .	29
3.3	Potential future accelerators and facilities at CERN . . . . .	30
3.3.1	Short Baseline Neutrino beam proposal . . . . .	30
3.3.2	Gamma Factory . . . . .	31
3.3.3	AWAKE and future proton-driven plasma wakefield accelerators . . . . .	32
3.3.4	Future colliders and their injectors . . . . .	33
<b>4</b>	<b>PBC proposed experiments and future opportunities at CERN and beyond</b>	<b>35</b>
4.1	SPS North Area . . . . .	36
4.1.1	NA61/SHINE-LE . . . . .	36
4.1.2	NA61/SHINE with ions . . . . .	36
4.1.3	NA64 ( $-e, -\mu, -h$ ) – Phase 2 . . . . .	37
4.1.4	NA66/AMBER – Phase 2 . . . . .	38
4.1.5	SHiP/NA67 in ECN3 . . . . .	39
4.1.6	MUonE . . . . .	40
4.1.7	DICE/NA60+ . . . . .	40
4.2	HL-LHC – Physics in the forward direction (neutrinos and FIPs) . . . . .	41
4.2.1	Forward Physics Facility . . . . .	41
4.2.2	Scattering and Neutrino detector at the HL-LHC (SND@HL-LHC) . . . . .	43
4.3	HL-LHC – FIPs Physics at large angle . . . . .	44
4.3.1	ANUBIS . . . . .	44
4.3.2	CODEX-b . . . . .	45

4.3.3	MAPP-2	46
4.3.4	MATHUSLA40	47
4.4	HL-LHC – Fixed Target	48
4.4.1	ALADDIN	48
4.4.2	LHCspin	49
4.5	ISOLDE	50
4.5.1	Symmetry violating effects in radioactive atoms and molecules	50
4.6	AD and ELENA Complex	50
4.7	Non-accelerator experiments	51
4.7.1	Atomic Interferometer@CERN	51
4.7.2	Axion Heterodyne Detection	51
4.7.3	FLASH	52
4.7.4	RADES	53
4.8	PBC Opportunities at new Facilities	53
4.8.1	SBN beam performance	53
4.8.2	Gamma Factory research opportunities	54
4.8.3	Experiments at AWAKE	55
4.8.4	PBC opportunities at FCC-ee and LC	55
4.8.5	cpEDM measurements	57
4.9	Other Early Stage Proposals Discussed within PBC	58
4.10	FPC – interfacing experiment and phenomenology	58
4.11	Summary of the proposals at CERN	59
<b>5</b>	<b>Physics reach of PBC projects in the global context</b>	<b>60</b>
5.1	Hadronic vacuum polarisation and the muon anomalous magnetic moment	60
5.2	Hadron structure and properties	61
5.3	Heavy-ion physics	65
5.4	Neutrino physics	68
5.5	Feebly-interacting particles and dark sectors	71
5.5.1	Benchmark models	72
5.5.2	Showcase models	73
5.5.3	Experiments table	80
5.6	Electric dipole moment	81
5.7	Gravitational Wave Detection	82
<b>List of Acronyms</b>		<b>114</b>

## 1 Executive summary

Physics Beyond Colliders (PBC) is a multidisciplinary study group to promote and facilitate a diverse physics programme at CERN. It was established by the CERN Directorate in 2016 to explore physics opportunities beyond high-energy frontier colliders and provide input into the 2020 European Particle Physics Strategy Update (EPPSU). Following the EPPSU process, the PBC Study Group was confirmed on a permanent basis with an updated mandate [1]. Taking into account the strategy recommendations, it has flourished since then and now serves as a gateway for new experimental ideas building on CERN infrastructure, technology and expertise. It helps developing experiments from their inception to a level ready for discussion in the relevant scientific committees. Notable recent examples in this direction are FASER, SMOG2, SHiP/NA67, and MuonE, the first two taking data since the beginning of LHC Run 3, the third in full swing in the TDR phase, and the fourth doing test measurements. This report provides an update to previous findings [2], outlines ongoing projects, the planned and potential evolution of CERN’s accelerator complex, and reviews existing proposals with their potential physics reach considering the international physics landscape.

PBC aims at addressing open questions in fundamental physics. Two main physics areas discussed within PBC are quantum chromodynamics (QCD) and beyond the Standard Model (BSM) physics. Both of them feature their own working groups to develop the experimental realization as well as the physics case. The BSM area is supported by a theory-experiment exchange hub, the Feebly Interacting Particle Physics Center (FPC), which also interacts with the worldwide community and scrutinizes and ensures the leading role of PBC experiments in this wider context. Dedicated accelerator and technology working groups assist preparing the proposals with integration into the CERN complex as well as with technological, siting, and engineering aspects relevant for implementation at CERN or outside.

### Worldwide and CERN Physics Beyond Colliders landscape

In the BSM area, the main targets are fundamental open questions such as: Are there new particles? What is Dark Matter? How to probe Dark Sectors? Can we shed light on the mysterious neutrino sector? Benefiting from both high-energy and high-intensity beams, PBC experiments are using a whole range of strategies to push this frontier forward. FASER, NA62, and NA64 have already taken data providing world-leading constraints on a wide range of new feebly interacting particles (FIPs). FASER and SND@LHC have been using the main LHC collisions but exploited them in a novel far-forward position. This enabled the detection of the first collider produced TeV neutrinos, opening new avenues for studying neutrino interactions at the TeV scale. NA62, in addition to observing the decay of a charged kaon into a charged pion and a neutrino-antineutrino pair, one of the rarest processes ever observed, took data with an SPS beam in a beam dump mode where the full primary proton beam is dumped on a collimator. In this mode, NA62 has provided world-leading constraints on hypothetical particles such as dark photons and axion-like particles. NA64 used high-energy electron and muon beams with an active beam dump able to measure missing energy. NA64 is a key player in the search for sub-GeV dark sector particles and probed a sizable range of the parameter space that would have been able to explain the deviation of the muon anomalous magnetic moment  $a_\mu$  from the Standard Model prediction. Recent pilot runs with muon beams have yielded critical constraints on lepton-flavor violating interactions.

QCD poses a number of critical challenges to our understanding. Being a strongly coupled system it requires developing and testing new computational methods beyond perturbation theory. Open questions include the phase diagram of QCD as well as predictions on the detailed structure of hadrons. The former is already a focus of NA61/SHINE. The AMBER/NA66 experiment focuses on the latter and the fundamental origins of mass within QCD. In its presently approved programme, AMBER/NA66 investigates the proton charge radius with high-energy muon-proton scattering, contributing to the resolution of long-standing discrepancies in proton radius measurements, as well as measures antiproton production cross sections. Likewise, SMOG2, a fixed-target program of LHCb at the LHC, utilizing a gas target immediately upstream of the experiment, offers a unique opportunity to study proton-nucleus collisions under controlled conditions. This experiment provides key insights into cosmic ray fluxes and cosmic ray showers, as well as on the QCD phase diagram and nuclear structure in general.

## Developments in the CERN accelerator complex

An overview of the CERN accelerator complex is shown Figure 1. Since the past EPPSU the accelerator complex was augmented with the LHC Injector Upgrade (LIU) aimed at providing high-brightness beams for the LHC in view of its high-luminosity upgrade (HL-LHC). The quality and intensity of the beams delivered to the fixed-target experimental areas of the complex from ISOLDE to the North Area (NA) have also improved as a result of these modifications. This benefits PBC experiments working with ions and protons to understand QCD as well as those looking for new physics using protons but also secondary beams of electrons, muons and other particles. Further specific improvements are discussed within PBC to address specific needs, e.g., the ability to quickly switch between ion species to allow experiments such as NA61/SHINE to explore quark gluon plasma (QGP) properties as a function of the system size while enabling DICE/NA60+ to further explore the chiral and QGP phase transitions. The ongoing NA consolidation programme together with the high intensity upgrade of ECN3 will extend the physics opportunities in this area and improve the beam availability. Importantly, the recently approved SHiP/NA67 experiment will use the underground cavern ECN3 to search for FIPs with a state-of-the-art beam dump absorber capable of absorbing high intensity and to operate reliably over several years. The HL-LHC upgrade taking place during LS3 will create unprecedented opportunities for hidden-sector searches, high-energy neutrino studies, and proton/nucleus structure measurements. These can be enhanced and fully realized by a range of suitable supplementary detectors, insertion of fixed targets and extraction of parts of the beam halo by means of crystals.

## Future facilities

A number of proposed and foreseen new facilities are considered within PBC. The envisioned Forward Physics Facility (FPF), discussed in more detail further below, would allow for a variety of experiments located in a new cavern some 600 m down the LHC collision axis from the ATLAS IP. These experiments, shielded by rock could make use of a massive amount of TeV-level neutrinos and possibly of dark matter particles coming “for free” from HL-LHC operations. In order to fully exploit the potential during the HL-LHC era, infrastructure work would have to start during LS3.

The need for a high-precision neutrino beam for cross-section measurements to reduce systematic uncertainties of future neutrino oscillation experiments like DUNE and Hyper-Kamiokande

has been recognized since the 2020 EPPSU. Recent studies within PBC of a short-baseline neutrino facility (SBN) have shown the possibility of providing a high-precision monitored and tagged medium-intensity neutrino beam, where the properties of the individual neutrinos are known. This would enable percent-level neutrino cross-section measurements at the GeV scale with a moderate amount of protons on target. A new slow-extraction system towards a new experimental area close to the HiRadMat facility would be required, allowing the use of existing transfer tunnels. A conceptual design of the new slow-extraction scheme from the SPS needs to be further developed, demonstrating its feasibility and the compatibility with LHC operation. The study, including the civil engineering and technical infrastructure design of the corresponding experimental area, should be completed by the end of LS3 in order to conduct the necessary modifications during LS4, if such proposal is approved.

First proposed within the PBC context, the Gamma Factory aims at reaching a new level of intensity and beam quality for MeV scale gamma rays. Partially stripped ions are accelerated to LHC energies and collided with a resonant optical laser. The de-excitation photons then are focused with an energy enhanced by the square of the ion relativistic boost. After first tests at the SPS and LHC, a proof-of-principle experiment is in preparation at the SPS and a wide range of physics applications from material science to fundamental physics are being developed.

PBC also closely follows developments for the FCC-ee injectors, CLIC, and AWAKE, exploring possibilities to use the respective beams directly for physics applications.

### **Status of experiments within PBC and opportunities**

NA64 plans to increase the number of particles on targets and using different species (electrons, positrons, muons, hadrons) thereby widening the range of accessible physics. In particular, the positron programme will enable the first probe of the so-called “thermal target lines”, which represent the dark sector coupling values predicted by astrophysical and cosmological arguments for selected model parameter values in the mass range 135 to 250 MeV. MUonE, aiming to measure the hadronic contributions to  $a_\mu$  in a novel way, has progressed to supervision by SPSC and is performing pilot runs in view of a possible approval for operation post-LS3. SHiP/NA67 is expected to start data taking from 2031 and it is designed to detect neutrino interactions and scattering events of hypothetical light dark matter particles produced in proton-target collisions as well as for searching for decays of FIPs.

A whole range of proposal aims at improving the exploitation of LHC in its high-luminosity phase with auxiliary detectors in the forward (SND@HL-LHC, FPF), intermediate (MoEDAL-MAPP2), and transverse (ANUBIS, CODEX-b, MATHUSLA40) directions with respect to the collision axis of the main LHC interaction points. Test setups are either being built or already taking data. Optimization of the physics reach and cost inside but also between experiments is driving the development. In particular, the FPF would provide space for a suite of far-forward small/medium-size detectors during the HL-LHC era. Experiments at the FPF can discover a wide variety of new particles that cannot be discovered at fixed-target facilities or other LHC experiments. The FPF is the only facility that will be able to detect millions of neutrinos with TeV energies, enabling precision probes of neutrino properties for all three flavors. These neutrinos will improve our understanding of proton and nuclear structure, enhancing the power of new particle searches at ATLAS and CMS, and providing valuable input for astro-particle experiments like IceCube, Auger and others. The studies conducted so far indicate that the civil engineering for the

construction of the experimental cavern could take place during HL-LHC operation though construction should start during LS3 in order to allow commissioning with beam of the FPF detectors before the end of LHC Run 4.

Exploitation and extension of the capabilities to perform experiments with ions in the North Area are pursued by DICE/NA60+ and NA61/SHINE with the aim to perform studies of the phase structure of QCD including the confinement and chiral phase transitions. The future programme at AMBER/NA66 focuses on studying hadron structure and the fundamental origins of mass within QCD. Through precision measurements of Drell-Yan and  $J/\psi$  production, it aims to extract parton distribution functions of pions and kaons, shedding light on the internal dynamics of strongly bound systems.

SMOG2 has opened the way to fixed-target physics at the LHC. The LHCspin proposal envisages to conduct unique spin-dependent measurements of Drell-Yan and heavy-flavour production processes, by studying collisions of both proton and lead beams on polarized hydrogen or deuterium gas targets. This would provide insight into details of the multi-dimensional structure of nucleons in terms of transverse momentum-dependent parton distributions.

Machine studies conducted at the SPS and LHC have demonstrated the suitability of crystals for the control of the beam halo and these devices are now used regularly in operation to enhance the collimation efficiency for LHC lead ion beams. The Double Crystal setup Proof of Principle Experiment (TWOCRYST) has the goal to demonstrate the feasibility of channeling the proton beam halo with a crystal onto an in-vacuum target and to bend TeV charmed baryons generated in the interaction by means of a second large bending-angle crystal that acts like a very powerful precession magnet. The TWOCRYST experiment, scheduled for 2025, will provide vital information for the technical design of ALADDIN, a proposed fixed-target experiment at the Insertion Region (IR) 3 of the LHC aiming to measure the magnetic and electric dipole moments of baryons, such as  $\Lambda_c^+$  and  $\Xi_c^+$ . These measurements are highly sensitive probes for BSM physics but have remained unexplored so far due to the extremely short lifetimes of these particles. The ALADDIN collaboration is working on a technical proposal of the detector aiming to start the installation of the required accelerator hardware and detector during LS3, if approved, to conduct beam commissioning and start data taking before the end of LHC Run 4.

A broad range of further experimental opportunities at CERN and elsewhere are being developed within PBC. Notably a number of small experiments to detect axion(-like particle) dark matter benefit from magnet and RF cavity expertise (RADES, FLASH and an experiment aiming for a heterodyne detection approach). Other proposals aim at the detection of CP-violating electric dipole moments of the proton (cpEDM) and nuclei, with the latter exploiting the existing ISOLDE facility. Stronger connections with PBC and further exploitation of the Antiproton Decelerator are also being investigated. Infrastructure such as large and deep access shafts (e.g., those of the LHC) may open possibilities for atomic interferometry (AION) to reach a new level in the exploration of gravitational waves.

## Physics targets and opportunities

While by their very nature of being a broad and diverse effort, the PBC experiments aim at and have powerful sensitivity to a number of important physics targets.

An important one is a broad and deep exploration of FIPs, i.e., dark sector particles. PBC experiments extend the reach of collider experiments to significantly smaller couplings (e.g., NA64,

SHiP/NA67), complementary flavour and generally different coupling structures (e.g., NA64), longer lifetimes (e.g., ANUBIS, CODEX-b, MATHUSLA40), as well as different mass regimes. They can thereby target candidates for dark matter of thermal (e.g., NA64, SHiP/NA67) and non-thermal origin (e.g., AION, FLASH, RADES).

Gravitational waves by now are proven to be an important driver in exploring astrophysics and the cosmos, but also fundamental processes such as phase transitions in the early Universe and the interactions giving rise to them. Using techniques such as atomic interferometry (AION) to enter new frequency ranges, allows to discover new sources as well as probing new underlying physics scales.

CP violation is a necessary ingredient for baryogenesis, but its absence is also a puzzle of the strong interactions. Suitable observables such as electric dipole moments (e.g., ALADDIN, cpEDM, ISOLDE EDM) can provide sensitivity to new physics at mass scales often many orders of magnitude in excess of the TeV scale.

Neutrino masses and mixings, possible non-standard interactions as well as the possible existence of sterile states are promising avenues to find physics beyond the Standard Model. At the same time, deep-inelastic neutrino scattering can serve as a unique probe of nucleons and nuclei. Both forward (e.g., FPF) and fixed-target experiments (e.g., NA64, SHiP/NA67) within PBC can contribute novel kinematic regions and unique sensitivities to these aspects. Novel precision neutrino beams (e.g., SBN) may provide crucial cross-section measurements for other endeavors such as DUNE and Hyper-Kamiokande.

Understanding the low-energy behavior of QCD and notably its phase structure remains an important challenge. Using the versatility of the SPS ion beams allows for the exploration of this question in promising kinematic regimes (e.g., DICE/NA60+) and with different ion species (e.g., NA61/SHINE), complementing other facilities worldwide. Spectroscopic information on QCD bound states (e.g., AMBER/NA66) can give complementary information on the low-energy QCD regime. Fixed-target experiments at the LHC supply valuable parton distribution functions for Standard Model measurements as well as BSM searches.

Highly precise measurements of electron muon scattering (MUonE) can shed light on the hadronic contributions to  $a_\mu$ , thereby providing new insights into this currently open puzzle, helping to decide whether it is a Standard Model effect or a sign of new physics.

## Concluding strategic remarks

Recent years have demonstrated that covering the full range of possibilities for fundamental particle physics requires a broad range of experimental strategies, complementing those at colliders. This notably includes dark matter and, connected with this, the search for FIPs, but also a better understanding of QCD. PBC realizes the idea of a diverse experimental programme (at CERN or elsewhere), making full use of the facilities, infrastructure and expertise at CERN. It thereby serves as a demonstrator for the possible role that large laboratories can play in this context. In addition, PBC also shows that large labs can serve as an incubator and facilitator bringing together theory, experiment as well as engineering. Together with the physics benefits, a diverse experimental landscape, including numerous smaller and medium scale experiments, also serves to improve the health and long-term viability of the community, allowing young researchers to take leading roles within an experiment, garnering experience in all aspects, from planning, construction to data taking and overseeing the whole experiment. Some of those experiments can be

performed making use of the existing infrastructures with minimal adaptions, others require further investments in facilities like the FPF or the SBN with timelines that require decisions as early as during the upcoming LS3.

Altogether, supporting a powerful and diverse programme at CERN and similar programmes at other labs is a crucial decision for a successful long-term strategy.

## 2 Physics landscape and current open questions targeted by PBC

### 2.1 CERN PBC Experimental landscape

A number of experimental proposals have seen the light and have been supported within the framework of the PBC initiative since its launch in 2016. The status of these proposals and their impact on the physics landscape are briefly summarized in this Section.

#### 2.1.1 NA61/SHINE

The SPS Heavy Ion and Neutrino Experiment (NA61/SHINE) is the only Fixed-Target (FT) hadron spectrometer operating at the CERN SPS, served by the H2 beam line in the SPS North Area (NA). It has the unique capability for large-acceptance measurements over a versatile set of beams and targets in the specific regime of collision energy,  $5\text{ GeV} < \sqrt{s_{\text{NN}}} < 17\text{ GeV}$ . Its accumulated data set includes  $p+p$ ,  $p+\text{C}$ ,  $\pi+\text{C}$ ,  $K+\text{C}$ ,  $p+\text{Pb}$ ,  $\text{Be}+\text{Be}$ ,  $\text{C}+\text{C}$ ,  $\text{Ar}+\text{Sc}$ ,  $\text{Xe}+\text{La}$ , and  $\text{Pb}+\text{Pb}$  collisions, each recorded at up to six beam momenta.

The most recent achievements of the experiment include (see Section 4.1): the first-ever direct measurement of open charm production in nucleus-nucleus collisions at SPS energies [3], the observation of a large excess of charged over neutral  $K$  meson production in  $\text{Ar}+\text{Sc}$  collisions at  $\sqrt{s_{\text{NN}}} = 11.9\text{ GeV}$ , interpreted as evidence for an unexpectedly large violation of isospin (flavour) symmetry in nucleus-nucleus reactions [4], and the completion of a 2D scan of hadron production in  $p+p$  and nucleus-nucleus collisions, each at six beam momenta, which brings insight into the changeover from confined to deconfined matter as a function of collision energy and colliding system size [5, 6, 7].

Presently, the upgraded NA61/SHINE detector operates a high-statistics  $\text{Pb}+\text{Pb}$  data-taking, bringing the first-ever differential measurement of open charm production in heavy-ion collisions close to the threshold (to be completed in 2026) [8].

At the same time, NA61/SHINE provides a substantial set of reference data to improve the precision of neutrino experiments and new measurements for cosmic-ray physics programs [9, 10, 11, 12].

#### 2.1.2 NA62

The NA62 Experiment was built to measure precisely the branching ratio  $\mathcal{B}(K^+ \rightarrow \pi^+ \nu \bar{\nu})$ , and has recently measured this decay with a 5 sigma significance [13, 14]. Thanks to its high intensity beam and detector performance (redundant particle-identification capability, extremely efficient veto system and high resolution measurements of momentum, time, and energy), NA62 has also achieved sensitivities to long-lived light mediators in a variety of new-physics scenarios by operating in the so-called Beam Dump (BD) mode, where the full primary proton beam is dumped on a collimator downstream of the production target, and a dedicated K12 beamline setup [15, 16] allows to reduce the muon background in the detector. Two analyses involving Hidden Sector (HS) particle decays to di-electrons [17] and di-muons [18] have been published and a search for hadronic decays of Dark Sector (DS) particles has been presented in 2024 [19].

### 2.1.3 NA64 ( $-e, -\mu, -h$ ) – PHASE 1

The NA64 Experiment (NA64) was designed to conduct a sensitive search for light, sub-GeV DS particles that could interact with ordinary matter via light mediators, potentially explaining the origin of the Dark Matter (DM) in the universe. These theoretically well-motivated and cosmologically viable scenarios are difficult to probe using traditional DM detection methods. NA64 effectively combines active target and missing-energy techniques to search for Light Dark Matter (LDM) particles. Using electron and positron beams with energies of 50–100 GeV, NA64 has achieved the best sensitivity to an important class of models based on the hypercharge kinetic mixing of a dark photon mediator. World-leading constraints have been set [20], allowing the experiment to explore the most compelling parameter space for LDM models, consistent with the observed DM relic abundance. The NA64 searches for LDM provide important inputs for other new physics scenarios, including  ${}^8\text{Be}$  anomaly [21], ALPs [22], inelastic DM [23, 24],  $B - L$  [25] and  $L_\mu - L_\tau Z'$  models [26], and Lepton Flavour Violation (LFV) processes [27]. Additionally, the experiment is highly complementary to other approaches, such as underground direct detection, neutrino, BD, and high-energy collider experiments. These results offer a crucial physics input and motivation for the current and future experimental research programme at CERN. In 2018, NA64 proposed to the CERN SPS and PS Experiments Committee (SPSC) the possibility to conduct a sensitive search for LDM in a higher mass range using a muon beam [28]. A key intermediate goal was to probe the parameter space of the  $L_\mu - L_\tau Z'$  model, which addresses the muon  $g - 2$  anomaly while explaining the DM relic density. NA64 completed its first muon pilot runs in 2022, nearly ruling out the  $g - 2$  explanation and setting first constraints on LDM for dark sectors primarily coupled to the second lepton generation [28]. These results demonstrate NA64’s capabilities to run with the M2 NA muon beamline [16] and provide a strong motivation to continue this unique research programme in the coming years. Furthermore, a short 2023 test run with a pion beam [29], searching for invisible decays of neutral  $\eta$  and  $\eta'$  mesons, revealed that NA64’s sensitivity to leptophobic DM (predominantly coupled to quarks) could be significantly enhanced with future active-target runs. This opens a new research direction for NA64 searches with hadron beams. Since its approval in 2016, NA64 has been pioneering searches for LDM across various modes: electron [20], positron [30], muon [28], and hadron [29]. The experiment has successfully met its primary objectives, as outlined in the input to the 2020 European Particle Physics Strategy Update (EPPSU), producing results which demonstrate its ability to operate in a near-background-free environment. These accomplishments have been recognized by the PBC and Feebly Interacting Particles (FIPs) communities as original, complementary to other ongoing and planned projects and worthy of continued exploration.

### 2.1.4 NA66/AMBER – PHASE 1

Selected topics of the physics programme of the Apparatus for Meson and Baryon Experimental Research (NA66/AMBER) were included in [2] and [31]. The NA66/AMBER Phase-1 proposal was approved by the CERN Research Board (CERN RB) in December 2020. This Fixed-Target (FT) experimental setup is located at the NA M2 beam line [16], which is capable of delivering beams of muons, pions, kaons, and protons as well as their anti-particles with beam momenta up to 250 GeV. In spite of the extremely important discovery of Higgs boson, the origin of 99 % of the mass of all visible universe is still unclear. The Higgs mechanism does not explain why the proton is so heavy and the pion is so light. The underlying physics process of the emergence of the

hadron mass is likely tightly related to the unique dynamical mass generation mechanism in continuum Quantum Chromo-Dynamics (QCD). A determination of the valence-quark Parton Distribution Function (PDF) of the pion and kaon—through Drell-Yan (DY) and  $J/\psi$  di-muon production, as well as direct-photon production—and high precision hadron spectroscopy measurements would provide sensitivity to the mechanisms responsible for the emergence of hadron mass in QCD. The present pre-LS3 measurements include that of the proton’s charge radius (from its form factor in  $\mu p$  elastic scattering) and of antiproton production cross sections in proton- ${}^4\text{He}/\text{H}_2/\text{D}_2$  collisions. A determination of the valence-quark PDF of the pion and kaon, through DY and  $J/\psi$  di-muon production will follow as one of three Phase-1 approved measurements.

### 2.1.5 FIXED-TARGET EXPERIMENTS AT THE LHC

The “forward” detector configuration of the Large Hadron Collider beauty Experiment (LHCb) at the LHC Interaction Point (IP)8, originally designed to perform detailed studies of beauty hadron decays (Charge Parity violation (CPV) and rare final states) [32], was exploited to extend the physics programme to a broad range of FT measurements. The programme started by using the System to Measure the beam Overlap with Gas (SMOG), a device developed to determine the LHC colliding beams luminosity by beam-gas imaging [33]. A gas target was obtained by injecting small amounts of light noble gases just upstream of the Vertex Locator (VELO) vacuum chamber. Pioneering LHC FT measurements were performed with He, Ne and Ar targets, obtaining unique results such as production cross sections of antiprotons in  $p$ -He collisions [34, 35] and of charm hadrons in  $p$ -He/Ne collisions [36, 37, 38]. The performance of the gaseous target was enhanced by installing a 1 cm diameter and 20 cm long open-ended storage cell around the beam path (SMOG upgrade, called SMOG2), just upstream of the VELO, and by injecting the gas directly into the middle of the cell via a capillary. The SMOG upgrade, in addition to increasing the target areal density by up to two orders of magnitude (depending on gas type), also included a more sophisticated gas-feed system which allowed to rapidly switch between injected gas types and which brought the possibility to deliver more gas target species (in particular  $\text{H}_2$ ,  $\text{D}_2$ ,  $\text{O}_2$ ) [39]. These improvements were facilitated by the studies performed in the LHC-FT Working Group (WG), where various challenges, such as aperture limitations, wake-field effects, dynamic vacuum phenomena and beam losses from beam-gas interactions, were addressed and adequate solutions were devised (such as an acceptable tube radius, appropriate wake-field suppression contacts, amorphous carbon coating, etc.) [40, 41]. Most importantly, thanks to the clear separation between the IP8 luminous region and the storage cell, and thanks to the LHCb upgraded detector capabilities [42], FT data and collider data are now acquired *simultaneously* at LHCb. A unique and diverse FT programme is now under way at LHCb which covers measurements of particles production spectra and cross sections with a variety of targets (mentioned above) and different beams ( $p$ , Pb, O) at several centre-of-mass (*c.m.*) energies (from 72 to 115 GeV) with a detector that covers a pseudorapidity range from about 1.8 to 5.5. These measurements are particularly important for the understanding of cosmic ray fluxes, cosmic ray showers, the Quark-Gluon Plasma (QGP) and nuclear structure in general.

### 2.1.6 FASER

The Forward Search Experiment (FASER) [43] was designed to search for light, weakly-coupled new particles, produced in the LHC collisions, and to study high-energy collider neutrinos of all flavours. The experiment is located in the junction between the Tunnel Injection (TI)12 service tunnel and the LHC, aligned with the A Toroidal LHC ApparatuS Experiment (ATLAS) collision-axis line of sight, which maximises the neutrino flux and energy, and the potential flux of light new particles.

After initial studies within PBC, the collaboration submitted a Letter of Intent (LoI) [44] and then a technical proposal [45] to the LHC Experiments Committee (LHCC) in September/November 2018, and was approved by the CERN research board in March 2019. The detector systems were designed, constructed and underwent standalone commissioning on the surface in 2019 and 2020, before being installed into the TI12 tunnel in the LHC complex in March 2021. During 2020 the experimental area was prepared by CERN technical teams, with a small trench excavated to allow the detector to be positioned on the collision-axis line of sight. The needed electrical, transport, cooling and communication infrastructure was installed. After the installation the experiment underwent a sustained period of in situ commissioning with cosmic-ray and single-beam data. Physics operation commenced in July 2022, at the start of LHC Run 3, with very smooth detector operations and overall above 97% of the delivered luminosity has been recorded (with a total dataset size of nearly  $200 \text{ fb}^{-1}$  recorded by the end of 2024).

The FASER detector [46] has two main parts: an electronic detector composed of a veto scintillator system, a tracking spectrometer, and an electromagnetic calorimeter, designed for long-lived particle searches; and a dedicated 1 t tungsten/emulsion detector called FASER Neutrino detector (FASERv) designed for neutrino measurements. The detector performance is very good, with all of the main design requirements achieved.

Based on the excellent detector operations and performance the experiment has been able to deliver impactful physics results in a timely fashion, with first search and neutrino results using the 2022 data released in time for the 2023 winter conferences. These were the search for dark photons, with unique sensitivity in an unexplored region of parameter space motivated by DM [47] and the first observation of muon neutrinos at a collider [48], with 153 neutrino candidate events observed. Further results have been released in 2024, with a search for Axion-Like Particles (ALPs) [49], the first measurements of the interaction cross section at TeV energies for electron and muon neutrinos [50] using the FASERv emulsion detector, and the first differential cross section measurement of neutrinos and antineutrinos [51] at TeV energies.

The FASER collaboration is considering an upgrade of its neutrino detector covering the rapidity range  $\eta > 7$ , hence allowing to probe both the on-axis region, currently probed by FASER, and the off-axis region, currently probed by Scattering and Neutrino Detector at the LHC (SND@LHC), in one detector [52].

### 2.1.7 SND@LHC

SND@LHC [53, 54] is a compact experiment exploiting the high flux of energetic neutrinos of all flavours from the LHC. It covers the pseudo-rapidity range of  $7.2 < \eta < 8.4$ , where a large fraction of neutrinos originates from charmed-hadrons decays. The experiment is located 480 m downstream of IP1 in the unused TI18 tunnel. The detector is composed of a hybrid system based on a 800 kg target mass of tungsten plates, interleaved with emulsions and electronic trackers,

followed downstream by an hadronic calorimeter and a muon identification system. The configuration allows efficiently distinguishing between all three neutrino flavours, thus probing physics of heavy-flavour production at the LHC in a region inaccessible to other experiments and enabling Lepton Flavour Universality (LFU) tests in the neutrino sector. The detector concept is also well suited to search for FIPs via signatures of scattering in the detector target.

The data-taking, which started at the beginning of the LHC Run 3, was immediately successful with the collection of an integrated luminosity of  $36.8 \text{ fb}^{-1}$  in 2022. The data sample from 2022 had a total of  $8.4 \times 10^9$  incoming muon tracks [55]. A rejection power at the level of  $10^{-12}$  was achieved by combining the veto system and the Scintillating Fibre (SciFi) stations of the two most upstream walls of the target. The only background left was due to neutral hadrons produced by muon interactions in the upstream rock which would in turn generate hadronic jets with a reconstructed muon track in the final state: this background was estimated to 0.086 expected events. Given the 8 candidate events found in the data, an observation of collider neutrinos was established with a significance of about  $7\sigma$  [56]. By adding the data taken in 2023 [57], an integrated luminosity of  $68.6 \text{ fb}^{-1}$  was achieved and the search for neutrino interactions without a muon in the final state was carried out. This sample consists essentially of Neutral Current (NC) neutrino interactions and Charged-Current (CC) electron neutrinos. Electron neutrinos produce typically an electron in the final state with more than 300 GeV energy on average, with a large energy density deposited in the neutrino target. The selection could therefore be tuned to enrich the sample of electron neutrinos by using the energy density. The data accumulated in a test beam carried out at the SPS in 2023 for the calorimeter calibration were used to validate the Monte Carlo simulation. A control region outside of the signal selection cuts was defined which showed a good agreement between data and simulation. As a result of the selection, 9 candidate events were found with an expected background of 0.3 events, dominated by muon neutrinos where the muon is not identified. This has led to the observation of neutrino interactions without a muon in the final state with a significance above  $6\sigma$  and to the evidence for electron neutrinos with  $3.7\sigma$  [58].

During 2022/2023 the Veto system did not completely cover the target area. In order to solve this problem and further reduce the veto inefficiency, a small trench was dug, the veto system was lowered and a third Veto plane was installed during the 2023-2024 Year-End Technical Stop (YETS) [59]. The inefficiency was reduced to  $(8.7 \pm 3.5) \times 10^{-9}$  on the full target area in 2024 when the experiment recorded a luminosity of about  $120 \text{ fb}^{-1}$ . The analysis of 2024 data is ongoing.

## 2.2 Theory and phenomenology support and interface

PBC provides both motivation and a forum for direct interactions between theory, phenomenology and experiment. This exchange enhances the physics case of the individual experiments, improving both the breadth and depth of the physics reach by working with the community to better understand and quantify existing signatures and to explore interesting new signatures suggested by theoretical considerations. At the same time these discussions also facilitate a comparison of different experimental capabilities and of the resulting sensitivities.

A crucial result of this effort during the first phase of PBC was the development of a set of benchmark cases [60] for new physics based on theoretically well-motivated models that can be viewed as simplifications of several broad classes of fundamental theories of Beyond the Standard Model (BSM) physics. By providing a detailed phenomenological description and a solid cal-

culational foundation for these models, it became possible to perform a consistent comparison of sensitivities across different experiments within PBC and across the world-wide landscape. Indeed, the benchmark cases and resulting discussions proved to have significant impact beyond PBC.

The original PBC benchmark models centered around the idea of Feebly Interacting Particles (FIPs) with masses at or below the GeV scale, which can be targeted by high-intensity and high-precision experiments. This focus led to the establishment of a dedicated PBC working group, the FIP Physics Centre (FPC), which serves as an interface between theory/phenomenology community and the experimental efforts within and beyond PBC. A series of dedicated workshops [61, 62] as well a school at Les Houches [63] strengthened this collaboration.

The FPC continually develops and refines the benchmark models and maintains an up-to-date collection of sensitivity projections, directly interacting with the experiments and the BSM working group. Crucially, this activity provided input for the discussion on the future use of the Experimental Cavern North 3 (ECN3) [64] by strengthening and sharpening the physics cases of the proposals for the High Intensity Kaon Experiment (HIKE) [65], Search for Hidden And Dark Objects With the SPS (SHADOWS) [66] and Search For Hidden Particles experiment (SHiP/NA67) [67] experiments.

Interfacing with theory is also crucial for the QCD-oriented experiments. This is done directly in the QCD working group. In the first PBC phase [68] this helped sharpen the targets of experiments in the area of QCD phase transition physics, but also discussed the sensitivity of experiments such as Muon On Electron Elastic Scattering (MUonE) to the hadronic vacuum polarization contribution to  $(g-2)_\mu$  with its potential impact on searching new physics via this observable.

Currently the QCD working group, and therefore also the phenomenological discussion within it, is focused on the opportunities presented by ion experiments in the NA. But efforts to support other experiments (e.g., LHC-FT, NA66/AMBER) continue to play an important role. Notably this also includes the exploitation of neutrinos that can be detected in experiments such as FASER, SND@LHC, and SHiP/NA67.

### 2.3 Worldwide landscape

The particle physics initiatives outlined by the PBC contribute to a broader international research landscape. This Section briefly introduces a number of relevant global efforts, highlighting those with closely related scientific objectives and significant evolution since the 2020 EPPSU (see [2, 60, 68] for the relevant PBC reports).

Among the various projects, the QCD experimental landscape is dominated by large experiments that evolve on a relatively large time scale and most of the world-wide experiments presented in Refs. [2, 68] are still active or foreseen. The time line of the future heavy-ion experiments CBM (FAIR) and CEE+ (HIAF) has been kept and they start taking data in the next 2 years.

The next-generation lepton-hadron machine, the Electron Ion Collider (EIC) [69], is to be built at BNL in the US, to start physics collisions in the first half of the 2030s. Key performance aspects include [70]:

- center-of-mass energy range: 29 to 140 GeV;
- ion beams from deuterons to the heaviest stable nuclei (e.g., Au, Pb, U);
- high collision luminosity from  $10^{33}$  to  $10^{34} \text{cm}^{-2} \text{s}^{-1}$  for electron-proton collisions;
- highly polarized (70%) electron, proton, and light-ion beams;

- an interaction region and integrated detector capable of nearly 100% kinematic coverage;
- the capability of incorporating a second such interaction region as needed;

allowing for a wide QCD physics programme, ranging from precision multi-dimensional imaging of nucleons with leptonic probes, the spin structure of nucleons and novel spin effects in QCD, exploration of gluon saturation at low parton momentum fractions, to modification of parton structure in the nuclear environment.

Jefferson Lab (JLab) has completed its luminosity-frontier 12 GeV energy update, enabling simultaneous delivery of highly (up to 90%) polarized electrons of up to 11 GeV to experiments conducted in Hall A, B, and C, and up to 12 GeV into Hall D, at luminosities of up to  $10^{35} \text{ cm}^{-2} \text{ s}^{-1}$  and potentially up to  $10^{39} \text{ cm}^{-2} \text{ s}^{-1}$  with the future SoLID fixed-target experiment. The experimental focus is on precision QCD studies—complementary to those at the future EIC in a different kinematic regime (e.g., valence-quark region)—and low-energy tests of the SM and BSM physics. Especially relevant in the context of this document is the approved Beam Dump Experiment (BDX) [71] searching for LDM. It is scheduled to run from 2026-2029 in a newly constructed facility (to be built) in front of the Hall-A beam dump, which will be served by a  $65 \mu\text{A}$  electron beam of 11 GeV.

Several upgrades of the complex are envisioned: A positron source could feed an unpolarized positron beam of order  $1 \mu\text{A}$ , less so for polarized positrons (of order 60% polarization), earliest in the first half of the 2030s [72]. An energy upgrade to 22 GeV beam energy could be realized with most of the existing accelerator installation for running as early as the second half of the 2030s, with hardly any impact on polarization and beam current as compared to the present configuration and with a broad physics program [73].

An exciting new direction are  $\eta/\eta'$  factories, which aim to exploit the special role of these particles in the SM to search for new physics in their rare decays. A first such experiment, JEF at JLab [74], is currently running and aims to extend the physics potential of the GlueX detector [75]. The proposed REDTOP experiment [76] at the European Spallation Source plans on collecting more than  $10^{13} \eta/\text{yr}$  ( $10^{11} \eta'/\text{year}$ ). The primary target is to search for new particles with mass below 950 MeV, such as dark photons or ALPs.

The Light Dark Matter eXperiment (LDMX) is a proposed beam-dump experiment at SLAC using the 8 GeV  $e^-$  beam from the Linac diverted to end station A [77]. The experiment aims to fully reconstruct the energy deposition of each incident electron using a high-granularity electromagnetic calorimeter and a hermetic hadronic calorimeter. LDMX then reconstructs the missing energy and transverse momentum to achieve (nearly) zero background with  $10^{14}$  electrons on target. The primary target of LDMX are invisibly decaying dark photons, but the experiment will also be sensitive to visible (displaced) decays. A first beam test with a prototype detector is planned for late 2025 and a detailed design report is currently in preparation. Another beam-dump experiment proposed in the US is DarkQuest [78], which plans to upgrade the SpinQuest experiment, a fixed-target experiment using a high-intensity 120 GeV proton beam at the Fermilab Main Injector. Using an electromagnetic calorimeter, DarkQuest aims to search for long-lived particles decaying to electron-positron pairs. A suitable detector has been identified and studied with a test beam in 2024 [79].

The Any Light Particle Search-II (ALPS-II) experiment [80] also searches for axions and axion-like particles. It is based on the “light-shining-through-a-wall” principle and has been set up over the past years in a currently unused part of the tunnel of DESY’s former Hadron-Elektron-

Ringanlage (HERA) around the HERA North Hall. The 250 m long experiment combines a string of 24 modified superconducting HERA dipole magnets with two 124 m long high-precision optical cavities [81, 82] and extremely low-power light detection [83, 84].

ALPS-II has the goal to improve the sensitivity on the axion-photon coupling by a factor of 1,000 compared to its predecessors. For the first time, ALPS-II will reach a parameter region in a model-independent fashion where the axion could also explain the dark matter in our universe and astrophysical anomalies. With its first run – concluded in May 2024 – ALPS-II has already reached an axion-photon coupling sensitivity roughly 30 times larger than earlier experiments (publication in preparation). The target sensitivity shall be reached in 2027.

The International AXion Observatory (IAXO) is a next-generation axion helioscope designed to search for solar axions with unprecedented sensitivity. In particular, it will explore QCD axion models in the mass range from meV to eV, covering scenarios motivated by astrophysical observations without relying on the dark matter paradigm. IAXO will build upon the two-decade experience gained with CAST, the detailed studies for BabyIAXO, which is expected to start construction at DESY soon, as well as new technologies. Several studies in recent years have demonstrated that IAXO has the potential to probe a wide range of new physics beyond solar axions, including dark photons, chameleons, gravitational waves, and axions from nearby supernovae.

The Laser Und XFEL Experiment (LUXE) [85, 86, 87] at the European XFEL (EuXFEL) facility aims to explore collisions between ultra-relativistic electrons (or photons) and intense laser pulses to study Strong-Field Quantum Electrodynamics (SFQED) and searches for new particles that couple primarily to photons. The installation timeline depends on EuXFEL’s operational schedule, particularly the T20 electron beam extraction line, requiring a facility shutdown of approximately 12 weeks. Following approval, LUXE could start operations around 2030.

There is currently no proposal for a non-collider experiment dedicated to measuring charged or neutral kaon decays within the PBC program. The CERN fixed-target kaon physics program is presently centered on the NA62 Experiment, which recently reported the first observation of the rare  $K^+ \rightarrow \pi^+ \nu \bar{\nu}$  decay [14]. The measured branching ratio is consistent with the SM prediction within  $1.7\sigma$ , though its central value is approximately 50% higher than the SM expectation. This result is particularly intriguing in light of recent measurements by the Belle II collaboration, which reported evidence for the  $B^+ \rightarrow K^+ \nu \bar{\nu}$  decay with a central value  $2.7\sigma$  above the SM expectation [88]. These flavor-changing neutral current transitions, with a neutrino-antineutrino pair in the final state, are theoretically well understood; thus, significant deviations from the SM predictions could indicate new physics.

While the HIKE experiment [65], proposed as a follow-up to NA62, was not approved by CERN, kaon physics continues with the study of neutral  $K_L$  decays at the KOTO experiment at J-PARC. Although KOTO continues to improve its sensitivity, it will not reach the level required to observe the SM-predicted  $K_L \rightarrow \pi^0 \nu \bar{\nu}$  decay. A letter of intent has recently been submitted for a successor experiment, KOTO II, which aims to achieve the necessary sensitivity to observe this decay [89].

Belle II, a next-generation flavor physics experiment at KEK’s SuperKEKB collider in Tsukuba, Japan, has collected electron–positron ( $e^+ e^-$ ) collision data since 2018. With peak luminosities exceeding  $5.0 \times 10^{34} \text{ cm}^{-2} \text{ s}^{-1}$  and strong European participation, it focuses on high-precision measurements in the fields of QCD and flavor physics, as well as in searches for New Physics. Data-taking resumed in 2024, aiming for an integrated luminosity of  $10 \text{ ab}^{-1}$  by 2032, followed by a detector upgrade to reach a total of  $50 \text{ ab}^{-1}$  [90].

Since the last European Strategy Update, neutrino oscillations have been confirmed as a central particle physics topic with a vivid competition. The main players in the field are Fermilab in the US, with the current NOvA experiment and future Deep Underground Neutrino Experiment (DUNE), J-PARC in Japan with the current T2K and future Hyper-Kamiokande (Hyper-K) experiments, and China with the JUNO reactor project. The ongoing NOvA and T2K programs are currently favoring the neutrino normal mass ordering and a non-0 CPV. In the coming years, their antineutrino (NOvA) and total (T2K) data samples are expected to be doubled, with the goal to approach the  $3\sigma$  level for the determination of the mass ordering and CPV detection. DUNE and Hyper-K are now both officially approved and in full construction swing, with start of data-taking expected before 2030. DUNE should quickly establish the mass ordering at  $5\sigma$  level within 1 to 3 years of data-taking. On the longer term, CPV is expected to be established at more than  $3\sigma$  within 75% of the possible ranges, with a measurement better than  $20^\circ$  in 10 years of data-taking for favorable values. The construction of the JUNO experiment in China is now close to completion and start of data-taking imminent. The mass hierarchy is expected to be established within 6 years at the  $3\sigma$  level.

### 3 Evolution of the CERN accelerator complex and post-LS3 outlook

#### 3.1 CERN Accelerator complex after LS2, planned upgrades during LS3 and future perspectives

##### 3.1.1 LHC INJECTORS

The CERN injector complex underwent an extensive upgrade during the Long Shutdown 2 (LS2), which lasted about two years (2019-20) and was driven by the LHC Injectors Upgrade (LIU) Project [91, 92] (Figure 1). The project included several baseline items to enable the LHC injector chain to deliver the high-brightness proton beams required by the High Luminosity LHC (HL-LHC) to reach a leveled luminosity of  $5 \times 10^{34} \text{ cm}^{-2}\text{s}^{-1}$ . Here is a list of the main ones:

- The connection of the Proton Synchrotron Booster (PSB) to the new 160 MeV H<sup>-</sup> linear accelerator, Linear Accelerator 4 (Linac 4), and the installation of the corresponding charge-exchange injection scheme.
- The increase of the extraction energy of the PSB to 2 GeV.
- The upgrade of the injection region and Radio Frequency (RF) systems of the Proton Synchrotron (PS) to allow 2 GeV injection and mitigate longitudinal instabilities.
- The power and Low Level Radio Frequency (LLRF) systems upgrade of the main SPS RF system (200 MHz), a new SPS beam dump and new protection devices in the transfer lines to LHC.

In the ion chain, the Low Energy Ion Ring (LEIR) was the object of an intense performance improvement campaign, which enabled it to double the amount of ions produced per cycle. In the SPS, the upgrade of the 200 MHz RF system allowed performing momentum slip-stacking, thus reducing the bunch spacing from 100 to 50 ns and doubling the number of bunches that can be packed in the LHC, another HL-LHC goal. During the present run (Run 3), the injector chain has proven to be able to achieve the LIU targets in terms of maximum bunch population  $N$  and minimum normalized emittance  $\varepsilon_{x,y}^n$ , and sometimes even surpass them as shown in Table 1.

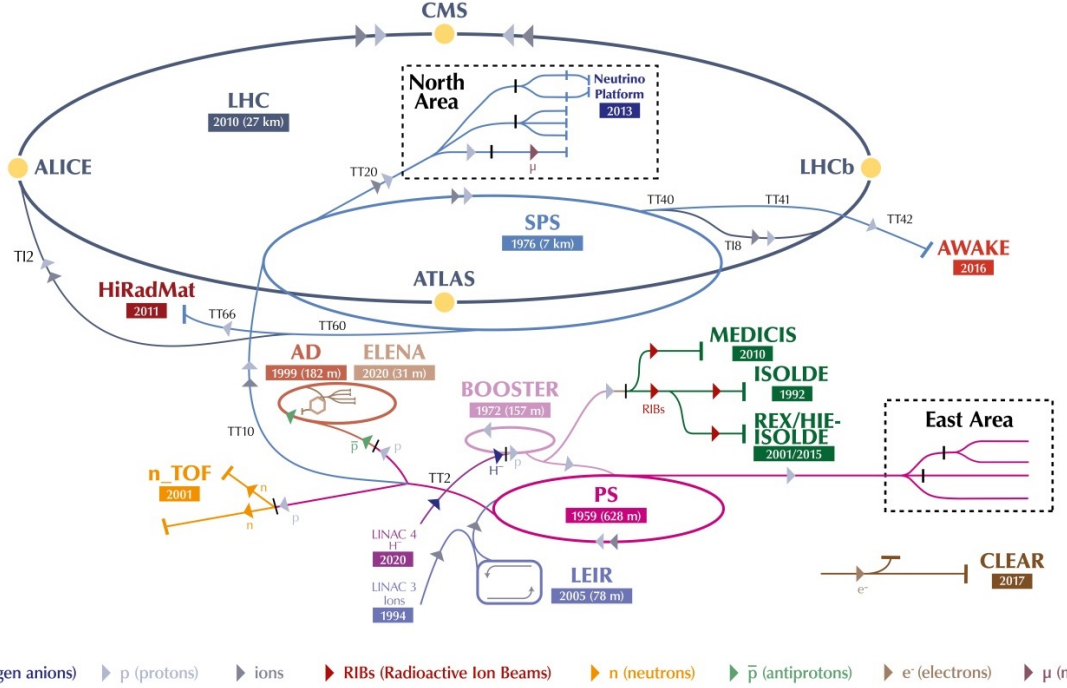


Figure 1: Overview of the LHC injectors chains, both for protons and heavy ions after LS2. Courtesy: CERN.

	$N [10^{11} \text{ p/b}]$	$\epsilon_{x,y}^n [\mu\text{m}]$	Bunch spacing [ns]	Train structure
LIU target	2.3	2.1	25	$4 \times 72$ bunches
Achieved	2.3	1.7	25	$4 \times 48$ bunches
	$N [10^8 \text{ ions/b}]$	$\epsilon_{x,y}^n [\mu\text{m}]$	Bunch spacing [ns]	Train structure
LIU target	2.0	1.5	50	$7 \times 8$ bunches
Achieved	2.8	1.8	50	$7 \times 8$ bunches

Table 1: Beam parameters at SPS extraction for protons and Pb ions, LIU target and best performance achieved so far in Run 3.

Beams used in the injectors for FT physics have also largely benefited from the LIU upgrades. Some of the new benefits have been put to fruition by improving the quality or increasing the intensity of the beams delivered to the experiments. For example, the production scheme of the beams for the NA has been improved in the PS thanks to the commissioning of the barrier bucket at extraction (to be used together with the Multi Turn Extraction (MTE), already operational for many years), made possible by using the same broad band cavity installed in the PS ring as a part of the feedback system against longitudinal instabilities. The losses at PS extraction of this beam have been thus significantly reduced, such that it will be possible to remove the element protecting the extraction septum (so-called *dummy septum*), improving the aperture for all beams [93]. Another example is the production of 5 bunches instead of 4 in the PSB (with one ring producing two bunches instead of one) for the Antiproton Decelerator (AD) beam, made possible by the lower transverse emittances achieved with the 160 MeV injection. This has led to 20 % larger intensity

per pulse on the AD target and consequently a higher number of antiprotons into AD and the Extra Low Energy Antiproton ring (ELENA) [94].

Other benefits have been studied during Machine Development (MD) sessions and are kept in store when potential requests for higher intensities might come after LS3. For instance, before LS3 the PSB accelerated a maximum of  $10^{13}$  p/ring, but with large losses during injection and RF capture (up to 40%). After the connection to Linac 4, the PSB has already unveiled its potential to produce 60% higher intensities (i.e., up to  $1.6 \times 10^{13}$  particles per pulse (ppp)/ring, a value so far successfully demonstrated in two of the four rings) with few percent losses only occurring in the very first phase of the acceleration [95]. Its routine operation has however stayed at  $0.8 \times 10^{13}$  p/ring, as this value currently fulfills the needs of the Isotope Separator On Line DEvice (ISOLDE) users with 30-40% cycles in the supercycle. Table 2 summarizes the currently achieved performances for the main FT beams.

	Intensity [ $10^{10}$ ppp]	$\epsilon_x^n, \epsilon_y^n$ [ $\mu\text{m}$ ]	Bunch length [ns]	# bunches
ISOLDE	5000	8, 8	240	4
nToF parasitic	800	9, 7	44	1
nToF dedicated	1020	14, 11	28/44	1
AD	2000	9, 6	35	5
EA	80	1.5, 1.3	-	unbunched
NA	4200	7, 4	-	unbunched
AWAKE	30	2, 2	0.5 - 0.7	1

Table 2: Beam parameters at extraction for protons, best performance achieved so far in Run 3. Here, ppp = particles per pulse; nToF = neutron Time of Flight facility; AWAKE = Advanced WAKEfield Experiment.

From Table 2 we can see that dedicated nToF beams have been produced with intensities slightly above  $1000 \times 10^{10}$  ppp, however around this value transverse stability becomes marginal upon transition crossing. This is the reason why the highest operational value is assumed to be  $920 \times 10^{10}$  ppp. The vertical instability limiting the intensity on the nToF beam has been widely studied in the past and found to be a Transverse Mode Coupling Instability (TMCI) mainly driven by the impedance of the PS kickers (e.g., [96]). To efficiently mitigate it, an impedance reduction campaign of these kickers would be needed.

The beam to the NA was operated routinely with an intensity of  $4200 \times 10^{10}$  ppp extracted from the SPS over an extended period of time in 2022, but this led to important losses in the region of the extraction electrostatic septum and at the splitter magnets in the transfer lines to the experiments, which resulted in high levels of radiation in these areas. Crystal shadowing and channeling measures have been meanwhile widely tested and optimized, and are planned to be put in place for the future operation at this intensity level [97, 98]. Higher intensities on this beam are being studied, with a high brightness version developed at the PSB and up to  $3300 \times 10^{10}$  ppp stably accelerated in the PS and extractable with MTE and barrier bucket [99]. In the SPS detailed studies of working point optimization along the cycle are ongoing before pushing the intensity to higher than operational values in order to check possible stability limitations or aperture bottlenecks.

Finally, it should be stressed that, although it was mentioned above that  $1600 \times 10^{10}$  ppp were successfully accelerated in two of the four PSB rings and can thus be seen as a peak performance

to be aimed at for future operation, the intensity value quoted for the ISOLDE beams in Table 2 considers  $1250 \times 10^{10}$  ppp/ring, a value stably and reproducibly achieved in autumn 2024 and used for yield measurements as a function of intensity on the General Purpose Separator (GPS) target.

No other major upgrades are foreseen in the injectors during the LS3 and the LHC ion experiments will operate with lead ions in Run 4. However, a number of proposals contemplating beam with ions lighter than lead, in addition to lead ones, have been made [100]. The LHC experiments, and in particular ALICE with an upgraded detector (ALICE3) [101] propose to maximize the nucleon-nucleon luminosity with ions of intermediate mass. The discovery at the LHC of the QGP properties in small systems, like proton-proton and proton-ion collisions, is motivating the physics community to study in more detail light ion collisions at the LHC [102, 103]. The NA61/SHINE [104] collaboration has proposed the continuation of their ion physics programme with beams of different species (lead and light ions) and energies and the Dilepton and Charm Experiment/NA60+ Collaboration (DICE/NA60+) has proposed experiments with lead beams at different energies [105, 100] after LS3. High Energy Accelerators for Radiation Testing and Shielding (HEARTS), a facility to study the effects of radiation to electronics, is being proposed at CERN [106]. It aims at delivering different ion species during the same day with switching times of maximum 15 minutes, which is not possible with the current ion complex. One of the reasons being the availability of a single ion source. Extensive studies have been conducted [107, 108, 109] showing the feasibility of producing and accelerating different ion species as requested by the above proposals. The intensities for boron, magnesium, oxygen and lead requested by the above-mentioned NA experiment proposals are expected to exceed the limits imposed by Radiation Protection (RP) considerations in the NA. A similar study is being conducted to address the performance reach of the ion complex for additional ion species requested by ALICE3 and HEARTS (argon, calcium, krypton, indium and xenon).

A pre-conceptual analysis has been performed to determine the upgrades of the ion complex [110] that would be required to deliver different ion species with switching times of around 15 minutes, mitigate space-charge effects in the injectors to increase the beam brightness and to halve the bunch spacing to almost double the number of bunches injected into the LHC.

### 3.1.2 EXPERIMENTAL AREAS

#### PS East Area (EA)

The EA at CERN was designed to use the protons from the PS and has served the physics community for over 50 years. With its perfect complementarity with the beam energies available at the CERN NA, which uses the protons from the SPS, it remains extremely popular and necessary for many different experiments and test beams. Given the upgrades needed for the HL-LHC, there is a growing request for test beams to calibrate the detectors over a wide range of energies. In addition, physics experiments like Cosmics Leaving Outdoor Droplets experiment (CLOUD) and irradiation facilities, like IRRAD and CERN High Energy Accelerator Mixed-field (CHARM), depend on the reliability and stable operation of the EA. An extensive renovation of the EA took place during the LS2 following a study phase between 2009 and 2015. The renovated EA started its operation in 2021 and has been serving the diverse user community since. The main goal of the project was to ensure the long-term operation of the EA experimental facilities in line with the operation needs and the physics requirements. It included a new beamline layout, a new cycled

powering scheme and refurbished beam elements and associated infrastructure [111]. In an effort to reduce the annual energy consumption of the facility, the EA building was upgraded with improved wall and roof cladding to better insulate it. The massive magnet yokes have been replaced with laminated ones to cycle all the magnets, and the power converters have been upgraded with energy recovery capacitor banks. The energy consumption has thus been reduced from 11 GWh to 0.6 GWh. To improve reliability, and maintainability the number of different families of the magnets has also been reduced from 22 to only 12. The upgrades and the new layout have also resulted in improved beam purities especially for the electron beam in the secondary beamlines at low energies which complements the energy ranges available in the NA.

## ISOLDE and nToF

The nToF facility underwent major renovation works during LS2, with the second-generation spallation lead target replaced by a new assembly. With an innovative design, the target consists of lead plates cooled by nitrogen gas, and it can receive a higher number of ppp, up to  $10^{13}$ , as an increased average proton flux. A new target replacement is planned for LS4, presently planned in 2034, most probably with minor design improvements with respect the current one. For the moment there are no other major modifications planned for the facility, which proved to be adequate to deliver the required flux of neutrons for the next decade while maintaining its unique features, mainly the longest flight path with short proton pulses (7 ns), the highest instantaneous proton (neutron) intensity and widest range of neutron energies spanning from meV to GeV [112].

ISOLDE is the only radioactive ion beam facility using GeV protons, giving access to several processes (fission, spallation, fragmentation) that contribute to radioisotope production. The ISOLDE primary area will undergo a major renovation in the coming years. The replacement of the two front-end beam dumps will take place during LS3. The two devices are approaching the end of their operational lifetime, and they will be replaced with two beam dumps capable of receiving higher power beams. This, together with the proposed upgrade of the primary proton beam line from 1.4 GeV to 2 GeV, will increase both the capability and the capacity of the facility. The higher power on target will open up the possibility of exploring new isotopes thanks to the increase of the production cross section with the higher energy. In addition, the increased yields will facilitate more detailed and higher precision studies, as well as increasing the throughput of experiments. Such advantages will be amplified if the potential of the PSB after the LIU upgrades can be used to deliver higher proton intensities [113]. The planned introduction of nanomaterial-based target also promises the possibility to produce shorter-lived isotopes. Other interventions to the facility will be focused on maintaining and improving its availability and performance, with particular attention to the superconducting linac of the High Intensity and Energy ISOLDE (HIE-ISOLDE) facility. Studies will be launched to make beams of radioactive molecules available in the framework of PBC (see Section 4.5.1).

## SPS North Area (NA)

The NA beamlines [16] are a cornerstone of the PBC programme, providing a versatile FT facility for exploring fundamental interactions. These beamlines deliver a broad mix of particle beams, ranging from protons and hadrons to electrons, muons, and ions, which are tailored to support both precision measurements and innovative new physics searches. Their design emphasizes

Parameter	H2	H4	H6	H8	M2	K12	P42
Max. momentum [GeV/c]	400/360	400/360	205	400/360	280	75	400
Max. acceptance [ $\mu\text{Sr}$ ]	1.5	1.5	2	2.5	5(h)	12.7	1.4(p) 0.3(e,h)
Maximum $\Delta p/p$ [%]	$\pm 2.0$	$\pm 1.4$	$\pm 1.5$	$\pm 1.5$	$\pm 4.0$	$\pm 2.0$	$\pm 0.5(p)$
Typical $\Delta p/p$ [%]						$\pm 1.0$	
Maximum intensity/spill	$10^7/10^5$	$10^7/10^5$	$10^7/10^5$	$10^7/10^5$	$5 \cdot 10^8$	$2 \cdot 10^9$	$6 \cdot 10^{12}$
Particle types ( <b>typical</b> )	$p, h, \mu,$ $e, \text{ ions}$	$p, h, \mu,$ $e, \text{ ions}$	$h, \mu, e$	$p, h, \mu,$ $e, \text{ ions}$	$\mu, h, e$	$h, \mu$	$p, h, \mu,$ $e, \text{ ions}$

Table 3: Overview of the characteristics of the NA beamlines. If multiple entries are provided for a specific value, the first one corresponds to primary beam operation, while the second one refers to secondary beams. The following abbreviations are used for particle types:  $p$  (protons),  $h$  (hadrons),  $e$  (electrons),  $\mu$  (muons). Intensities are given for a typical spill of 4.8 s.

flexibility and high performance, ensuring that experiments can be optimized for a wide range of research objectives. Table 3 summarises the beam characteristics of the NA beamlines.

The NA is fed by a slow-extracted beam from the SPS, typically delivered in 4.8 s spills at 400 GeV/c. The beam impinges on the primary production targets T2, T4, and T6, located in the Tunnel Target Cavern 2 (TCC2). From these targets, secondary beams are produced and distributed via dedicated beamlines. The H2, H4, H6, and H8 lines, each extending over 600–700 m, deliver secondary and tertiary beams to Experimental Hall North 1 (EHN1) for test-beam applications and fixed-target experiments [e.g., NA61/SHINE, NA64–e, and the Gamma Irradiation Facility++ (GIF++)]. In contrast, the M2 beamline, which spans nearly 1.2 km, is designed for high-intensity muon production and also provides hadron and low-energy electron calibration beams to Experimental Hall North 2 (EHN2), serving currently the NA66/AMBER and NA64– $\mu$  experiments. Furthermore, the K12 beamline delivers beams to ECN3, serving the NA62 experiment. Unlike the other beamlines, the K12 beamline starts in Tunnel Target Cavern 8 (TCC8), which receives the non-interacting protons surviving the T4 target that are transported via the P42 beamline to the T10 production target. Figure 2 shows a schematic overview of the different beamlines, experiments, facilities, and experimental areas as of 2025.

#### North Area Consolidation Project (NA-CONS)

A North Area Consolidation Project (NA-CONS) has been approved in 2021 with two phases covering the renovation of infrastructures and services to recover reliability and bring the facility into compliance with modern safety requirements. The first phase of the consolidation programme is targeting the single-point-of-failure with particular focus on the primary beam delivery systems. The second phase of the consolidation will guarantee the compatibility with future upgrades and new experiments. Figure 3 gives an overview on the locations that are targeted by both consolidation phases: Phase 1 of NA-CONS (2019 – 2029), in blue, aims at the consolidation of the primary beam areas and the high-intensity beamline towards TCC8 and ECN3. Phase 2 (2030 – 2035), in orange, will address the consolidation of EHN1 and EHN2 together with their associated beamlines and technical buildings.

The NA-CONS baseline does not cover a full renovation of TCC2 but discussions are ongoing to extend its scope to address a series of faults in TCC2 hinting to a potential end-of-life scenario

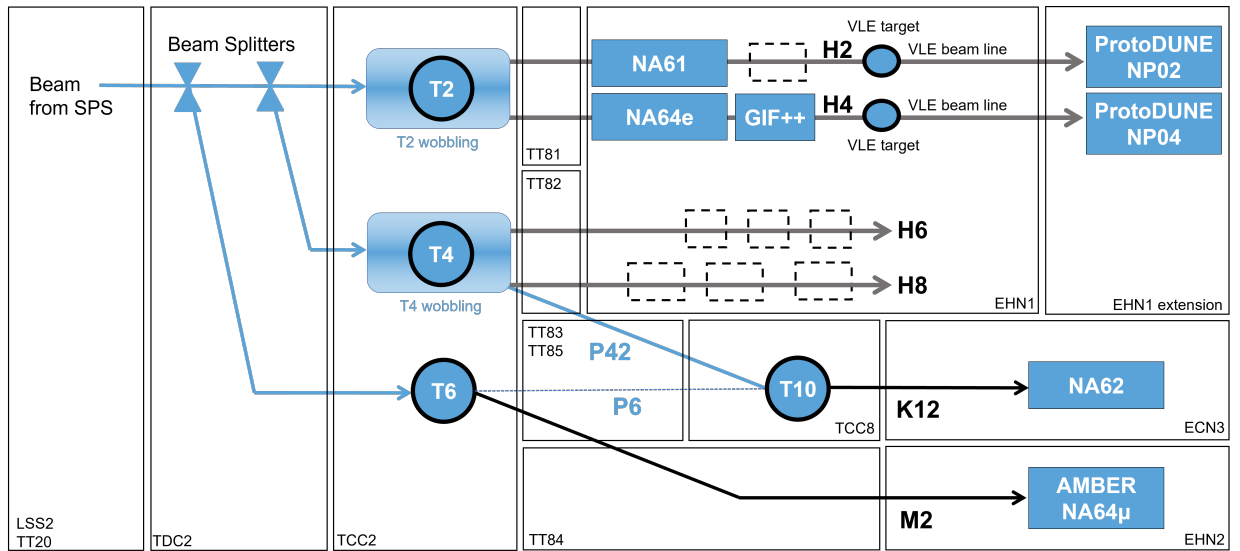


Figure 2: A schematic layout of the NA beamline and experiment complex as of 2025 [64].

of various components. It is proposed to carry out a full renovation of TCC2 including the entire re-alignment of the beamlines, the replacement of the old magnets and production of additional spares, the replacement of plug-in supports and damaged magnet supports, extensive cabling/de-cabling, shielding removal and re-routing of all the services to provide better accessibility. Such an extension of scope will ensure a safe and reliable operation.

#### *High Intensity ECN3 (HI-ECN3)*

The consolidation efforts go hand in hand with the recent decision to host a new experimental facility to search for HS particles, for which an Expression of Interest (EoI) [114] was submitted to the SPSC in October 2013, identifying underground locations around the SPS (Tunnel Target Cavern 4 (TCC4), Tunnel Neutrino Cavern (TNC), ECN3 and Transfer Tunnel 61 (TT61)) [115]. At that time, all the suitable locations had recently approved programmes (AWAKE, High Radiation to Material (HiRadMat) and NA62, respectively) and TT61 was disfavoured for environmental reasons. Studies continued with a focus on the construction of an entirely new facility at a new underground cavern in the NA, coined ECN4. Following a Technical Proposal [116, 117] submitted to the SPSC in 2015, a three-year Comprehensive Design Study (CDS) was carried out under the auspices of PBC to present the proposal for the Beam Dump Facility (BDF) [118] and the SHiP/NA67 experiment [119, 120] to the 2020 EPPSU. The SHiP/NA67 proposal was recognised as one of the front-runners among the new facilities investigated within the PBC studies but for reasons of cost, the project could not, as of 2020, be recommended for construction considering the overall recommendations of the EPPSU [121]. Following a thorough assessment of alternative sitings [122], focus moved to ECN3 to reduce the investment cost for the facility implementation. Several options were studied within the PBC Study Group for the long term use of ECN3 [64]. After evaluation by the SPSC, the CERN RB selected the SHiP/NA67 experiment [67] for the future exploitation of the ECN3 experimental facility after LS3 in conjunction with the implementation of BDF and an upgrade of the facility to higher beam intensity. Figure 4 shows an overview of SHiP/NA67 in ECN3.

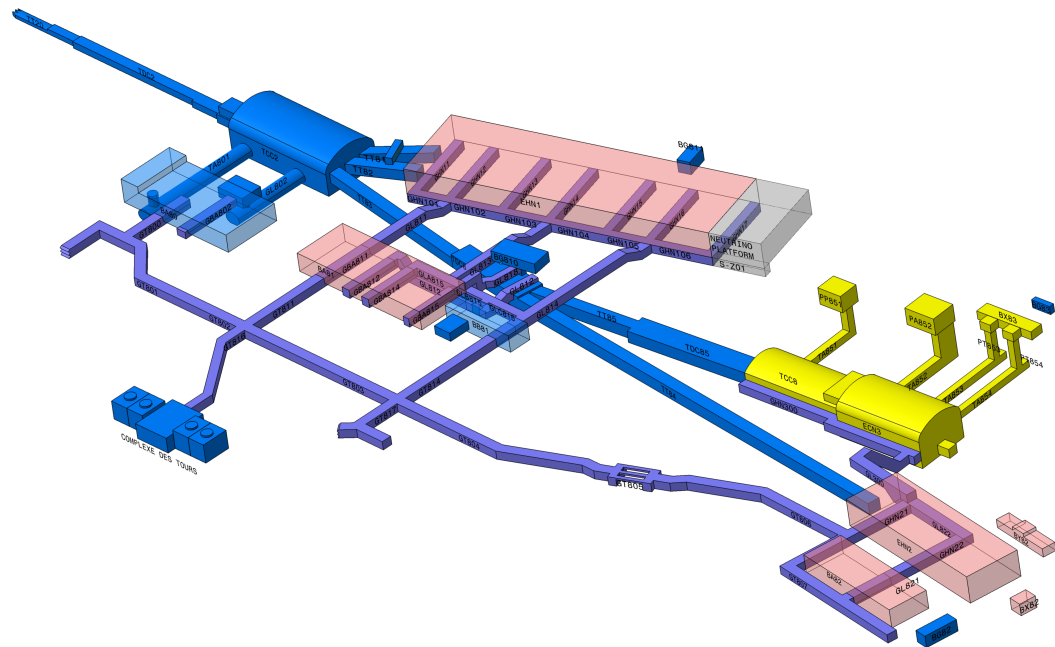


Figure 3: Overview of the experimental areas, beam tunnels, target caverns, and technical galleries in the CERN NA. The locations affected by Phase 1 of NA-CONS are depicted in blue (caverns, tunnels, service buildings) and in violet (technical galleries), areas targeted by Phase 2 are shown in orange, and locations under HI-ECN3 are in light green. Courtesy: CERN.

The cost of upgrading and implementing BDF in ECN3 for SHiP/NA67 came in at approximately 100 MCHF lower than the original ECN4 proposal by removing the need for major civil engineering works and by re-using existing infrastructure, as well as profiting from the ongoing investment in NA-CONS. Alongside the NA-CONS project, the upgrade of ECN3 will secure the long-term future of the SPS FT physics programme at CERN. The High Intensity ECN3 (HI-ECN3) project is presently in a rapid technical design phase with the delivery of the Technical Design Report (TDR) expected mid-2026. The project is working in close synergy with the NA-CONS project to upgrade the required accelerator infrastructure as part of the foreseen consolidation programme during LS3. The TDR for SHiP/NA67 is expected around mid-2027. The construction plan foresees commissioning of the facility in 2031 and detector in 2032 with at least one year of initial physics data-taking before LS4 with a programme extending to the mid of the century.

## *Proton Sharing*

A common feature of most proposals received for the NA 61/FT programme is the request for higher intensities. Proton-sharing scenarios across the CERN accelerator complex have been analyzed and possible optimizations considering future PBC experiments have been studied.

Since the cessation of CNGS operations, the NA experiments have received spills with a duration of 4.8 s at the highest possible repetition rate. The proton sharing scenarios for the high-intensity operation of ECN3 in parallel to other NA experiments has been studied also considering

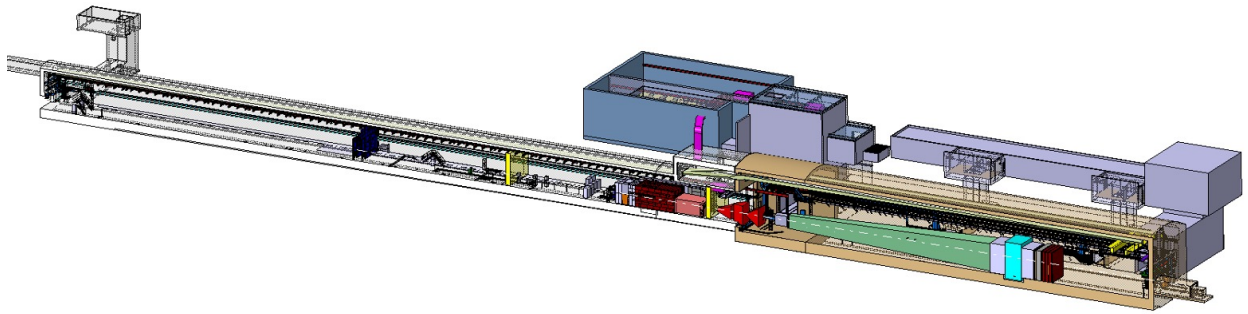


Figure 4: BDF/SHiP/NA67 integrated inside the ECN3 experimental cavern. Courtesy: CERN.

the parallel operation of the LHC, AWAKE, HiRadMat and MD sessions [123, 124]:  $1.2 \times 10^{19}$  Protons on Target (PoT)/year will be available to the EHN1 and EHN2 experiments, provided no ion run (1 month) takes place and  $0.8 \times 10^{19}$  PoT/year can be delivered in case an ion run is included. The integrated intensity to the other NA experiments is maximised by assuming the acceleration of  $4.2 \times 10^{13}$  ppp with a 4.8 s spill. For some NA users this might be problematic due to rate limitations and an alternative approach (previously adopted during CNGS operation) would be to extend the flat top while proportionally increasing the accelerated beam intensity up to  $4.2 \times 10^{13}$  ppp (which has been already achieved at the SPS):  $0.8 \times 10^{19}$  PoT/year ( $0.6 \times 10^{19}$  PoT/year with an ion run) can be delivered to the EHN1 and EHN2 users with 9.6 s long spills.

Following the decision to launch a TDR for SHiP/NA67, additional studies are being performed by the bSAC (Beam Sharing across Complex) and SOX (Spill Optimisation for eXperiments) working groups, mandated by the Injectors and Experimental Facilities Committee (IEFC), to cope with potentially higher proton requirements for the NA experiments while minimizing the impact on the users of the upstream PS complex [125]. The reports from these working groups are expected by the end of Q1 2025.

### 3.1.3 AD COMPLEX AND ELENA

The Antimatter Factory at CERN comprises the proton-to-antiproton target area, two synchrotrons [the Antiproton Decelerator (AD) and the Extra Low Energy Antiproton ring (ELENA)], and several experimental zones housed within the AD hall.

The AD ring has been operational since early 2000 [126], delivering approximately  $3 \times 10^7 \bar{p}$  at 5.3 MeV in a single bunch every two minutes to experiments, which, before LS2, operated in 8-hour shifts. In 2018, the ELENA ring was commissioned [127, 128] and became fully operational after LS2 in 2021 [129, 130]. The introduction of ELENA has enabled a further deceleration of antiprotons extracted from AD to energies as low as 100 keV. This advancement significantly improved experimental efficiency, increasing trapping rates by up to two orders of magnitude. In addition, ELENA allows the available intensity to be split into four bunches, enabling up to four experiments to run simultaneously.

Since its integration, ELENA has exceeded expectations, doubling the antiproton flux compared to its original design specifications, as shown in Table 4.

A comprehensive review of the facility's status is presented in [131], while a broader overview

	PoT [ $\times 10^{13}$ ]	$\bar{p}/\text{bunch} [\times 10^6]$	# $\bar{p}$ bunches	rep. period [s]
AD pre-LS2 (achieved)	1.4	30	1	110
ELENA (design)	1.4	4.5	4	$\approx 100$
ELENA (achieved)	1.9	12	4	110

Table 4: Overall performance of the Antimatter Factory.

of potential upgrades can be found in [132]. These upgrades include essential consolidations of legacy AD equipment to ensure maintaining high availability and operational reliability, with the assumption of operating the facility till the end of Run 5 (end of 2041). Short-term performance improvements, such as enhanced beam stability and reduced cycle times, are already underway.

### 3.1.4 HIGH LUMINOSITY LHC (HL-LHC)

The completion of the LIU project and a number of HL-LHC upgrades already deployed in LS2 [133] have offered to the LHC the opportunity and the challenge to operate with up to two times higher beam brightness compared to the design parameters and 50 % higher as compared to Run 2. The main beam parameters achieved and planned for the LHC and the HL-LHC [134] at the start of collisions are given in Table 5. The complete installation of the HL-LHC will take place in LS3. In this context, Run 3 is clearly a transition between the LHC and the HL-LHC.

The HL-LHC Project has the following targets:

- A peak luminosity of  $5 \times 10^{34} \text{ cm}^{-2}\text{s}^{-1}$  with levelling operation (corresponding to an average event pile-up  $\langle \mu \rangle$  (PU), i.e. the number of events per bunch crossing in the detectors, of  $\approx 140$ ) with the possibility to reach a peak levelled luminosity of  $7.5 \times 10^{34} \text{ cm}^{-2}\text{s}^{-1}$  (corresponding to  $\langle \mu \rangle > 200$ ).
- An integrated luminosity of  $250 \text{ fb}^{-1}$  per year, with the goal of achieving a total of  $3000 \text{ fb}^{-1}$  in the decade following the upgrade.

These ambitious goals will be achieved through a number of important upgrades throughout the accelerator. In particular, a complete renovation of the experimental insertions IR1 and IR5 is planned, involving about 1.2 km of the accelerator. The upgrades include the installation of high-field Nb<sub>3</sub>Sn quadrupole magnets, which will replace the current focusing magnets around the IPs to achieve smaller beam sizes. This is complemented by the deployment of crab cavities, which will rotate particle bunches to maximize their overlap at the collision points, thereby enhancing effective luminosity. To support these modifications, additional cryogenic plants, HTS-based superconducting links, new power converters and beam instrumentation will be installed. The project also relies on an improved beam collimation system designed to handle the higher beam intensities. These upgrades will also ensure the LHC efficient operation until the end of the physics programme, presently planned until 2041.

The transition from the LHC to HL-LHC in Run 4 foresees a carefully staged performance ramp-up during the initial years of operation. This approach balances machine protection, operational experience with new hardware systems, and the progressive validation of beam dynamics at higher intensities. Luminosity will also be increased incrementally, while the accelerator and experiments gather essential experience with higher pile-up conditions and increased radiation levels in critical areas such as collimation and experimental insertions.

Parameter	Nominal LHC (design report)	LHC (2024)	HL-LHC
Beam energy in collision [TeV]	7	6.8	7
Particles per bunch $N_b$ [ $10^{11}$ ppb]	1.15	1.6	2.2
# bunches per beam	2808	2352	2760
Half-crossing angle in IP1 and IP5 [ $\mu\text{rad}$ ]	142.5	150	250
Minimum $\beta^*$ [m]	0.55	0.30	0.15
Norm. transverse emittance start of collisions $\epsilon_n$ [ $\mu\text{m}$ ]	3.75	2.50	2.50
Levelled luminosity in IP1/5 [ $10^{34} \text{ cm}^{-2}\text{s}^{-1}$ ]	1 (peak)	2.0	5.0
Max. average event pile-up $\langle\mu\rangle$ [events/crossing]	27	60	132

Table 5: HL-LHC nominal parameters compared to the LHC design and achieved parameters [135].

The availability of these upgraded beams at the LHC starting in Run 4 offer further PBC experimental opportunities presently under consideration. These PBC experiments, operating parasitically or semi-parasitically alongside the main collider programme, represent a cost-effective and complementary path to new physics in the HL-LHC era, making full use of the upgraded accelerator infrastructure and physics opportunities presented by the high-luminosity environment.

### 3.2 Accelerator Technology developments

CERN has developed a number of technologies to support the design and construction of accelerators and detectors for particle physics experiments. The experience and expertise in technological domains such as Superconducting (SC) and normal conducting magnet and RF technology, cryogenics, optics, vacuum and surface technology can benefit and contribute to the development of new detection methods like quantum sensing. It can also support the development and assessment of the feasibility of accelerator and non-accelerator experiment proposals aiming at fundamental SM or BSM physics measurements. As examples of such contributions we can mention the design of the SC dipole for the Baby International AXion Observatory (BabyIAXO) experiment [136], the contribution to the DarkSide-20k experiment cryogenic and argon purification system [137] (including the support for commissioning the Aria argon distillation plant [138]), or the current ongoing development of High-Temperature Superconductors (HTS) for the Relic Axion Detector Exploratory Setup (RADES) experiment [139]. To further foster exchanges between technology experts at CERN and collaborating institutes, the PBC Technology WG has organized five workshops on the following topics: SC RF [140], lasers and optics [141], vacuum, coating and surface technologies [142], cryogenic technologies [143] and superconductivity technologies [144].

Since its inception PBC [2] has supported the feasibility study of several experiments, some of which have now reached maturity, being fully fledged collaborations and funded by the respective agencies. Among the experiments that were part of the WG are Any Light Particle Search-II (ALPS-II) [145], which is presently taking data at Deutsche Elektronen-Synchrotron (DESY), and the already mentioned BabyIAXO and DarkSide-20k, which are now in the construction stage. Some other experiments have instead either concluded that their proposal could not reach technical feasibility (Vacuum Magnetic Birefringence experiment at CERN (VMB@CERN)), or are running

their facilities without further contribution required from the Technology WG (Ptolemy, Sub-THz Axion eXperiment (STAX)). The experiments participating in the WG at the date of this report are

- Grenoble Axion Haloscope (GrAHal) [146],
- advanced Kinetic Weakly interacting Sub-eV Particle experiment (aKWISP) [147],
- FINUDA magnet for Light Axion SearchH (FLASH) [148],
- RADES [149],
- Axion heterodyne detection [150], and
- Atom Interferometer Observatory and Network (AION)-100 @ CERN.

GrAHal and aKWISP joined PBC from its launch [151], while the other experiments have joined more recently. FLASH has just started interacting with the Technology WG at the date of this report thanks to preliminary discussion established during the workshops. The four new experiments are described in more detail in Section 4.7, and they all are in synergy with the CERN Quantum Technology Initiative (CERN QTI) [152] and the European Committee for Future Accelerators (ECFA) Detector Research and Development programme (DRD) 5 on quantum sensors [153], as they all rely on the support of both programmes, to different extents.

### 3.3 Potential future accelerators and facilities at CERN

#### 3.3.1 SHORT BASELINE NEUTRINO BEAM PROPOSAL

The need for a high-precision neutrino beam for cross-section measurements has been recognized since the 2020 EPPSU and is currently being explored at CERN within the framework of PBC. This effort builds upon CERN’s investments in neutrino physics, particularly in the development of the proto-DUNE detectors, along with advances in high-precision neutrino-beam design spearheaded by the Enhanced NeUtrino BEams from kaon Tagging (ENUBET) and Neutrino Tagging (NuTag) collaborations [154, 155, 156]. The aim of the Short Baseline Neutrino (SBN) beamline [157] is to provide a medium-intensity, high-precision neutrino beam that advances our knowledge of neutrino cross sections at the GeV scale in all channels that cannot be addressed by current neutrino cross-section experiments or the upcoming near detectors of Deep Underground Neutrino Experiment (DUNE) and Hyper-Kamiokande (Hyper-K).

A conceptual study of the SBN beamline has been performed, and an extensive report is under preparation [158]. The proposed design (Figure 5) includes a slow extraction of the SPS protons towards a production target, a 23-meter-long secondary meson beamline and a 40-meter-long decay tunnel, both instrumented with fast radiation-hard detectors for a high-precision monitoring of the neutrino fluxes and individual neutrino tagging (see Section 4.8.1). Following an extensive optimisation of the target and acceptance of the secondary beamline the expected particle production rates at a particle momentum of  $8.5 \text{ GeV}/c$  are  $12.7 \times 10^{-4} K^+$  per PoT and  $1.9 \times 10^{-2} \pi^+/\text{PoT}$ . In order to meet pile-up constraints, the ideal spill instantaneous intensity should be in the range of  $\sim 1.0 \times 10^{12} \text{ PoT}/\text{s}$ . To collect  $10^4 \nu_e$  CC interactions at the neutrino detector, roughly  $2 - 3 \times 10^{18} \text{ PoT}$  per year over five to seven years are required, with the yearly intensity never exceeding 30 % of the maximum PoT per year that could be available for TCC2 during SHiP/NA67 operation [124].

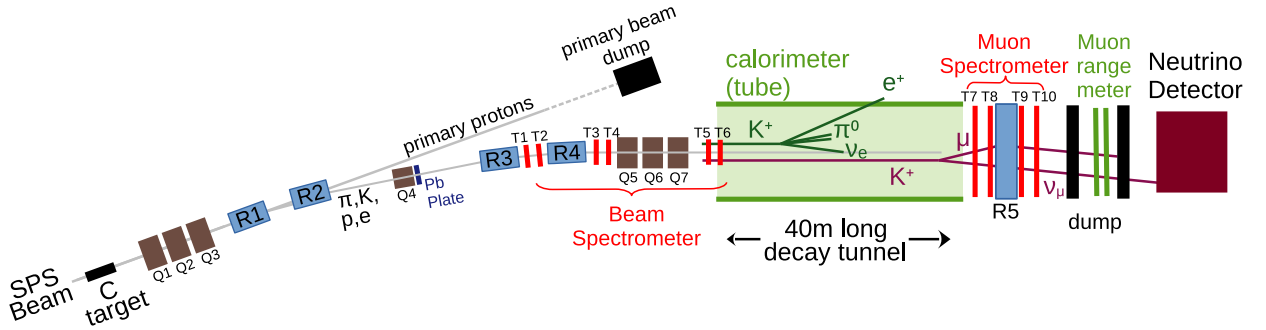


Figure 5: Conceptual layout of the SBN beamline [157]. The secondary mesons produced in a target by the slow-extracted SPS protons are focused with quadrupoles (in brown) and selected in the 8.5 GeV/c momentum range by a set of dipoles (in blue) before entering the decay tunnel. The secondary beamline, decay tunnel and downstream region are instrumented with calorimeters (in green) and trackers (in red) to monitor the neutrino fluxes and tag individual neutrinos.

The studies conducted so far indicate that the considered beam line can be integrated neither in EHN1 nor EHN2 due to radiation-protection considerations as well as geometric (survey) reasons. Hence, an installation in the NA would require the excavation of a new underground infrastructure and extensive Research and Development (R&D) on the feasibility of the beam delivery. A new experimental area close to TCC6 (where the HiRadMat facility is installed) could also be considered, given that infrastructure already exists there (like the side tunnel TT61, that is currently empty and not used). This could partly use existing transfer lines and therefore reduce the implementation costs. In this case the extraction system should allow simultaneous slow-extraction to the new experimental area and to the NA, similarly to what was done to serve simultaneously the SPS NA and West Area (WA) until the beginning of the 2000's. Such a system would now have to be compatible with the LHC extraction. A conceptual slow extraction scheme has been proposed [159] and more studies would be required to demonstrate its feasibility. The installation of a new slow extraction system cannot occur before LS4 as it would require significant modifications of the SPS. Significant civil engineering for the construction of the new experimental area would also be necessary.

### 3.3.2 GAMMA FACTORY

The key GF idea [160, 161, 162] is to produce, accelerate, and store highly relativistic atomic (Partially Stripped Ions (PSI)) beams in the LHC rings and to resonantly excite their atomic degrees of freedom by laser photons to: (1) cool and study highly-charged ions, and (2) produce high-energy, polarised photon beams with intensities reaching  $10^{17}$  photons/s. Emitted photons in the energy range from 40 keV to 400 MeV with the above-mentioned intensities can be achieved at the LHC with laser photon energies varying from 0.7 eV to 12 eV and Fabry-Perot-cavity-stored photon pulses with an average power of up to 200 kW. The above performance might require a significant upgrade of the LHC RF system, depending on the specific implementation.

Emitted photons in the above energy range can be used as a source of unprecedented-intensity secondary beams of polarised electrons and positrons [ $\approx 10^{17} e^+(e^-)/s$ ] [163], polarised muons [ $\approx 10^{14} \mu^+(\mu^-)/s$ ] [163], quasi-monochromatic neutrons ( $\approx 10^{16} n/s$ ) [164], and radioactive ions

( $\approx 10^{13}$  r.i./s) [165].

Dedicated simulation tools [166, 167, 168] have been developed to conduct detailed feasibility studies [169, 170, 171].

The technical feasibility of the GF photon beam generation and the PSI laser beam cooling schemes are being investigated and a Gamma Factory SPS Proof of Principle (GF SPS PoP) experiment has been proposed [172] for installation in the SPS tunnel starting from LS3. Essential milestones towards the GF SPS PoP have already been achieved since the last EPPSU:

1. demonstration of efficient production, storage and operation of the PSI beams in the SPS and LHC [173, 174, 175, 176, 177], including the assessment of the stability and measurement precision in beam position and momentum in the SPS area where laser pulses would interact with atomic beam bunches [178];
2. design [179] and experimental demonstration of the stable storage of more than 200 kW of average power in a Fabry-Perot resonator, in fact up to 700 kW was achieved at the Laboratory of the Physics of the two Infinities Irène Joliot-Curie (IJCLab) [179, 180, 181, 182].

The successful implementation of the GF requires the validation of the following additional elements:

- stable laser transport and injection of the laser beam into the long Fabry-Perot cavity with fully remote controls and diagnostics. The beam stability is comparable to that of the interferometric systems of the Laser Interferometer Gravitational-Wave Observatory (LIGO);
- fully remote and continuous operation of the laser source system in a high intensity hadron accelerator tunnel;
- operational tools to guarantee the requisite control of the PSI beam momentum and its spread, and the spatial and temporal overlap of the ion and laser beams in a reproducible fashion;
- agreement between simulations and measurements of atomic excitation and ion beam cooling rates;
- atomic and photon beams diagnostic methods to measure and characterise the photon flux from the spontaneous emissions allowing to unfold the photon spectrum and angular distribution.

The modelling of the radiation environment at the GF SPS PoP experiment site has been performed [183] and measurements are ongoing to validate them. Procurement of an ultra low-phase noise laser and amplification chain is being finalised. The final design of the controls, diagnostics of the laser beam transport system and optical cavity are in progress, with dedicated studies on stabilisation reported in [184].

Scientific opportunities opened by the GF across the fields of science are briefly discussed in Section 4.8.

### 3.3.3 AWAKE AND FUTURE PROTON-DRIVEN PLASMA WAKEFIELD ACCELERATORS

AWAKE, is a proton-driven plasma wakefield acceleration experiment, using self-modulation of a long bunch of 400 GeV protons in plasma to resonantly excite high amplitude wakefields and accelerate externally injected electrons to high energies [ $\mathcal{O}(\text{GeV})$ ]. Building on its successful Proof of Concept (PoC) results [185, 186, 187, 188] during its first run period (2016 – 2018), the AWAKE

collaboration has developed a well-defined program for Run 2 [189], which started in 2021 and will last until LS4.

The experimental layout for Run 2 incorporates several key changes from Run 1, particularly the introduction of two distinct plasma sources. The first plasma source serves as the “self-modulator”, where the proton bunch undergoes seeded self-modulation, which was successfully demonstrated [190]. Introducing a density step in the plasma source maintains high-amplitude wakefields [191]. Recent measurements are very promising, showing a clear effect, e.g., higher achieved accelerated electron energies.

The second plasma source is the “accelerator” source, where electrons are injected and accelerated, while controlling the beam quality. With this layout, which will be ready after LS3, AWAKE Run 2 aims to achieve the next milestone: the acceleration of electrons in the range of 4 to 10 GeV in 10 m of plasma, a low electron energy spread (5–8 %) with an accelerated bunch charge of approximately 100 pC and a normalized emittance of 2–30 mm mrad. To meet these goals, beam loading is required to flatten the wakefield and to control the emittance growth. This necessitates the use of a new electron beam system featuring a RF photo-injector, two X-band accelerating structures and a new beamline. A prototype of the new electron source has already been installed and successfully commissioned at CERN’s CLIC Test Facility 2 (CTF2) facility, validating the new design.

An additional milestone is the demonstration of the scalability of the acceleration process. In the last phase of Run 2, i.e., before LS4, it is planned to replace the second plasma source with a new plasma technology (discharge or helicon plasma source) scalable to lengths of tens to hundreds of meters, which will be crucial for achieving high-energy electron beams. A 10 m-long prototype of a discharge plasma source was successfully commissioned and operated in AWAKE in 2023.

To accommodate the necessary space for the installation of the second plasma source and the associated electron injection system for achieving the acceleration and scalability milestones, the AWAKE facility will undergo major modifications, with works starting in 2025. This includes dismantling the CERN Neutrino beam to Gran Sasso (CNGS) target area, which currently occupies a 100 m-long tunnel section downstream of the AWAKE experimental facility.

Once the goals of Run 2 will be demonstrated, the AWAKE acceleration scheme could be used in first particle physics applications, including the production of electron beams with energies between 40 and 200 GeV for fixed-target experiments (see Section 4.8.3).

### 3.3.4 FUTURE COLLIDERS AND THEIR INJECTORS

#### Future electron-positron Circular Collider (FCC-ee)

The FCC-ee will require a dedicated injector complex for delivering positron and electron beams to the booster for the top-up operation of the collider [192]. The presently studied injector complex, as shown in Figure 6, consists of a low energy electron linac, a positron linac and a damping ring at 2.86 GeV. For positron production, the electron beam from the low energy linac is sent on a positron target, and the positron linac accelerates the beam to the damping ring injection energy 2.86 GeV. A high energy linac accelerates either positrons or electrons to the final energy of 20 GeV. This injector complex will be placed on the CERN Prévessin site, with the beam exiting the high energy linac close to the NA, which could provide additional science opportunities beyond collider physics.

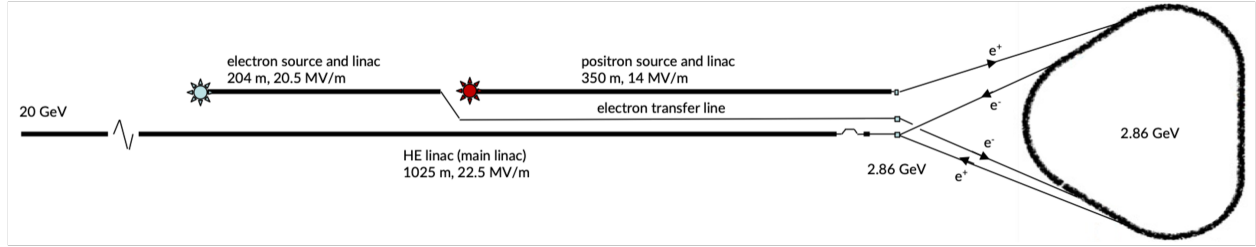


Figure 6: Schematic representation of the proposed FCC-ee injector complex [193].

The FCC-ee injector complex will provide pulses of 4 bunches with a bunch spacing of 25 ns, with  $2.5 \times 10^{10}$  particles per bunch (ppb) (corresponding to 4 nC). A summary of relevant beam parameters is given in Table 6. It is important to note that the duty cycle of the injector complex required for providing beam to the booster in top-up mode varies significantly depending on the operation mode of the collider. The injector complex will be used with a duty cycle of 73 % for the  $Z$ -pole, 40 % in  $WW$ , 19 % for  $ZH$  and 5 % for  $t\bar{t}$ .

	FCC-ee	PBC users
Beam energy [GeV]	20	$\leq 20$
Max. bunch charge [nC]	4	4
Max. bunch population	0.1–2.5	2.5
Bunches per pulse	2–4	1–4
Linac repetition rate [Hz]	50–100	100
Normalized emittance $x/y$ [mm mrad]	$\leq 20/2$	$\leq 20/2$
Physical emittance $x/y$ [nm rad]	$\leq 0.5/0.05$	$\leq 0.5/0.05$
Bunch length rms [mm]	4	1–4
Energy spread [%]	0.1	0.1–0.75
Bunch spacing [ns]	25	25 or 50
Pre-injector duty cycle [%]	5–73	27–95

Table 6: Beam parameters of the FCC-ee injector complex [193].

Science opportunities offered by the FCC-ee injectors have been discussed in a workshop [194] and are summarized in [193], those related to PBC are outlined in Section 4.8.

The positron beams of the FCC-ee booster could be exploited for DM searches. These experiments typically require an almost continuous beam with low instantaneous rate [ $\mathcal{O}(1\text{ ns}^{-1})$ ]. First considerations of producing such beams in between top-up injections of the booster to the collider have been presented in [195]. The most promising options are to perform a slow extraction directly from the damping ring at 2.86 GeV, which would result in about  $1 \times 10^{13}$  positrons on target per day with a bunch spacing of 2.5 ns when considering a duty cycle of 70 %. Alternatively, a slow extraction at 20 GeV from the booster, could deliver  $2.7 \times 10^{13}$  positrons on target per day with 1.25 ns bunch spacing assuming a 40 % booster duty cycle (available during  $H$  and  $t\bar{t}$ , while only 20 % booster duty cycle would be available during  $WW$ ).

## Linear Collider (LC)

A future Linear Collider (LC) at CERN could host a number of additional detectors, including detectors for FT experiments and BD experiments making use of the high energy main linac beams or the lower energy injector beams. A LC provides very high energy, high intensity, low emittance electron and positron beams. The single pass nature of the LC allows us to use the beams even destructively as long as the influence to the collider experiments is not significant. PBC opportunities at an LC are outlined in detail in Ref. [196].

The main purpose of these experiments will be to search for DS particles interacting only feebly with the SM particles. The intense and high-energy electron and positron beams that the LC makes available also have uses in nuclear and hadron physics and in studies of strong-field Quantum Electro-Dynamics (QED).

The most appropriate locations for using the beams are the beam dumps. There, very high intensity electron and positron beams interact with thick targets, producing large numbers of highly penetrating particles. There are several beam dumps distributed over a LC facility. Also the injector linacs and damping rings provide opportunities for lower energy beams. In the case of CLIC the very high intensity drive beam surface installation provides another beam available for physics or equipment R&D.

A significant numbers of concrete studies have been made for the International Linear Collider (ILC) as documented in [197]. These studies also indicate a not exhaustive list of possible locations for experimental facilities as shown in Figure 7. The possibilities offered by injectors and damping rings are not fully shown. For CLIC or other LC options similar possibilities exist for providing electron and positron beams at varying energy and intensity.

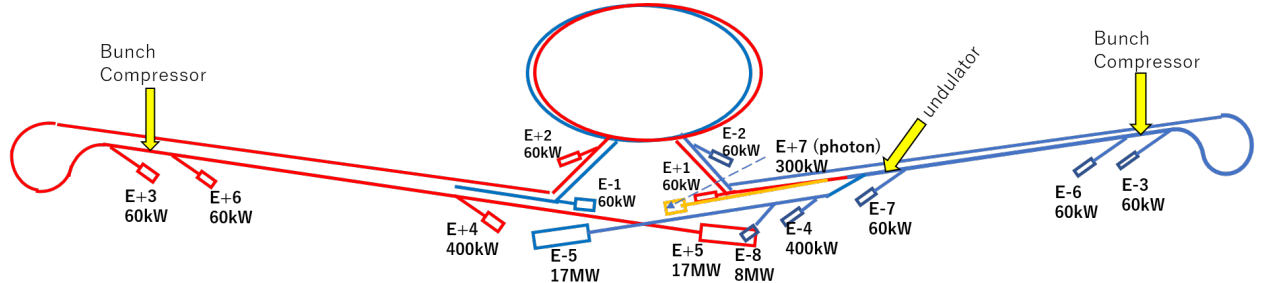


Figure 7: Distribution of beam dumps over the ILC facility labeled E1-E8 [197]. The electron, positron and photon beamlines are colored blue, red and yellow, respectively. Similar possibilities exists for other LC implementation providing a wide range of energies from injectors to full beam energies, using the opportunities offered by a single pass accelerators to provide beams according to proprieties and needs for collider and FT experiments operating at the same time.

## 4 PBC proposed experiments and future opportunities at CERN and beyond

PBC has been and is currently supporting the development and feasibility study of a wide range of experimental proposals for submission to the relevant scientific committees. Below, experiments

previously supported and now being followed-up by these committees, are briefly described as well as the opportunities that are currently being scrutinized and studied to support a diverse particle physics programme at CERN and elsewhere.

## 4.1 SPS North Area

### 4.1.1 NA61/SHINE-LE

NA61/SHINE plans to conduct studies of hadron production on nuclear targets using a new very-low-energy (LE) tertiary branch of the H2 beam. These measurements will include both proton- and meson-incident interactions on nitrogen as well as solid materials in order to improve predictions for the flux of neutrinos from atmospheric sources, accelerator beams, and spallation sources.

Among the highlights of the NA61/SHINE-LE program [198, 199] are:

- A comprehensive study of proton-nitrogen interactions at energies below 20 GeV. These will be used to improve models of atmospheric neutrinos, potentially resulting in improvements to the neutrino flux errors of more than a factor of two.
- Measurements of meson production and rescattering from low-energy interactions on aluminium, water, and iron. These will reduce the current large uncertainties on wrong-sign neutrinos (especially  $\nu_e$  and  $\bar{\nu}_e$ ) that result from interactions outside the target at long-baseline beams and are especially significant backgrounds in precise studies of Charge Parity (CP) symmetry. These measurements will be geared to the specific needs of the Hyper-K and DUNE experiments.
- A study of 8 GeV  $p + Be$  interactions geared toward reducing the flux uncertainty of Fermilab's Booster Neutrino Beam from 7–40% down to 5–6% across the entire energy spectrum. This will translate directly into improved  $\nu + Ar$  cross-section measurements.

The NA61/SHINE-LE beam project has been supported by the leadership of eleven neutrino and muon physics collaborations in a November 2024 letter to CERN's management. From the CERN side, a technical study was prepared in the framework of PBC-CBWG [200]. The study is currently on hold waiting for the official approval by the relevant CERN committees (SPSC, CERN RB). The new beam will be installed parallel to the existing one, which will remain available for NA61/SHINE and downstream users. A CAD drawing of this proposed tertiary branch is shown in Figure 8.

### 4.1.2 NA61/SHINE WITH IONS

The immediate physics goals of the NA61/SHINE include: (i) measurements of oxygen-oxygen collisions at  $\sqrt{s_{NN}} = 5.1, 7.6$  and  $16.8$  GeV, by the end of Run 3 and the beginning of Run 4, to elucidate the diagram of high-energy nuclear collisions [201, 104] and for a precision study of violation of isospin symmetry [4]; (ii) construction and installation of a new Large Acceptance Silicon Tracker (LAST) during LS3; (iii) a new series of measurements of charm and anti-charm hadron correlations in  $Pb+Pb$  collisions. This would be accompanied by extensive measurements of Event-by-Event (EbyE) fluctuations in  $Pb+Pb$  collisions as a function of energy and by new data-taking of  $B+B$  and/or  $Mg+Mg$  collisions [104]. The realization of oxygen data-taking does not necessitate any additions to the fully operational NA61/SHINE experiment. Implementing the

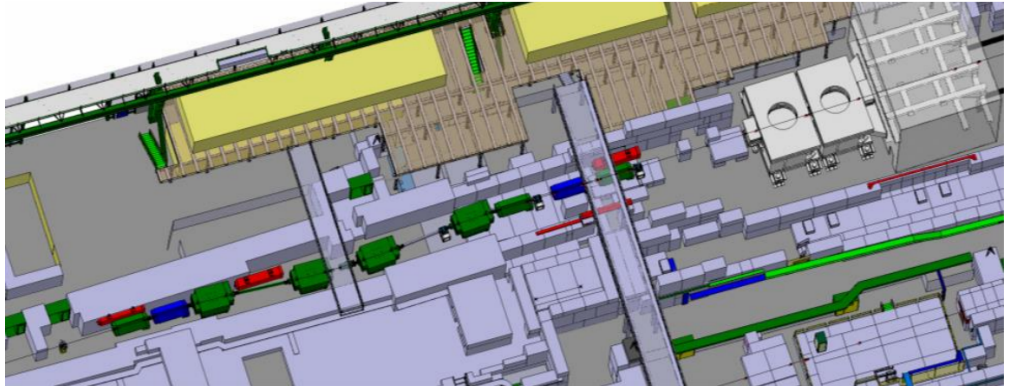


Figure 8: The proposed low-energy branch for NA61/SHINE. The new magnets for the low-energy particles appear in green, while a rail system would allow the changeover between this low-energy and the normal high-energy configuration. More details on the proposed implementation can be found in [200].

LAST for charm and anti-charm hadron correlation studies constitutes a major upgrade of the detector to be completed at the end of LS3. These measurements will be fully complementary to the operation of the considered DICE/NA60+ experiment during Run 4. Studies of EbyE fluctuations are meant as an independent verification of recent observations made at the Relativistic Heavy-Ion Collider (RHIC), argued as a possible indication of a Critical Point in the phase diagram of strongly interacting matter.

The proposed large-acceptance measurements are not possible in the foreseeable future at accelerator facilities other than the SPS.

#### 4.1.3 NA64 ( $-e, -\mu, -h$ ) – PHASE 2

The great advantage of the NA64 approach compared e.g. to the BD approach is that the signal rate in NA64 scales as  $(coupling)^2$ , while for the latter one it is  $(coupling)^4$ . Thus, much less beam particles on target are required for the same sensitivity. In order to use this feature effectively in the future a setup upgrade during LS3 is required which will allow NA64 to enter an exciting new phase, leveraging higher particle rates to search for light sub-GeV dark matter by running in background-free mode. After completing the corresponding R&D phase, the upgrades for the electron/positron and muon programs will primarily focus on (i) improving the hermeticity of the detector by installing a new veto hadron calorimeter system; (ii) enhancing Particle Identification (PID) capabilities with a new synchrotron radiation detector; and (iii) increasing the beam rate through upgraded read-out electronics. The best location for running in hadron mode is still under study, including the possibility to use the PS T9 beamline. The target for true muonium production at H4 is being optimized [202]. With the projected  $\approx 10^{13}$  electrons,  $\approx 10^{11}$  positrons (at 40 and 60 GeV) and  $\approx 2 \times 10^{13}$  muons accumulated on target, the next stage of the experiment has the potential to probe entirely new regions of canonical LDM models involving kinetic mixing, offering the possibility to decisively discover, or conclusively disprove, several well motivated models by the end of Run 4.

#### 4.1.4 NA66/AMBER – PHASE 2

Phase 2 of the NA66/AMBER experiment is planned to start in 2031 and will focus on world-wide unique measurements of the internal structure and the excitation spectrum of kaons and other hadrons.

In the last 20 years, considerable progress has been made in our understanding of the excitation spectrum of light hadrons containing up and down quarks as well as heavy hadrons containing charm and bottom quarks. States beyond the ordinary quark model picture have been firmly established in both the light-quark and heavy-quark sectors. In stark contrast to this, the strange-quark sector has seen very little progress. Most of the experimental data on strange mesons are based on experiments that were performed more than 30 years ago. Only four additional kaon states were included in the Particle Data Group (PDG) listings since 1990. Many claimed states still need confirmation. In order to progress in our understanding of the internal structure of hadrons, it is extremely important to bridge the gap between the light up-/down-quark and the heavy-quark hadrons. Using a high-intensity kaon beam, NA66/AMBER will perform unprecedented measurements of the full kaon spectrum up to masses of about  $3\text{ GeV}/c^2$ . The goal is to collect at least  $2 \times 10^7$  exclusive events for the  $K^-\pi^-\pi^+$  final state with kaon beam. This will allow for precision measurements of strange mesons and the identification of possible strange exotic states, e.g., multi-quark states or states with gluonic excitations. In addition, the new data will have impact on other fields, e.g., CP-violation studies in multi-body heavy-meson decays at  $B$  factories, where excited strange mesons appear as intermediate states.

Understanding the emergence of hadron sizes is a crucial measurement in hadron physics and beyond. These radius measurement can be performed in inverse kinematics, i.e., scattering of a hadron off an electron in the target material. NA66/AMBER – Phase 2 aims at determining the kaon charge radius with a factor 10 better precision than currently known. Since pions are predominant in the secondary hadron beam delivered to the experiment, the measurement on the pion can be done in parallel with high statistics. At the same time, this opens the opportunity for a first determination of the radius of an anti-nucleus, namely the antiproton.

The internal structure of pions and kaons is of great theoretical interest due to their dual roles as Goldstone bosons and quark-antiquark bound states [203]. Nowadays, the experimentally available information on the partonic structure of the kaon is extremely limited. It consists of the  $K^-$ -induced DY data by the NA3 experiment based on  $\sim 700$  events [204]. The analysis based on these data revealed evidence of the softer behavior of the valence  $\bar{u}$  quark distribution of  $K^-$  in comparison to the one in  $\pi^-$ . This difference was attributed to the breaking of the flavor SU(3) symmetry, resulting in a larger fraction of the kaon's momentum being carried by the  $s$  quark than the lighter  $\bar{u}$  quark [203, 205], which has triggered intense theoretical investigations of the quark and gluon content of kaons. To study the quark and gluon component of the kaon, a measurement of the prompt photon production with a composite hadron beam at NA66/AMBER is proposed. A system of three electromagnetic calorimeters is able to cover the kinematic region  $-0.5 < x_F < 0.7$  and  $p_T > 3\text{ GeV}/c$ . The  $K^+$ -induced prompt-photon production via gluon Compton scattering at negative  $x_F$  provides information about the gluon content of kaons while the cross-section difference for negative and positive kaons is proportional to the valence  $\bar{u}$ -quark contribution.

All three above-mentioned physics programs require the availability of positive and negative hadron beams with medium and high intensity of up to  $10^9$  hadrons per spill delivered to the NA66/AMBER spectrometer in EHN2. The hadron beam at the M2 beamline has a natural mix of

protons, kaons, and pions requiring efficient and reliable beam particle identification. To allow for the delivery of the high-intensity kaon beams and maximum tagging efficiency, upgrades on the beamline and spectrometer shielding as well as improvements on the beamline vacuum are needed. The full physics program of NA66/AMBER – Phase 2 is expected to cover running also post-LS4.

#### 4.1.5 SHiP/NA67 in ECN3

SHiP/NA67 will be installed in ECN3 and will operate with  $4 \times 10^{19}$  PoT/year colliding with a thick, high-density target. The target is followed by background-reducing systems – a hadron absorber and a muon deflector (or muon shield) – and two SHiP/NA67 detectors. The first one is the Scattering and Neutrino Detector (SND). It is designed to detect neutrino interactions and scattering events of hypothetical LDM particles produced in proton-target collisions. The second detector is the Hidden Sector Decay Spectrometer (HSDS), aimed at searching for decays of FIPs. It is made of a 50 m-long decay volume, a magnetic spectrometer based on straw technology, and an electromagnetic calorimeter that also serves as a particle identification system. The hadron absorber, the muon shield, veto systems surrounding the HSDS, and the precise straw tracker allow for the reduction of the backgrounds in the HSDS down to a negligible level.

The validity of the predictions of the SHiP/NA67 simulation framework on the particle fluxes has been verified by comparing [206] them to the data from the CERN HAmberg Rome Moscow Experiment (CHARM Experiment) [207] and a dedicated experiment performed in 2018 with a replica of the BDF/SHiP/NA67 target [208]. With a total of  $6 \times 10^{20}$  PoT, generating large amounts of heavy hadrons such as  $D$  and  $B$  mesons, and thanks to efficient background reduction techniques, SHiP/NA67 has a rich physics case that covers neutrino physics and will explore previously inaccessible regions of the FIPs parameter space in the GeV mass range, complementing ongoing searches at the LHC and future searches at FCC-ee, which mainly focus on the energy frontier and precision physics.

Neutrino physics is explored with the SND. It comprises measurements of neutrino DIS cross section in the range 5–100 GeV; the structure functions  $F_4, F_5$  parametrizing the differential cross section; tests of the LFU; precision measurements of the Cabibbo Kobayashi Maskawa (CKM) matrix elements, and neutrino-induced charm production. It especially benefits from the large flux of  $\tau$  neutrinos and antineutrinos.

The new physics case may be generically split into exploring scattering signatures, to be studied by SND, and decay signatures, to be searched for at the HSDS detector. The scattering case covers models of LDM, both elastic and inelastic [209], as well as millicharged particles [210]. The decay signatures cover various portal models adding unstable particles [60], including (but not restricted to) Heavy Neutral Leptons (HNLs), dark photons and other vector mediators, Higgs-like scalars, and ALPs [67, 211, 212].

Depending on the new physics model, SHiP/NA67 may explore the parameter space orders of magnitude larger than the currently excluded couplings in the mass range up to  $\mathcal{O}(10 \text{ GeV})$ , being complementary to the main program of ATLAS, CMS, and LHCb experiments. Moreover, the detector will allow for careful reconstruction of the events' kinematics and identification of the particles' type, which makes it possible not only to push the domain of excluded couplings but also to obtain important insights in the case of discovery. For example, in case of a discovery of Long-Lived Particles (LLPs), SHiP/NA67 will be able to check if they are consistent with the resolution of BSM problems [213, 214].

#### 4.1.6 MUONE

The MUonE project [215, 216] aims to shed light on the potential discrepancy between the theory prediction of the muon's anomalous magnetic moment and its measurement results. Specifically, MUonE plans to measure the terms related to the Hadronic Vacuum Polarisation (HVP), which are one of the limiting factors in the precise calculation of the anomalous magnetic moment, by measuring the hadronic contribution to the running of the electromagnetic coupling constant  $\alpha$  in elastic high-energy muon-electron scattering. It is thus entirely complementary to experimental efforts using  $e^+e^-$  annihilation into hadrons, including independent systematic uncertainties.

In 2025, MUonE will perform a test run with a complete scaled-down setup of the final detector with a possible sensitivity to the hadronic corrections to the running of  $\alpha$  [217]. The 160 GeV/c M2 muon beam, with its present performance and parameters, is adequate for this first measurement. The apparatus will consist of three silicon-based tracking stations (the final experiment will have 40 of them), the calorimeter of 25 PbWO<sub>4</sub> crystals in use now, and a muon identification downstream the calorimeter. An upgrade of the present hardware of the Beam Momentum Spectrometer (BMS), which measures the incoming muon energy, is in preparation to improve the accuracy of this muon momentum determination.

Discussions are ongoing within the collaboration about the possibility and the opportunity to run in 2026. The possibility to operate at different beam momenta (e.g., 60 GeV/c and 200 GeV/c) to improve the control of the systematic uncertainties is being investigated.

If the final proposal will be approved, the experiment will run after LS3, with the ultimate goal of achieving a 0.3 % statistical accuracy on the leading-order hadronic vacuum polarization contribution  $a_\mu^{\text{HLO}}$  to the muon's anomalous magnetic moment. For that purpose, the collaboration is considering two possible upgrades:

- increase the beam intensity by at least a factor of two, up to about  $(4 - 5) \times 10^8 \mu/\text{spill}$ ;
- thermalise the beam tunnel ( $\pm 2^\circ\text{C}$  or better), for a length of 50 m and an estimated volume of 800 m<sup>3</sup>.

#### 4.1.7 DICE/NA60+

The SPS can provide intense beams ( $\approx 10^7/\text{spill}$ ) of ions at *c.m.* energies  $6 \text{ GeV} < \sqrt{s_{\text{NN}}} < 17 \text{ GeV}$ . It represents the ideal location for an experiment aiming at the measurement of rare probes of the QGP, and in particular of heavy quarks and thermal lepton pairs. Such measurements allow an investigation of the order of the phase transition to the QGP, restoration of the QCD chiral symmetry and modification of the hadron spectrum in its vicinity. Studies of various QGP properties, such as its diffusion coefficients and the modification of the QCD binding force from large to small distances can also be carried out. None of these studies were performed until now below top SPS energy with a decent integrated luminosity, nor will they become possible in the foreseeable future at any other facility in the collision energy range under discussion. On the contrary, this research domain is complementary to that already explored at hadron colliders (RHIC, LHC), in particular for heavy-quark measurements, and to that expected from lower-energy facilities [Facility for Antiproton and Ion Research (FAIR)], in particular for dilepton-related observables. The use of a heavy-nucleus beam (Pb) is mandatory for these measurements, to ensure the largest size and lifetime of the QGP droplet that will possibly be formed.

The DICE/NA60+ project proposes a setup that includes a muon spectrometer coupled to a vertex spectrometer to perform the measurements sketched above [105]. The need for a high-interaction rate ( $10^5 \text{ s}^{-1}$ ) poses significant challenges on (i) the availability of focused high-intensity Pb beams down to low SPS energy, and of proton beams at the same energies, which represent a needed reference; (ii) use of state-of-the-art large area Monolithic Active Pixel Sensors (MAPS) that can be operated in the large charged-hadron multiplicity of Pb–Pb collisions, reaching hundreds of particles. In addition, an essential requisite for the realization of the experiment are two large-volume dipole magnets needed for the two spectrometers. Both magnets are available at CERN.

After submission of an EoI in 2019 [218] and the discussion of an LoI in February 2023 [105], the collaboration aims to submit a proposal to the SPSC by mid-2025. According to this proposal, data-taking is expected to start in 2029/2030 and to last approximately seven years, with a run with a Pb beam at a different energy each year and periods with proton beams, exploring at least three different energies and with an equivalent integrated luminosity per nucleon-nucleon collision. The technology challenges are mainly related to the project of the MAPS for the vertex detector, with corresponding R&D being carried out in synergy with the ALICE Inner Tracking System 3 (ITS3) project [219], which has the same timeline. For the muon spectrometer, Multi-Wire Proportional Chamber (MWPC) detectors will be used, covering a total surface of about  $60\text{--}70 \text{ m}^2$ . The collaboration is in the process of strengthening its manpower to ensure that all the items are duly covered. In particular, discussions to extend the participation of groups from the US are currently in progress.

## 4.2 HL-LHC – Physics in the forward direction (neutrinos and FIPs)

### 4.2.1 FORWARD PHYSICS FACILITY

The Forward Physics Facility (FPF) is a proposal to build a new underground cavern at CERN to house a suite of far forward experiments during the HL-LHC era [220, 221, 222, 223]. These experiments will cover the blind spots of the existing LHC detectors and will maximise the physics potential in the very forward region of the LHC collisions. The physics program of the FPF covers searches for BSM particles, neutrino physics, and QCD with important implications for astro-particle physics. The FPF can discover a wide variety of new particles that cannot be discovered at fixed target facilities or other LHC experiments. In the event of a discovery, the FPF, with other experiments, will play an essential role in determining the precise nature of the new physics and its possible connection to the dark universe. In addition, the FPF is the only facility that will be able to detect millions of neutrinos with TeV energies, enabling precision probes of neutrino properties for all three flavors. These neutrinos will also sharpen our understanding of proton and nuclear structure, enhancing the power of new particle searches at ATLAS and CMS, and enabling IceCube Neutrino Observatory (IceCube), Pierre Auger Observatory (Auger), Cubic Kilometre Neutrino Telescope (KM3NeT) and other astro-particle experiments to make the most of the new era of multi-messenger astronomy.

An extensive site selection study has been conducted and the resulting site is shown in Figure 9. The facility dimensions have been optimized following integration studies to demonstrate that it can house the proposed detectors and the main technical infrastructure [224]. The FPF location is shielded from the ATLAS IP by over 200 m of rock, providing an ideal location to search for rare processes and very weakly interacting particles. Vibration [225], radiation [226], and safety

studies [226] have shown that the FPF can be constructed independently of the LHC without interfering with its operation. A core sample, taken along the location of the 88 m-deep shaft to provide information about the geological conditions, has confirmed that the site is suitable for construction [224]. RP studies [226] have concluded that the facility can be safely accessed with appropriate controls during beam operations.

The FPF is uniquely suited to explore physics in the forward region because it will house a diverse set of experiments based on different detector technologies and optimized for particular physics goals. The proposed experiments are shown in Figure 9 and include:

- Forward Search Experiment 2 (FASER2), a magnetic tracking spectrometer, designed to search for light and weakly-interacting states, including new force carriers, sterile neutrinos, ALPs, and dark sector particles, and to distinguish  $\nu$  and  $\bar{\nu}$  charged current scattering in the upstream detectors.
- FASER Neutrino Detector 2 (FASER $\nu$ 2), an on-axis emulsion detector, with pseudorapidity range  $\eta > 8.4$ , that will detect  $\approx 10^6$  neutrinos at TeV energies with unparalleled spatial resolution, including several thousands of tau neutrinos, among the least well-studied of all the known particles.
- Forward Liquid Argon Experiment (FLArE), a 10-ton-scale, noble liquid, fine-grained time projection chamber that will detect neutrinos and search for LDM with high kinematic resolution, wide dynamic range and good particle-identification capabilities.
- FORward MicrOcharge SeArch detector (FORMOSA), a detector composed of scintillating bars, with world-leading sensitivity to millicharged particles across a large range of masses [227].

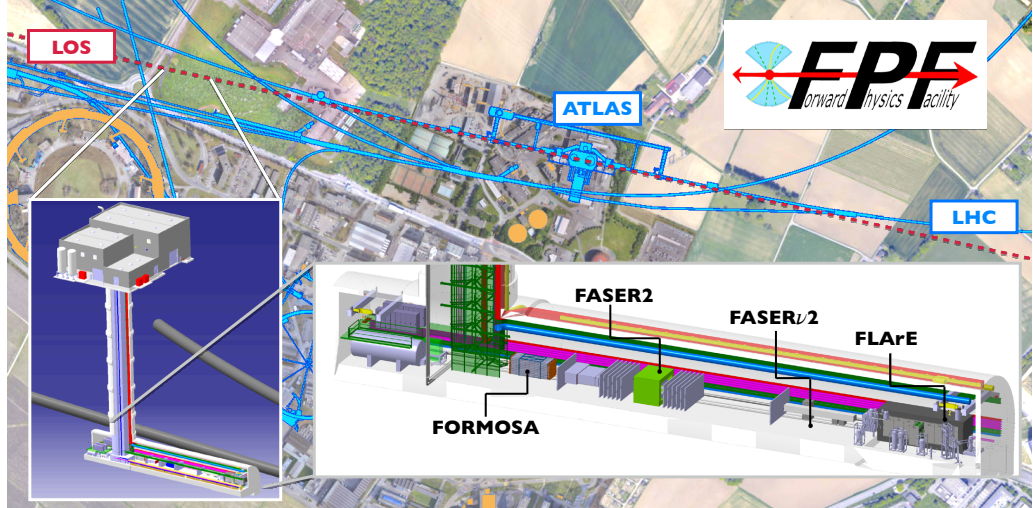


Figure 9: The FPF is located 627 to 702 m west of the ATLAS IP along the line of sight. The FPF cavern, 75 m long and 12 m wide, will house a diverse set of experiments to fully explore the forward region. (Figure taken from [223].)

Three of the four proposed detectors have existing pathfinder experiments running at the LHC [FASER, FASER $\nu$  and the MilliQan Experiment (MilliQan) [228] — see Section 2.1.6], and have

released world-leading results, already demonstrating the ability to carry out searches and measurements in the forward region of the LHC.

All of the planned experiments are relatively small, low cost, require limited R&D, and can be constructed in a timely way. A Class 4 cost estimate for the Facility by the CERN engineering and technical teams is 35 MCHF for the construction of the new shaft and cavern [223] and 10 MCHF for the technical infrastructure. An estimate of the core costs for the full suite of experiments (without labour) is around 40 MCHF [223]. The FPF requires no modifications to the LHC and will support a sustainable experimental program, without additional power consumption for the beam beyond the existing LHC program.

To fully exploit the forward physics opportunities, the FPF and its experiments should be ready for physics as early as possible in Run 4. A possible timeline is for the FPF cavern to be built during LS3, the support services and experiments to be installed starting in 2030, and the experiments to begin taking data during Run 4. All of the experiments will be supported by international collaborations, and they will attract a large and diverse global community. The FPF is a mid-scale project composed of smaller experiments that can be realized on short and flexible timescales, which are well aligned with the Advancing Science and Technology using Agile Experiments (ASTAE) programme recommended from the US Particle Physics Project Prioritization Panel (P5) report [229]. In addition, it will provide a multitude of scientific and leadership opportunities for junior researchers, who can make important contributions from construction to data analysis in a single graduate student lifetime.

#### 4.2.2 SCATTERING AND NEUTRINO DETECTOR AT THE HL-LHC (SND@HL-LHC)

First results [56, 58] provide a clear picture of the signal and background environment for further exploitation of the neutrino physics potential at the LHC. The physics program in Run 3 will be statistically limited in most channels. The exploitation of the potential of the HL-LHC with some key improvements will largely extend the physics reach of the experiment both in neutrino physics and in BSM searches.

The SND@LHC detector upgrade for the HL-LHC is expected to observe over  $10^4$  neutrino interactions. This high statistics will allow for reducing the uncertainties in all of the main physics measurements using neutrinos: forward charm production, lepton flavour universality tests, and high energy neutrino interactions. The experiment is expected to observe a few hundred tau neutrino interactions and will possibly observe tau antineutrino interactions for the first time [230].

The experiment's relatively large cross-sectional area of 40 by 40 cm<sup>2</sup> allows for a wide coverage in pseudo-rapidity ( $6.9 < \eta < 7.7$ ), which is complementary to all other HL-LHC experiments, including FASER. This wide  $\eta$  coverage enhances the fraction of neutrinos originating in charm decays and allows for measurements differential in  $\eta$  which are sensitive to the gluon PDF in unexplored low- $x$  regions. In addition to the different  $\eta$  coverage compared to FASER, the experiments also differ significantly in their implementation, with the SND@HL-LHC design including precise instrumentation of the neutrino target and of the hadronic calorimeter and muon spectrometer [230]. This design, which also foresees high precision timing layers, provides the unique opportunity to correlate neutrino-like events with ATLAS data via a dedicated trigger.

The detector will be located in the same TI18 tunnel where the SND@LHC experiment currently operates. The experiment will use silicon strip detector modules inherited from the CMS outer barrel tracker and is divided into two sections. The upstream section includes tungsten as

the neutrino interaction target, and denser instrumentation. The downstream section includes magnetized iron as an absorber and has sparser instrumentation. The latter section of the experiment acts as a hadronic calorimeter and muon spectrometer. Fast detector planes using either plastic scintillator or resistive-plate chamber technology will be used to trigger the read out.

The large yield of neutrino events offers a unique opportunity to identify sub-samples of neutrino events in coincidence with charm hadrons detected in ATLAS. While the charm hadron that decays into the neutrino detected in SND@HL-LHC is always outside of the ATLAS detector acceptance, in about 11% of these events the charm hadron produced in association with the neutrino parent is emitted within the acceptance of ATLAS, and therefore it can, potentially, be detected.

A detailed design exists for the components of the detector and their integration. A prototype of a silicon strip layer has been assembled with CMS spare components, and timing detector components have been exposed to a hadron test-beam in 2024. Significant synergy exists in detector R&D for the SHiP/NA67 experiment, which has a highly complementary physics case.

It is worth noting that a modest civil engineering work, with an excavation of  $4.5 \text{ m}^3$ , would improve by a factor  $\approx 7$  the accumulated statistics and hence the physics reach, in particular in the tau neutrino sector.

### 4.3 HL-LHC – FIPs Physics at large angle

The programme to search for LLPs at ATLAS, CMS, and LHCb is vibrant and draws on the expertise of data analysts, instrumentation specialists, and theory experts [231]. The sensitivity of both ATLAS and CMS to the decay-in-flight of LLPs is greatest when these particles are relatively heavy ( $m_{llp} \gtrsim 10 \text{ GeV}$ ), though there are some important exceptions (e.g., [232, 233]). This is due to the presence of large backgrounds when exploring the low-mass region (below a few GeV) in a high-energy hadron collider, where data acquisition systems are overwhelmed with primarily hadronic activity. Transverse detectors that can probe FIPs physics at large angles are imperative as they provide complementary sensitivity to FT and forward detectors discussed in Sections 4.1 and 4.2, which kinematically cannot probe heavy LLPs produced at the Electro-Weak (EW) scale and above. Furthermore, transverse detectors provide complementary sensitivity to the main LHC detectors ATLAS, CMS, and LHCb, which cannot probe LLPs with large decay lengths of 10 m and above. To achieve comprehensive coverage of the full LLPs parameter landscape, and in particular, to have a large sensitivity to LLPs produced from Higgs-boson decays, one or more high-volume, transverse LLPs detectors are needed.

#### 4.3.1 ANUBIS

The primary physics motivation of AN Underground Belayed In-Shaft search experiment (ANUBIS) is providing unique sensitivity to massive LLPs ( $m_{llp} > 1 \text{ GeV}$ ) with significant lifetimes ( $c\tau > \mathcal{O}(10^2 \text{ m})$ ) produced in high- $Q^2$  collisions at the EW scale or above [234, 235]. Such models cannot be probed either at existing general purpose detectors like ATLAS and CMS due to their finite geometrical acceptance nor at dedicated forward detectors like FASER or beam dump experiments like SHiP/NA67 as they cannot probe phenomena produced at an effective *c.m.* energy  $\sqrt{s} \gtrsim 10 \text{ GeV}$ .

The ANUBIS and ATLAS trigger and data acquisition system should be fully integrated allowing the full information about LLPs candidate events registered by the two detectors to be

exploited. This would provide unique sensitivity to the associated production of new particles together with a Higgs boson or  $W$  or  $Z$  bosons, enabling new searches for HNLs [236], ALPs [237, 238] and hidden photons [239] that could not be performed otherwise. ANUBIS would extend the reach of all current LHC detectors to LLPs produced via the Higgs portal by 3 orders of magnitude [235].

The detector requirements are (i) high efficiency of  $> 98\%$  per detector layer, (ii) angular resolution of  $\lesssim 0.01$  rad, (iii) spatial resolution of  $\lesssim 0.5$  cm, and (iv) time resolution of  $\lesssim 0.5$  ns. The large instrumented detector area of  $\approx 1600\text{ m}^2$  imposes stringent constraints on the detector costs. Resistive Plate Chamber (RPC) is the optimal choice of technology given the requirements above. For cost optimization and to benefit from a mature technology, a technology based on the ATLAS Phase 2 RPCs [240] is adopted.

The proposed implementation of the ANUBIS detector takes a staged approach:

- First, a small-scale  $\approx 1 \times 2 \times 2\text{ m}^3$  prototype, ANUBIS prototype (proANUBIS), was commissioned in 2024 and is currently taking physics data in a representative location close to the ceiling of the ATLAS cavern. The primary physics goals of proANUBIS are: (i) directly measuring the expected background levels in combination with ATLAS, and (ii) validating the experimental setup and its technology.
- proANUBIS is scheduled to run during Run 3, while R&D of the full ANUBIS detector electronics is performed and the civil engineering related to its installation is finalized.
- It is foreseen to partially deploy ANUBIS in LS3, allowing for partial data-taking in Run 4 before the full deployment in LS4 for data-taking in Run 5.

Currently, proANUBIS has collected  $104\text{ fb}^{-1}$  of  $pp$  collisions. This is being used to develop analysis techniques and detector calibrations that would allow for easier commissioning and early data-taking for the full detector. ATLAS can be used as an active veto against high-energy charged tracks and ‘punch-through jets’ (jets that are not fully contained in the calorimeter) that are likely to produce displaced vertex candidates from hadronic interactions. Hence, displaced vertices aligned with punch-through jets and energetic charged tracks are vetoed. Synchronization with ATLAS would allow for a strong PoC for the active-veto concept and the expected background level, ANUBIS would operate under.

The R&D efforts focus on the detector geometry and sensor layout to optimize its performance, the identification of an eco-friendly gas mixture for operating the RPCs, and on the serialization and daisy-chaining of the data acquisition system and its integration with the ATLAS detector.

#### 4.3.2 CODEX-B

The COmpact Detector for EXotics at LHCb (CODEX-b) proposal is a low-cost transverse LLPs detector option that uses existing technology and infrastructure. CODEX-b is a special-purpose detector to be installed near the LHCb IP8 to search for displaced decays of exotic LLPs [241, 242, 243]. A recent EoI presented the physics case with extensive experimental and simulation studies for the proposal [242]. The proposed CODEX-b detector would be located roughly 25 meters from IP8 and have a nominal fiducial volume of  $10 \times 10 \times 10\text{ m}^3$ . Backgrounds would be controlled by passive shielding provided by the existing concrete shielding wall in Underground Experimental Cavern (UX)85, combined with an array of active vetoes and passive

shielding to be installed nearer to the interaction point. The installation of the detector and the passive shielding would not impact LHCb operation. The core advantages of CODEX-b are

1. competitive sensitivity to a wide range of BSM LLPs scenarios, exceeding or complementing the sensitivity of other dedicated LLPs or general purpose detectors, both existing and proposed [242];
2. a near-zero background environment, as well as an accessible experimental location with many of the necessary services already in place;
3. the ability to tag events of interest within the existing LHCb detector, independently from the LHCb physics program;
4. a relatively compact size, instrumented with low-cost RPCs, results in a modest cost. There is also the realistic possibility of extending detector capabilities for final-state neutral particles using technologies like scintillating tiles.

A smaller proof-of-concept demonstrator detector, CODEX- $\beta$ , consisting of 42 RPC singlets, is currently being installed and will be integrated with LHCb and operated during a fraction of Run 3 [244]. This demonstrator has been approved as an LHCb R&D project and will be placed close to the proposed location of CODEX-b, shielded only by the existing concrete wall. The assembly and first commissioning of the RPCs for CODEX- $\beta$  is complete, and the first steps towards installation have been taken. Data-taking with CODEX- $\beta$  will commence in 2025 and continue to the end of Run 3. A RPC gas mixture compliant with CERN regulations in terms of Greenhouse Gas (GHG) emissions will be used during the production of the CODEX-b detector.

#### 4.3.3 MAPP-2

The physics programme of MoEDAL Apparatus for Penetrating Particles, Phase-2 (MAPP-2) focuses on searching for LLPs and weakly interacting particle avatars of new BSM physics at the HL-LHC. MAPP-2 targets a wide range of exotic particles, including dark photons, new scalars, ALPs, HNLs, and supersymmetric particles. By searching for LLPs and weakly interacting particles, MAPP-2 addresses fundamental questions related to dark matter, new physics, and HSSs.

The MAPP-2 detector would be located in the UGC1 gallery near IP8 and it would cover an intermediate pseudorapidity range ( $1.4 \leq \eta \leq 3$ ) not addressed by other detectors dedicated to LLPs searches. Additionally, MAPP-2's  $1000 \text{ m}^3$ , fully open, monitored decay zone would allow to detect charged particles with kinetic energies as low as 50 MeV and photons with energies down to 100 MeV, enabling the observation of low-mass LLPs decays. MAPP-2 would use position-sensitive scintillator technology instead of RPCs, removing the need of using gases. The estimated cost of the detector is 6 to 7 MCHF.

MAPP-2 would consist of three position-sensitive scintillator layers arranged in 14 “houses” along UGC1’s length, following its cross section and leaving the central decay region free of material. MAPP-2 covers a pseudorapidity range from 1.3 to about 3. The detector is shielded from SM backgrounds by at least 24 m of rock and concrete and from cosmic rays by about 110 m of rock. Each MAPP-2 “house” contains  $1 \text{ m} \times 1 \text{ m}$  scintillator panels with embedded Wavelength Shifting (WLS) fibers on both sides. These fibers form an X-Y grid with a 2 cm pitch, read out by Silicon Photo Multipliers (SiPM). The electronic readout, software trigger, and calibration systems mirror those of the MAPP-1 detector presently installed in the UA83 gallery near IP8. MAPP-2 is expecting to integrate  $300 \text{ fb}^{-1}$  during the HL-LHC phase.

A LoI for the LHCC is in preparation and a TDR will be submitted for approval in 2026. the MoEDAL-MAPP collaboration plans to test a MAPP-2 demonstrator unit in 2026/27 and to apply for funding to construct the full MAPP-2 detector during LS3. In this scenario, MAPP-2 data-taking would take place during Run 4 and beyond.

#### 4.3.4 MATHUSLA40

The proposed MAssive Timing Hodoscope for Ultra-Stable neutrAL pArticles,  $40 \times 40 \text{ m}^2$  area) (MATHUSLA40) experiment is a dedicated LLPs detector for the HL-LHC, situated on the surface near CMS. LLPs that are produced at CMS IP5, travel to the surface, and decaying in the MATHUSLA40 decay volume would be reconstructed as displaced vertices by six plastic scintillator tracking layers installed in the ceiling and rear wall of the decay volume (see Figure 10). The primary physics target are LLPs in the  $\mathcal{O}(10\text{GeV}) - \mathcal{O}(100\text{GeV})$  mass range with lifetimes  $\gtrsim 100\text{m}$  that decay hadronically. This highly motivated [245] new physics signal, including exotic Higgs decays to LLPs, arises in many BSM theories, including the Neutral Naturalness solutions to the little Hierarchy Problem [246, 247]. The LHC is the only collider that can produce these LLPs today, but they are in a blind spot for ATLAS and CMS due to high backgrounds and severe trigger limitations [248]. MATHUSLA40 could search for these LLPs with near-zero background, with an ultimate sensitivity that surpasses the main detectors by orders of magnitude in LLPs cross section and long lifetime.

The current proposal consists of an LLPs decay volume with area  $\approx 40\text{m}^2$  and height  $\approx 11\text{m}$  (see Figure 10). Veto detectors in the floor and front wall help reject cosmic, LHC muon, and atmospheric backgrounds. A trigger system identifies upward traveling tracks, prompting the detector to be read out for permanent storage and offline analysis. The MATHUSLA40 trigger system can

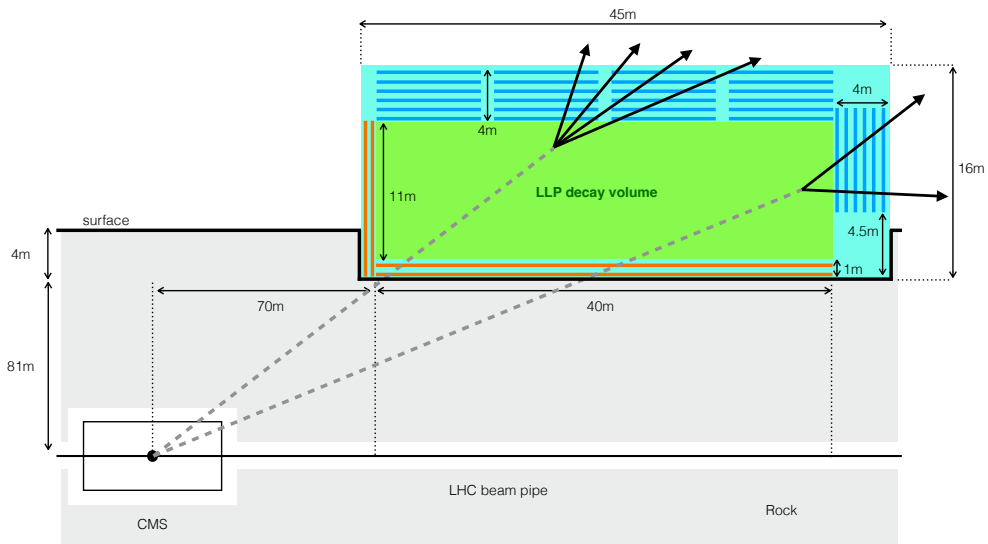


Figure 10: LLPs (gray dashed lines) can decay into SM charged states (black arrows) in the MATHUSLA40 decay volume (green), and be reconstructed as displaced vertices by the  $9 \times 9 \times 4 \text{ m}^3$  tracking modules (thin blue rectangles), with veto layers (orange) aiding in background rejection. (Figure taken from [249].)

also provide a Level 1 (L1) trigger signal to CMS, enabling correlated offline analyses to determine the underlying new physics model in the event of a discovery [250].

The MATHUSLA40 collaboration presented an LoI to the LHCC in 2018 [251] and an update in 2020 [252], and operated a test-stand on the surface above ATLAS in 2018 [253]. Canadian MATHUSLA40 groups constructed and operate R&D test-stands at the University of Toronto and the University of Victoria. The collaboration developed a proposal for a 100 m-scale detector towards the conceptual design stage, but over the last year, downscaled its proposal to the current 40 m version in response to recent developments in the US funding landscape [254], which made explicitly clear that the original proposal was too large to attract US (and international) support. MATHUSLA40’s inherent modularity facilitates this rescaling, and also suggests a clear progression towards implementation of the full detector, by first building a 10 m prototype which then becomes the first module of MATHUSLA40. This redesign is now complete, and reflected in the recently released MATHUSLA40 CDR [249] for an achievable 40 m geometry, covering the design, fabrication, and installation at CERN Point 5 [255]. The collaboration aims to submit the proposal to the LHCC in 2025.

## 4.4 HL-LHC – Fixed Target

### 4.4.1 ALADDIN

An Lhc Apparatus for Direct Dipole moments INvestigation (ALADDIN) is a proposed fixed-target experiment at the Insertion Region (IR)3 of the LHC aiming to measure the Electric Dipole Moment (EDM) of charm baryons, such as  $\Lambda_c^+$  and  $\Xi_c^+$  [256]. These measurements are highly sensitive probes of the SM and to potential new physics but remain unexplored due to the challenges imposed by the short lifetimes of these particles. ALADDIN employs a technique using two bent crystals to channel forward-produced charm baryons from proton collisions, as sketched in Figure 11, inducing spin precession to enable the determination of their Magnetic Dipole Moment (MDM) and EDM. The first crystal, with 50  $\mu$ rad bending, splits part of the halo from the 7 TeV circulating proton beam, and steers it onto the target, itself paired to the second crystal with 5–10 mrad bending. It is followed by a compact detector including a spectrometer and a Ring-Imaging Cherenkov (RICH) detector for particle identification. ALADDIN not only provides a unique opportunity to probe uncharted charm baryon properties but also paves the way for innovative advancements in experimental techniques and detector technologies. Its deployment during Run 4 builds upon validation tests from machine experiment called Double Crystal set-up Proof of Principle Experiment (TWOCRYST) scheduled for 2025 to demonstrate the feasibility of the technique [257].

The operation of a double-crystal setup, parasitically to standard proton-proton collisions [258], is both complex and challenging. A number of critical issues were identified early on by the LHC-FT study team [259], which call for a direct demonstration of this scheme. The machine experiment TWOCRYST was conceived to validate the feasibility of this setup and to characterize precisely the performance reach in the HL-LHC era. The TWOCRYST setup is installed in the LHC IR3 to address the performance in the multi-TeV range of the new long-crystals required for the charmed baryons precession experiments. The double-crystal setup has been installed in IR3 together with two Roman Pots that will enable transverse profile monitoring of single- and double-channeled beams. The specifications of these crystals are identical to those planned for ALADDIN. Two detector technologies will be applied: a fibre tracker system recovered from the ATLAS-ALFA

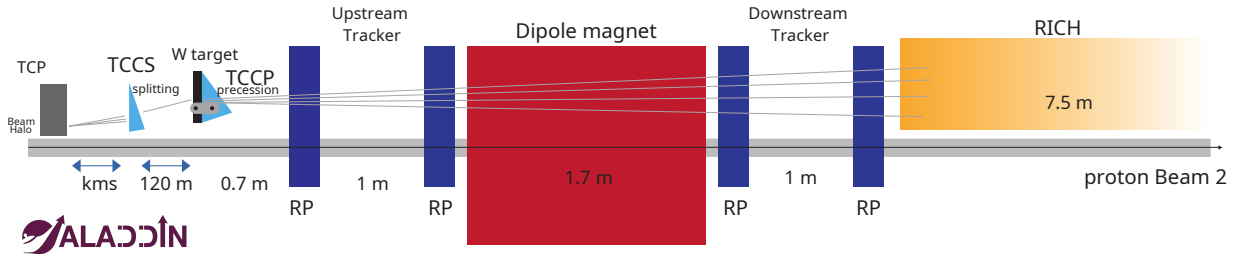


Figure 11: Sketch of the ALADDIN experiment (not to scale), illustrating the primary collimator (TCP), the splitting (TCCS) and precession (TCCP) crystals, the tungsten target just upstream of the TCCP, the spectrometer including the dipole magnet, and the upstream and downstream trackers, housed in Roman Pots, and the RICH detector. (Figure adapted from [256].)

experiment and a pixel detector derived from the LHCb VELO, which is close to the technology for the final experiment.

The goal is to exploit the last two years of operation of the LHC before the LS3 to collect important data as an input to the future MDM/EDM experiment: performance of the long 7 mrad crystal in the multi-TeV energy range; operational aspects of the double-crystal setup; background checks with the final sensors. An ambitious MD plan is expected in 2025 and 2026, with the goal of performing the relevant measurements to establish the achievable PoT and the rate of channeled  $\Lambda_c^+$  that the machine can deliver.

#### 4.4.2 LHCSPIN

Building on the experience obtained with SMOG2 (see Section 2.1.5), a proposal called LHC-spin [260, 261] is being studied which envisages to install a transversely polarized hydrogen (and deuterium) target inside the LHC. This setup would facilitate unique spin-dependent measurements of DY and heavy-flavour production processes, by using both proton and lead beams, providing insight into details of the nucleonic transverse momentum-dependent parton distributions [262, 263, 264]. The setup would use an Atomic Beam Source (ABS) to inject a nuclear-polarized H or D beam into a storage cell just in front of the LHCb VELO. The main challenge lies in the ability to maintain a high nuclear target polarization inside the storage cell, which requires finding an adequate coating of the inner cell wall compatible with LHC operation. Measurements performed with an amorphous carbon coating produced promising results which revealed that a high degree of nuclear polarization is maintained despite a substantial hydrogen recombination rate [265], thus providing an almost ideal storage cell target (molecular hydrogen, being slower than atomic hydrogen, produces a denser target). However, if a molecule-dominated nuclear-polarized hydrogen target is used, a technique must be developed to measure its polarization *in situ*. This could be achieved by using a calibrated single-spin asymmetry, such as in elastic scattering near the Coulomb-nuclear interference region [266, 267, 268, 269]. Therefore, an auxiliary experiment is also proposed [270] which would be installed in IR4 and which would measure the asymmetry of a free atomic beam of known polarization. The details of this setup are being developed and include the integration with the LHC beam pipe of an ABS, a Breit-Rabi-type polarimeter and large-angle (MeV range) proton recoil detectors.

## 4.5 ISOLDE

### 4.5.1 SYMMETRY VIOLATING EFFECTS IN RADIOACTIVE ATOMS AND MOLECULES

The unique environments within heavy, radioactive atoms and molecules provide opportunities to probe BSM physics [271]. CP-violating interactions manifest in these systems as observable Electro-Magnetic (EM) moments such as anEDM. These measurements of CP-violation in EM moments can provide sensitivity to new particles and interactions on energy scales comparable to those achievable at the LHC and the FCC [272], enabling discovery of new physics or imposing extremely stringent constraints on models of new interactions [273].

To disentangle possible sources of CP-violation, multiple searches are required in complementary probe systems. The aim of the radioactive molecules initiative is firstly to develop a catalogue of probe systems at ISOLDE and enable preliminary characterization at the existing experimental facility. Secondly, the initiative aims to make a selection of long-lived radioactive probes available to offline experiments. Finally, investigations are underway towards the feasibility of adapting the high-precision techniques used for stable molecules in offline symmetry-violating experiments towards online experiments with radioactive probes.

## 4.6 AD and ELENA Complex

The Antimatter Factory at CERN is unmatched worldwide in producing low-energy antiprotons ( $\bar{p}$ ). It supports over 60 institutes and about 350 scientists organised into six collaborations, which conduct precise comparisons of the fundamental properties of stable matter-antimatter conjugates at low energies, and study antimatter gravity [274].

With increased  $\bar{p}$  flux and improved beam availability, ELENA has supported groundbreaking studies in fundamental physics. Highlights include the most precise comparisons of fundamental properties of protons and antiprotons [275, 276], the first observation of the ballistic behaviour of antihydrogen in the gravitational field of the earth [277], the 1S-2S spectroscopy of laser-cooled antihydrogen atoms [278, 279], and the antiproton-to-electron mass ratio measurements in buffer-gas cooling of antiprotonic helium [280]. Some of the collaborations are progressing towards production of an anti-hydrogen beam [281] and anti-hydrogen production via charge-exchange [282, 283]. The recently reported observation of positronium laser cooling [284] is a crucial step towards this goal. Two collaborations, Baryon Antibaryon Symmetry Experiment (BASE) and antiProton Unstable Matter Annihilation (PUMA), are working toward transporting antiprotons out of the ELENA facility, and BASE-Symmetry Tests in Experiments with Portable antiprotons (STEP) reported very recently on first transport of protons [285]. PUMA will soon move the antiprotons from ELENA to ISOLDE aiming at probing the surface properties of stable and rare isotopes using low-energy antiprotons [286].

Looking ahead, physicists are interested in studying the properties of the antineutron and strongly interacting antimatter with high precision. In another attempt, some AD physicists are currently looking into the production and spectroscopy of anti-hydrogen molecular ions. These techniques have potential to study fundamental antimatter properties with resolutions on the  $10^{-16}$ -level and below [287], which could pave the way for novel experiments in the long-term future [288].

In response to those needs, the feasibility of producing anti-deuterons at the AD target is being explored. Further upgrade studies being considered include the ability to vary the  $\bar{p}$  extraction

energy and the introduction of slow extraction, aiming at antineutron-related studies by the current users as well as to broaden the facility’s scientific reach beyond the present user community.

## 4.7 Non-accelerator experiments

### 4.7.1 ATOMIC INTERFEROMETER @ CERN

Atom Interferometry (AI) is a promising quantum sensing technology [289] with great promise for searching for Ultra-Light Dark Matter (ULDM) and measuring Gravitational Waves (GWs). The sensitivity of AI is maximised in experiments manipulating with the same laser two or more atom clouds that are as widely separated as possible. Two geometric configurations are being considered, using either a vertical shaft or a horizontal gallery, with the former being pursued by the Matter-wave Atomic Gradiometer Interferometric Sensor (MAGIS) experiment [290] in the US and the Atom Interferometer Observatory and Network (AION) project [291] in the UK. The AION Collaboration has already demonstrated quantum interference between superposed clouds of atoms and the cancellation of laser noise between the interference patterns in a pair of  $^{87}\text{Sr}$  clouds manipulated by the same laser in a vertical gradiometer configuration. The AION collaboration has proposed to build a 10 m prototype in the UK, to be followed by full-scale 100 m and 1 km experiments [291].

One of the CERN access shafts, PX46, has been identified as a possible site for a 100 m AI detector based on AION technology, see Figure 12, and a conceptual feasibility study [292] has established its suitability as far as infrastructure, seismic stability and electromagnetic interference are concerned. The installation in PX46 of an international experiment is currently being discussed within the framework of the Terrestrial Very Long Baseline Atom Interferometry (TVLBAI) proto-collaboration [293]. Assuming successful evolution of the current technical R&D programme and the availability of funding, it is suggested to undertake preparatory work at Point 4 during LS3 to enable the subsequent installation and operation of the AI detector in PX46 without compromising LHC operation. The preparatory work would consist primarily of installing radiation shielding at the base of PX46 and an access control system.

No equally suitable European site for a 100 m vertical AI experiment has yet been identified, and this project would maximise the exploitation of unique CERN infrastructure to make world-leading probes of ULDM and GWs.

### 4.7.2 AXION HETERODYNE DETECTION

The proposal in [294, 150] for the heterodyne detection of axion DM in microwave cavities was realized in the form of two prototypes that are currently taking data at Stanford Linear Accelerator Center (SLAC) [295] and within the Superconducting Quantum Materials and Systems Center (SQMS) initiative at Fermilab [296]. A third prototype has been funded by the CERN Quantum Technology Initiative (CERN QTI), but has not been built, yet.

The basic idea consists in designing a cavity with two modes that have a small frequency splitting compared to their frequencies. Their geometry is designed to maximize photon transitions between them when an axion DM background is present and one of the two modes is loaded. This setup gives a large parametric advantage, of order  $1/(m_a L)^2$  in signal power compared to traditional resonant searches, when exploring small axion masses  $m_a < L^{-1}$ , where  $L$  is the size of the cavity.

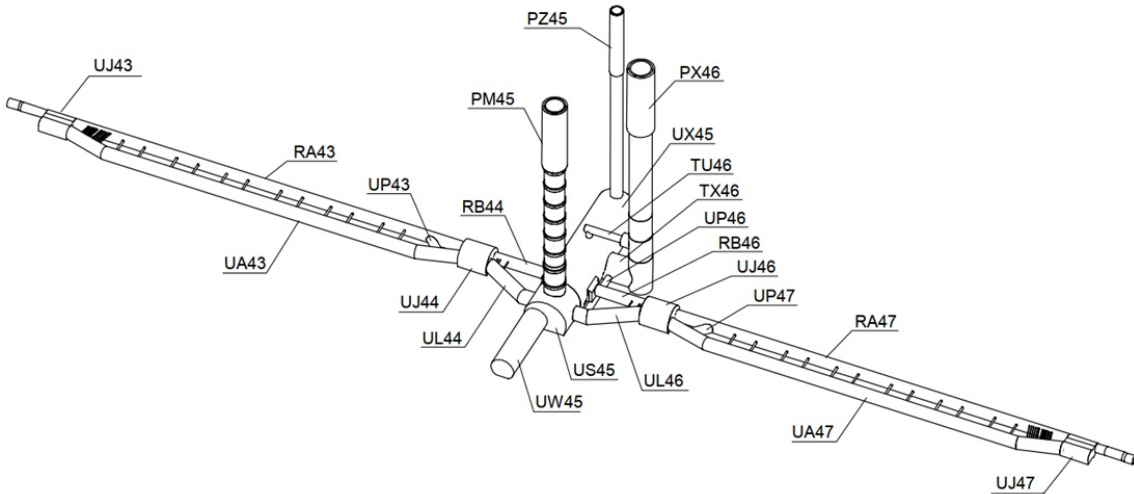


Figure 12: Schematic drawing of the civil engineering infrastructure at Point 4 on the LHC, including the LHC tunnel, the PX46 shaft and other underground locations [292].

Preliminary results of the prototype at SLAC have demonstrated a good mode separation in the readout of the signal mode and the possibility to tune the frequency splitting between the modes by about a MHz. The recorded mode separation is better than a part in  $10^7$ , i.e., if the loaded mode is readout through the signal mode port, less than  $10^{-7}$  of its input power is measured. These preliminary results are still unpublished but demonstrate the key features needed to realize a full future experiment [294, 150]. The SLAC prototype is a 50 L-copper cavity, while the CERN QTI prototype will demonstrate the same features in a SC cavity of similar size. It is projected to have sensitivity to unexplored axion DM parameter space.

The long-term goal of this initiative is to build a full scale experiment as proposed in [294, 150], based on a  $\text{m}^3$  SC cavity cooled to 2 K. A future experiment based on this idea can probe about two orders of magnitude in axion mass on the QCD line [294], the prime target of all axion searches. Additionally, it is the only existing proposal that can probe in the laboratory the lightest viable DM candidates [150], whose De Broglie wavelength is comparable to the size of dwarf galaxies and whose coherence time is about ten times longer than recorded human history.

#### 4.7.3 FLASH

FINUDA magnet for Light Axion SearchH (FLASH) [297] is a large resonant-cavity haloscope in a high static magnetic field which is planned to probe new physics in the form of DM axions, scalar fields, chameleons, hidden photons, as well as High Frequency Gravitational Waves (HFGW). Concerning the QCD axion, FLASH will search for these particles as the DM in the mass range  $0.49\text{--}1.49\text{ }\mu\text{eV}$ , thus filling the mass gap between the ranges covered by other planned searches. A dedicated microstrip Superconducting QUantum Interference Device (SQUID) operating at ultra-cryogenic temperatures will amplify the signal. The frequency range accessible overlaps with the Very High Frequency (VHF) RF spectrum and allows for a search of GWs in the frequency range  $100\text{--}300\text{ MHz}$ . The experiment will make use of the cryogenic plant and magnet of the FIIsica NUCleare a DA $\phi$ NE (FINUDA) experiment at Istituto Nazionale di Fisica Nucleare

(INFN) – Laboratori Nazionali di Frascati (LNF) (Italy). Recently, an European Research Council (ERC) Synergy Grant has been awarded to the project *GravNet*, which has the ambition to search for HFGW with a network of haloscopes, including QUaerere AXions experiment @ LNF (QUAX@LNF) [298], already operating at LNF, and FLASH.

#### 4.7.4 RADES

RADES is a haloscope for axion DM searches using RF cavities in dipole magnets, with physics results obtained at around 8–9 GHz [299, 300]. The use of HTS tapes on the cavity walls, gives also a unique synergy with studies that explore HTS coating for the Future hadron-hadron Circular Collider (FCC-hh) beam-pipes [301, 139]. In addition, it has resulted in the development of a novel type of cavity tuning mechanism through a ‘split-cavity’ [302].

The ERC Synergy Grant *Dark Quantum* and the Quantum Relic Axion DEtection Sensors (QRADES) Grant within QuantERA [303], which have been awarded to RADES collaborators for the development of single photon detection in RADES, have started in 2024 with relevant contracts in place. In addition, many RADES collaborators are members of the IAXO collaboration. In 2024, a LoI has been submitted by RADES to the Canfranc Underground Laboratory (Spain) in order to run the experiment shielded from cosmic radiation.

The long-term goal of RADES will be the installation of a haloscope in the BabyIAXO magnet [304]. In terms of axion-mass-range to be probed, there is a unique experimental reach in axion masses between 1 and 2  $\mu\text{eV}$  (except for FLASH [297]). Within the ERC Synergy Grant there is also the plan to explore quantum-limited detection with magnetic-field-resilient transmons for axion masses corresponding to frequencies of 10–20 GHz.

## 4.8 PBC Opportunities at new Facilities

### 4.8.1 SBN BEAM PERFORMANCE

The proposed novel SBN beam facility introduced in Section 3.3.1 would provide an outstanding playground for precision neutrino physics. In order to evaluate its experimental performance, a reference experimental setup has been defined with realistic ingredients as detailed below (see Figure 5).

The SBN reference beam consists of 9.6 s spills of  $1.0 \times 10^{13}$  protons and an 8.5 GeV energy tune of the secondary meson narrow-band beam. A possible lower secondary energy tune at, e.g., 4 GeV, optimized for Hyper-K, is being evaluated [157]. The calorimetric instrumentation of the decay tunnel monitors the  $\nu_e$  flux by measuring the continuous yield of electrons produced in the kaon  $K_{3e}$  decays. The instrumentation on the tunnel walls also monitors muons from  $K_{2\mu}$ , while a muon range-meter based on PICOSEC micromegas [305] (instrumented hadron dump) can access muons from pion decays, thus monitoring the  $\nu_\mu$  fluxes of the facility [154]. Rate capability, radiation hardness, and ability to discriminate electrons from photons and pions are key specifications of these devices. The SBN reference calorimeter is based on the results of the prototype built and beam-tested within the Neutrino Platform 06 Experiment (NP06)/ENUBET [154]. The tracking instrumentation of the beam and muon spectrometers is designed to measure individual 2-body decays of charged pions and kaons to tag each  $\nu_\mu$  of the beam, similarly to what the current NA62 GTK tracker performs. The peak meson rate at the entrance of the decay tunnel is 20 MHz/mm<sup>2</sup>,

10 times higher than the present NA62 conditions. Rate capability, radiation hardness, time resolution, and material budget are key specifications of these devices. The SBN reference trackers anticipate the expected performance of Si detectors developed for the HL-LHC era [306]. The SBN reference neutrino detector is a ProtoDUNE-like LAr Time Projection Chamber (TPC) of 500 t with a fiducial transverse size of  $4 \times 4 \text{ m}^2$  and an entry plane located 25 m from the end of the decay tunnel. With this detector statistical samples of about  $10^4 \nu_e$  and  $5 \times 10^5 \nu_\mu$  CC events are expected for  $1.4 \times 10^{19}$  PoT, corresponding to  $\approx 5$  years of data-taking. An additional water Cherenkov detector of interest for Hyper-K is being considered [157].

The quantitative response of this reference setup has been simulated based on a detailed propagation of secondary particles in the optimized beam optics. Some key results are listed below:

- $\nu_e$  and  $\nu_\mu$  flux: the simulation confirms that the flux can be controlled within 1 %, in line with the expected statistical precision of the  $\nu_e$  CC total sample.
- $\nu_\mu$  tagging: the  $\nu_\mu$  CC events in the detector are associated to the tagged  $\pi$  and  $K$  decays using time and space coincidence. The simulation shows that most of the observed events can be associated to a single decay, with mis-associations at the level of a few %. In addition,  $\pi$  and  $K$  parents can be discriminated using the decay kinematics, which should allow for providing complementary control of the  $K$  flux and hence the  $\nu_e$  flux. A proof of principle of neutrino tagging was recently provided by NA62 with the first detection of a tagged neutrino [307].
- $\nu_\mu$  energy resolution: with a detector close to the source, the transverse position of interacting vertices is correlated with the neutrino energy by the two-body kinematics of a Narrow-Band beam. The Narrow-Band Off-Axis (NBOA) technique exploits this correlation, similarly to the approach currently used in experiments such as Short-Baseline Near Detector (SBND) at Fermilab. NBOA provides a  $\nu_\mu$  energy resolution of approximately 10 %. For the tagged  $\nu_\mu$  CC sample the energy resolution is improved to the sub-% level thanks to full reconstruction of the individual decays.

The physics impact of the SBN expected from these experimental performances is discussed in Section 5.4.

#### 4.8.2 GAMMA FACTORY RESEARCH OPPORTUNITIES

The GF facility, introduced in Section 3.3, proposes to extend the CERN scientific programme in the domains of particle, nuclear, atomic, fundamental, accelerator, and applied physics, delivering technological leaps opening new research opportunities and creating potential for unexpected discoveries in many branches of physics. Its multidisciplinary research could re-use the existing CERN accelerator infrastructure, including LHC. It could be conducted over the time interval between the end of HL-LHC proton and ion collision programme, and the start of a new, high-energy-frontier collider operation.

The GF primary goal is to create novel research tools and novel research methods for the high-intensity frontier research. Several application domains of the GF tools have already been studied:

- **Particle physics** [163, 308, 309] – precision QED and EW studies, Higgs boson studies in the  $\gamma\gamma$  collision mode, searches for very rare muon decays, precision studies in the neutrino sector, electron-proton collision physics at the LHC, QCD-confinement studies;

- **Nuclear physics** [310, 165, 311] – nuclear spectroscopy, studies of cross-talk of nuclear and atomic processes, nuclear photo-physics studies, photo-fission research, precision studies of rare radioactive nuclides;
- **Atomic physics** [312, 313, 314, 315, 311] – studies of highly charged atoms, high precision studies of muonic and pionic atoms;
- **Fundamental physics** [316, 317, 318, 319, 311] – studies of the basic symmetries of the universe, vacuum birefringence studies, dark matter searches, atomic interferometry;
- **Accelerator physics** [169, 320, 171, 321, 322, 182, 323, 324, 163] – laser beam cooling techniques, high-intensity sources of polarised positrons and muons, beams of radioactive ions and neutrons, very narrow band, CP and flavour-tagged neutrino beams;
- **Applied physics** [164] – beam-driven energy sources, fusion research, medical isotopes and isomers, precision lithography.

#### 4.8.3 EXPERIMENTS AT AWAKE

The demonstration of the AWAKE programme technology (see Section 3.3.3) would enable the upgrade and extension of the accelerator facility and the acceleration of electrons to  $\mathcal{O}(50\text{ GeV})$  for use in particle physics experiments. Some possibilities have already been discussed elsewhere [189, 325, 326], although this list is by no means exhaustive and other possibilities could provide a compelling particle physics motivation. A brief summary of some of the experiments is given here, principally the possibility to search for dark photons in a BD experiment or the investigation of strong-field QED in electron–laser interactions.

Using protons from the SPS, experiments could be performed under the assumption of electrons delivered at 50 GeV in bunches with  $5 \times 10^9$  particles and a total running time of, e.g., 3 months giving  $10^{16}$  Electrons on Target (EoT) [327]. As this would be a BD experiment, searches for dark photons would be performed in the  $e^+e^-$  decay channel. Given these parameters, the search can be extended to higher dark photon masses ( $m_{A'} \approx 0.1\text{ GeV}$ ) in the coupling range,  $10^{-5} < \epsilon < 10^{-3}$ , a region not covered by current searches. If protons from the LHC could be used to drive the wakefields, TeV energy electrons could be produced and a similar search for dark photons would extend to even higher masses ( $m_{A'} \approx 1\text{ GeV}$ ) and for the same  $\epsilon$  region, beyond any currently planned experiment.

The E144 Experiment (E144) [328] at SLAC in the 1990s pioneered studies in strong-field QED [329] through investigation of electron–laser interactions. Understanding how QED becomes non-linear is relevant for a number of physical systems, such as in astrophysics, and can be investigated in the laboratory through experiments in which high-energy electrons and a high-power laser interact. These studies have undergone a resurgence with the improvement in laser technology and the consequent increase in laser power. Experiments could be performed with electrons of energy 50 GeV, as in the E144 experiment, and beyond other current experiments [330, 331]. As the rate will be limited by the Hz-level laser system, high bunch rates for electrons are not required and so this is an ideal first experiment for the AWAKE facility.

#### 4.8.4 PBC OPPORTUNITIES AT FCC-EE AND LC

Future colliders, such as the FCC-ee or a LC, and their injectors, as described in Section 3.3.4, will offer various options for PBC. Both types of facilities have the potential to test QED in the

strong-field regime. This is possible due to the very high particle energy available of 100 GeV and beyond and the developments in the available peak intensity of high-power laser systems. Combining both in an electron-laser collision allows the investigation of the harmonic structure of the non-linear Breit–Wheeler pair production and eventually also delve into the fully non-perturbative domain of QED where there is no reliable theory at all [329]. A viable and sustainable approach to testing strong-field QED is the use of oriented crystals. At FCC-ee energies, electrons and positrons traversing a crystal along its main lattice axes experience an average electric field in their rest frame that is amplified by a factor  $\gamma$  due to Lorentz contraction. This enhancement brings the field to values comparable to the Schwinger critical field of QED, beyond which electrodynamics becomes non-linear [332, 333, 334]. A linear collider additionally enables to explore strong-field QED effects in the beam-beam interaction, which becomes particularly relevant in possible energy upgrades above the 1 TeV scale [335, 336]. Since strong-field QED processes produce a high flux of energetic photons, they can also be further used in a FT experiment to search for new physics [87, 337].

### PBC opportunities at FCC-ee

The science opportunities of FCC-ee are detailed in [193]. The high-intensity positron source from the FCC-ee booster, operating at 20 GeV and possibly up to 46 GeV, offers opportunities for dark sector searches and studies of true muonium. If positrons slow extraction can be realized, an experiment akin to NA64 could significantly extend the sensitivity to LDM, leveraging resonant annihilation to enhance reach in the dark photon parameter space. True muonium, the yet-unobserved bound state of a muon and antimuon, presents a unique test for bound-state QED and potential New Physics. Previous proposals suggested production at the SPS H4 beam line with 43.7 GeV positrons, requiring precise energy resolution. The FCC-ee booster could dramatically increase positron availability, enabling true-muonium production with a controlled energy spread and with expected production rates of  $10^3 – 10^4$  true muonium atoms per day. This would allow studies of its decay properties, hyperfine structure, and possibly the Lamb shift. The FCC-ee accelerator complex will provide high-energy, high-quality positron and electron beams, reaching energies up to 183 GeV, with an intense primary beam and low divergence. This unprecedented beam availability would significantly enhance the experimental performance and increase statistics, which is essential for advancing strong-field QED studies in crystals. Indeed, it could enable the observation of spin dynamics effects in strong-field QED. At FCC-ee, spin rotation via channeling in bent crystals would offer a unique opportunity to investigate strong-field QED spin dynamics, particularly the significant reduction of the anomalous magnetic moment  $\mu'$  in strong fields at high particle energies [338, 339]. Thus, measuring the spin precession angle of positrons in a bent crystal at FCC-ee energies would provide a direct test of strong-field QED. Bent crystals would not only facilitate the measurement of the drastic decrease in the positron (electron) magnetic moment, but also enable the observation of radiative self-polarization in strong fields [340], observing circularly polarized gamma-radiation by positrons, polarized electron-positron pair production by gamma-quanta and spin rotation in the circularly polarized crystal field harmonics [341, 342, 343].

## PBC opportunities at the LC

In addition to the capabilities to test strong-field QED, which are similar for FCC-ee and an LC, a future LC facility offers other options for PBC, which are elaborated in [196]. The main difference is that a LC will continuously dump its beam. As an example, the main beam dump of ILC is designed to handle 17 MW of power [344], indicated in Figure 7. The extremely large quantity of electrons and positrons on target is unique, and high production rates of heavy mesons and tau leptons are expected [345]. It enables the exploration of uncharted regions of parameter space for dark-sector particles, like ALPs, light scalar particles, HNLs, and LDM. The electrons are highly polarized, above 80%, which enhances certain mechanisms of production of new physics. On the other hand, positrons enhance the production via resonant annihilation. Besides the main beam dumps, an LC has other beam dumps, such as the tune-up dump. At such a location, single bunches can be extracted from each bunch train at full energy after the linear accelerator. They can be used, for example, for FT searches with thin targets, where lower rates are desired [346] or for the R&D of electron-driven plasma-wakefield acceleration at 100 GeV [347].

### 4.8.5 CPEDM MEASUREMENTS

Proposals to build a synchrotron to measure a possible EDM of charged particles [348, 349, 350] are motivated by the physics case described in Section 5.6. Whereas the EDM of electrically neutral particles such as neutrons can be measured with particles at rest, charged particle Electric Dipole Moment (cpEDM) measurements require to confine the particles in a precision storage ring. Most proposals to measure static EDMs are based on circulating polarized bunches satisfying the “frozen spin” condition as sketched in Figure 13. In a perfect machine and particles without EDM and the well known MDM of the particles, an initially longitudinal polarization is maintained by appropriate choice of the magnetic and electric field bending the beam. This means that the angular frequencies  $\omega_M$  describing the rotation of the spin and  $\omega_p$  describing the rotation of the particle momentum or direction are identical. A finite EDM generates a rotation of the polarization out of the horizontal plane into the vertical direction. A common proposal by an international community for proton EDM measurements is a ring with only Electro-Static (ES) bendings operated at the “magic energy” ( $\approx 232.8$  MeV), where the magnetic fields to satisfy the frozen spin condition vanish. Focusing can be done with electric [349] or magnetic [350] quadrupolar components and a typical circumference is 500 m to keep the required electric fields at reasonable values.

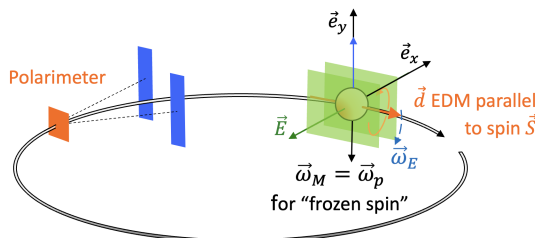


Figure 13: Sketch of a frozen-spin cpEDM measurement ring.

The main challenge of cpEDM measurement proposals is to show that the achievable sensitivity, i.e., the smallest detectable EDM, is superior to current limits, e.g., for the neutron [351]. This requires that a sufficient spin coherence time can be reached and that systematic effects, i.e., spin

rotations caused by machine imperfections for particles with a MDM only, can be understood and sufficiently suppressed. The former requires that the beam is bunched and sextupole families are used to suppress contributions to spin decoherence related to betatron and synchrotron oscillations. Some systematic effects are mitigated for “magic energy” rings by circulating counter-rotating beams, state-of-the-art magnetic shielding (in particular for fully Electro-Static (ES) rings), magnetic focusing and high symmetry lattices (in particular for the “hybrid” ring with magnetic focusing). However, many possible systematic effects remain and require thorough and careful evaluations [352, 353, 354, 355, 356].

Many experimental studies relevant for the design of any cpEDM ring have been done with the COoler SYnchrotron (COSY) ring [357, 358, 359, 360] in Jülich using a different method not relying on frozen spin concept.

A proposal to design and construct a smaller  $\approx 100$  m-circumference prototype EDM ring [349] is motivated by the observation that achieving the required cpEDM measurement sensitivity is very challenging without thorough in-depth investigations. Such a prototype ring would be an intermediate step to gain expertise in operating a large scale ES facility, to develop key technologies (as very sensitive beam position pick-ups and high electric field equipment), and to study in-depth systematic effects and mitigation measures.

## 4.9 Other Early Stage Proposals Discussed within PBC

Below a brief summary of ideas presently discussed within the PBC (in alphabetical order):

- **AQN@LHC**: Search for axion-antiquark-nuggets at the LHC through energy deposition from their strong interaction with the LHC environment leading to a measurable warm up (cf. [361]).
- **FAMU**: Measurement of the Zemach proton radius with an accuracy better than 1% via high-precision spectroscopy of the 1S hyperfine splitting in muonic hydrogen [362].
- **FLOUNDER, SINE & UNDINE**: DM searches and TeV neutrino physics studies with under-water and ground detectors from very forward production in LHC collisions [363, 364].
- **Gravitational effects of the LHC beam**: Measurement of the gravitational near-field of the LHC beam with optomechanical detectors testing gravity in a completely different domain from previous test of general relativity [365].
- **PAX**: Test of strong-field quantum electrodynamics via high-precision X-ray spectroscopy of antiprotonic atoms at the CERN AD facility [366].
- **SHIFT@LHC**: Search for long-lived low-mass BSM particles with a fixed-target setup upstream of the CMS experiment at the LHC [367].

## 4.10 FPC – interfacing experiment and phenomenology

As the spectrum of PBC experiments targeting FIPs and other types of HSs broadens, the role of the FPC continues to grow.

With data from the CERN experiments NA62, NA64, and FASER coming in, and with the construction of SHiP/NA67 on the horizon, maintaining the benchmark models that facilitate a comparison of different results is an important indicator of the achieved progress – both within

PBC and in the worldwide context. The improved sensitivity and sophistication of experimental analyses also require more accurate signal calculations, especially in difficult hadronic channels (cf., e.g., [368] for some recent measurements of NA62) as well as the development of tools facilitating sensitivity calculations and reinterpretations, e.g., [369, 370]. Further updates of the benchmark models may be needed to improve overall consistency and agreement with data from a broader range of experiments, such as, e.g., neutrino experiments. Many of these updates are driven by contributions from individual members of the FPC, but the hub that the FPC provides is central for disseminating these developments and identifying the requirements of the different experiments and the wider community.

This exchange will become even more important with the broadening landscape of fixed target experiments, LHC searches for long-lived particles and forward physics, as well as other types of experiments and facilities. These developments stimulate new discussions on interesting new physics targets that are within reach of PBC experiments, such as exotic bound states called quirks [371]. In exchange with the BSM working group, the FPC also aims to identify experimental capabilities that are not yet captured by PBC benchmark models and new ways to present them. Some of these new developments will be discussed in Section 5.5.

Maintaining and expanding this lively, collaborative and adaptive effort between theory and experiment, but also promoting individual investigations will be central to continuing the successful and broad physics program supported by PBC.

## 4.11 Summary of the proposals at CERN

Location	Proposal	Status	Cost category	Earliest operation
EHN1	NA61/SHINE ions	Addendum submitted to SPSC in 2024	C0	Run 4
	NA61/SHINE-LE	Proposal submitted to SPSC in 2024	C1	Run 4
	NA64 - Phase 2 - e	Proposal to be submitted to SPSC	C0	Run 4
	NA64 - Phase 2 - e <sup>+</sup>	Conceptual Design	N/A	Run 4
	NA64 - Phase 2 - h	Conceptual Design	N/A	Run 4
EHN2	DICE/NA60+	Proposal to be submitted to SPSC in 2025	C2	Run 4
	NA64 - Phase 2 - $\mu$	Proposal to be submitted to SPSC	C0	Run 4
	NA66/AMBER - Phase 2	Conceptual Design	C1/C2	Run 4
To be defined	MUonE	Conceptual Design	C1	Run 4
	SBN	Conceptual Study	N/A	Run 5
LHC	FPF	LoI to be submitted to LHCC in 2025	C3	Run 4
	SND@HL-LHC	Proposal submitted to LHCC in 2024	C1	Run 4
	ANUBIS	Data-taking with prototype detector (proANUBIS)	N/A	Run 4
	CODEX-b	Data-taking with prototype detector (CODEX- $\beta$ )	N/A	Run 4
	MAPP-2	LoI to be submitted to LHCC in 2025	C1	Run 4
	MATHUSLA40	Data-taking with prototype detectors	N/A	Run 4
	ALADDIN	Preparation of proposal to LHCC	C2	Run 4
	LHCspin	Conceptual Study	N/A	Run 5
	AION	EoI to be submitted to LHCC in 2025	C1	Run 4
	GF	Conceptual Study	N/A	After Run 5

Table 7: Preliminary cost estimates for beam and infrastructure upgrades as obtained by a PBC working group for the initial proposals where available. The definition of cost categories is explained in the text. N/A = Not Available.

The list of proposed experiments and facilities with an overview of the present status and indicative cost are shown in Table 7. The cost estimates are limited to the beam and infrastructure

upgrades and do not account for the costs of the experiments themselves. The cost categories are defined as follows:

- C0: Up to 300 kCHF
- C1: From 300 kCHF to 2 MCHF
- C2: From 2 MCHF to 10 MCHF
- C3: From 10 MCHF to 50 MCHF
- C4: Above 50 MCHF

## 5 Physics reach of PBC projects in the global context

### 5.1 Hadronic vacuum polarisation and the muon anomalous magnetic moment

The apparent discrepancy between the experimental value and theoretical prediction of the muon anomalous magnetic moment  $(g - 2)_\mu$  has triggered enormous activities in improving both the experimental results and theoretical predictions [372], but also in formulating extensions to the Standard Model. Recent experimental results on  $(g - 2)_\mu$  confirm the earlier measurements [373] with reduced uncertainties of 0.19 ppm when combined, and a final goal of 0.10 ppm [374, 375]. Additional data is also expected from the planned Japan Proton Accelerator Research Complex (J-PARC) E34 (g-2/EDM) experiment [376].

The experimental determination is significantly more precise than phenomenology, which is above 0.3 ppm. To improve on that it is of utter importance to better understand the contributions from the leading-order Hadronic Vacuum Polarisation (HVP) and from the hadronic contribution to light-by-light scattering, which are main drivers of current theory uncertainties [372].

A traditionally promising way of calculating the leading hadronic contribution is the use of time-like dispersion relation, which relies on the knowledge of the  $e^+e^-$  annihilation cross section into hadrons from the  $\pi^0$  mass threshold upwards. The low-energy range is affected by large non-perturbative effects, and experimental data from  $e^+e^-$  machines are needed. At present, large amounts of data have been collected at different machines for many exclusive and inclusive channels, through direct energy scan or radiative return methods, which – in principle – allow for a rather precise determination of the leading hadronic contribution. However, from Figure 14 it also becomes clear that there is a clear tension between results that use different experimental data sets.

More recently, lattice QCD has become more competitive in the calculation of the leading-order HVP. Not only that, they suggest much smaller discrepancies between the experimental results of  $(g - 2)_\mu$  and its theoretical determination, reducing them to less than a one-sigma effect [377].

An overview of current experimental and theoretical results on the muon anomalous magnetic moment is given in Figure 14, highlighting a large spread in the theory predictions, which indicates a lack of a full understanding of the systematics involved. In this situation, corroboration from independent methods, like the space-like approach [215] with muon-electron scattering data of the MUonE experiment [216] would be extremely valuable. MUonE aims to measure the leading-order hadronic contribution to  $(g - 2)_\mu$  with a statistical precision of 0.3%, in line with current determinations. The goal in accuracy and the novel technique will make this measurement an important contribution to the test of the Standard Model prediction of  $(g - 2)_\mu$ .

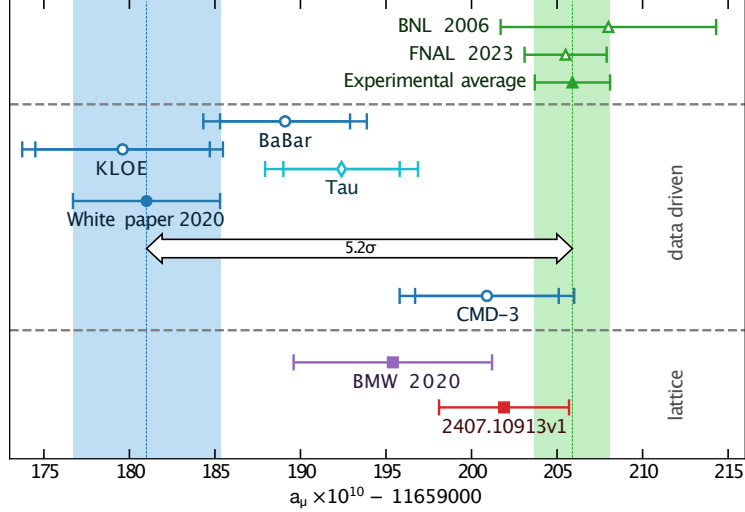


Figure 14: Overview of current experimental [373, 374, 375] and data-driven [378, 379, 380, 381, 382, 383, 384, 385, 386, 387] as well as theoretical [377, 388, 372] results related to the muon anomalous magnetic moment  $a_\mu$ . (Figure adapted from Ref. [377].)

## 5.2 Hadron structure and properties

Hadron structure studies remain an important part of high-energy physics, addressing such questions as the origin of mass of ordinary matter, partons with a very large fraction of the parent hadron’s momentum, or the onset of saturation at very low Bjorken- $x$ . Although the physics program of related PBC projects partially overlaps with that of ongoing and future experiments, like at the EIC at BNL, which is scheduled to begin data-taking in the middle of 2030s, it is important to note that the covered kinematical regions are often different and complementary (see, e.g., Figure 15). While the EIC will mainly cover the low- $x$  region with good coverage also of intermediate-to-high  $x$  at high- $Q^2$ , fixed-target collisions at the LHC—such as those achievable with SMOG2 and LHCspin—mainly cover the intermediate-to-high  $x$  region at intermediate  $Q^2$ . Furthermore, while EIC exploits DIS measurements, LHCspin (and SMOG2) will allow one to explore the nucleon structure by means of hadronic collisions, providing a fully complementary approach. This is of crucial importance, especially to constrain poorly explored aspects of the nucleon structure, such as the essentially unknown gluon Transverse Momentum Distribution (TMD). In addition, comparisons between EIC and LHCspin results will be extremely useful to test fundamental QCD predictions, such as evolution, universality and factorization. Likewise, the FPF will probe high- $x$  but also very low- $x$  PDFs at low scales, virtually unreachable at current and upcoming experiments. NA66/AMBER’s focus is on pion and kaon PDFs using the theoretically clean DY process, typical DIS experiments can contribute to this avenue only in a model-dependent approach.

### LHCb-FT

**SMOG2:** Unpolarized fixed-target collisions at LHCb open a new chapter in LHC physics, offering novel opportunities that complement the traditional beam-beam studies. These opportunities notably include: (i) access to nucleon and nuclear PDFs at large Bjorken- $x$ , including the

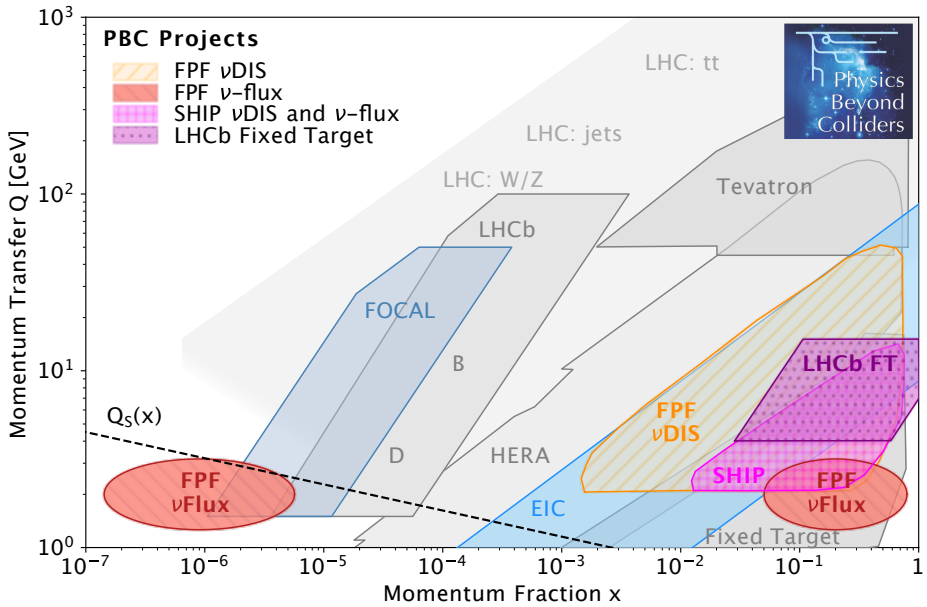


Figure 15: Kinematic coverage of proposed PBC experiments (as labelled), past/existing experiments (gray), and other proposed experiments (blue) in the momentum transfer  $Q$  versus momentum fraction  $x$  plane. Also indicated is the expected saturation scale  $Q_s$  in protons (dashed line) [389].

unpolarized TMDs, and (ii) studies of effects arising from (non-perturbative) intrinsic-charm contributions, expected at large  $x$ . Opportunities regarding nuclear matter and dark matter studies with SMOG2 will be addressed further below.

**LHCspin:** The physics case of LHCspin is mainly focused on the investigation of the nucleon spin structure, with a special emphasis on the TMDs and the GPDs of quarks and gluons. Polarized quark and gluon distributions can be studied at LHC with LHCspin through high-energy collisions of proton beams on transversely polarized hydrogen or deuterium targets. The golden process for accessing quark TMDs is DY, where a quark and an anti-quark annihilate to produce a charged lepton pair (e.g.,  $\mu^+ \mu^-$ ) in the final state. Another key aspect of this project is the possibility to access heavy quarks, which are primarily produced via gluon-gluon fusion. The production of quarkonia and open heavy-flavour states provides an efficient way to study the gluon dynamics inside nucleons and probe gluon TMDs. This is achieved by measuring inclusive production of heavy mesons such as  $J/\Psi$ ,  $D^0$ ,  $\eta_c$ ,  $\chi_c$ ,  $\chi_b$ , etc., for which the LHCb detector is well suited and optimized. Furthermore, isospin effects can be studied by comparing  $pp^\uparrow$  and  $pd^\uparrow$  collisions. Finally, by studying collisions of heavy-ion beams with polarized p or d targets, LHCspin enables innovative investigations of collectivity in small systems as well as access to higher-twist contribution to fragmentation functions.

### Gamma Factory possibilities/opportunities

The secondary photons of the GF at LHC would have an energy between 40 keV and 400 MeV. Unprecedentedly high intensity of the polarized photon beam will allow to study a number of low-energy observables relevant to nuclear and nucleon structure and to tests of fundamental

symmetries, hitherto inaccessible with the available photon sources. If the secondary photons of the GF can collide with a polarized fixed target at the LHC, then further opportunities would arise. The *c.m.* energy would be at most  $\sqrt{s} = 1$  GeV at a photon energy of 400 MeV, hence insufficient to probe nucleon partonic structure, but polarized structure functions  $g_1$  and  $g_5$  would be accessible in case of longitudinally polarized proton or nuclear targets. The polarized structure function  $g_1$  is of relevance to the Gerasimov-Drell-Hearn sum rule. The parity-violating polarized structure function  $g_5$  has never been measured with real photons before.

The further possibility of colliding these secondary photons with the LHC proton/ion beam would yield a *c.m.* energy  $\sqrt{s}$  up to 100 GeV, allowing one to perform studies of nucleon structure at (sub)asymptotic photon energies. This would allow to study with high statistics the parity violating structure function  $F_3$  with real photons that are circularly polarized, arising from loop contributions, rather than through  $\gamma$ -Z interference. This would be complementary to  $F_3$  studies at the future EIC, which will require high  $Q^2$  (electroproduction rather than photoproduction). Parity-violation studies with circularly polarized real photons moreover will provide information on odderon exchange without the need for comparison to antiparticle beams. Further opportunities are offered by exclusive and semi-inclusive vector-meson photoproduction, which would allow for studies of GPDs and TMDs.

### SHiP/NA67 possibilities/opportunities

The SHiP/NA67 experiment will provide information about the internal structure of the nucleon using neutrino interactions as a probe (see a discussion in [390] and in section 1.3 and 4.4.4 of [67]). First, it can measure the structure functions  $F_{4,5}$  with the precision of around 5%, corresponding to the systematic uncertainty in neutrino production flux. This estimate is reasonable assuming that the charm hadron production will be well measured; this may be done via combining the charm production measurements at the thin target NA65/DsTau experiment and  $J/\psi$  production in the thick SHiP/NA67-like target (section 4.5 of [67]). Second, the neutrino-induced charm production will allow probing the strange content of the nucleon. Last but not least, the neutrino cross-section measurements in the range of energies accessible at SHiP/NA67 (mainly within the range  $E_\nu < 100$  GeV) can be used in fitting nuclear PDFs. These questions will be studied in detail once the collaboration decides on the technology, dimensions, and placement of the SND@SHiP/NA67.

### FPF possibilities/opportunities

The FPF will also enable unique studies of the strong interaction and proton structure both via measurements of neutrino fluxes and interactions. Both high-energy electron neutrinos and tau neutrinos primarily originate from charm hadrons. These are mainly produced via gluon fusion with one gluon carrying a momentum fraction  $x \sim 1$  and the other  $x \sim 4m_c/s \sim 10^{-7}$ . Neutrino flux measurements at the FPF will therefore constrain the gluon PDFs in the low- $x$  region, beyond the coverage of all other existing and proposed experiments, as shown in the left panel of Figure 16. This will allow to probe BFKL dynamics [391] and gluon saturation [392]. Stringent constraints on models of  $D$ -meson fragmentation will also be provided.

The FPF also augments the LHC program with a *neutrino-ion collider* to probe charged current DIS. This complements the planned EIC, which will probe neutral current DIS in a similar

energy range. The large neutrino sample enables differential cross-section measurements to constrain PDFs. An example is shown in the right panel of Figure 16. These improvements will benefit key measurements at the LHC central detectors, such as Higgs or weak boson production [393], and help to break the degeneracy between QCD and new physics effects in LHC data interpretations [394].

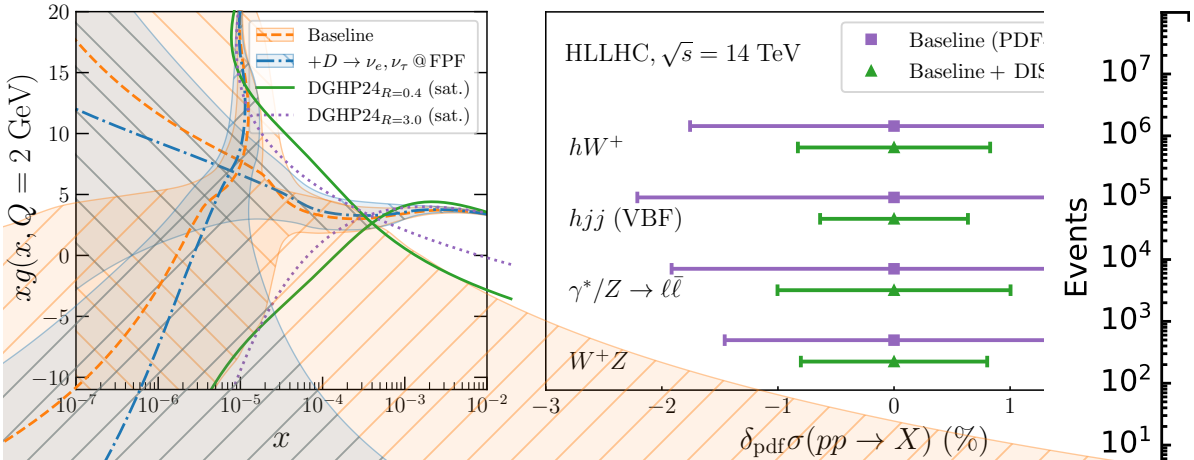


Figure 16: Left: Impact of neutrino flux measurements at the FPF on the small- $x$  gluon PDF. Right: Reduction of the PDF uncertainties on Higgs and weak gauge-boson cross sections at the HL-LHC, enabled by neutrino DIS measurements at the FPF. (Figures adapted from Ref. [223].)

## NA66/AMBER

The partonic structure of light mesons (e.g., pions and kaons) has garnered significant interest recently, driven by both phenomenological analyses of existing data and advancements in lattice QCD calculations [395, 396, 397, 398, 399, 400]. The observed differences in the relative momentum fractions carried by quarks and gluons in mesons compared to protons may provide valuable insights into fundamental questions, such as the mechanisms of baryon mass generation in QCD. However, the existing pion and especially kaon DY cross-section data, collected primarily in the 1980s, partially suffer from limited precision and notable tensions between experiments. This underscores the importance of the NA66/AMBER experiment’s physics program, which aims to measure the structures and charge radii of pions and kaons with unprecedented precision. NA66/AMBER’s efforts will provide the first comprehensive data on kaon PDFs while significantly enhancing the accuracy of pion structure determinations.

The kaon spectroscopy program of NA66/AMBER offers worldwide unique possibilities to deliver much-awaited new data for the strange-meson sector, allowing for a detailed comparison to theory predictions and for the search of strange exotic mesons like hybrids and tetraquarks. The envisaged  $2 \times 10^7$  exclusive events for the  $K^- \pi^- \pi^+$  final state with kaon beam would correspond to 100 times more data than that of the ACCMOR experiment [401], and 30 times more than the (acceptance-limited) COMPASS/NA58 data. Kaon spectroscopy with kaon beams could, in principle, be pursued with JLab Hall D’s tertiary  $K_L$  beam, but with a limited flux of about  $10^4 \text{ s}^{-1}$  in the momentum range  $0\text{--}11 \text{ GeV}/c$  [402]. Besides the low flux, there is an additional uncertainty in the production mechanism due to the rather low beam energy. Likewise, the new hall and

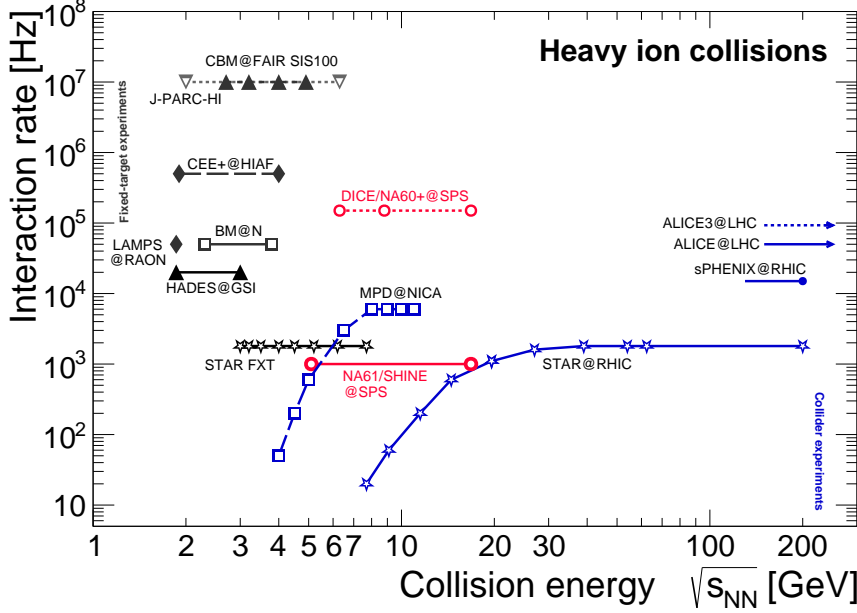


Figure 17: Interaction rate for existing (solid line), under construction (long-dashed line) and planned (short-dashed line) heavy-ion (Au–Au or Pb–Pb) experiments. Figure and caption from [100], which is adopted and updated from [404, 405, 406, 68]. Highlighted in red are the SPS DICE/NA60+ and NA61/SHINE projects.

beamline in planning at J-PARC (funding and timelines unclear), with a very high ( $10^7 \text{ s}^{-1}$ ) flux and reach of about 10 GeV [403], could, in principle, be used for kaon spectroscopy. However, there is no program for strange meson spectroscopy so far and the low energy, again, makes the separation between beam and target excitation very challenging. BES III, Belle II, as well as LHCb can study strange mesons in  $D$  or  $B$ -meson decays.  $D$ -meson decays are limited by the mass of the  $D$ -meson, and both channels need the knowledge of strong phases and final-state interactions, where input from NA66/AMBER is actually crucial.

### 5.3 Heavy-ion physics

Within PBC, heavy-ion physics is pursued both at the SPS (DICE/NA60+ and NA61/SHINE) and LHC (SMOG2) fixed-target setups. The SPS experiments occupy a unique and crucially important energy range from  $5.1 - 16.8 \text{ GeV} \sqrt{s_{NN}}$  in the global landscape of heavy-ion experiments, see Figure 17 and Table 8. In this regime we expect a change of the dynamics of heavy-ion collisions. This includes the approach to the potential critical end point of QCD and the emergence of inhomogeneous patterns such as a moat regime. In combination, DICE/NA60+ and NA61/SHINE offer a rather complete cover of interesting observables, see Table 8. Furthermore, SPS and LHC-FT measurements will also impact astroparticle physics via production studies relevant to cosmic-ray physics and DM searches. Collisions on hydrogen and helium targets reproduce primary cosmic-ray collisions in the interstellar medium, while data from nitrogen or oxygen targets (or proxies like neon) contribute to modeling extensive air showers from Ultra-High-Energy (UHE) cosmic rays in the atmosphere.

DICE/NA60+ aims at measuring rare probes of the QGP, and in particular heavy quarks and

	SIS18 / SIS100 HADES CBM		SPS NA61/SHINE DICE/NA60+		RHIC STAR	LHC ALICE / ALICE3
$\sqrt{s_{NN}}$ [GeV] Start date	1.9 – 4.9 running	2.7 – 4.9 2028	5.1 – 16.8 running light ions	6.3 – 16.8 >2029 Pb+Pb	3 – 200 running	2760 – 5440 running / 2035
Bulk properties	+	+	+	+	+	+
E-by-E fluctuations	+	+	+	+	+	+
Resonances	+	+	+	+	+	+
Open charm	higher energies		+	+	only top energy	
$c - \bar{c}$ correlations	higher energies		+	+	+	
Quarkonium	+	higher energies		+	+	+
Dileptons	+	+		+	+	+

Table 8: Synergy between SPS and *selected* other heavy-ion physics programs, covering a broad range of topics with a gradual transition from (left to right) properties of dense hadronic matter over onset of deconfinement and the location of the critical endpoint to the properties of quark-gluon plasma without always clear boundaries between them at the various experiments. Table and caption taken from [100].

lepton pairs. None of these studies were performed until now below top SPS energy with a decent integrated luminosity, nor will they become possible in the foreseeable future at any other facility in the collision energy range under discussion. On the contrary, this research domain is complementary to that already explored at hadron colliders (RHIC, LHC), in particular for heavy-quark measurements, and to that expected from lower-energy facilities (FAIR), in particular for dilepton-related observables.

More in detail, an energy scan in the region  $6 \text{ GeV} < \sqrt{s_{NN}} < 17 \text{ GeV}$  is planned. With the foreseen experimental setup, which includes a muon spectrometer coupled to a vertex spectrometer, the dimuon spectrum from threshold up to the charmonium region will be addressed. Lepton pairs are a unique tool to determine the temperatures and lifetime of the strongly interacting medium created in the collisions. Those are key quantities to investigate a possible anomalous behavior related to the onset of a first-order transition. In addition, dileptons provide direct information about hadron spectral functions, in particular the  $\rho$ -meson and its mixing with the chiral partner  $a_1$ , sensitive to chiral symmetry restoration which occurs in vicinity of the transition from hadrons to a QGP.

The investigation of charmonium states, and in particular  $J/\psi$ , has always been of paramount importance in QGP studies. Anomalous suppression effects are likely due to color screening in the QGP. They were observed at top SPS energies in the 1990s (NA50/NA60 experiments). They should disappear when moving toward lower energies. It would be particularly interesting to correlate them with a precise measurement of the temperature of the fireball, and perform comparisons with the temperature dependence of the modifications of the inter-quark potential, which can be computed starting from lattice QCD results.

Open heavy flavor hadrons ( $D^0, D^+, \Lambda_c$ ) represent excellent probes of the strongly interacting matter created in nuclear collisions, as demonstrated by extensive studies at RHIC/LHC energy. The initial temperature of system will be lower and more time will be spent in the hadronic phase, allowing stringent tests of theory predictions for the diffusion coefficient in this region. The degree of thermalization of charm quarks may also be accurately measured, through studies of the elliptic flow of charmed hadrons. Finally, the hadronization of a baryon-rich QGP may lead to even larger enhancement of baryon/meson ratios with respect to LHC energies.

NA61/SHINE is a fixed-target hadron spectrometer operating at the SPS, with the unique capability for large-acceptance hadron measurements over a versatile set of beams and targets in the specific regime of collision energy:  $5 \text{ GeV} < \sqrt{s_{\text{NN}}} < 17 \text{ GeV}$ . Its accumulated data set includes  $p+p$ ,  $p+C$ ,  $\pi+C$ ,  $K+C$ ,  $p+\text{Pb}$ ,  $\text{Be}+\text{Be}$ ,  $C+C$ ,  $\text{Ar}+\text{Sc}$ ,  $\text{Xe}+\text{La}$ , and  $\text{Pb}+\text{Pb}$  reactions, recorded at up to six beam momenta per reaction.

The primary objectives of the Collaboration are **(a)** to further explore QGP-related signatures in light-ion systems (oxygen-oxygen collisions) at  $\sqrt{s_{\text{NN}}} = 5.1, 7.6, \text{ and } 16.8 \text{ GeV}$  by the end of Run 3 (2026) and the beginning of Run 4 [201, 104], **(b)** a precision study of the violation of isospin symmetry in the  $\text{O}+\text{O}$  system, **(c)** the construction and installation of a new LAST during LS3 (2027-2029), and **(d)** a new series of measurements of charm and anti-charm hadron correlations in  $\text{Pb}+\text{Pb}$  collisions in Run 4, to investigate the space correlation (locality) of the  $c\bar{c}$  pair [407]. The studies performed in  $\text{O}+\text{O}$  reactions will be continued in  $\text{B}+\text{B}$  and/or  $\text{Mg}+\text{Mg}$  collisions [104]. Being charge-symmetric systems ( $Z=A-Z$ ),  $\text{O}+\text{O}$  and  $\text{Mg}+\text{Mg}$  reactions give a unique experimental opportunity to address the issue of the isospin-symmetry-violating charged-kaon excess [4]. On the other hand, the expected multiplicity of about one  $c\bar{c}$  pair in central  $\text{Pb}+\text{Pb}$  collisions at top SPS energy makes studies of  $c\bar{c}$  hadron correlations very promising for testing heavy-quark production locality and transport properties [407]. Also, extensive measurements of even-by-event (EbyE) fluctuations in  $\text{Pb}+\text{Pb}$  collisions are planned as a function of energy. They are meant as an independent verification of recent observations made at RHIC, argued as a possible indication of a Critical Point in the phase diagram of strongly interacting matter. The realization of oxygen data-taking does not necessitate any additions to the fully operational NA61/SHINE experiment. Implementing the LAST for  $c\bar{c}$  hadron correlation studies constitutes a major upgrade of the detector to be completed at the end of LS3.

The proposed large-acceptance measurements are not possible in the foreseeable future at accelerator facilities other than the SPS.

**SMOG2:** Studies of nuclear-matter effects can be performed using hydrogen as a reference system for comparison with larger nuclear targets such as argon, krypton, and xenon. Quarkonia production is a key tool to study the high temperature and density QCD regime. In these collisions, where on average only one  $c\bar{c}$  bound state is produced, one can probe charmonium suppression in a regime where contributions from charm quark recombination are expected to be negligible. Jet measurements represent an additional tool to explore cold nuclear matter in this unique phase space and collision system. Using  $p\text{H}_2$  collisions as a pp reference, measurements of nuclear modification factors ( $R_{pA}$ ) can be performed with jets produced in FT  $p\text{A}$  collisions, enabling precise studies of parton energy loss in cold nuclear matter as a function of the nuclear size  $A$  and of the relevant kinematic variables. Measurements with photon-tagged jets and charm jets will further allow flavour-dependent studies of parton energy loss with increasing nuclear size.

Precise antiproton and anti-nuclei production measurements in  $p\text{H}$  and  $p\text{He}$  collisions in the relevant energy regime of  $\sqrt{s_{\text{NN}}} \sim 100 \text{ GeV}$  allow for significant reduction of the present uncertainties on the production cross sections, which constitute the main limitation to the interpretation of data collected by space-borne experiments (PAMELA, AMS) searching for signals of DM.

## 5.4 Neutrino physics

### The Short Baseline Neutrino (SBN) beam

The novel short-baseline neutrino beam facility introduced in Sections 3.3.1 and 4.8.1 would represent a paradigm shift in the field by enabling the determination of neutrino-nucleus scattering amplitudes with a precision comparable to that achieved in electron-nucleus scattering. In particular, achieving sub-percent precision in cross-section measurements within the neutrino energy range of 0.6 to 5 GeV would be invaluable for DUNE and Hyper-K since their current uncertainties,  $\mathcal{O}(4\%)$ , exceed the expected experiment statistical uncertainties and would be the limiting factor in their systematics budgets.

The physics potential of the SBN experimental reference setup presented in Section 4.8.1 has been quantified for an integrated luminosity of  $1.4 \times 10^{19}$  PoTs, corresponding to  $\approx 5$  years of data-taking. The main highlights are:

- An absolute measurement of the inclusive  $\nu_\mu$  CC cross section in argon (and possibly water) with a precision of 1 % as function of energy from 0.6 to 5 GeV. Unlike current experiments, the neutrino energy is determined a priori, independent of final state particles reconstruction in the neutrino detector (which is biased by nuclear effects), with precisions of 10–20 % using the NBOA technique and below 1% for the tagged events. Figure 18 shows the expected energy distributions and the corresponding cross-section precision using both methods.
- A measurement of differential  $\nu_\mu$  cross sections where the momentum transfer is known a priori with a  $\approx 10$  % precision ( $\approx 1\%$  for tagging). This precision can be achieved in exclusive channels such as single-pion production in CC and NC events, thanks to the unprecedented resolution of the liquid argon TPC.
- An absolute measurement of the inclusive  $\nu_e$  CC cross section in argon (and possibly water) with a precision of 2 % (5 %) in the region of interest for DUNE (Hyper-K). By comparing measurements of  $\nu_e$  and  $\nu_\mu$ , the ratio of the cross sections, which is currently responsible for the largest projected source of systematic uncertainties on measurements of the CP-violating phase  $\delta$  with DUNE and Hyper-K, can also be measured to a similar level of precision.
- A direct determination from data of the energy smearing function (an essential input to neutrino oscillation studies but notoriously challenging to model) by comparing the reconstructed neutrino energy in the neutrino detector (as used in oscillation analyses) to the true neutrino energy estimated with neutrino tagging.

Given the outstanding precision in source characterization, SBN could also explore BSM processes, such as Non-Standard Interactions (NSI), the oscillation of sterile neutrinos at the 1 eV<sup>2</sup> mass scale, and the production of neutral LLPs. Additionally, the facility’s performance in anti-neutrino mode for the study of  $\bar{\nu}_\mu$  cross sections and the first direct measurement of  $\bar{\nu}_e$  interactions are under evaluation.

Last but not least, the neutrino tagging technique may pave the way to a post DUNE/Hyper-K sustainable high-precision Long Baseline Program in synergy with large deep-sea detectors developed for neutrino astronomy [155, 156].

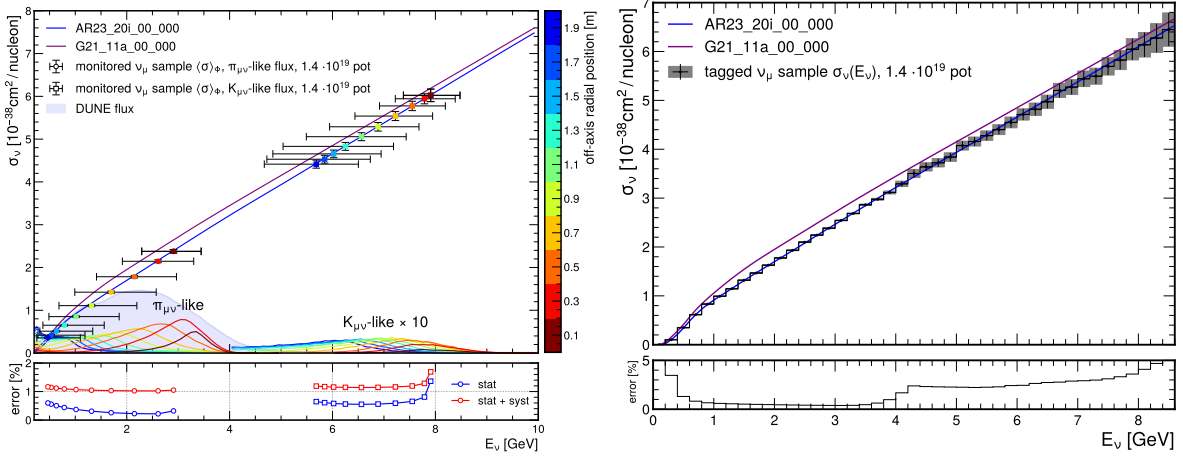
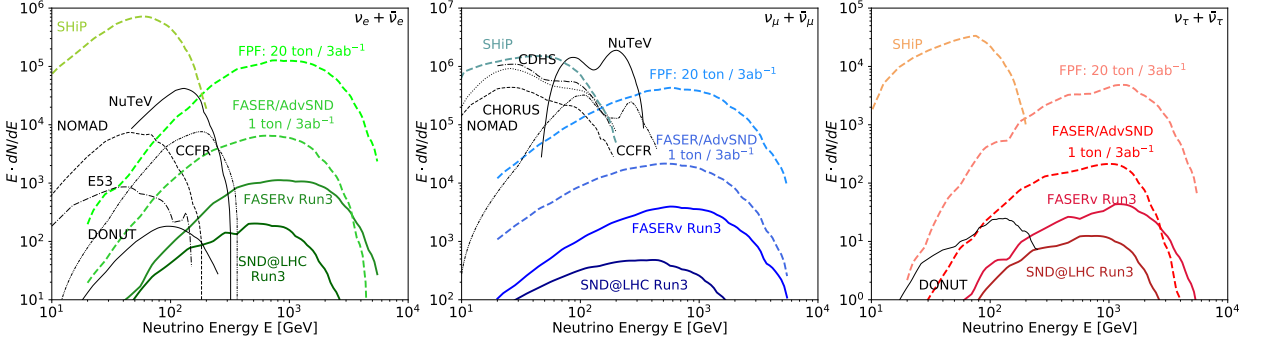


Figure 18: Determinations of the  $\nu_\mu$  CC inclusive cross section with the SBN facility. The measurements are compared to two models (blue and red lines). Left: Flux averaged cross section as a function of neutrino energy using the NBOA technique. The colored lines correspond to the fluxes at different radial distances, given by the colored scale to the right of the figure. The  $K_{\mu\nu}$  decay component of each flux has been artificially inflated by a factor of 10 for illustration purposes. Each NBOA flux has a corresponding predicted measurement point of the same color. Horizontal error bars encase the 68% percentiles with respect to the mean energy for the NBOA fluxes. The underlying figure shows the size of uncertainties due to available statistics (blue) and considering also systematic uncertainties related to the monitored flux prediction, assumed to be  $\sim 1\%$ , (red). The DUNE near-detector flux is shown for reference using an arbitrary normalization. Right: Projected measurement of the cross section as a function of neutrino energy using tagged neutrinos. In this case, the individual neutrino energies are measured with a sub-percent precision by reconstructing the kinematics of the parent meson 2-body decays. The error bars represent the statistical error expected on the measurement, also shown below the main figure. (Figures taken from [157].)

## Collider Neutrino Experiments

As the highest-energy particle collider built to date, the LHC is also the source of the most energetic human-made neutrinos. Indeed, it generates an intense, collimated beam of neutrinos of all three flavors with TeV energies in the forward direction. These neutrinos have been detected for the first time by the LHC far-forward FASER and SND@LHC experiments in 2023 [48, 56], a breakthrough observation making the *dawn of collider neutrino physics* [410], and first measurements of the neutrino flux and cross section have already been performed [50, 51]. Both FASER [411] and SND@LHC will operate until the end of LHC Run 3, where they are expected to collect about  $10^4$  neutrino interactions, and plan to continue operation with upgraded neutrino detectors during the HL-LHC era, where they could collect and study about  $10^5$  interactions. Additional neutrino detectors, FASERv2 and FLArE, with significantly larger target mass have been proposed as part of the FPF [221, 222, 223, 220], and could collect more than  $10^6$  neutrino interactions. Additional detector places at the surface exit points of the neutrino beam were also considered, but would require 1000 times larger detectors and correspondingly cheaper detector technologies to collect a comparable event rate [363, 364].

Figure 19 shows the event rates and energy spectra for these experiments, which will probe



**Figure 19: Neutrino yields at existing and proposed LHC neutrino experiments.** The plots show the expected event rate and energy spectrum of neutrinos interacting at collider neutrino experiments for all three neutrino flavors, following Ref. [408]. Spectra from previous accelerator experiments and the planned SHiP/NA67 experiment are shown for comparison [64]. (Figure adapted from Ref. [409].)

neutrino energies from hundreds of GeV to several TeV, i.e., well beyond current accelerator experiments, and with far higher event rates than FASER and SND@LHC in Run 3. The high statistics enable precision studies, including measurements of neutrino cross sections for all three flavors and tests of lepton flavor universality in neutrino scattering, complementing results from flavor physics and main LHC experiments. Notably, the large number of expected tau neutrino interactions, identifiable in the FASERv2 emulsion detectors, will allow for detailed studies of tau neutrinos, the least known of all SM particles. Measurements at FASERv2 will also allow for detecting the anti-tau neutrino for the first time.

LHC neutrino flux measurements will significantly impact astroparticle physics by validating and improving models of forward particle production. These models are essential for understanding particle production in extreme astrophysical environments and cosmic-ray interactions with Earth’s atmosphere. Collider neutrino experiments offer a unique opportunity to test these models at comparable energies under controlled conditions. For instance, they will shed light on the cosmic ray muon puzzle—a long-standing tension between measured and predicted muon counts in high-energy cosmic-ray air showers [416]. Thorough analyses suggest that an enhanced forward strangeness production could resolve this discrepancy [417]: this scenario can be tested using the LHC neutrino flux as shown in Figure 20. Additionally, the figure shows how collider data will reduce uncertainties in the prompt atmospheric neutrino flux [413]—arising from charmed hadron decays in cosmic-ray collisions—which is the dominating background for astrophysical neutrino searches above a few 100 TeV [415]. Collider neutrino data will therefore enhance astrophysical neutrino studies and multi-messenger astronomy [415].

## Neutrinos at SHiP/NA67

Proton interactions on the tungsten target produce a very intense neutrino flux, of all three flavors. Indeed, the beam dump is the ideal instrument to enrich the neutrino yield of tau neutrinos, since the thick and high-density target absorbs most of the hadrons rather than letting them decay, thus enhancing neutrinos from prompt, i.e., charmed hadron, decays. This feature enhances enormously the tau as well as the electron neutrino components when compared to muon neutrinos,

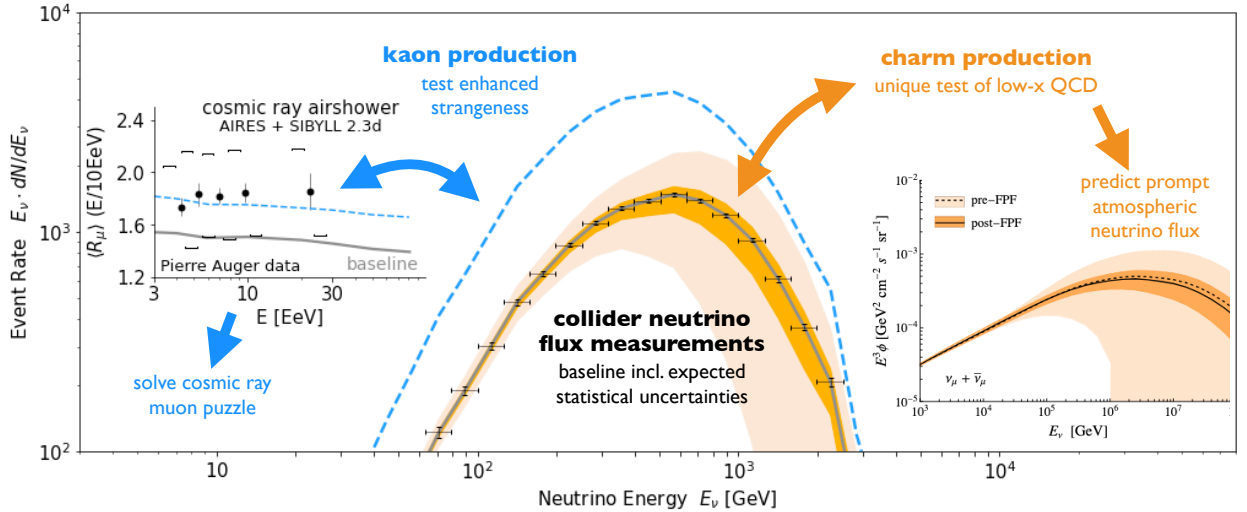


Figure 20: **Astroparticle physics at collider neutrino experiments.** The central part of the figure show expected energy spectrum of interacting electron neutrinos in the FLArE detector at the FPF (solid gray curve) and expected statistical uncertainties (black error bars). The left part considers a model of strangeness enhancement introduced in Ref. [412] which can resolve the discrepancy in the dimensionless muon shower content  $R_\mu$  for air shower data and would lead to sizable changes of the neutrino energy spectrum at the FPF and can therefore be tested. The right side of the figure shows how FPF data will reduce PDF uncertainties (orange band) on the prompt neutrino flux  $\Phi$  as a function of  $E_\nu$  [413, 414, 415]. (Figure from Ref. [223].)

thus allowing for unique studies of their behavior when interacting with matter. More than 90% of the  $\nu_e$ s interacting in the neutrino detector target are expected to originate from charmed hadron decays. Therefore, systematic uncertainties from the neutrino flux cancel out when, e.g., forming the  $\nu_e/\nu_\tau$  ratio, thus enabling LFU studies with neutrino interactions with unprecedented accuracy. The collected dataset will enable a rich program of neutrino physics measurements, providing valuable SM tests and serving as an essential benchmark for future neutrino experiments. SHiP/NA67 will measure nucleon/nucleus structure functions, probe the strange quark content of the nucleons, study neutrino-induced charm production and  $V_{cd}$  matrix elements with unprecedented accuracy. Notably, this aspect of SHiP/NA67's program offers a set of guaranteed measurements, ensuring high-impact physics results even in the absence of BSM discoveries.

## 5.5 Feebly-interacting particles and dark sectors

In spite of the many successes of the SM of particle physics, there are strong reasons for expecting new physics beyond the SM. From the theoretical viewpoint, it would be desirable to explain the large hierarchies of masses and apparent fine-tuning of parameters present in the SM. On the experimental side, there are various observations that cannot be explained within the SM, such as the amount of particle-antiparticle asymmetry in the universe, non-zero neutrino masses and the existence of a new form of matter called Dark Matter. All these problems may be addressed by postulating the existence of new particles at or below the GeV scale that have thus far evaded detection because of their feeble couplings to known matter. Examples include QCD axions [418, 419], relaxions [420, 421], right-handed neutrinos [422, 423] and mediators of DM interactions [424],

such as new scalar or gauge bosons arising from a spontaneously broken symmetry. All these particles, collectively referred to as Feebly Interacting Particles (FIPs), have been the focus of great experimental and theoretical efforts [2, 60, 61, 62].

To manage the large number of potential FIPs models with different coupling structures, PBC pursues a model-agnostic bottom-up approach [425], considering a small number of benchmark scenarios with coupling structures that resemble interactions known from the SM [60]. These benchmark scenarios highlight the complementarity of different FIPs production modes (including for example Higgs decays, meson decays and bremsstrahlung) and decay channels (including both charged and fully neutral final states). A key feature of FIPs is that, due to their small masses and feeble couplings, their proper decay length can be comparable to typical detector dimensions, and they can be produced with substantial boost factors. In large regions of parameter space, FIPs are therefore predicted to escape from the LHC main detectors before decaying, but they can be targeted with lower-energy accelerators or new LHC detectors placed further away from the production point. Depending on the specific processes under consideration, these dedicated detectors can be situated either in the forward direction or at large angles from the beam axis.

In the following, we present the sensitivity of various PBC experiments for a variety of different FIPs models. The sensitivities corresponds to an integrated luminosity of  $300 \text{ fb}^{-1}$  for projects using collisions at LHCb and  $3000 \text{ fb}^{-1}$  for projects using collisions at CMS or ATLAS, and  $6 \times 10^{20} \text{ PoT}$  for SHiP/NA67.

### 5.5.1 BENCHMARK MODELS

The PBC Benchmark Cases (BCs) were proposed originally in [60], then developed further in [61, 62], and have by now become a community standard. While several of these benchmarks are of primary relevance for high-intensity beam-dump experiments, others can be targeted by a wider range of complementary search strategies. The former BCs have been presented in detail in [64]; therefore we focus here on the latter. We emphasize that in spite of substantial efforts by the community, the various production and decay modes of FIPs are still subject to sizable theoretical uncertainties. The sensitivity projections of the various experiments treat these uncertainties in different ways. Hence, care must be taken when comparing different curves.

BC3 considers particles  $\chi$  with a fractional electric charge (so-called millicharge). In Figure 21, we show the sensitivity projections and existing limits for the parameter space of this model in the plane of the effective charge  $Q_\chi$  in units of elementary charge  $e$  versus mass  $m_\chi$ .

BC5 considers a dark scalar  $S$  mixing with the SM Higgs boson. The dark scalar can be produced both through rare meson decays (relevant for intensity-frontier experiments) and at the LHC through Higgs boson decays (with  $\text{BR}(h \rightarrow SS) = 0.01$ ). In Figure 22, we show sensitivity projections and existing limits on the parameter space of this model in the  $\sin \theta$  vs.  $m_S$  plane under the assumption that both  $\lambda$  and  $\mu$  are nonzero, see [60] for details.

BC7 considers HNLs coupling exclusively to the second lepton generation. They can be produced both in rare meson decays (relevant for intensity-frontier experiments) and in electroweak processes at the LHC. In Figure 23, we show sensitivity projections and existing limits on the parameter space of this model in the  $|U_\mu|^2 = \theta_\mu^2$  versus  $m_N$  plane under the hypothesis that  $|U_e|^2 = |U_\tau|^2 = 0$ , see [60] for details. We note that models of HNLs linked to the generation of neutrino masses typically have a more complex flavour structure [451] but lead to a rather similar phenomenology [452].

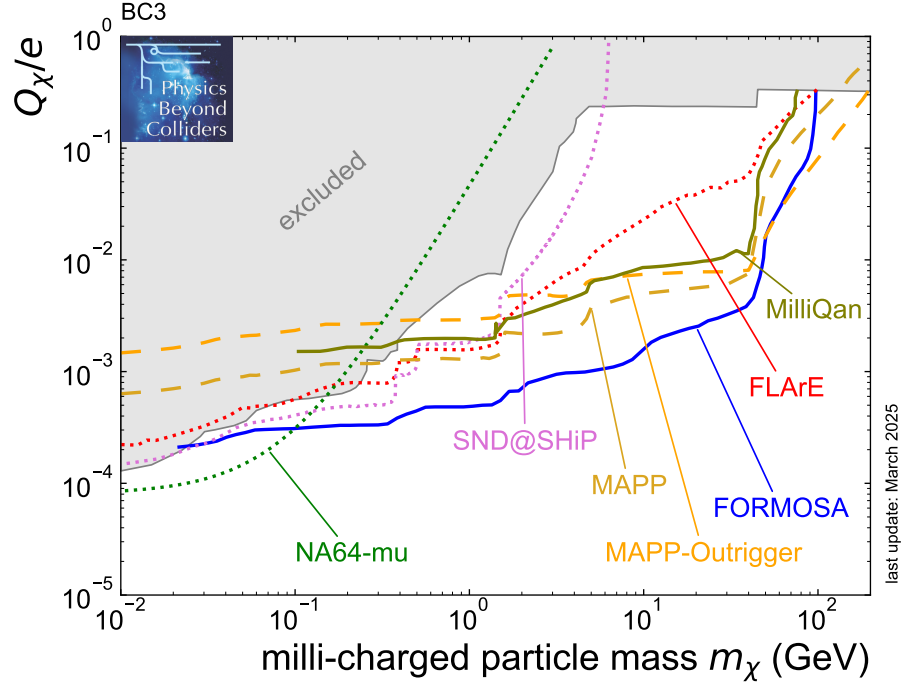


Figure 21: Sensitivity projections for the FPC benchmark BC3 for millicharged particles  $\chi$  in the plane of the effective charge  $Q_\chi$  in units of elementary charge  $e$  versus  $\chi$  mass  $m_\chi$ . For the various projections, the line style reflects the maturity of the background estimates: solid lines correspond to background estimates based on the extrapolation of existing data sets, dashed lines indicate background estimates based on full Monte Carlo simulations, and dotted lines represent projections based on toy Monte Carlo simulations or on the assumption that backgrounds are negligible. Upper limits on the effective charge  $Q_\chi/e$  as function of the milli-charged particle mass  $m_\chi$  stem from ArgoNeuT [426], MilliQan-Prototype [427], MilliQ/SLAC [428], LSND [429, 430], SuperK [431], SENSEI [432], and CMS [433] as well as from reinterpretations of BEBC [434] and a combination of LEP-based results [427]. Note that these reinterpretations were not performed by the experimental collaborations and without access to raw data. Relevant sensitivity is expected also for a proposed LAr detector at SHiP/NA67, but no detailed estimates are available [210].

### 5.5.2 SHOWCASE MODELS

While the benchmark models established by the PBC initiative [60] have been a worldwide success and a valuable asset for the development and presentation of experimental proposals, the landscape of these models is not at all static. New or modified models are constantly being proposed and discussed by the FPC, in order to refine the phenomenological description and determine benchmark cases of particular interest. In the following, we present several examples of such models, which have been selected to highlight exciting physics opportunities for specific PBC experiments not covered by the usual benchmark models. We emphasize that these models have not yet reached the same level of sophistication as the benchmark models discussed above, which means in particular that not all potentially relevant experiments have been able to perform the signal and background simulations needed for detailed sensitivity studies. Just because a specific experiment is not shown in these plots therefore does not mean that the experiment is insensitive. We comment

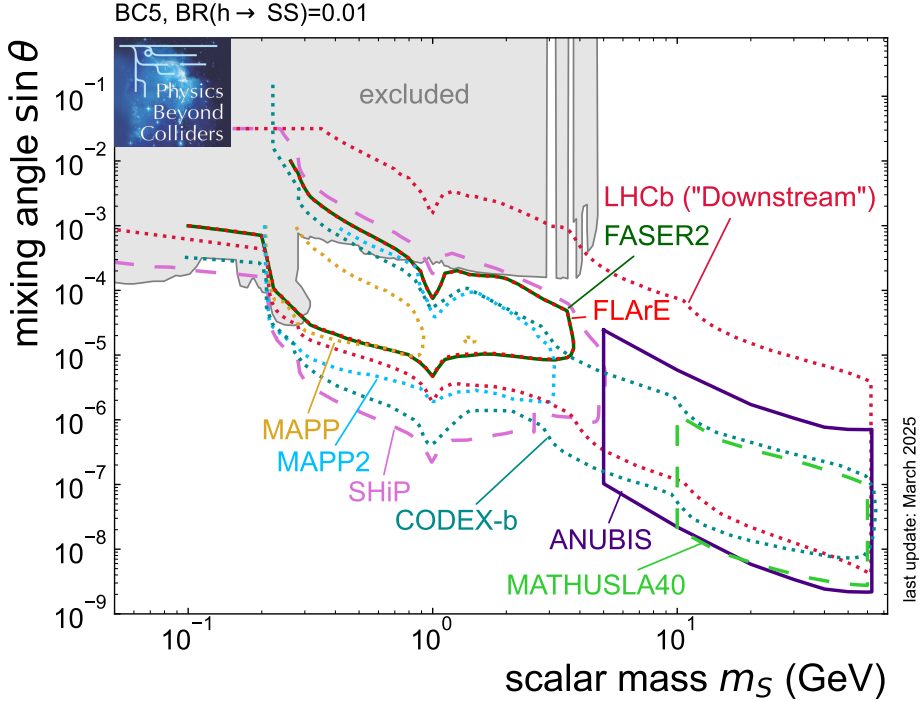


Figure 22: Sensitivity projections for the FPC benchmark BC5 for the dark scalar mixing with the Higgs in the plane of mixing angle  $\sin \theta$  versus dark scalar mass  $m_S$  under the hypothesis that both parameters  $\lambda$  and  $\mu$  are different from zero. For the various projections, the line style reflects the maturity of the background estimates: solid lines correspond to background estimates based on the extrapolation of existing data sets, dashed lines indicate background estimates based on full Monte Carlo simulations, and dotted lines represent projections based on toy Monte Carlo simulations or on the assumption that backgrounds are negligible. The sensitivity projections have been obtained assuming  $\text{BR}(h \rightarrow SS) = 10^{-2}$ . The sensitivity projection labeled ‘LHCb (“Downstream”)’ is taken from [435]. Upper limits on the mixing angle  $\sin \theta$  as function of scalar mass  $m_S$  from E949 [436], NA62 [437, 438], MicroBooNE [439, 440, 441], KOTO [442, 441], ICARUS [443], LHCb [444, 445, 446], Belle II [447]) as well as reinterpretations of PS191 [448], CHARM [207, 446], and LSND [449]. Note that these reinterpretations were not performed by the experimental collaborations and without access to raw data. The sensitivity of MATHUSLA40 for smaller masses is under study. Belle II is expected to providing a distinctive handle on the production mode by reconstructing the complete  $B$ -meson decay [450].

on these additional opportunities in the respective figure captions.

### Exotic Higgs decays to long-lived scalars

Extended Higgs sectors often feature additional scalar or pseudoscalar states ( $X$ ) lighter than the SM Higgs boson, which couple to the latter through mixed quartic terms in the scalar potential [247]. For  $m_X < m_h/2$ , this opens up the possibility that the SM Higgs boson decays into pairs of such (pseudo)scalars [470]. Based on the hypothesis of minimal flavour violation, these particles are expected to couple to fermions proportional to their mass. Couplings to down-type quarks

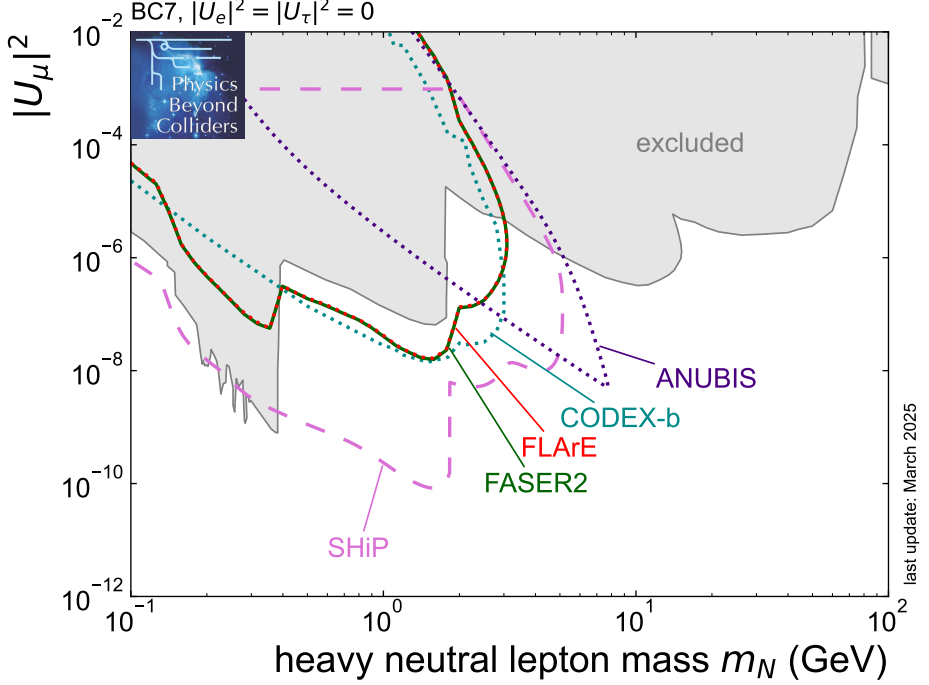


Figure 23: Sensitivity projections for the FPC benchmark BC7 for HNLs with coupling to the second lepton generation only in the plane of the squared magnitude  $|U_\mu|^2 = \theta_\mu^2$  of the mixing angle  $\theta_\mu$  versus HNLs mass  $m_N$  under the hypothesis that  $|U_e|^2 = |U_\tau|^2 = 0$ . For the various projections, the line style reflects the maturity of the background estimates: solid lines correspond to background estimates based on the extrapolation of existing data sets, dashed lines indicate background estimates based on full Monte Carlo simulations, and dotted lines represent projections based on toy Monte Carlo simulations or on the assumption that backgrounds are negligible. Upper limits on the mixing angle  $|U_\mu|^2$  as function of HNLs mass  $m_N$  from NuTeV (90 % CL [453]), BEBC (90 % CL [454]), T2K (90 % CL [455]), NA62 (90 % CL [456]), E949 (90 % CL [457]), MicroBooNE (90 % CL [458]), CMS (95 % CL [459, 460, 461]), ATLAS (95 % CL [462]), CHARM-II (90 % CL [463]), and DELPHI (90 % CL [464]). Relevant sensitivity is expected also for MATH-USLA40 as well as for long-lived particle searches at ATLAS and CMS using HL-LHC data, but no detailed estimates are available. Projected sensitivities for LHCb ("Downstream") using HL-LHC data can be found in [435].

may be further enhanced for example in Two-Higgs doublet models [471]. In such a setup, the (pseudo)scalar is expected to decay with nearly 100% probability into  $b$ -quark pairs. The decay width, and hence the proper decay length  $c\tau_X$ , is however independent from the production mode, such that detectors placed at different distance from the interaction points at the LHC are needed for optimal coverage of the model parameter space. We show current constraints and sensitivity projections in Figure 24.

### Exotic Higgs decays to long-lived dark photons

Models of dark photons ( $A'$ ) often do not specify the mechanism that generates the gauge boson mass. If the mass is generated via a new scalar field analogous to the Higgs mechanism of the SM,

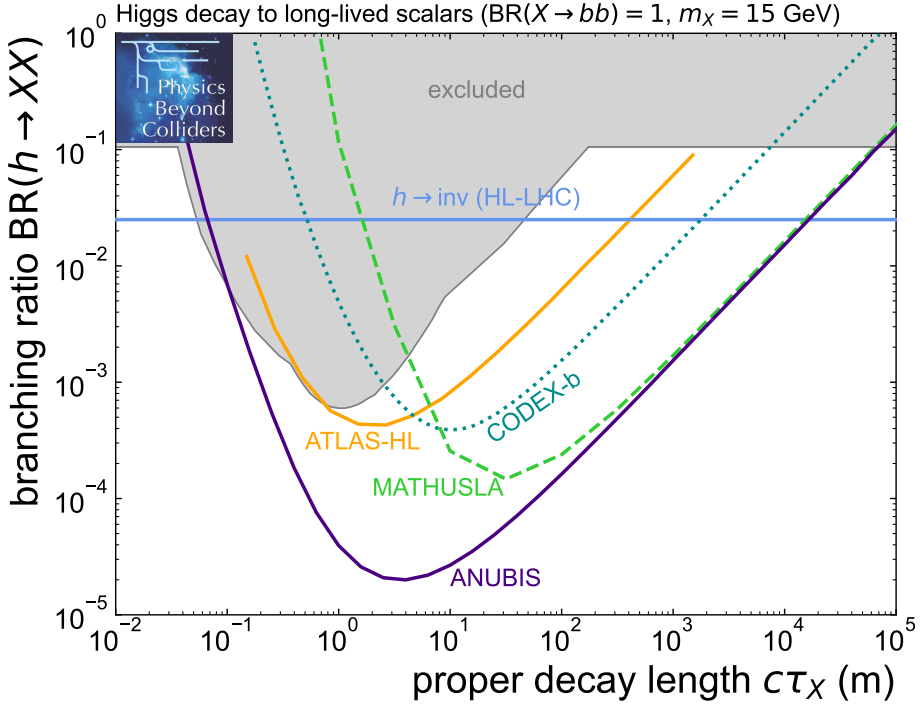


Figure 24: Sensitivity projections for Higgs boson decays into long-lived (pseudo)scalars with  $m_X = 15 \text{ GeV}$  in the plane of proper decay length  $c\tau_X$  versus the exotic Higgs branching ratio  $\text{BR}(h \rightarrow XX)$ . For concreteness we assume that the (pseudo)scalars have 100% branching ratio into  $b$ -quark pairs, but similar sensitivities are expected for other hadronic final states. For the various projections, the line style reflects the maturity of the background estimates: solid lines correspond to background estimates based on the extrapolation of existing data sets, dashed lines indicate background estimates based on full Monte Carlo simulations, and dotted lines represent projections based on toy Monte Carlo simulations or on the assumption that backgrounds are negligible. Existing exclusion limits come from ATLAS [465] and CMS [466], as well as from a combination of different bounds on the Higgs invisible branching ratio [467]. The corresponding projection for HL-LHC is taken from ref. [468], while the projection for LLP searches at ATLAS is taken from Ref. [469]. Relevant sensitivity is expected also for LLP searches at ATLAS and CMS using HL-LHC data, but no detailed estimates are available. In addition, LHCb ("Downstream") may also have sensitivity to this model, utilizing the same search strategy as for the BC5 model [435].

the two Higgs fields can mix with each other [473, 474]. As a result, the SM Higgs boson obtains a new tree-level decay mode  $h \rightarrow A'A'$  analogous to the SM decay modes into  $Z$  and  $W$  bosons [475]. The branching ratio depends primarily on the Higgs mixing and can be varied independently from the dark photon mass  $m_{A'}$  and the other couplings of the dark photon such as the kinetic mixing, which determine its proper decay length  $c\tau_{A'}$  [476]. These so-called Hidden Abelian Higgs Models can be probed by searches for LLPs produced in Higgs boson decays [441]. Dark photons with mass below a few GeV will decay from a displaced vertex into a low multiplicity of charged leptons or hadrons. This signature presents a challenge for the LHC main detectors but can be targeted with dedicated detectors for LLPs such as CODEX-b. Complementary constraints come

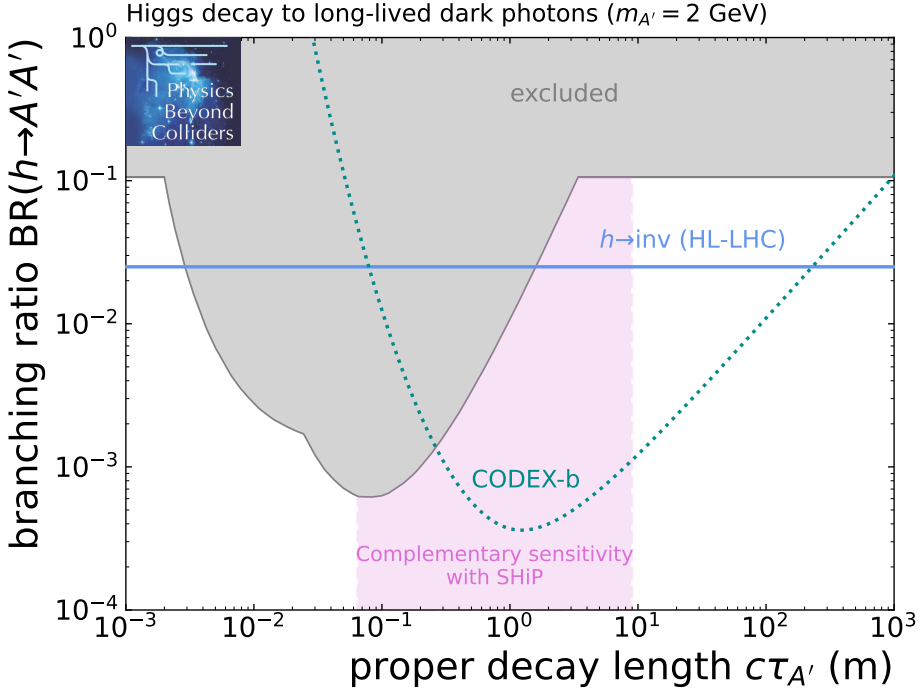


Figure 25: Sensitivity projections for Higgs boson decays into long-lived dark photons with mass  $m_{A'} = 2\text{ GeV}$  in the plane of proper decay length  $c\tau_{A'}$  versus the exotic Higgs branching ratio  $\text{BR}(h \rightarrow A'A')$ . For the various projections, the line style reflects the maturity of the background estimates: solid lines correspond to background estimates based on the extrapolation of existing data sets, dashed lines indicate background estimates based on full Monte Carlo simulations, and dotted lines represent projections based on toy Monte Carlo simulations or on the assumption that backgrounds are negligible. Existing exclusion limits come from an ATLAS search [472] and from a combination of different bounds on the Higgs invisible branching ratio [467]. The corresponding projection for HL-LHC is taken from Ref. [468]. In the red shaded region, dark photons can be directly produced via kinetic mixing and detected at SHiP/NA67, offering complementary detection prospects. Relevant sensitivity is expected also for MATHUSLA40 and ANUBIS, as well as for ATLAS and CMS using HL-LHC data, but no detailed estimates are available.

from SHiP, which is not sensitive to exotic Higgs boson decays but can search for dark photons produced directly via kinetic mixing, which gives an independent parameter that does not directly affect the branching ratio. Other experiments that are sensitive to long-lived dark photons produced via kinetic mixing either probe shorter lifetimes (e.g., Belle II [477]) or are not sensitive to such heavy dark photons. We show current constraints and sensitivity projections in Figure 25.

### Inelastic-Dipole Dark Matter

Models of inelastic DM, which involve transitions between two states  $\chi$  and  $\chi^*$  of slightly different mass, provide attractive targets for accelerator experiments, since the strong constraints from direct and indirect detection experiments can be evaded and the observed DM relic density can be reproduced [478]. A particularly simple realisation of this idea is inelastic dipole DM, in which DM particles possess a transition dipole moment that couples directly to the electromagnetic

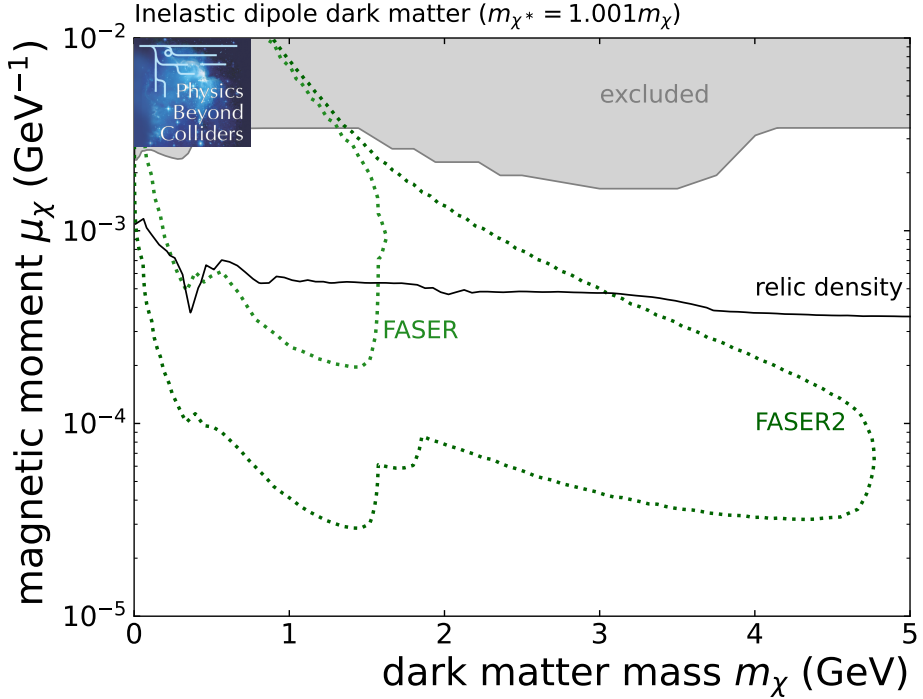


Figure 26: Sensitivity projections for inelastic-dipole DM in the plane of DM mass  $m_\chi$  versus magnetic dipole moment  $\mu_\chi$  for a very small mass splitting of  $m_{\chi^*} = 1.001m_\chi$ . For the various projections, the line style reflects the maturity of the background estimates: solid lines correspond to background estimates based on the extrapolation of existing data sets, dashed lines indicate background estimates based on full Monte Carlo simulations, and dotted lines represent projections based on toy Monte Carlo simulations or on the assumption that backgrounds are negligible. Existing exclusion limits come from reinterpretations [478] of LEP [479] and BaBar [480] data. Note that these reinterpretations were not performed by the experimental collaborations and without access to raw data. For larger mass splittings than considered here, relevant sensitivity is expected also for SHiP/NA67 (using both SND and LAr detectors) and for LLP searches at Belle II.

field strength tensor, such that the entire model is characterised by the two masses and the dipole moment [481]. For sufficiently large mass splitting ( $m_{\chi^*} \gtrsim 1.1m_\chi$ ) the model can be constrained with a variety of collider and fixed-target experiments, such as Belle II [482] and long-lived particle detectors such as SHiP/NA67 [483] or NA64 [24]. However, for much smaller mass splittings, the energy released in the de-excitation process  $\chi^* \rightarrow \chi + \gamma$  is so small that it can only be detected if  $\chi^*$  is highly boosted. In this case, forward experiments like FASER2 have particularly promising prospects [481]. We show current constraints and sensitivity projections in Figure 26.

### $L_\mu - L_\tau$ gauge boson

Among the simplest gauge extensions of the SM are models involving gauged lepton number  $L$  and/or baryon number  $B$  [488]. These models can be made anomaly-free if one includes three right-handed neutrinos that are singlets under the SM gauge group. While gauged  $B - L$  is tightly

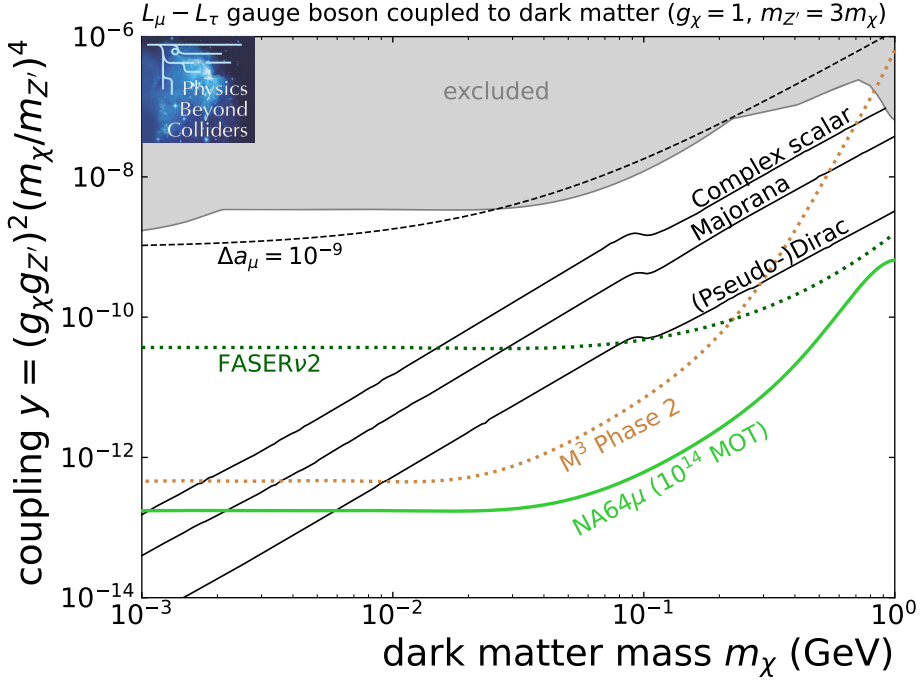


Figure 27: Sensitivity projections for a  $L_\mu - L_\tau$  gauge boson coupled to DM in the plane of DM mass  $m_\chi$  versus the effective DM-SM coupling  $y = (g_\chi g_{Z'})^2 (m_\chi/m_{Z'})^4$ . Here  $g_\chi = 1$  denotes the coupling of the DM particle to the  $Z'$  gauge boson and the mass ratio has been fixed to  $m_{Z'} = 3m_\chi$ , while the gauge coupling  $g_{Z'}$  is a free parameter. For the various projections, the line style reflects the maturity of the background estimates: solid lines correspond to background estimates based on the extrapolation of existing data sets, dashed lines indicate background estimates based on full Monte Carlo simulations, and dotted lines represent projections based on toy Monte Carlo simulations or on the assumption that backgrounds are negligible. Existing exclusion limits come from NA64e [26], NA64μ [484], Belle II [485] and a reinterpretation [486] of data from CCFR [487]. Note that this reinterpretation was not performed by the experimental collaboration and without access to raw data. Relevant sensitivity is expected also for future Belle II searches with more data, but no detailed estimates are available.

constrained by electron-positron colliders and electron beam-dump experiments, these constraints are evaded in models of gauged  $L_\mu - L_\tau$ , where couplings to electrons are absent [489]. As a result, these models can give a sizable contribution to the muon anomalous magnetic moment  $\Delta a_\mu$  [490]. If the corresponding gauge boson  $Z'$  acts as mediator between the SM and a DM particle  $\chi$ , it is possible to reproduce the observed DM relic abundance for complex scalar DM, Majorana DM and (Pseudo-)Dirac DM [491]. The most promising experiments to probe the interesting regions of parameter space are those involving muon beams, such as NA64μ [484] or the proposed  $M^3$  experiment [492], as well as experiments sensitive to particle scattering in forward detectors, such as FASERv2. We show current constraints and sensitivity projections in Figure 27.

### 5.5.3 EXPERIMENTS TABLE

Several experiments within PBC have been proposed to investigate signatures of BSM physics. These experiments primarily target LLPs, DM candidates, neutrinos, and milli-charged particles. Table 9 provides a summary of the experimental parameters for these proposed experiments. The comparison shows accelerator facilities, interaction points, detector acceptance in pseudorapidity and azimuthal coverage, decay volume specifications, and detector instrumentation.

	MATHUSLA40	CODEX-b	ANUBIS	FASER2	FASERv2	FORMOSA	FLArE
Accelerator	HL-LHC	HL-LHC	HL-LHC	HL-LHC	HL-LHC	HL-LHC	HL-LHC
IP/Facility	CMS	LHCb	ATLAS	FPF	FPF	FPF	FPF
Physics focus	LLP	LLP	LLP	$\nu$ , LLP	$\nu$ , DM	mQP	$\nu$ , DM, LLP, mQP
$\eta$ coverage	0.69 – 1.1	0.13 – 0.54	-0.965 – 0.965*	> 6.7	> 8	> 7	> 5.6
$\phi$ coverage [rad]	0.5	0.36	1.53*	$2\pi$	$2\pi$	$2\pi$	$2\pi$
Distance [m]	120	25	23*	620	620	620	620
Overburden [mwe $^\diamond$ ]	0	250	150**	250	250	250	250
Decay volume length [m]	14	10	15	10	6 $^\dagger$	5	7
Magnetic field	no	no	yes $^\ddagger$	yes	no	no	yes $^\ddagger$
Timing [ps]	1000	100	250	100	no	100	300
Calorimeter	no	no	no	yes	yes	no	yes
Tracking	yes	yes	yes	yes	yes	approximate	yes
Charge threshold	1e	1e	1e	1e	1e	<0.001e	0.01e
Reference	[249]	[242]	[234, 235]	[223, 222, 493]	[50]	[227, 222]	[494, 495]

	NA64	SND	SHiP/NA67	MAPP-Outrigger	MAPP-2	SND@HL-LHC
Accelerator	SPS	SPS	SPS	LHC, HL-LHC	LHC, HL-LHC	HL-LHC
IP/Facility	-	BDF	BDF	LHCb	LHCb	ATLAS
Physics focus	LLP, DM	$\nu$ , DM	LLP	mQP, LLP	LLP	$\nu$ , DM
$\eta$ coverage	fixed target	> 2.2	> 1.7	-4.4 – -3.3	1.4 – 3.0	6.9 – 7.6
$\phi$ coverage [rad]	$2\pi$	$2\pi$	$2\pi$	0.07–0.2	0.2–0.9	0.79
Distance [m]	active dump	28	32	120	25–55	480
Overburden [mwe $^\diamond$ ]	0	0	0	270	270	250
Decay volume length [m]	5	1.2 $^\dagger$	50	up to 60 $^\$$	6–15	0.9 $^\dagger$
Magnetic field	yes	yes	yes	no	no	yes
Timing [ps]	1000	500	100	500	1000	50
Calorimeter	yes	yes	yes	no	no	yes
Tracking	yes	yes	yes	approximate	yes	yes
Charge threshold	1e	1e	1e	0.01e	1e	1e
Reference	[496]	[497]	[67, 497]	[498]	[499]	[230]

Table 9: Summary of experimental parameters for proposed PBC BSM experiments designed to probe LLPs, DM candidates, neutrinos, and mQPs.

\* This is the ANUBIS "ceiling" configuration described in [235].

\*\* This value does not account for the two access shafts to the ATLAS cavern that are air-filled. Depending on the angle of the incoming cosmic ray and its position, the effective overburden is significantly lower.

$^\dagger$  Length of instrumented target instead of an empty decay volume.

$^\$$  The distance between LHCb and the MAPP-Outrigger is filled with concrete and rock. LLP decay products must have sufficient momentum to avoid being absorbed. No decay vertex reconstruction is possible.

$^\ddagger$  Stray magnetic field of the ATLAS muon spectrometer.

$^\ddagger$  Magnet only in HCAL section, not in LAr.

$^\diamond$  The approximate shielding against cosmic particles is given in meter water equivalent (mwe), which represents the depth of water that would provide the same level of attenuation, assuming a rock density of 2.51 g/cm $^3$ .

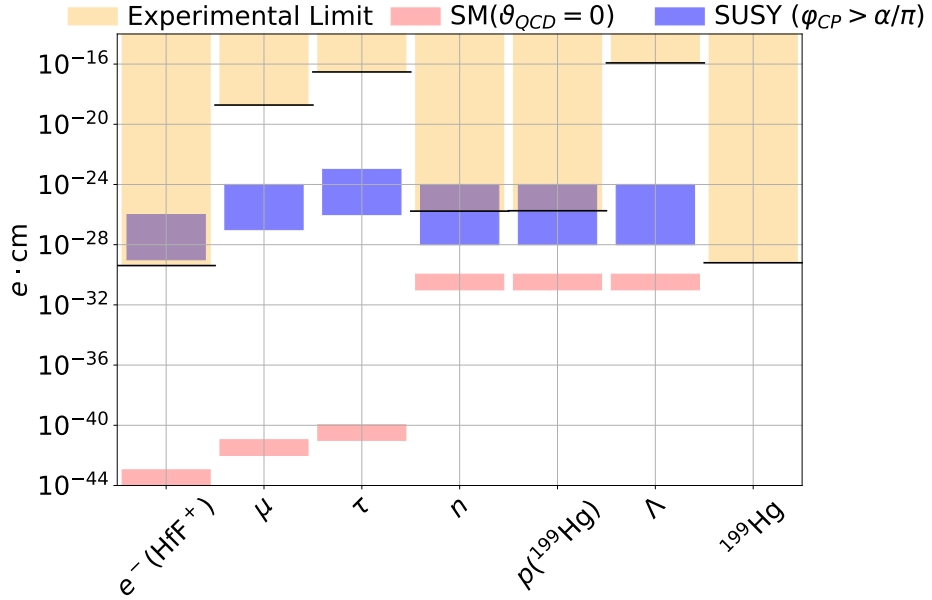


Figure 28: Upper Limits on EDMs for various leptons, hadrons and the Hg atom [504, 505, 506, 507, 508, 509, 510], and corresponding expectations from the SM and its super-symmetric extension. (Figure adapted from Ref. [511]; cf., e.g., Refs. [500, 501, 502] for some SUSY estimates.)

## 5.6 Electric dipole moment

Particles with spin, not identical to their antiparticles, possess an MDM, which characterizes the strength of the spin coupling to external magnetic field. In addition to the MDM, the spin can also contain a coupling to the external electric field, with the strength regulated by the EDM. These have long been identified as powerful probes of new BSM physics (cf., e.g., [500, 501, 502, 503] for some overviews). The EDMs are forbidden if  $P$  and  $T$  are exact symmetries, and the search for EDMs is equivalent to searches of CP violation. Unlike the decays of  $K, B, D$  mesons, where CP violation has been observed, EDMs represent the test of CP violation in the flavour-diagonal channel. Such violation is extremely well motivated by theories of baryogenesis, i.e., the dynamical generation of the baryon asymmetry of the Universe from the initially particle-antiparticle symmetric state. Multi-decade efforts to detect EDMs resulted in the upper limits on the EDMs of neutrons, nuclei, electrons, and muons. Only indirect limits exist for the EDMs of heavier flavours. Also, the proton EDM  $d_p$  limit can be extracted from the atomic EDM experiments, but right now lag behind sensitivity to neutron EDM,  $d_n$ .

The SM is believed to have two sources of CP violation. One firmly established source, the Kobayashi-Maskawa phase of the quark weak charged currents, predicts tiny EDMs not observable in the near future. The second source of CP violation, the QCD theta term, if large, would predict very large EDMs for neutrons, protons and nuclei, and therefore is severely limited. The absence of the EDMs induced by theta motivates the dynamical mechanism of its removal, connected to a new particle, the QCD axion. Thus, searches of EDMs represent the searches of new CP-violating physics, that manifest itself over the expected EDMs from the Kobayashi-Maskawa phase.

Current EDM sensitivities (with the limit on electron EDM being at  $4 \times 10^{-30} e\cdot\text{cm}$  [504]), depending on the model of New Physics, may be sensitive to energy scales vastly exceeding the

electroweak scale, and indeed even the reach of the LHC, being truly a probe “beyond the collider reach”. Therefore, the continuation of the EDM program worldwide is one of the priorities of fundamental physics searches. Current experimental limits and predictions for selected cases is presented in Figure 28.

The main goal of the cpEDM project is to advance sensitivity to the EDMs of charged particles, and in particular, proton EDM  $d_p$ . The main idea is to circulate a well controlled and spin-polarized proton beam in a storage ring in the configuration that minimizes spin evolution due to the proton MDM. The stated goal (cf., e.g., [512]) of the experiment is to reach the level of  $10^{-29}e\cdot\text{cm}$ , which would make proton probe even more valuable than the current  $d_n$  sensitivity and on par with  $d_e$ , but naturally sensitive to a wider variety of new physics models that involve strongly-interacting particles. ALADDIN on the other hand aims at measuring the MDM and EDM of charmed baryons, such as  $\Lambda_c^+$  and  $\Xi_c^+$ , produced in a fixed-target setup in which protons from the LHC halo are deflected on a tungsten target and produced baryons channeled through a bent crystal inducing spin precession. Simulation studies suggest that ALADDIN can achieve a 10 % precision on the MDMs and can set first direct limits on the EDMs at the  $10^{-16}e\cdot\text{cm}$  level within some years of data-taking. It also offers the opportunity to explore the EDM of the  $\tau$  lepton.

## 5.7 Gravitational Wave Detection

Measurements of Gravitational Waves (GWs) have become essential tools for exploring astrophysics and cosmology, opening a new way to study the Universe beyond traditional electromagnetic observations. Figure 29 illustrates some astrophysical sources of GWs and the sensitivities of selected detectors. Experiments based on Atom Interferometry (AI), such as that suggested for the PX46 access shaft at CERN [292], offer sensitivity in a frequency range that is inaccessible to current and planned laser interferometers such as LIGO [513], Virgo [514], KAGRA [515], ET [516] and LISA [517]. Among the targets in this frequency range are GWs from the mergers of black holes with masses intermediate between the stellar-mass black holes discovered by LIGO, Virgo and KAGRA and the supermassive black holes (SMBHs) found in the cores of galaxies [518]. Measurements of the mergers of such intermediate mass black holes may cast light on the formation of SMBHs. FLASH targets GWs at very high frequencies beyond 100 MHz: for a survey of possible sources of high-frequency GWs from physics beyond the Standard Model, see [519].

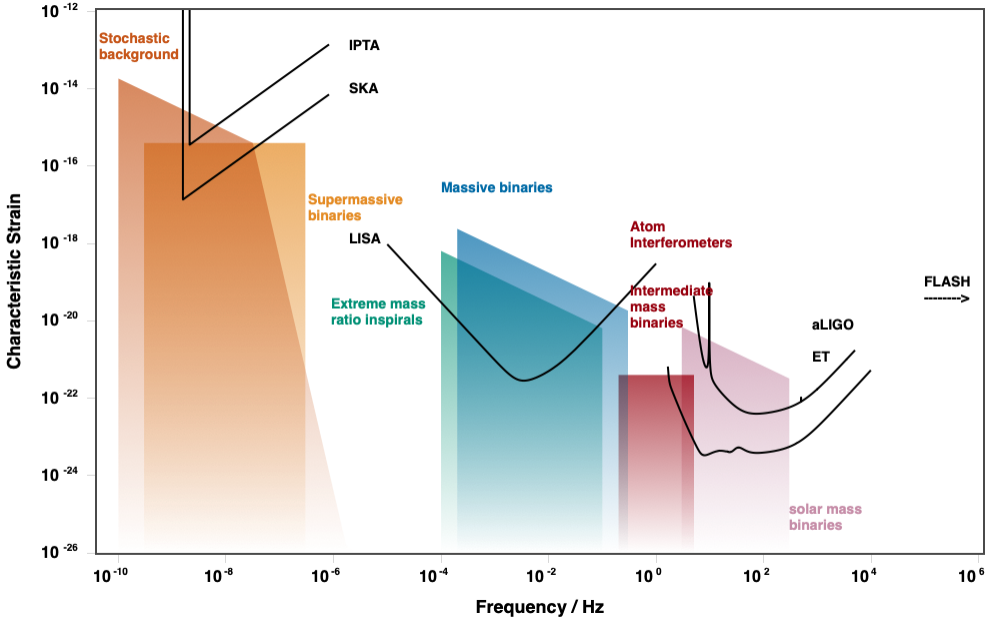


Figure 29: Spectrum of possible sources of GWs and the sensitivities of existing and planned detectors. AI experiments such as that suggested for CERN [292] target the range of frequencies intermediate between LIGO [513]/ET [516] and LISA [517], while FLASH [297] targets HFGW with frequencies above 100 MHz. Plot prepared using `GWplotter` [520].

## Acknowledgments

The work of F.Kl. was supported by the Deutsche Forschungsgemeinschaft under Germany’s Excellence Strategy – EXC 2121 Quantum Universe – 390833306. G.S. acknowledges support by the State Agency for Research of the Spanish Ministry of Science and Innovation through the grant PID2022-136510NB-C33 as well as via the QuantERA project T-NiSQ grant PCI2022-132984 funded by MCIN/AEI/10.13039/501100011033 and by the European Union “NextGenerationEU”/PRTR. The work of I.S. was supported by the Swiss National Science Foundation under grant no. 214492. The work of G.V. was supported by the Leverhulme Trust, LIP-2021-01. M.M.P. and A.R. acknowledge the support by the Polish Minister of Education and Science (contract No. 2021/WK/10); the work of MMP was also supported by WUT IDUB.

## References

- [1] “Mandate of the Physics Beyond Colliders Study Group (Revised January 2021),” 2021. <https://pbc.web.cern.ch/mandate-physics-beyond-colliders-study-group-revised-january-2021>. Last accessed 21 June 2022.
- [2] R. Alemany *et al.*, “Summary Report of Physics Beyond Colliders at CERN,” [arXiv:1902.00260 \[hep-ex\]](https://arxiv.org/abs/1902.00260). <https://arxiv.org/abs/1902.00260>.

- [3] **NA61/SHINE** Collaboration, A. Merzlaya, “First  $D^0 + \bar{D}^0$  measurement in nucleus-nucleus collisions at SPS energies with NA61/SHINE,” *EPJ Web Conf.* **316** (2025) 04004, [arXiv:2410.24014 \[nucl-ex\]](https://arxiv.org/abs/2410.24014).
- [4] **NA61/SHINE** Collaboration, H. Adhikary *et al.*, “Evidence of isospin-symmetry violation in high-energy collisions of atomic nuclei,” *Nature Commun.* **16** (2025) no. 1, 2849, [arXiv:2312.06572 \[nucl-ex\]](https://arxiv.org/abs/2312.06572).
- [5] **NA61/SHINE** Collaboration, A. Aduszkiewicz *et al.*, “Measurements of  $\pi^\pm$ ,  $K^\pm$ ,  $p$  and  $\bar{p}$  spectra in proton-proton interactions at 20, 31, 40, 80 and 158 GeV/c with the NA61/SHINE spectrometer at the CERN SPS,” *Eur. Phys. J. C* **77** (2017) no. 10, 671, [arXiv:1705.02467 \[nucl-ex\]](https://arxiv.org/abs/1705.02467).
- [6] **NA61/SHINE** Collaboration, A. Acharya *et al.*, “Measurements of  $\pi^\pm$ ,  $K^\pm$ ,  $p$  and  $\bar{p}$  spectra in  $^7\text{Be} + ^9\text{Be}$  collisions at beam momenta from 19A to 150A GeV/c with the NA61/SHINE spectrometer at the CERN SPS,” *Eur. Phys. J. C* **81** (2021) no. 1, 73, [arXiv:2010.01864 \[hep-ex\]](https://arxiv.org/abs/2010.01864).
- [7] **NA61/SHINE** Collaboration, A. Acharya *et al.*, “Spectra and mean multiplicities of  $\pi^-$  in central  $^{40}\text{Ar} + ^{45}\text{Sc}$  collisions at 13A, 19A, 30A, 40A, 75A and 150A GeV/c beam momenta measured by the NA61/SHINE spectrometer at the CERN SPS,” *Eur. Phys. J. C* **81** (2021) no. 5, 397, [arXiv:2101.08494 \[hep-ex\]](https://arxiv.org/abs/2101.08494).
- [8] **NA61/SHINE Collaboration** Collaboration, M. Gazdzicki and S. Kowalski, “Open Charm Measurements: Pb-beam schedule and detector upgrade,” Tech. Rep. CERN-SPSC-2022-005, SPSC-M-792, CERN, Geneva, Jan, 2022. <https://cds.cern.ch/record/2799311>.
- [9] **NA61/SHINE** Collaboration, H. Adhikary *et al.*, “Measurements of  $K_S^0$ ,  $\Lambda$ , and  $\bar{\Lambda}$  production in 120 GeV/c p+C interactions,” *Phys. Rev. D* **107** (2023) no. 7, 072004, [arXiv:2211.00183 \[hep-ex\]](https://arxiv.org/abs/2211.00183).
- [10] **NA61/SHINE** Collaboration, H. Adhikary *et al.*, “Measurements of  $\pi^+$ ,  $\pi^-$ ,  $p$ ,  $\bar{p}$ ,  $K^+$  and  $K^-$  production in 120 GeV/c p + C interactions,” *Phys. Rev. D* **108** (2023) 072013, [arXiv:2306.02961 \[hep-ex\]](https://arxiv.org/abs/2306.02961).
- [11] **NA61/SHINE** Collaboration, H. Adhikary *et al.*, “Measurement of hadron production in  $\pi$ -C interactions at 158 and 350 GeV/c with NA61/SHINE at the CERN SPS,” *Phys. Rev. D* **107** (2023) no. 6, 062004, [arXiv:2209.10561 \[nucl-ex\]](https://arxiv.org/abs/2209.10561).
- [12] **NA61/SHINE** Collaboration, H. Adhikary *et al.*, “Measurement of the mass-changing, charge-changing and production cross sections of  $^{11}\text{C}$ ,  $^{11}\text{B}$  and  $^{10}\text{B}$  nuclei in  $^{12}\text{C} + \text{p}$  interactions at 13.5 GeV/c per nucleon,” [arXiv:2410.18273 \[nucl-ex\]](https://arxiv.org/abs/2410.18273).
- [13] “CERN article news on NA62 result,” 2024. <https://home.cern/news/press-release/physics/na62-experiment-cern-observes-ultra-rare-particle-decay>. Last accessed 29 October 2022.
- [14] **NA62** Collaboration, E. Cortina Gil *et al.*, “Observation of the  $K^+ \rightarrow \pi^+ \nu \bar{\nu}$  decay and measurement of its branching ratio,” *JHEP* **02** (2025) 191, [arXiv:2412.12015 \[hep-ex\]](https://arxiv.org/abs/2412.12015).
- [15] M. Rosenthal *et al.*, “Single-muon rate reduction for beam dump operation of the K12 beam line at CERN,” *Int. J. Mod. Phys. A* **34** (2019) no. 36, 1942026.
- [16] J. Bernhard, L. Gatignon, and S. Schuh, eds., *Report from the Conventional Beams Working Group to the Physics Beyond Colliders Study and to the 2026 European Strategy for Particle Physics Update*. CERN Yellow Reports: Monographs. CERN, Geneva, Switzerland, 2025. <https://cds.cern.ch/record/2925964>.
- [17] **NA62** Collaboration, E. Cortina Gil *et al.*, “Search for Leptonic Decays of Dark Photons at NA62,” *Phys. Rev. Lett.* **133** (2024) no. 11, 111802, [arXiv:2312.12055 \[hep-ex\]](https://arxiv.org/abs/2312.12055).

[18] **NA62** Collaboration, E. Cortina Gil *et al.*, “Search for dark photon decays to  $\mu^+ \mu^-$  at NA62,” *JHEP* **09** (2023) 035, [arXiv:2303.08666 \[hep-ex\]](https://arxiv.org/abs/2303.08666).

[19] “First NA62 search for long-lived new physics particle hadronic decays,” 2024. <https://moriond.in2p3.fr/QCD/2024/FridayMorning/Jerhot.pdf>. Last accessed 29 October 2022.

[20] **NA64** Collaboration, Y. M. Andreev *et al.*, “Search for Light Dark Matter with NA64 at CERN,” *Phys. Rev. Lett.* **131** (2023) no. 16, 161801, [arXiv:2307.02404 \[hep-ex\]](https://arxiv.org/abs/2307.02404).

[21] **NA64** Collaboration, D. Banerjee *et al.*, “Search for a Hypothetical 16.7 MeV Gauge Boson and Dark Photons in the NA64 Experiment at CERN,” *Phys. Rev. Lett.* **120** (2018) no. 23, 231802, [arXiv:1803.07748 \[hep-ex\]](https://arxiv.org/abs/1803.07748).

[22] **NA64** Collaboration, D. Banerjee *et al.*, “Search for Axionlike and Scalar Particles with the NA64 Experiment,” *Phys. Rev. Lett.* **125** (2020) no. 8, 081801, [arXiv:2005.02710 \[hep-ex\]](https://arxiv.org/abs/2005.02710).

[23] **NA64** Collaboration, C. Cazzaniga *et al.*, “Probing the explanation of the muon (g-2) anomaly and thermal light dark matter with the semi-visible dark photon channel,” *Eur. Phys. J. C* **81** (2021) no. 10, 959, [arXiv:2107.02021 \[hep-ex\]](https://arxiv.org/abs/2107.02021).

[24] M. Mongillo, A. Abdullahi, B. B. Oberhauser, P. Crivelli, M. Hostert, D. Massaro, L. M. Bueno, and S. Pascoli, “Constraining light thermal inelastic dark matter with NA64,” *Eur. Phys. J. C* **83** (2023) no. 5, 391, [arXiv:2302.05414 \[hep-ph\]](https://arxiv.org/abs/2302.05414).

[25] **NA64** Collaboration, Y. M. Andreev *et al.*, “Search for a New  $B - L Z'$  Gauge Boson with the NA64 Experiment at CERN,” *Phys. Rev. Lett.* **129** (2022) no. 16, 161801, [arXiv:2207.09979 \[hep-ex\]](https://arxiv.org/abs/2207.09979).

[26] Y. M. Andreev *et al.*, “First constraints on the  $L_\mu - L_\tau$  explanation of the muon g-2 anomaly from NA64-e at CERN,” *JHEP* **07** (2024) 212, [arXiv:2404.06982 \[hep-ex\]](https://arxiv.org/abs/2404.06982).

[27] A. Ponten, H. Sieber, B. B. Oberhauser, P. Crivelli, D. Kirpichnikov, S. N. Glinenko, M. Hösgen, L. M. Bueno, M. Mongillo, and A. Zhevlakov, “Probing hidden leptonic scalar portals using the NA64 experiment at CERN,” *Eur. Phys. J. C* **84** (2024) no. 10, 1035, [arXiv:2404.15931 \[hep-ph\]](https://arxiv.org/abs/2404.15931).

[28] **NA64** Collaboration, Y. M. Andreev *et al.*, “Shedding light on dark sectors with high-energy muons at the NA64 experiment at the CERN SPS,” *Phys. Rev. D* **110** (2024) no. 11, 112015, [arXiv:2409.10128 \[hep-ex\]](https://arxiv.org/abs/2409.10128).

[29] **NA64** Collaboration, Y. M. Andreev *et al.*, “Dark-Sector Search via Pion-Produced  $\eta$  and  $\eta'$  Mesons Decaying Invisibly in the NA64h Detector,” *Phys. Rev. Lett.* **133** (2024) no. 12, 121803.

[30] **NA64** Collaboration, Y. M. Andreev *et al.*, “Probing light dark matter with positron beams at NA64,” *Phys. Rev. D* **109** (2024) no. 3, L031103, [arXiv:2308.15612 \[hep-ex\]](https://arxiv.org/abs/2308.15612).

[31] European Strategy Group, “2020 Update of the European Strategy for Particle Physics,” Tech. Rep. CERN-ESU-013, CERN, Geneva, 2020.

[32] **LHCb** Collaboration, R. Aaij *et al.*, “LHCb Detector Performance,” *Int. J. Mod. Phys. A* **30** (2015) no. 07, 1530022, [arXiv:1412.6352 \[hep-ex\]](https://arxiv.org/abs/1412.6352).

[33] **LHCb** Collaboration, R. Aaij *et al.*, “Precision luminosity measurements at LHCb,” *JINST* **9** (2014) no. 12, P12005, [arXiv:1410.0149 \[hep-ex\]](https://arxiv.org/abs/1410.0149).

[34] **LHCb** Collaboration, R. Aaij *et al.*, “Measurement of Antiproton Production in pHe Collisions at  $\sqrt{s_{NN}} = 110$  GeV,” *Phys. Rev. Lett.* **121** (2018) no. 22, 222001, [arXiv:1808.06127 \[hep-ex\]](https://arxiv.org/abs/1808.06127).

[35] **LHCb** Collaboration, R. Aaij *et al.*, “Measurement of antiproton production from antihyperon decays in  $p\text{He}$  collisions at  $\sqrt{s_{\text{NN}}} = 110\text{ GeV}$ ,” *Eur. Phys. J. C* **83** (2023) no. 6, 543, [arXiv:2205.09009 \[hep-ex\]](https://arxiv.org/abs/2205.09009).

[36] **LHCb** Collaboration, R. Aaij *et al.*, “First Measurement of Charm Production in its Fixed-Target Configuration at the LHC,” *Phys. Rev. Lett.* **122** (2019) no. 13, 132002, [arXiv:1810.07907 \[hep-ex\]](https://arxiv.org/abs/1810.07907).

[37] **LHCb** Collaboration, R. Aaij *et al.*, “Open charm production and asymmetry in  $p\text{Ne}$  collisions at  $\sqrt{s_{\text{NN}}} = 68.5\text{ GeV}$ ,” *Eur. Phys. J. C* **83** (2023) no. 6, 541, [arXiv:2211.11633 \[hep-ex\]](https://arxiv.org/abs/2211.11633). [Erratum: Eur. Phys. J. C 83 (2023) 708].

[38] **LHCb** Collaboration, R. Aaij *et al.*, “Open charm production and asymmetry in  $p\text{Ne}$  collisions at  $\sqrt{s_{\text{NN}}} = 68.5\text{ GeV}$ ,” *Eur. Phys. J. C* **83** (2023) no. 6, 541, [arXiv:2211.11633 \[hep-ex\]](https://arxiv.org/abs/2211.11633). [Erratum: Eur. Phys. J. C 83 (2023) 708].

[39] O. Boente Garcia *et al.*, “High-density gas target at the LHCb experiment,” *Phys. Rev. Accel. Beams* **27** (2024) no. 11, 111001, [arXiv:2407.14200 \[physics.ins-det\]](https://arxiv.org/abs/2407.14200).

[40] C. Boscolo Meneguolo, R. Bruce, M. Ferro-Luzzi, M. Giovannozzi, and S. Redaelli, “Calculation of the allowed aperture for a gas storage cell in IP8,” Tech. Rep. CERN-PBC-Notes-2018-008, CERN, 2018. <https://cds.cern.ch/record/2651289>.

[41] D. M. Parragh, “Hydrogen Embrittlement of TiZrV Non-Evaporable Getter Coating,” Master’s thesis, KU Leuven, 2022. [http://cds.cern.ch/record/2836903](https://cds.cern.ch/record/2836903). Presented 26 Aug 2022.

[42] **LHCb** Collaboration, R. Aaij *et al.*, “The LHCb Upgrade I,” *JINST* **19** (2024) no. 05, P05065, [arXiv:2305.10515 \[hep-ex\]](https://arxiv.org/abs/2305.10515).

[43] J. L. Feng, I. Galon, F. Kling, and S. Trojanowski, “ForwArd Search ExpeRiment at the LHC,” *Phys. Rev. D* **97** (2018) no. 3, 035001, [arXiv:1708.09389 \[hep-ph\]](https://arxiv.org/abs/1708.09389).

[44] **FASER** Collaboration, A. Ariga *et al.*, “Letter of Intent for FASER: ForwArd Search ExpeRiment at the LHC,” [arXiv:1811.10243 \[physics.ins-det\]](https://arxiv.org/abs/1811.10243).

[45] **FASER** Collaboration, A. Ariga *et al.*, “Technical Proposal for FASER: ForwArd Search ExpeRiment at the LHC,” [arXiv:1812.09139 \[physics.ins-det\]](https://arxiv.org/abs/1812.09139).

[46] **FASER** Collaboration, H. Abreu *et al.*, “The FASER detector,” *JINST* **19** (2024) no. 05, P05066, [arXiv:2207.11427 \[physics.ins-det\]](https://arxiv.org/abs/2207.11427).

[47] **FASER** Collaboration, H. Abreu *et al.*, “Search for dark photons with the FASER detector at the LHC,” *Phys. Lett. B* **848** (2024) 138378, [arXiv:2308.05587 \[hep-ex\]](https://arxiv.org/abs/2308.05587).

[48] **FASER** Collaboration, H. Abreu *et al.*, “First Direct Observation of Collider Neutrinos with FASER at the LHC,” *Phys. Rev. Lett.* **131** (2023) no. 3, 031801, [arXiv:2303.14185 \[hep-ex\]](https://arxiv.org/abs/2303.14185).

[49] **FASER** Collaboration, R. Mammen Abraham *et al.*, “Shining light on the dark sector: search for axion-like particles and other new physics in photonic final states with FASER,” *JHEP* **01** (2025) 199, [arXiv:2410.10363 \[hep-ex\]](https://arxiv.org/abs/2410.10363).

[50] **FASER** Collaboration, R. Mammen Abraham *et al.*, “First Measurement of  $\nu_e$  and  $\nu_\mu$  Interaction Cross Sections at the LHC with FASER’s Emulsion Detector,” *Phys. Rev. Lett.* **133** (2024) no. 2, 021802, [arXiv:2403.12520 \[hep-ex\]](https://arxiv.org/abs/2403.12520).

[51] **FASER** Collaboration, R. Mammen Abraham *et al.*, “First Measurement of the Muon Neutrino Interaction Cross Section and Flux as a Function of Energy at the LHC with FASER,” [arXiv:2412.03186 \[hep-ex\]](https://arxiv.org/abs/2412.03186).

[52] **FASER** Collaboration, R. Mammen Abraham *et al.*, “Prospects and Opportunities with an upgraded FASER Neutrino Detector during the HL-LHC era: Input to the EPPSU,” [arXiv:2503.19775](https://arxiv.org/abs/2503.19775) [hep-ex].

[53] **SND@LHC** Collaboration, C. Ahdida *et al.*, “SND@LHC - Scattering and Neutrino Detector at the LHC,” Technical Proposal CERN-LHCC-2021-003, LHCC-P-016, CERN, Geneva, 2021. <https://cds.cern.ch/record/2750060>.

[54] **SND@LHC** Collaboration, G. Acampora *et al.*, “SND@LHC: the scattering and neutrino detector at the LHC,” *JINST* **19** (2024) no. 05, P05067, [arXiv:2210.02784](https://arxiv.org/abs/2210.02784) [hep-ex].

[55] **SND@LHC** Collaboration, R. Albanese *et al.*, “Measurement of the muon flux at the SND@LHC experiment,” *Eur. Phys. J. C* **84** (2024) no. 1, 90, [arXiv:2310.05536](https://arxiv.org/abs/2310.05536) [hep-ex].

[56] **SND@LHC** Collaboration, R. Albanese *et al.*, “Observation of Collider Muon Neutrinos with the SND@LHC Experiment,” *Phys. Rev. Lett.* **131** (2023) no. 3, 031802, [arXiv:2305.09383](https://arxiv.org/abs/2305.09383) [hep-ex].

[57] **SND@LHC** Collaboration, D. Abbaneo *et al.*, “Results and Perspectives from the First Two Years of Neutrino Physics at the LHC by the SND@LHC Experiment,” *Symmetry* **16** (2024) no. 6, 702.

[58] **SND@LHC** Collaboration, D. Abbaneo *et al.*, “Observation of collider neutrinos without final state muons with the SND@LHC experiment,” [arXiv:2411.18787](https://arxiv.org/abs/2411.18787) [hep-ex].

[59] **SND@LHC** Collaboration, D. Abbaneo *et al.*, “Installation and performance of the 3rd Veto plane at the SND@LHC detector,” [arXiv:2502.10188](https://arxiv.org/abs/2502.10188) [physics.ins-det].

[60] J. Beacham *et al.*, “Physics Beyond Colliders at CERN: Beyond the Standard Model Working Group Report,” *J. Phys. G* **47** (2020) no. 1, 010501, [arXiv:1901.09966](https://arxiv.org/abs/1901.09966) [hep-ex].

[61] P. Agrawal *et al.*, “Feebly-interacting particles: FIPs 2020 workshop report,” *Eur. Phys. J. C* **81** (2021) no. 11, 1015, [arXiv:2102.12143](https://arxiv.org/abs/2102.12143) [hep-ph].

[62] C. Antel *et al.*, “Feebly-interacting particles: FIPs 2022 Workshop Report,” *Eur. Phys. J. C* **83** (2023) no. 12, 1122, [arXiv:2305.01715](https://arxiv.org/abs/2305.01715) [hep-ph].

[63] “FIPs in the ALPs,” 2021. <https://indico.cern.ch/event/1247323/>. Last accessed 27 February 2025.

[64] C. Ahdida *et al.*, “Post-LS3 Experimental Options in ECN3,” Tech. Rep. CERN-PBC-REPORT-2023-003, CERN, 10, 2023. [arXiv:2310.17726](https://arxiv.org/abs/2310.17726) [hep-ex]. <https://cds.cern.ch/record/2867743>.

[65] **HIKE** Collaboration, M. Ashraf *et al.*, “High Intensity Kaon Experiments (HIKE) at the CERN SPS: Proposal for Phases 1 and 2,” tech. rep., CERN, Geneva, 2023. [arXiv:2311.08231](https://arxiv.org/abs/2311.08231). <https://cds.cern.ch/record/2878543>.

[66] **SHADOWS** Collaboration, M. Alviggi *et al.*, “SHADOWS Technical Proposal,” Tech. Rep. CERN-SPSC-2023-029, SPSC-P-367, CERN, Geneva, 2023. <https://cds.cern.ch/record/2878470>.

[67] **SHiP** Collaboration, R. Albanese *et al.*, “BDF/SHiP at the ECN3 high-intensity beam facility,” Tech. Rep. CERN-SPSC-2023-033, SPSC-P-369, CERN, Geneva, 2023. <https://cds.cern.ch/record/2878604>.

[68] **QCD Working Group** Collaboration, A. Dainese *et al.*, “Physics Beyond Colliders: QCD Working Group Report,” Tech. Rep. CERN-PBC-REPORT-2018-008, CERN, 1, 2019. [arXiv:1901.04482](https://arxiv.org/abs/1901.04482) [hep-ex].

[69] R. Abdul Khalek *et al.*, “Science Requirements and Detector Concepts for the Electron-Ion Collider: EIC Yellow Report,” *Nucl. Phys. A* **1026** (2022) 122447, [arXiv:2103.05419 \[physics.ins-det\]](https://arxiv.org/abs/2103.05419).

[70] F. Willeke, “Electron-Ion Collider Global Requirements,” Tech. Rep. EIC-ORG-PLN-010, BNL, 2023. <https://eic.jlab.org/Documents/EIC-SEG/Electron-Ion%20Collider%20Global%20Requirements.pdf>.

[71] **BDX** Collaboration, M. Battaglieri *et al.*, “Dark Matter Search in a Beam-Dump eXperiment (BDX) at Jefferson Lab,” [arXiv:1607.01390 \[hep-ex\]](https://arxiv.org/abs/1607.01390).

[72] A. Afanasev *et al.*, “Physics with Positron Beams at Jefferson Lab 12 GeV,” tech. rep., Jefferson Lab, 6, 2019. [arXiv:1906.09419 \[nucl-ex\]](https://arxiv.org/abs/1906.09419).

[73] A. Accardi *et al.*, “Strong interaction physics at the luminosity frontier with 22 GeV electrons at Jefferson Lab,” *Eur. Phys. J. A* **60** (2024) no. 9, 173, [arXiv:2306.09360 \[nucl-ex\]](https://arxiv.org/abs/2306.09360).

[74] A. Somov, “Jlab Eta Factory Experiment in Hall D,” *PoS CD2021* (2024) 029.

[75] **GlueX** Collaboration, S. Adhikari *et al.*, “The GLUEX beamline and detector,” *Nucl. Instrum. Meth. A* **987** (2021) 164807, [arXiv:2005.14272 \[physics.ins-det\]](https://arxiv.org/abs/2005.14272).

[76] C. Gatto, “The REDTOP experiment: a low energy meson factory to explore dark matter and physics beyond the Standard Model.,” *PoS CD2021* (2024) 043.

[77] T. Åkesson *et al.*, “Current Status and Future Prospects for the Light Dark Matter eXperiment,” in *Snowmass 2021*. 3, 2022. [arXiv:2203.08192 \[hep-ex\]](https://arxiv.org/abs/2203.08192).

[78] A. Apyan *et al.*, “DarkQuest: A dark sector upgrade to SpinQuest at the 120 GeV Fermilab Main Injector,” in *Snowmass 2021*. 3, 2022. [arXiv:2203.08322 \[hep-ex\]](https://arxiv.org/abs/2203.08322).

[79] A. Apyan *et al.*, “Performance measurements of the electromagnetic calorimeter and readout electronics system for the DarkQuest experiment,” [arXiv:2502.20590 \[physics.ins-det\]](https://arxiv.org/abs/2502.20590).

[80] R. Bähre *et al.*, “Any light particle search II —Technical Design Report,” *JINST* **8** (2013) T09001, [arXiv:1302.5647 \[physics.ins-det\]](https://arxiv.org/abs/1302.5647).

[81] T. Kozlowski *et al.*, “Design and Performance of the ALPS II Regeneration Cavity,” [arXiv:2408.13218 \[physics.optics\]](https://arxiv.org/abs/2408.13218).

[82] M. D. Ortiz *et al.*, “Design of the ALPS II optical system,” *Phys. Dark Univ.* **35** (2022) 100968, [arXiv:2009.14294 \[physics.optics\]](https://arxiv.org/abs/2009.14294).

[83] A. Hallal, G. Messineo, M. D. Ortiz, J. Gleason, H. Hollis, D. B. Tanner, G. Mueller, and A. Spector, “The heterodyne sensing system for the ALPS II search for sub-eV weakly interacting particles,” *Phys. Dark Univ.* **35** (2022) 100914, [arXiv:2010.02334 \[physics.ins-det\]](https://arxiv.org/abs/2010.02334).

[84] J. A. Rubiera Gimeno, K.-S. Isleif, F. Januscheck, A. Lindner, M. Meyer, G. Othman, M. Schott, R. Shah, and L. Sohl, “The TES detector of the ALPS II experiment,” *Nucl. Instrum. Meth. A* **1046** (2023) 167588.

[85] H. Abramowicz *et al.*, “Letter of Intent for the LUXE Experiment,” [arXiv:1909.00860 \[physics.ins-det\]](https://arxiv.org/abs/1909.00860).

[86] H. Abramowicz *et al.*, “Conceptual design report for the LUXE experiment,” *Eur. Phys. J. ST* **230** (2021) no. 11, 2445–2560, [arXiv:2102.02032 \[hep-ex\]](https://arxiv.org/abs/2102.02032).

[87] Z. Bai *et al.*, “New physics searches with an optical dump at LUXE,” *Phys. Rev. D* **106** (2022) no. 11, 115034, [arXiv:2107.13554 \[hep-ph\]](https://arxiv.org/abs/2107.13554).

[88] **Belle II** Collaboration, I. Adachi *et al.*, “Evidence for  $B^+ \rightarrow K^+ v\bar{v}$  decays,” *Phys. Rev. D* **109** (2024) no. 11, 112006, [arXiv:2311.14647](https://arxiv.org/abs/2311.14647) [hep-ex].

[89] **KOTO** Collaboration, J. Fry *et al.*, “Proposal of the KOTO II experiment,” [arXiv:2501.14827](https://arxiv.org/abs/2501.14827) [hep-ex].

[90] H. Aihara *et al.*, “The Belle II Detector Upgrades Framework Conceptual Design Report,” [arXiv:2406.19421](https://arxiv.org/abs/2406.19421) [hep-ex].

[91] J. Coupard *et al.*, “LIU Technical design report, vol. I: Protons,” Tech. Rep. CERN-ACC-2014-0337, CERN, 2014. <https://cds.cern.ch/record/1976692>.

[92] J. Coupard *et al.*, “LIU Technical design report, vol. II: Ions,” Tech. Rep. CERN-ACC-2016-0041, CERN, 2016. [http://cds.cern.ch/record/2153863](https://cds.cern.ch/record/2153863).

[93] M. Vadai, H. Damerau, M. Giovannozzi, A. Huschauer, and A. Lasheen, “Implementation of synchronised PS-SPS transfer with barrier buckets,” 2022. <https://arxiv.org/abs/2210.05416>.

[94] C. Lombard *et al.*, “Improved Antiproton Beam Production at CERN,” in *14th International Particle Accelerator Conference*. 6, 2023.

[95] F. Asvesta *et al.*, “Pushing High Intensity and High Brightness Limits in the CERN PSB after the LIU Upgrades,” *JACoW HB* **2023** (2024) 458–461. <https://cds.cern.ch/record/2900904>.

[96] M. Migliorati, S. Aumon, E. Koukovini-Platia, A. Huschauer, E. Métral, G. Sterbini, and N. Wang, “Instability studies at the CERN Proton Synchrotron during transition crossing,” *Phys. Rev. Accel. Beams* **21** (2018) no. 12, 120101. [Erratum: *Phys. Rev. Accel. Beams* 22 (2019) 068002].

[97] F. M. Velotti *et al.*, “Demonstration of non-local crystal shadowing at the CERN SPS,” *JACoW IPAC 2023* (2023) MOPA098. <https://cds.cern.ch/record/2886012>.

[98] P. A. Arrutia Sota, Y. Dutheil, M. A. Fraser, and F. M. Velotti, “TT20 Transport and Splitting of Beams Extracted Using Crystal Shadowing in LSS2 of the SPS,” Tech. Rep. CERN-ACC-Note-2020-0040, CERN, 2020. <https://cds.cern.ch/record/2724487>.

[99] M. Cuvelier, “Longitudinal dynamics of the Barrier Bucket Multi-Turn Extraction transfer from PS to SPS,” Tech. Rep. CERN-STUDENTS-Note-2023-204, CERN, 2023. <https://cds.cern.ch/record/2876316>.

[100] C. Ahdida *et al.*, “Ion beams requirements for the North Area Experiments post-LS3,” Tech. Rep. CERN-PBC-REPORT-2025-002, CERN, Geneva, 2025. <https://cds.cern.ch/record/2926928>.

[101] **ALICE** Collaboration, “Letter of intent for ALICE 3: A next-generation heavy-ion experiment at the LHC Version 2,” Tech. Rep. CERN-LHCC-2022-009, LHCC-I-038, LHCC-I-038, CERN, Geneva, 2022. [arXiv:2211.02491](https://arxiv.org/abs/2211.02491). <https://cds.cern.ch/record/2803563>.

[102] R. Alemany Fernandez *et al.*, “Light ion collisions at the LHC,” Geneva, Switzerland, Nov, 2024. <https://indico.cern.ch/event/1436085/>. Last accessed 11 November 2024.

[103] J. F. Grosse-Oetringhaus and U. A. Wiedemann, “A Decade of Collectivity in Small systems,” [arXiv:2407.07484](https://arxiv.org/abs/2407.07484) [hep-ex].

[104] **NA61/SHINE** Collaboration, M. Mackowiak-Pawlowska *et al.*, “Addendum to the NA61/SHINE Proposal: Request for light ions beams in Run 4,” Tech. Rep. CERN-SPSC-2023-022, SPSC-P-330-ADD-14, CERN, Geneva, 2023. <https://cds.cern.ch/record/2867952>.

[105] **NA60+** Collaboration, C. Ahdida *et al.*, “Letter of Intent: the NA60+ experiment,” Tech. Rep. CERN-SPSC-2022-036, SPSC-I-259, CERN, Geneva, 2022. [http://cds.cern.ch/record/2845241](https://cds.cern.ch/record/2845241).

[106] HEARTS, “High-Energy Accelerators for Radiation Testing and Shielding.” <https://hearts-project.eu/>.

[107] R. Alemany Fernandez *et al.*, “Future Ions in the CERN Accelerator Complex WG: Post-LS3 NA61 ion beam requirements feasibility study: source operation, radiation protection impact and risk assessment,” tech. rep., CERN, CERN-ACC-NOTE-2024-0020, Geneva, 2024. <http://cds.cern.ch/record/2916353>.

[108] M. Slupecki *et al.*, “LHC Oxygen Run Preparation in the CERN Injector Complex,” tech. rep., CERN, CERN-ACC-NOTE-2024-0001, Geneva, 2024. <https://cds.cern.ch/record/2888741>.

[109] M. Slupecki *et al.*, “CERN ion injector complex performance during 2024 magnesium test,” Tech. Rep. CERN-ACC-NOTE-2025-0006, CERN, 2025. <https://cds.cern.ch/record/2929494>.

[110] R. Alemany Fernandez and M. Slupecki, “Ion Complex Upgrade (ICU) project proposal - kickoff meeting,” Geneva, Switzerland, Nov, 2024. <https://indico.cern.ch/event/1481171/>. Last accessed 11 November 2024.

[111] J. Bernhard, F. Carvalho, S. Evrard, E. Harrouch, and G. Romagnoli, eds., *CERN Proton Synchrotron East Area Facility: Upgrades and renovation during Long Shutdown 2*, vol. CERN-2021-004 of *CERN Yellow Reports: Monographs*. CERN, Geneva, Switzerland, 2021.

[112] **n\_TOF** Collaboration, A. Mengoni *et al.*, “n\_TOF,” Tech. Rep. CERN-INTC-2023-072, CERN, 2023. <https://cds.cern.ch/record/2872442>.

[113] Freeman, S. on behalf or the ISOLDE Collaboration, “Isolde consolidation and improvement,” Tech. Rep. CERN-INTC-2023-028, CERN, 2023. <https://cds.cern.ch/record/2846021>.

[114] W. Bonivento *et al.*, “Proposal to Search for Heavy Neutral Leptons at the SPS,” Tech. Rep. CERN-SPSC-2013-024, SPSC-EOI-010, SPSC-EOI-010 [1310.1762], CERN, Geneva, Oct, 2013. [arXiv:\[arXiv:1310.1762\]](https://arxiv.org/abs/1310.1762). <https://cds.cern.ch/record/1606085>.

[115] G. Arduini *et al.*, “A new Experiment to Search for Hidden Particles (SHIP) at the SPS North Area,” Tech. Rep. EDMS 1369559, EN-DH-2014-007, July, 2014.

[116] **SHiP** Collaboration, M. Anelli *et al.*, “A Facility to Search for Hidden Particles (SHiP) at the CERN SPS - Technical Proposal,” Tech. Rep. CERN-SPSC-2015-016, SPSC-P-350, SPSC-P-350, [1504.04956], CERN, Geneva, Apr, 2015. [arXiv:1504.04956](https://arxiv.org/abs/1504.04956). <https://cds.cern.ch/record/2007512>. Technical Proposal.

[117] **SHiP** Collaboration, M. Anelli *et al.*, “A Facility to Search for Hidden Particles (SHiP) at the CERN SPS (Addendum to Technical Proposal),” Tech. Rep. CERN-SPSC-2015-040, SPSC-P-350-ADD-2, CERN, Geneva, Oct, 2015. <https://cds.cern.ch/record/2060742>. Technical Proposal.

[118] C. Ahdida *et al.*, *SPS Beam Dump Facility - Comprehensive Design Study*. CERN Yellow Reports: Monographs. CERN, Geneva, Dec, 2019. 1912.06356. <http://cds.cern.ch/record/2703984>.

[119] **SHiP** Collaboration, C. Ahdida *et al.*, “SHiP Experiment - Progress Report,” Tech. Rep. CERN-SPSC-2019-010, SPSC-SR-248, CERN, Geneva, Jan, 2019. <https://cds.cern.ch/record/2654870>.

[120] **SHiP** Collaboration, C. Ahdida *et al.*, “SHiP Experiment - Comprehensive Design Study report,” Tech. Rep. CERN-SPSC-2019-049, SPSC-SR-263, CERN, Geneva, Dec, 2019. <https://cds.cern.ch/record/2704147>.

[121] The European Strategy Group, “[Deliberation document on the 2020 Update of the European Strategy for Particle Physics](https://cds.cern.ch/record/2720131),” Tech. Rep. CERN-ESU-014, CERN, Geneva, 2020. <https://cds.cern.ch/record/2720131>.

[122] O. Aberle *et al.*, “Study of alternative locations for the SPS Beam Dump Facility,” tech. rep., CERN, Geneva, 2022. [arXiv:2204.03549](https://cds.cern.ch/record/2802785). <https://cds.cern.ch/record/2802785>. The report is an update of the Comprehensive Design Study of the SPS Beam Dump Facility (CERN-PBC-REPORT-2019-005; CERN-2020-002), complementing the BDF/SHiP proposal.

[123] H. Bartosik *et al.*, “SPS Operation and Future Proton Sharing scenarios for the SHiP experiment at the BDF facility,” Tech. Rep. CERN-ACC-NOTE-2018-0082, CERN-PBC-Notes-2021-008, CERN, Dec, 2018. <http://cds.cern.ch/record/2650722>.

[124] T. Prebibaj, G. Arduini, H. Bartosik, and M. A. Fraser, “SPS Operation and Future Proton Sharing Scenarios for the ECN3 facility,” Tech. Rep. CERN-PBC-Notes-2023-001, CERN, Geneva, 2023. <https://cds.cern.ch/record/2848908>.

[125] T. Prebibaj, “Proton sharing in the injector complex post LS3.” [https://indico.cern.ch/event/1469359/contributions/6233099/attachments/3004638/5296113/Proton\\_Sharing\\_in\\_the.Injector\\_Complex\\_Chamonix2025\\_v1p0.pptx](https://indico.cern.ch/event/1469359/contributions/6233099/attachments/3004638/5296113/Proton_Sharing_in_the.Injector_Complex_Chamonix2025_v1p0.pptx), 2025.

[126] P. Belochitskii *et al.*, “Commissioning and First Operation of the Antiproton Decelerator (AD),” in *Proc. PAC’2001*. Chicago, USA, June, 2001.

[127] D. Gamba *et al.*, “[ELENA Commissioning](#),” in *Proc. NAPAC 2019*, pp. 626–631. Lansing, MI, USA, Sep., 2019.

[128] C. Carli *et al.*, “[ELENA Commissioning and Status](#),” in *Proc. IPAC’2021*, pp. 598–601. Online, May, 2021.

[129] L. Ponce *et al.*, “[ELENA - From Commissioning to Operation](#),” in *Proc. IPAC’2022*. Bangkok, Thailand, June, 2022.

[130] Y. Dutheil *et al.*, “[Commissioning of the ELENA Electrostatic Transfer Lines for the Antimatter Facility at CERN](#),” in *Proc. IPAC’2022*. Bangkok, Thailand, June, 2022.

[131] F. Butin, “AD/ELENA facility Mini Workshop,” Geneva, Switzerland, Mar, 2023. <https://indico.cern.ch/event/1255500/>. Last accessed 11 November 2024.

[132] D. Gamba and L. Ponce, “AD/ELENA operation & consolidation for the next 10-20 years,” Chamonix, France, Jan, 2024. <https://indico.cern.ch/event/1343931/>. Presented at the Chamonix Workshop 2024.

[133] G. Arduini *et al.*, “LHC Upgrades in preparation of Run 3,” *JINST* **19** (2024) no. 05, P05061.

[134] O. Aberle *et al.*, *High-Luminosity Large Hadron Collider (HL-LHC): Technical design report*. CERN Yellow Reports: Monographs. CERN, Geneva, 2020. <http://cds.cern.ch/record/2749422>.

[135] O. S. Brüning, P. Collier, P. Lebrun, S. Myers, R. Ostojic, J. Poole, and P. Proudlock, *LHC Design Report*. CERN Yellow Reports: Monographs. CERN, Geneva, 2004. <https://cds.cern.ch/record/782076>.

[136] “IAXO web page,” 2024. <https://iaxo.desy.de/>. Last accessed 11 October 2024.

[137] **DarkSide-20k** Collaboration, C. E. Aalseth *et al.*, “DarkSide-20k: A 20 tonne two-phase LAr TPC for direct dark matter detection at LNGS,” *Eur. Phys. J. Plus* **133** (2018) 131, [arXiv:1707.08145 \[physics.ins-det\]](https://arxiv.org/abs/1707.08145).

[138] **DarkSide-20k** Collaboration, P. Agnes *et al.*, “Separating  $^{39}\text{Ar}$  from  $^{40}\text{Ar}$  by cryogenic distillation with Aria for dark-matter searches,” *Eur. Phys. J. C* **81** (2021) no. 4, 359, [arXiv:2101.08686 \[physics.ins-det\]](https://arxiv.org/abs/2101.08686).

[139] J. Golm *et al.*, “Thin Film (High Temperature) Superconducting Radiofrequency Cavities for the Search of Axion Dark Matter,” *IEEE Trans. Appl. Supercond.* **32** (2022) no. 4, 1500605, [arXiv:2110.01296 \[hep-ex\]](https://arxiv.org/abs/2110.01296).

[140] “First PBC technology mini workshop: superconducting RF,” 2021. <https://indico.cern.ch/event/1057715/>. Last accessed 11 October 2024.

[141] “Second PBC technology mini workshop: lasers & optics,” 2021. <https://indico.cern.ch/event/1092283/>. Last accessed 11 October 2024.

[142] “Third PBC technology mini workshop: vacuum, coating and surface technologies,” 2022. <https://indico.cern.ch/event/1134154/>. Last accessed 11 October 2024.

[143] “Fourth PBC technology mini workshop: cryogenics technologies,” 2022. <https://indico.cern.ch/event/1180067/>. Last accessed 11 October 2024.

[144] “Fifth PBC technology mini workshop: Superconductivity Technologies,” 2024. <https://indico.cern.ch/event/1418701/>. Last accessed 11 October 2024.

[145] “ALPS-II web page,” 2024. [https://alps.desy.de/our\\_activities/axion\\_wisp\\_experiments/alps\\_ii/](https://alps.desy.de/our_activities/axion_wisp_experiments/alps_ii/). Last accessed 11 October 2024.

[146] T. Grenet, R. Ballou, Q. Basto, K. Martineau, P. Perrier, P. Pugnat, J. Quevillon, N. Roch, and C. Smith, “The Grenoble Axion Haloscope platform (GrAHal): development plan and first results,” [arXiv:2110.14406 \[hep-ex\]](https://arxiv.org/abs/2110.14406).

[147] G. Cantatore *et al.*, “aKWISP: investigating short-distance interactions at sub-micron scales,” in *13th Patras Workshop on Axions, WIMPs and WISPs*, pp. 200–203. 2018. [arXiv:1803.07685 \[physics.ins-det\]](https://arxiv.org/abs/1803.07685).

[148] D. Alesini *et al.*, “The future search for low-frequency axions and new physics with the FLASH resonant cavity experiment at Frascati National Laboratories,” *Phys. Dark Univ.* **42** (2023) 101370, [arXiv:2309.00351 \[physics.ins-det\]](https://arxiv.org/abs/2309.00351).

[149] A. A. Melcón *et al.*, “Axion Searches with Microwave Filters: the RADES project,” *JCAP* **05** (2018) 040, [arXiv:1803.01243 \[hep-ex\]](https://arxiv.org/abs/1803.01243).

[150] A. Berlin, R. T. D’Agnolo, S. A. R. Ellis, and K. Zhou, “Heterodyne broadband detection of axion dark matter,” *Phys. Rev. D* **104** (2021) no. 11, L111701, [arXiv:2007.15656 \[hep-ph\]](https://arxiv.org/abs/2007.15656).

[151] A. Siemko *et al.*, “PBC technology subgroup report,” Tech. Rep. CERN-PBC-REPORT-2018-006, CERN, Geneva, 2018. <https://cds.cern.ch/record/2652165>.

[152] “CERN Quantum Technology Initiative web page,” 2024. <https://quantum.cern/>. Last accessed 11 October 2024.

[153] “DRD5 / RDq - Quantum Sensor R&D for Particle Physics web page,” 2024. <https://drd5.web.cern.ch/>. Last accessed 11 October 2024.

[154] **ENUBET** Collaboration, F. Acerbi *et al.*, “Design and performance of the ENUBET monitored neutrino beam,” *Eur. Phys. J. C* **83** (2023) no. 10, 964, [arXiv:2308.09402 \[hep-ex\]](https://arxiv.org/abs/2308.09402).

[155] M. Perrin-Terrin, “Neutrino tagging: a new tool for accelerator based neutrino experiments,” *Eur. Phys. J. C* **82** (2022) no. 5, 465, [arXiv:2112.12848 \[hep-ex\]](https://arxiv.org/abs/2112.12848).

[156] A. Baratto-Roldán, M. Perrin-Terrin, E. G. Parozzi, M. A. Jebramcik, and N. Charitonidis, “NuTag: a proof-of-concept study for a long-baseline neutrino beam,” *Eur. Phys. J. C* **84** (2024) no. 10, 1024, [arXiv:2401.17068 \[physics.acc-ph\]](https://arxiv.org/abs/2401.17068).

[157] F. Acerbi *et al.*, “SBN@CERN: A short-baseline neutrino beam at CERN for high-precision cross-section measurements,” 2025. <https://arxiv.org/abs/2503.21589>. Contribution to the EPPSU.

[158] M. Jebramcik and N. Charitonidis, “Conceptual comparative analysis of the PBC-SBN beamline implementation at CERN,” Tech. Rep. CERN-PBC-NOTE-2025-004, CERN, 2024. <https://cds.cern.ch/record/2926318>.

[159] M. Jebramcik, N. Charitonidis, and P. Arrutia, “Ideas for a slow extraction via SPS LSS4 or LSS to a future PBC-SBN beamline,” Tech. Rep. CERN-PBC-NOTE-2024-006, CERN, 2024. <https://cds.cern.ch/record/2918573>.

[160] M. W. Krasny, “The Gamma Factory proposal for CERN,” [arXiv:1511.07794 \[hep-ex\]](https://arxiv.org/abs/1511.07794).

[161] A. Wu Chao, M. Tigner, H. Weise, and F. Zimmermann, eds., *Handbook of Accelerator Physics and Engineering, Gamma Factory chapter*. World Scientific, 2, 2023.

[162] M. W. Krasny, “Gamma Factory,” in *The Future of the Large Hadron Collider: A Super-Accelerator with Multiple Possible Lives*, O. Brüning, M. Klein, L. Rossi, and P. Spagnolo, eds., pp. 297–303. World Scientific, Singapore, November, 2023.

[163] A. Apyan, M. W. Krasny, and W. Płaczek, “Gamma Factory high-intensity muon and positron source: Exploratory studies,” *Phys. Rev. Accel. Beams* **26** (2023) no. 8, 083401, [arXiv:2212.06311 \[hep-ex\]](https://arxiv.org/abs/2212.06311).

[164] H. Baolong *et al.*, “Efficient transmutation of long-lived fission products in a Gamma Factory beam driven advanced nuclear energy system,” [arXiv:2409.12473 \[physics.acc-ph\]](https://arxiv.org/abs/2409.12473).

[165] D. Nichita, D. L. Balabanski, P. Constantin, M. W. Krasny, and W. Placzek, “Radioactive Ion Beam Production at the Gamma Factory,” *Annalen Phys.* **534** (2022) no. 3, 2100207, [arXiv:2105.13058 \[nucl-ex\]](https://arxiv.org/abs/2105.13058).

[166] W. Placzek *et al.*, “Gamma Factory at CERN - Novel Research Tools Made of Light,” *Acta Phys. Polon. B* **50** (2019) no. 6, 1191–1203, [arXiv:1903.09032 \[physics.acc-ph\]](https://arxiv.org/abs/1903.09032).

[167] C. Curatolo, M. Krasny, W. Placzek, and L. Serafini, “New Simulation Programs for Partially Stripped Ions - Laser Light Collisions,” in *9th International Particle Accelerator Conference*. 6, 2018.

[168] M. W. Krasny, A. Petrenko, and W. Placzek, “BE-ABP Gamma Factory Software Workshop,” <https://indico.cern.ch/event/1076086/>.

[169] M. W. Krasny, A. Petrenko, and W. Płaczek, “The Gamma Factory path to high-luminosity LHC with isoscalar beams,” *PoS ICHEP2020* (2021) 690.

[170] P. Kruyt, D. Gamba, and G. Franchetti, “Simulation studies of laser cooling for the Gamma Factory proof-of-principle experiment at the CERN SPS,” *JACoW IPAC2024* (2024) MOPS50.

[171] M. W. Krasny, A. Petrenko, and W. Płaczek, “High-luminosity Large Hadron Collider with laser-cooled isoscalar ion beams,” *Prog. Part. Nucl. Phys.* **114** (2020) 103792, [arXiv:2003.11407 \[physics.acc-ph\]](https://arxiv.org/abs/2003.11407).

[172] **Gamma Factory Study Group** Collaboration, M. W. Krasny *et al.*, “Gamma Factory Proof-of-Principle experiment - Letter of Intent,” Tech. Rep. CERN-SPSC-2019-031, SPSC-I-253, CERN, 2019.

[173] S. Hirlaender *et al.*, “Lifetime and Beam Losses Studies of Partially Strip Ions in the SPS ( $^{129}\text{Xe}^{39+}$ ),” in *9th International Particle Accelerator Conference*. 6, 2018.

[174] Y. Dutheil *et al.*, “Gamma Factory for CERN initiative - progress report,” *PoS EPS-HEP2019* (2020) 020.

[175] F. M. Kröger *et al.*, “Charge state tailoring of relativistic heavy ion beams for the Gamma Factory project at CERN,” *X Ray Spectrom.* **49** (2019) no. 1, 25–28.

[176] A. Gorzawski *et al.*, “Collimation of partially stripped ions in the CERN Large Hadron Collider,” *Phys. Rev. Accel. Beams* **23** (2020) no. 10, 101002, [arXiv:2007.12507 \[physics.acc-ph\]](https://arxiv.org/abs/2007.12507).

[177] M. Schaumann *et al.*, “MD3284: Partially Stripped Ions in the LHC,” Tech. Rep. CERN-ACC-NOTE-2019-0012, CERN-PBC-Note-2021-019, CERN, 2019. <https://cds.cern.ch/record/2670544>.

[178] R. L. Ramjiawan *et al.*, “SPS MD5044: machine stability characterisation of Gamma Factory SPS Proof-of-Principle Experiment,” Tech. Rep. CERN-ACC-NOTE-2022-0014, CERN-PBC-Notes-2022-006, CERN, 2022. <https://cds.cern.ch/record/2807037>.

[179] A. Martens *et al.*, “Design of the optical system for the gamma factory proof of principle experiment at the CERN Super Proton Synchrotron,” *Phys. Rev. Accel. Beams* **25** (2022) no. 10, 101601.

[180] X. Y. Lu *et al.*, “Stable 500 kW average power of infrared light in a finesse 35 000 enhancement cavity,” *Appl. Phys. Lett.* **124** (2024) no. 25, 251105.

[181] X. Y. Lu *et al.*, “710 kW stable average power in a 45,000 finesse two-mirror optical cavity,” *Opt. Lett.* **49** (2024) no. 23, 6884–6887.

[182] E. Granados *et al.*, “Prospects for extreme light sources at the CERN accelerator complex,” in *High-Brightness Sources and Light-Driven Interactions Congress*, p. ETu3A.3. Optica Publishing Group, 9, 2024.

[183] G. Mazzola *et al.*, “Radiation to electronics studies for CERN gamma factory-proof of principle experiment in SPS,” *JACoW IPAC2024* (2024) TUPC80.

[184] E. Granados, Y. Dutheil, B. Marsh, and G. Arduini, “Laser beam transport and stabilization considerations for the Gamma Factory proof-of-principle experiment,” Tech. Rep. CERN-PBC-Notes-2023-007, CERN, 2023. <https://cds.cern.ch/record/2868829>.

[185] AWAKE Collaboration, F. Batsch *et al.*, “Transition between Instability and Seeded Self-Modulation of a Relativistic Particle Bunch in Plasma,” *Phys. Rev. Lett.* **126** (2021) no. 16, 164802, [arXiv:2012.09676 \[physics.plasm-ph\]](https://arxiv.org/abs/2012.09676).

[186] AWAKE Collaboration, E. Adli *et al.*, “Experimental Observation of Proton Bunch Modulation in a Plasma at Varying Plasma Densities,” *Phys. Rev. Lett.* **122** (2019) no. 5, 054802, [arXiv:1809.04478 \[physics.acc-ph\]](https://arxiv.org/abs/1809.04478).

[187] AWAKE Collaboration, M. Turner *et al.*, “Experimental Observation of Plasma Wakefield Growth Driven by the Seeded Self-Modulation of a Proton Bunch,” *Phys. Rev. Lett.* **122** (2019) no. 5, 054801, [arXiv:1809.01191 \[physics.acc-ph\]](https://arxiv.org/abs/1809.01191).

[188] AWAKE Collaboration, E. Adli *et al.*, “Acceleration of electrons in the plasma wakefield of a proton bunch,” *Nature* **561** (2018) no. 7723, 363–367, [arXiv:1808.09759 \[physics.acc-ph\]](https://arxiv.org/abs/1808.09759).

[189] E. Gschwendtner *et al.*, “The AWAKE Run 2 Programme and Beyond,” *Symmetry* **14** (2022) no. 8, .

[190] AWAKE Collaboration, L. Verra *et al.*, “Controlled Growth of the Self-Modulation of a Relativistic Proton Bunch in Plasma,” *Phys. Rev. Lett.* **129** (2022) no. 2, 024802, [arXiv:2203.13752 \[physics.plasm-ph\]](https://arxiv.org/abs/2203.13752).

[191] K. V. Lotov, “Physics of beam self-modulation in plasma wakefield accelerators,” *Phys. Plasmas* **22** (2015) 103110, [arXiv:1503.05104 \[physics.plasm-ph\]](https://arxiv.org/abs/1503.05104).

[192] Craievich, Paolo *et al.*, “Injector complex status and outlook,” 2024. [https://indico.cern.ch/event/1298458/contributions/5977869/attachments/2875469/5040026/FCCweek\\_2024\\_Craievich.pdf](https://indico.cern.ch/event/1298458/contributions/5977869/attachments/2875469/5040026/FCCweek_2024_Craievich.pdf).

[193] I. Agapov *et al.*, “Other Science Opportunities at the FCC-ee,” Tech. Rep. CERN-FCC-ACC-2025-0005, CERN, Geneva, 2025. <https://cds.cern.ch/record/2928809>.

[194] “Other Science opportunities at the FCC-ee,” 2024. <https://indico.cern.ch/event/1454873/>. Last accessed 11 December 2024.

[195] H. Bartosik *et al.*, “Possibilities in the FCC-ee pre-injector complex,” Geneva, Switzerland, November, 2024. <https://indico.cern.ch/event/1454873/>. Presented at the Other Science Opportunities at the FCC-ee workshop.

[196] **Linear Collider Vision** Collaboration, H. Abramowicz *et al.*, “A Linear Collider Vision for the Future of Particle Physics,” [arXiv:2503.19983 \[hep-ex\]](https://arxiv.org/abs/2503.19983).

[197] A. Aryshev *et al.*, “The International Linear Collider: Report to Snowmass 2021,” [arXiv:2203.07622 \[physics.acc-ph\]](https://arxiv.org/abs/2203.07622).

[198] **NA61/SHINE** Collaboration, A. Acharya *et al.*, “Addendum to the NA61/SHINE Proposal: A Low-Energy Beamline at the SPS H2,” Tech. Rep. CERN-SPSC-2021-028, SPSC-P-330-ADD-12, CERN, 2021. <https://cds.cern.ch/record/2783037>.

[199] **NA61/SHINE** Collaboration, “Additional Information concerning the Low Energy beam project,” Tech. Rep. CERN-SPSC-2022-022, SPSC-M-793, CERN, 2022. <https://cds.cern.ch/record/2810696>.

[200] N. Charitonidis and C. Mussolini, “A New Tertiary Branch of the H2 beamline for low-energy particle beams,” tech. rep., CERN, 2023. <https://edms.cern.ch/document/2803011>.

[201] **NA61/SHINE** Collaboration, M. Gazdzicki, “Addendum to the NA61/SHINE Proposal: Request for oxygen beam in Run 3,” Tech. Rep. CERN-SPSC-2022-021, SPSC-P-330-ADD-13, CERN, Geneva, 2022. <https://cds.cern.ch/record/2810689>.

[202] R. Gargiulo, S. Palmisano, and E. Di Meco, “Feasibility study of true muonium discovery with the CERN-SPS H4 positron beam,” *Phys. Rev. D* **110** (2024) no. 9, 092015, [arXiv:2409.11342 \[hep-ex\]](https://arxiv.org/abs/2409.11342).

[203] W.-C. Chang, J.-C. Peng, S. Platchkov, and T. Sawada, “Constraining kaon PDFs from Drell-Yan and  $J/\psi$  production,” *Phys. Lett. B* **855** (2024) 138820, [arXiv:2402.02860 \[hep-ph\]](https://arxiv.org/abs/2402.02860).

[204] **Saclay-CERN-College de France-Ecole Poly-Orsay** Collaboration, J. Badier *et al.*, “Measurement of the  $K^-/\pi^-$  Structure Function Ratio Using the Drell-Yan Process,” *Phys. Lett. B* **93** (1980) 354–356.

[205] C. Bourrely, F. Buccella, W.-C. Chang, and J.-C. Peng, “Extraction of kaon partonic distribution functions from Drell-Yan and  $J/\psi$  production data,” *Phys. Lett. B* **848** (2024) 138395, [arXiv:2305.18117 \[hep-ph\]](https://arxiv.org/abs/2305.18117).

[206] **SHiP** Collaboration, C. Ahdida *et al.*, “Measurement of the muon flux from 400 GeV/c protons interacting in a thick molybdenum/tungsten target,” *Eur. Phys. J. C* **80** (2020) no. 3, 284, [arXiv:2001.04784 \[physics.ins-det\]](https://arxiv.org/abs/2001.04784).

[207] **CHARM** Collaboration, F. Bergsma *et al.*, “Search for axion-like particle production in 400 GeV proton-copper interactions,” *Phys. Lett. B* **157** (1985) 458–462.

[208] **SHiP** Collaboration, E. van Herwijnen, “Muon-flux measurements for SHiP at H4,” Tech. Rep. CERN-SPSC-2017-020, SPSC-EOI-016, CERN, Geneva, 2017. <https://cds.cern.ch/record/2267770>.

[209] **SHiP** Collaboration, C. Ahdida *et al.*, “Sensitivity of the SHiP experiment to light dark matter,” *JHEP* **04** (2021) 199, [arXiv:2010.11057](https://arxiv.org/abs/2010.11057) [hep-ex].

[210] M. Ferrillo, M. Ovchinnikov, F. Resnati, and A. De Roeck, “Improving the potential of BDF@SPS to search for new physics with liquid argon time projection chambers,” *JHEP* **02** (2024) 196, [arXiv:2312.14868](https://arxiv.org/abs/2312.14868) [hep-ph].

[211] **SHiP** Collaboration, C. Ahdida *et al.*, “Sensitivity of the SHiP experiment to Heavy Neutral Leptons,” *JHEP* **04** (2019) 077, [arXiv:1811.00930](https://arxiv.org/abs/1811.00930) [hep-ph].

[212] **SHiP** Collaboration, C. Ahdida *et al.*, “Sensitivity of the SHiP experiment to dark photons decaying to a pair of charged particles,” *Eur. Phys. J. C* **81** (2021) no. 5, 451, [arXiv:2011.05115](https://arxiv.org/abs/2011.05115) [hep-ex].

[213] J.-L. Tastet and I. Timiryasov, “Dirac vs. Majorana HNLs (and their oscillations) at SHiP,” *JHEP* **04** (2020) 005, [arXiv:1912.05520](https://arxiv.org/abs/1912.05520) [hep-ph].

[214] O. Mikulenko, K. Bondarenko, A. Boyarsky, and O. Ruchayskiy, “Unveiling new physics with discoveries at Intensity Frontier,” [arXiv:2312.05163](https://arxiv.org/abs/2312.05163) [hep-ph].

[215] C. M. Carloni Calame, M. Passera, L. Trentadue, and G. Venanzoni, “A new approach to evaluate the leading hadronic corrections to the muon  $g-2$ ,” *Phys. Lett. B* **746** (2015) 325–329, [arXiv:1504.02228](https://arxiv.org/abs/1504.02228) [hep-ph].

[216] **MUonE** Collaboration, G. Abbiendi *et al.*, “Measuring the leading hadronic contribution to the muon  $g-2$  via  $\mu e$  scattering,” *Eur. Phys. J. C* **77** (2017) no. 3, 139, [arXiv:1609.08987](https://arxiv.org/abs/1609.08987) [hep-ex].

[217] **MUone** Collaboration, J. Komijani *et al.*, “Proposal for phase 1 of the MUonE experiment,” Tech. Rep. CERN-SPSC-2024-015, SPSC-P-370, CERN, Geneva, 2024. <https://cds.cern.ch/record/2896293>.

[218] **NA60+** Collaboration, T. Dahms, E. Scomparin, and G. Usai, “Expression of Interest for a new experiment at the CERN SPS: NA60+,” Tech. Rep. CERN-SPSC-2019-017, SPSC-EOI-019, CERN, Geneva, 2019. <https://cds.cern.ch/record/2673280>.

[219] **ALICE** Collaboration, “Technical Design report for the ALICE Inner Tracking System 3 - ITS3; A bent wafer-scale monolithic pixel detector,” Tech. Rep. CERN-LHCC-2024-003, ALICE-TDR-021, CERN, Geneva, 2024. <https://cds.cern.ch/record/2890181>.

[220] **FPF Working Groups** Collaboration, L. A. Anchordoqui *et al.*, “The Forward Physics Facility at the Large Hadron Collider,” 3, 2025. [arXiv:2503.19010](https://arxiv.org/abs/2503.19010) [hep-ex]. Contribution to the ESPPU, March 2025.

[221] L. A. Anchordoqui *et al.*, “The Forward Physics Facility: Sites, experiments, and physics potential,” *Phys. Rept.* **968** (2022) 1–50, [arXiv:2109.10905](https://arxiv.org/abs/2109.10905) [hep-ph].

[222] J. L. Feng *et al.*, “The Forward Physics Facility at the High-Luminosity LHC,” *J. Phys. G* **50** (2023) no. 3, 030501, [arXiv:2203.05090](https://arxiv.org/abs/2203.05090) [hep-ex].

[223] J. Adhikary *et al.*, “Science and Project Planning for the Forward Physics Facility in Preparation for the 2024-2026 European Particle Physics Strategy Update,” [arXiv:2411.04175](https://arxiv.org/abs/2411.04175) [hep-ex].

[224] J. Boyd *et al.*, “Update of Facility Technical Studies for the FPF,” Tech. Rep. CERN-PBC-Notes-2024-004, CERN, 2024. <https://cds.cern.ch/record/2904086>.

[225] D. Gamba *et al.*, “Impact of Vibration to HL-LHC Performance During the FPF Facility Construction,” Tech. Rep. CERN-PBC-Notes-2024-003, CERN, 2024. <https://cds.cern.ch/record/2901520>.

[226] J. Boyd *et al.*, “Update on the FPF Facility technical studies,” Tech. Rep. CERN-PBC-Notes-2023-002, CERN, 2023. <https://cds.cern.ch/record/2851822>.

[227] S. Foroughi-Abari, F. Kling, and Y.-D. Tsai, “Looking forward to millicharged dark sectors at the LHC,” *Phys. Rev. D* **104** (2021) no. 3, 035014, [arXiv:2010.07941](https://arxiv.org/abs/2010.07941) [hep-ph].

[228] A. Haas, C. S. Hill, E. Izaguirre, and I. Yavin, “Looking for milli-charged particles with a new experiment at the LHC,” *Phys. Lett. B* **746** (2015) 117–120, [arXiv:1410.6816](https://arxiv.org/abs/1410.6816) [hep-ph].

[229] “Report of the 2023 Particle Physics Project Prioritization Panel: Executive Summary.” [https://www.usparticlephysics.org/2023-p5-report/assets/pdf/2023\\_P5\\_Executive\\_Summary.pdf](https://www.usparticlephysics.org/2023-p5-report/assets/pdf/2023_P5_Executive_Summary.pdf), 2024.

[230] **SNDLHC** Collaboration, D. Abbaneo *et al.*, “SND@HL-LHC, Scattering and Neutrino Detector in Run 4 of the LHC,” Tech. Rep. CERN-LHCC-2025-004, LHCC-P-026, CERN, Geneva, 2025. <https://cds.cern.ch/record/2926288>.

[231] J. Alimena *et al.*, “Searching for long-lived particles beyond the Standard Model at the Large Hadron Collider,” *J. Phys. G* **47** (2020) no. 9, 090501, [arXiv:1903.04497](https://arxiv.org/abs/1903.04497) [hep-ex].

[232] **CMS** Collaboration, A. Tumasyan *et al.*, “Search for long-lived particles decaying into muon pairs in proton-proton collisions at  $\sqrt{s} = 13$  TeV collected with a dedicated high-rate data stream,” *JHEP* **04** (2022) 062, [arXiv:2112.13769](https://arxiv.org/abs/2112.13769) [hep-ex].

[233] **CMS** Collaboration, A. Tumasyan *et al.*, “Search for Long-Lived Particles Decaying in the CMS End Cap Muon Detectors in Proton-Proton Collisions at  $\sqrt{s} = 13$  TeV,” *Phys. Rev. Lett.* **127** (2021) no. 26, 261804, [arXiv:2107.04838](https://arxiv.org/abs/2107.04838) [hep-ex].

[234] M. Bauer, O. Brandt, L. Lee, and C. Ohm, “ANUBIS: Proposal to search for long-lived neutral particles in CERN service shafts,” [arXiv:1909.13022](https://arxiv.org/abs/1909.13022) [physics.ins-det].

[235] T. P. Satterthwaite, *Sensitivity of the ANUBIS and ATLAS Detectors to Neutral Long-Lived Particles Produced in pp Collisions at the Large Hadron Collider (Unpublished)*. PhD thesis, Cambridge U., 2022. <https://cds.cern.ch/record/2839063>. Presented 08 Sep 2022.

[236] M. Hirsch and Z. S. Wang, “Heavy neutral leptons at ANUBIS,” *Phys. Rev. D* **101** (2020) no. 5, 055034, [arXiv:2001.04750](https://arxiv.org/abs/2001.04750) [hep-ph].

[237] M. Bauer, M. Neubert, and A. Thamm, “Collider Probes of Axion-Like Particles,” *JHEP* **12** (2017) 044, [arXiv:1708.00443](https://arxiv.org/abs/1708.00443) [hep-ph].

[238] I. Brivio *et al.*, “ALPs Effective Field Theory and Collider Signatures,” *Eur. Phys. J. C* **77** (2017) no. 8, 572, [arXiv:1701.05379](https://arxiv.org/abs/1701.05379) [hep-ph].

[239] S. Argyropoulos, O. Brandt, and U. Haisch, “Collider Searches for Dark Matter through the Higgs Lens,” *Symmetry* **13** (2021) no. 12, 2406, [arXiv:2109.13597](https://arxiv.org/abs/2109.13597) [hep-ph].

[240] **ATLAS** Collaboration, J. B. Sola *et al.*, “Technical Design Report for the Phase-II Upgrade of the ATLAS Muon Spectrometer,” Tech. Rep. CERN-LHCC-2017-017, ATLAS-TDR-026, CERN, Geneva, 2017. <https://cds.cern.ch/record/2285580>.

[241] V. V. Gligorov, S. Knapen, M. Papucci, and D. J. Robinson, “Searching for Long-lived Particles: A Compact Detector for Exotics at LHCb,” *Phys. Rev. D* **97** (2018) no. 1, 015023, [arXiv:1708.09395 \[hep-ph\]](https://arxiv.org/abs/1708.09395).

[242] G. Aielli *et al.*, “Expression of interest for the CODEX-b detector,” *Eur. Phys. J. C* **80** (2020) no. 12, 1177, [arXiv:1911.00481 \[hep-ex\]](https://arxiv.org/abs/1911.00481).

[243] G. Aielli *et al.*, “The Road Ahead for CODEX-b,” [arXiv:2203.07316 \[hep-ex\]](https://arxiv.org/abs/2203.07316).

[244] **CODEX-b** Collaboration, G. Aielli *et al.*, “Technical design report for the CODEX- $\beta$  demonstrator,” [arXiv:2406.12880 \[physics.ins-det\]](https://arxiv.org/abs/2406.12880).

[245] D. Curtin *et al.*, “Long-Lived Particles at the Energy Frontier: The MATHUSLA Physics Case,” *Rept. Prog. Phys.* **82** (2019) no. 11, 116201, [arXiv:1806.07396 \[hep-ph\]](https://arxiv.org/abs/1806.07396).

[246] Z. Chacko, H.-S. Goh, and R. Harnik, “The Twin Higgs: Natural electroweak breaking from mirror symmetry,” *Phys. Rev. Lett.* **96** (2006) 231802, [arXiv:hep-ph/0506256](https://arxiv.org/abs/hep-ph/0506256).

[247] N. Craig, A. Katz, M. Strassler, and R. Sundrum, “Naturalness in the Dark at the LHC,” *JHEP* **07** (2015) 105, [arXiv:1501.05310 \[hep-ph\]](https://arxiv.org/abs/1501.05310).

[248] D. Acosta *et al.*, “Review of opportunities for new long-lived particle triggers in Run 3 of the Large Hadron Collider,” [arXiv:2110.14675 \[hep-ex\]](https://arxiv.org/abs/2110.14675).

[249] B. Aitken *et al.*, “Conceptual Design Report for the MATHUSLA Long-Lived Particle Detector near CMS,” [arXiv:2503.20893 \[physics.ins-det\]](https://arxiv.org/abs/2503.20893).

[250] J. Barron and D. Curtin, “On the Origin of Long-Lived Particles,” *JHEP* **12** (2020) 061, [arXiv:2007.05538 \[hep-ph\]](https://arxiv.org/abs/2007.05538).

[251] C. Alpigiani *et al.*, “A Letter of Intent for MATHUSLA: a dedicated displaced vertex detector above ATLAS or CMS,” [arXiv:1811.00927 \[physics.ins-det\]](https://arxiv.org/abs/1811.00927).

[252] **MATHUSLA** Collaboration, C. Alpigiani *et al.*, “An Update to the Letter of Intent for MATHUSLA: Search for Long-Lived Particles at the HL-LHC,” [arXiv:2009.01693 \[physics.ins-det\]](https://arxiv.org/abs/2009.01693).

[253] M. Alidra *et al.*, “The MATHUSLA test stand,” *Nucl. Instrum. Meth. A* **985** (2021) 164661, [arXiv:2005.02018 \[physics.ins-det\]](https://arxiv.org/abs/2005.02018).

[254] **P5** Collaboration, S. Asai *et al.*, “Exploring the Quantum Universe: Pathways to Innovation and Discovery in Particle Physics,” [arXiv:2407.19176 \[hep-ex\]](https://arxiv.org/abs/2407.19176).

[255] **MATHUSLA** Collaboration, B. Aitken *et al.*, “Conceptual Design Report for the MATHUSLA Long-Lived Particle Detector near CMS,” [arXiv:2503.20893 \[physics.ins-det\]](https://arxiv.org/abs/2503.20893).

[256] K. Akiba *et al.*, “**ALADDIN**: An Lhc Apparatus for Direct Dipole moments INvestigation,” Tech. Rep. CERN-LHCC-2024-011, LHCC-I-041, CERN, Geneva, 2024. <https://cds.cern.ch/record/2905467>.

[257] P. Hermes *et al.*, “Update on TWOCRYST: the feasibility of double-crystal fixed-target experiments at the LHC,” *PoS ICHEP2024* (2025) 844.

[258] D. Mirarchi, A. S. Fomin, S. Redaelli, and W. Scandale, “Layouts for fixed-target experiments and dipole moment measurements of short-lived baryons using bent crystals at the LHC,” *Eur. Phys. J. C* **80** (2020) no. 10, 929, [arXiv:1906.08551 \[physics.acc-ph\]](https://arxiv.org/abs/1906.08551).

[259] C. Barschel *et al.*, “**LHC fixed target experiments**,” Tech. Rep. CERN-PBC-REPORT-2019-001, CERN-2020-004, CERN, Geneva, 2019. <https://cds.cern.ch/record/2653780>.

[260] C. A. Aidala *et al.*, “The LHCspin Project,” [arXiv:1901.08002 \[hep-ex\]](https://arxiv.org/abs/1901.08002).

[261] P. Di Nezza *et al.*, “The LHCspin project,” *PoS PANIC2021* (2022) 347.

[262] H. Avakian, A. Bressan, and M. Contalbrigo, “Experimental results on TMDs,” *Eur. Phys. J. A* **52** (2016) no. 6, 150. [Erratum: Eur. Phys. J. A 52 (2016) 165].

[263] C. Hadjidakis *et al.*, “A fixed-target programme at the LHC: Physics case and projected performances for heavy-ion, hadron, spin and astroparticle studies,” *Phys. Rept.* **911** (2021) 1–83, [arXiv:1807.00603 \[hep-ex\]](https://arxiv.org/abs/1807.00603).

[264] F. Gross *et al.*, “50 Years of Quantum Chromodynamics,” *Eur. Phys. J. C* **83** (2023) 1125, [arXiv:2212.11107 \[hep-ph\]](https://arxiv.org/abs/2212.11107).

[265] T. El-Kordy *et al.*, “Amorphous carbon-coated storage cell tests for the polarized gas target at LHCb,” *Nucl. Instrum. Meth. A* **1068** (2024) 169707.

[266] N. H. Buttimore, E. Leader, and T. L. Trueman, “An Absolute polarimeter for high-energy protons,” *Phys. Rev. D* **64** (2001) 094021, [arXiv:hep-ph/0107013](https://arxiv.org/abs/hep-ph/0107013).

[267] A. Zelenski *et al.*, “Absolute polarized H-jet polarimeter development, for RHIC,” *Nucl. Instrum. Meth. A* **536** (2005) 248–254.

[268] A. A. Pobladuev, A. Zelenski, G. Atoian, Y. Makdisi, and J. Ritter, “Systematic error analysis in the absolute hydrogen gas jet polarimeter at RHIC,” *Nucl. Instrum. Meth. A* **976** (2020) 164261, [arXiv:2006.08393 \[physics.ins-det\]](https://arxiv.org/abs/2006.08393).

[269] H. Huang *et al.*, “A p-carbon CNI polarimeter for RHIC,” in *Proceedings of the 1999 Particle Accelerator Conference (Cat. No.99CH36366)*, vol. 1, pp. 471–473. 1999.

[270] P. Di Nezza *et al.*, “LHCspin: a Polarized Gas Target for LHC,” Tech. Rep. CERN-PBC-Notes-2025-008, CERN, Geneva, 2025. <https://cds.cern.ch/record/2928086>.

[271] M. S. Safronova, D. Budker, D. DeMille, D. F. J. Kimball, A. Derevianko, and C. W. Clark, “Search for new physics with atoms and molecules,” *Rev. Mod. Phys.* **90** (2018) no. 2, 025008, [arXiv:1710.01833 \[physics.atom-ph\]](https://arxiv.org/abs/1710.01833).

[272] T. S. Roussy *et al.*, “An improved bound on the electron’s electric dipole moment,” *Science* **381** (2023) no. 6653, 46–50.

[273] G. Arrowsmith-Kron *et al.*, “Opportunities for fundamental physics research with radioactive molecules,” *Rept. Prog. Phys.* **87** (2024) no. 8, 084301, [arXiv:2302.02165 \[nucl-ex\]](https://arxiv.org/abs/2302.02165).

[274] C. Carli, D. Gamba, C. Malbrunot, L. Ponce, and S. Ulmer, “ELENA: Bright Perspectives for Low Energy Antiproton Physics,” *Nuclear Physics News* **32** (2022) no. 3, 21–27.

[275] **BASE** Collaboration, M. J. Borchert *et al.*, “A 16-parts-per-trillion measurement of the antiproton-to-proton charge–mass ratio,” *Nature* **601** (2022) no. 7891, 53–57.

[276] **BASE** Collaboration, C. Smorra *et al.*, “A parts-per-billion measurement of the antiproton magnetic moment,” *Nature* **550** (2017) no. 7676, 371–374.

[277] **ALPHA** Collaboration, E. K. Anderson *et al.*, “Observation of the effect of gravity on the motion of antimatter,” *Nature* **621** (2023) no. 7980, 716–722.

[278] M. Ahmadi *et al.*, “Characterization of the 1S–2S transition in antihydrogen,” *Nature* **557** (2018) no. 7703, 71–75.

[279] **ALPHA** Collaboration, C. J. Baker *et al.*, “Laser cooling of antihydrogen atoms,” *Nature* **592** (2021) no. 7852, 35–52.

[280] **ASACUSA** Collaboration, M. Hori *et al.*, “Buffer-gas cooling of antiprotonic helium to 1.5 to 1.7 K, and antiproton-to-electron mass ratio,” *Science* **354** (2016) no. 6312, 610–614.

[281] **ASACUSA** Collaboration, N. Kuroda *et al.*, “A source of antihydrogen for in-flight hyperfine spectroscopy,” *Nature Commun.* **5** (2014) 3089–3092.

[282] **AEgIS** Collaboration, N. Zurlo *et al.*, “Pulsed Production of Antihydrogen in AEgIS,” *EPJ Web Conf.* **290** (2023) 07001.

[283] P. Adrich *et al.*, “Production of antihydrogen atoms by 6 keV antiprotons through a positronium cloud,” *Eur. Phys. J. C* **83** (2023) no. 11, 1004, [arXiv:2306.15801 \[hep-ex\]](https://arxiv.org/abs/2306.15801). [Erratum: Eur. Phys. J. C 83 (2023) 1069, Eur. Phys. J. C 84 (2024) 1143].

[284] **AEgis** Collaboration, L. T. Glöggler *et al.*, “Positronium Laser Cooling via the 13S-23P Transition with a Broadband Laser Pulse,” *Phys. Rev. Lett.* **132** (2024) no. 8, 083402, [arXiv:2310.08760 \[physics.atom-ph\]](https://arxiv.org/abs/2310.08760).

[285] **BASE-STEP** Collaboration, C. Smorra *et al.*, “Proton Transport from the Antimatter Factory of CERN,” *Nature Portfolio, PREPRINT (Version 1)* (2024) .

[286] **PUMA** Collaboration, T. Aumann *et al.*, “PUMA, antiProton unstable matter annihilation,” *Eur. Phys. J. A* **58** (2022) no. 5, 88.

[287] E. G. Myers, “CPT tests with the antihydrogen molecular ion,” *Phys. Rev. A* **98** (2018) no. 1, 010101, [arXiv:1802.01514 \[physics.atom-ph\]](https://arxiv.org/abs/1802.01514).

[288] R. Caravita, A. C. Mathad, J. S. Hangst, M. Hori, B. M. Latacz, A. Obertelli, P. Perez, S. Ulmer, and E. Widmann, “CERN AD/ELENA Antimatter Program,” [arXiv:2503.22471 \[nucl-ex\]](https://arxiv.org/abs/2503.22471).

[289] O. Buchmueller, J. Ellis, and U. Schneider, “Large-scale atom interferometry for fundamental physics,” *Contemp. Phys.* **64** (2023) no. 2, 93–110, [arXiv:2306.17726 \[astro-ph.CO\]](https://arxiv.org/abs/2306.17726).

[290] **MAGIS-100** Collaboration, M. Abe *et al.*, “Matter-wave Atomic Gradiometer Interferometric Sensor (MAGIS-100),” *Quantum Sci. Technol.* **6** (2021) no. 4, 044003, [arXiv:2104.02835 \[physics.atom-ph\]](https://arxiv.org/abs/2104.02835).

[291] L. Badurina *et al.*, “AION: An Atom Interferometer Observatory and Network,” *JCAP* **05** (2020) 011, [arXiv:1911.11755 \[astro-ph.CO\]](https://arxiv.org/abs/1911.11755).

[292] G. Arduini *et al.*, “A Long-Baseline Atom Interferometer at CERN: Conceptual Feasibility Study,” Tech. Rep. CERN-PBC-REPORT-2023-002, CERN, 2023. [arXiv:2304.00614 \[physics.atom-ph\]](https://arxiv.org/abs/2304.00614).

[293] A. Abdalla *et al.*, “Terrestrial Very-Long-Baseline Atom Interferometry: summary of the second workshop,” *EPJ Quant. Technol.* **12** (2025) no. 1, 42, [arXiv:2412.14960 \[hep-ex\]](https://arxiv.org/abs/2412.14960).

[294] A. Berlin *et al.*, “Axion Dark Matter Detection by Superconducting Resonant Frequency Conversion,” *JHEP* **07** (2020) no. 07, 088, [arXiv:1912.11048 \[hep-ph\]](https://arxiv.org/abs/1912.11048).

[295] “An SRF Cavity for Dark Matter Axion Detection - FY2022.” <https://ldrd.slac.stanford.edu/active-projects/active-projects-fy-2022>.

[296] B. Giaccone *et al.*, “Design of axion and axion dark matter searches based on ultra high Q SRF cavities,” [arXiv:2207.11346 \[hep-ex\]](https://arxiv.org/abs/2207.11346).

[297] D. Alesini *et al.*, “The future search for low-frequency axions and new physics with the FLASH resonant cavity experiment at Frascati National Laboratories,” *Phys. Dark Univ.* **42** (2023) 101370, [arXiv:2309.00351 \[physics.ins-det\]](https://arxiv.org/abs/2309.00351).

[298] **QUAX** Collaboration, A. Rettaroli *et al.*, “Search for axion dark matter with the QUAX–LNF tunable haloscope,” *Phys. Rev. D* **110** (2024) no. 2, 022008, [arXiv:2402.19063 \[physics.ins-det\]](https://arxiv.org/abs/2402.19063).

[299] **CAST** Collaboration, A. A. Melcón *et al.*, “First results of the CAST-RADES haloscope search for axions at  $34.67\text{ }\mu\text{eV}$ ,” *JHEP* **21** (2020) 075, [arXiv:2104.13798 \[hep-ex\]](https://arxiv.org/abs/2104.13798).

[300] S. Ahyoune *et al.*, “RADES axion search results with a high-temperature superconducting cavity in an 11.7 T magnet,” *JHEP* **04** (2025) 113, [arXiv:2403.07790 \[hep-ex\]](https://arxiv.org/abs/2403.07790).

[301] A. Dhar *et al.*, “REBCO sample testing at high power X-band,” *JACoW IPAC2024* (2024) WEPS37.

[302] J. Golm *et al.*, “Split-cavity tuning of a rectangular axion haloscope operating around 8.4 GHz,” *Front. in Phys.* **12** (2024) 1372846, [arXiv:2312.13109 \[physics.ins-det\]](https://arxiv.org/abs/2312.13109).

[303] “Quantera QRADES.” <https://quantera.eu/qrades/>.

[304] S. Ahyoune *et al.*, “A Proposal for a Low-Frequency Axion Search in the  $1\text{--}2\text{ }\mu\text{eV}$  Range and Below with the BabyIAXO Magnet,” *Annalen Phys.* **535** (2023) no. 12, 2300326, [arXiv:2306.17243 \[physics.ins-det\]](https://arxiv.org/abs/2306.17243).

[305] A. Kallitsopoulou *et al.*, “PICOSEC-Micromegas Detector, an innovative solution for Lepton Time Tagging,” *Nucl. Instrum. Meth. A* **1069** (2024) 169920, [arXiv:2411.02532 \[physics.ins-det\]](https://arxiv.org/abs/2411.02532).

[306] **LHCb** Collaboration, J. B. Leite *et al.*, “Framework TDR for the LHCb Upgrade II,” Tech. Rep. CERN-LHCC-2021-012, LHCb-TDR-023, CERN, Geneva, 2021. <http://cds.cern.ch/record/2776420>.

[307] **NA62** Collaboration, E. Cortina Gil *et al.*, “First detection of a tagged neutrino in the NA62 experiment,” *Phys. Lett. B* **863** (2025) 139345, [arXiv:2412.04033 \[hep-ex\]](https://arxiv.org/abs/2412.04033).

[308] M. W. Krasny, “Electron beam for LHC,” *Nucl. Instrum. Meth. A* **540** (2005) 222–234, [arXiv:hep-ex/0405028](https://arxiv.org/abs/hep-ex/0405028).

[309] W. Placzek and M. W. Krasny, “Gamma Factory and Precision Physics at the LHC,” *Acta Phys. Polon. Supp.* **17** (2024) no. 5, A28.

[310] D. Budker *et al.*, “Expanding Nuclear Physics Horizons with the Gamma Factory,” *Annalen Phys.* **534** (2021) no. 3, 2100284, [arXiv:2106.06584 \[nucl-ex\]](https://arxiv.org/abs/2106.06584).

[311] D. Budker, M. Gorchtein, M. W. Krasny, A. Pálffy, and A. Surzhykov, “Physics Opportunities with the Gamma Factory,” *Annalen Phys.* **534** (2022) no. 3, 2200004.

[312] D. Budker *et al.*, “Atomic Physics Studies at the Gamma Factory at CERN,” *Annalen Phys.* **532** (2020) no. 8, 2000204, [arXiv:2003.03855 \[physics.atom-ph\]](https://arxiv.org/abs/2003.03855).

[313] J. Bieroń, M. W. Krasny, W. Placzek, and S. Pustelný, “Optical Excitation of Ultra-Relativistic Partially Stripped Ions,” *Annalen Phys.* **534** (2022) no. 3, 2100250, [arXiv:2106.00330 \[physics.atom-ph\]](https://arxiv.org/abs/2106.00330).

[314] V. G. Serbo, A. Surzhykov, and A. Volotka, “Resonant Scattering of Plane-Wave and Twisted Photons at the Gamma Factory,” *Annalen Phys.* **534** (2022) no. 3, 2100199, [arXiv:2108.01859 \[physics.atom-ph\]](https://arxiv.org/abs/2108.01859).

[315] V. V. Flambaum, J. Jin, and D. Budker, “Resonance photoproduction of pionic atoms at the proposed Gamma Factory,” *Phys. Rev. C* **103** (2021) no. 5, 054603, [arXiv:2010.06912 \[nucl-ex\]](https://arxiv.org/abs/2010.06912).

[316] B. Wojtsekhowski and D. Budker, “Local Lorentz Invariance Tests for Photons and Hadrons at the Gamma Factory,” *Annalen Phys.* **534** (2022) no. 3, 2100141, [arXiv:2104.03784 \[hep-ex\]](https://arxiv.org/abs/2104.03784).

[317] F. Karbstein, “Vacuum Birefringence at the Gamma Factory,” *Annalen Phys.* **534** (2022) no. 3, 2100137, [arXiv:2106.06359 \[hep-ph\]](https://arxiv.org/abs/2106.06359).

[318] R. Balkin, M. W. Krasny, T. Ma, B. R. Safdi, and Y. Soreq, “Probing Axion-Like-Particles at the CERN Gamma Factory,” *Annalen Phys.* **534** (2022) no. 3, 2100222, [arXiv:2105.15072 \[hep-ph\]](https://arxiv.org/abs/2105.15072).

[319] S. Chakraborti, J. L. Feng, J. K. Koga, and M. Valli, “Gamma factory searches for extremely weakly interacting particles,” *Phys. Rev. D* **104** (2021) no. 5, 055023, [arXiv:2105.10289 \[hep-ph\]](https://arxiv.org/abs/2105.10289).

[320] F. Zimmermann, “Accelerator Technology and Beam Physics of Future Colliders,” *Front. in Phys.* **10** (2022) 888395.

[321] D. A. Cooke *et al.*, “Measurement and application of electron stripping of ultrarelativistic  $^{208}\text{Pb}^{81+}$ ,” *Nucl. Instrum. Meth. A* **988** (2021) 164902, [arXiv:2006.16160 \[physics.acc-ph\]](https://arxiv.org/abs/2006.16160).

[322] F. Zimmermann *et al.*, “Muon Collider Based on Gamma Factory, FCC-ee and Plasma Target,” *JACoW IPAC2022* (2022) 1691–1694.

[323] F. Zimmermann *et al.*, “Advanced accelerator concepts for dark sector searches and fast muon acceleration,” *JACoW IPAC2024* (2024) MOPR17.

[324] F. Zimmermann, “Beam Physics Frontier Problems,” *JACoW eeFACT2022* (2023) 42–51.

[325] A. Caldwell *et al.*, “Particle physics applications of the AWAKE acceleration scheme,” [arXiv:1812.11164 \[physics.acc-ph\]](https://arxiv.org/abs/1812.11164).

[326] M. Wing, “Particle physics experiments based on the AWAKE acceleration scheme,” *Phil. Trans. R. Soc. A* **377** (2019) 20180185, [arXiv:1810.12254 \[physics.acc-ph\]](https://arxiv.org/abs/1810.12254).

[327] **NA64** Collaboration, E. Gschwendtner *et al.*, “AWAKE++: The AWAKE Acceleration Scheme for New Particle Physics Experiments at CERN,” Tech. Rep. CERN-PBC-REPORT-2018-005, CERN, Geneva, 2018. <https://cds.cern.ch/record/2651319>.

[328] C. Bamber *et al.*, “Studies of nonlinear QED in collisions of 46.6 GeV electrons with intense laser pulses,” *Phys. Rev. D* **60** (1999) 092004.

[329] A. Fedotov *et al.*, “Advances in QED with intense background fields,” *Phys. Rept.* **1010** (2023) 1–138, [arXiv:2203.00019 \[hep-ph\]](https://arxiv.org/abs/2203.00019).

[330] **E320** Collaboration, D. Reis and S. Meuren, “E-320 Progress in FY24 and Plans for FY25,”. <https://indico.slac.stanford.edu/event/9280/contributions/10855/>.

[331] **LUXE** Collaboration, H. Abramowicz *et al.*, “Technical Design Report for the LUXE experiment,” *Eur. Phys. J. ST* **233** (2024) no. 10, 1709–1974, [arXiv:2308.00515 \[hep-ex\]](https://arxiv.org/abs/2308.00515).

[332] V. N. Baier, V. M. Katkov, and V. M. Strakhovenko, *Electromagnetic processes at high energies in oriented single crystals*. World Scientific, 6, 1998.

[333] U. I. Uggerhj, “The interaction of relativistic particles with strong crystalline fields,” *Rev. Mod. Phys.* **77** (2005) 1131–1171.

[334] V. G. Baryshevsky and V. V. Tikhomirov, “Synchrotron type radiation processes in crystals and polarization phenomena accompanying them,” *Sov. Phys. Usp.* **32** (1989) 1013–1032.

[335] D. Schulte, “High-energy beam-beam effects in CLIC,” Tech. Rep. CERN-PS-99-017-LP, CERN-PS-99-17-LP, CERN-CLIC-NOTE-391, CLIC-NOTE-391, CERN, Geneva, 1999. <https://cds.cern.ch/record/2828394>.

[336] M. Filipovic, C. Baumann, A. M. Pukhov, A. S. Samsonov, and I. Y. Kostyukov, “Effect of transverse displacement of charged particle beams on quantum electrodynamic processes during their collision,” *Quantum Electron.* **51** (2021) no. 9, 807–811.

[337] I. Schulthess and F. Meloni, “New Physics Search with the Optical Dump Concept at Future Colliders,” [arXiv:2503.20996 \[hep-ph\]](https://arxiv.org/abs/2503.20996).

[338] V. G. Baryshevsky, “Spin rotation and depolarization of relativistic particles traveling through a crystal,” *Nucl. Instrum. Meth. B* **44** (1990) 266–272.

[339] V. G. Baryshevsky and A. O. Grubich, “POSSIBILITY OF MEASURING THE ANOMALOUS MAGNETIC MOMENT OF ULTRARELATIVISTIC E- (E+) AS A FUNCTION OF PARTICLE ENERGY AND STRENGTH OF THE EXTERNAL FIELD. (IN RUSSIAN),” *Yad. Fiz.* **44** (1986) 1114–1115.

[340] V. V. Tikhomirov, “Possibility of observing radiative self-polarization and the production of polarized  $e^+e^-$  pairs in crystals at accessible energies,” *JETP Lett.* **58** (1993) 166–170. [http://jetpletters.ru/ps/0/article\\_17893.shtml](http://jetpletters.ru/ps/0/article_17893.shtml).

[341] V. V. Tikhomirov, “On the circular polarization and spin dependence of surface radiation of positrons,” *JETP* **109** (1996) 639–646.

[342] V. V. Tikhomirov, “Spin precession of ultrarelativistic electrons in a circularly polarized electromagnetic wave,” *Phys. Rev. D* **53** (1996) 7213–7222.

[343] V. V. Tikhomirov, “Electron-Spin Precession in a Plane Electromagnetic Wave,” *Phys. Rev. Lett.* **87** (2001) 181801.

[344] P. Satyamurthy *et al.*, “Design of an 18-MW vortex flow water beam dump for 500-GeV electrons/positrons of an international linear collider,” *Nucl. Instrum. Meth. A* **679** (2012) 67–81.

[345] M. M. Nojiri, Y. Sakaki, K. Tobioka, and D. Ueda, “First evaluation of meson and  $\tau$  lepton spectra and search for heavy neutral leptons at ILC beam dump,” *JHEP* **12** (2022) 145, [arXiv:2206.13523 \[hep-ph\]](https://arxiv.org/abs/2206.13523).

[346] A. Ishikawa, Y. Sakaki, and Y. Takubo, “Search for axion-like particles with electron and positron beams at the KEK linac,” *PTEP* **2022** (2022) no. 11, 113B05, [arXiv:2107.06431 \[hep-ph\]](https://arxiv.org/abs/2107.06431).

[347] M. Litos *et al.*, “High-efficiency acceleration of an electron beam in a plasma wakefield accelerator,” *Nature* **515** (2014) no. 7525, 92–95.

[348] F. J. M. Farley, K. Jungmann, J. P. Miller, W. M. Morse, Y. F. Orlov, B. L. Roberts, Y. K. Semertzidis, A. Silenko, and E. J. Stephenson, “New Method of Measuring Electric Dipole Moments in Storage Rings,” *Phys. Rev. Lett.* **93** (2004) 052001, [arXiv:hep-ex/0307006](https://arxiv.org/abs/hep-ex/0307006).

[349] **CPEDM** Collaboration, F. Abusaif *et al.*, *Storage ring to search for electric dipole moments of charged particles: Feasibility study*. CERN, Geneva, 6, 2021. [arXiv:1912.07881 \[hep-ex\]](https://arxiv.org/abs/1912.07881).

[350] Z. Omarov, H. Davoudiasl, S. Haciomeroglu, V. Lebedev, W. M. Morse, Y. K. Semertzidis, A. J. Silenko, E. J. Stephenson, and R. Suleiman, “Comprehensive symmetric-hybrid ring design for a proton EDM experiment at below 10-29e·cm,” *Phys. Rev. D* **105** (2022) no. 3, 032001, [arXiv:2007.10332 \[physics.acc-ph\]](https://arxiv.org/abs/2007.10332).

[351] C. Abel *et al.*, “Measurement of the Permanent Electric Dipole Moment of the Neutron,” *Phys. Rev. Lett.* **124** (2020) no. 8, 081803, [arXiv:2001.11966 \[hep-ex\]](https://arxiv.org/abs/2001.11966).

[352] S. Haciömeroğlu and Y. K. Semertzidis, “Systematic errors related to quadrupole misplacement in an all-electric storage ring for proton EDM experiment,” [arXiv:1709.01208 \[physics.acc-ph\]](https://arxiv.org/abs/1709.01208).

[353] M. Haj Tahar and C. Carli, “Benchmarking of analytical estimates to study systematic errors for the charged particle electric dipole moment measurements,” *Phys. Rev. Accel. Beams* **24** (2021) no. 3, 034003, [arXiv:2008.12058 \[physics.acc-ph\]](https://arxiv.org/abs/2008.12058).

[354] C. Carli and M. Haj Tahar, “Geometric phase effect study in electric dipole moment rings,” *Phys. Rev. Accel. Beams* **25** (2022) no. 6, 064001.

[355] V. Cilento and C. Carli, “Vertical Spin build-up due to Vertical Offset in Quadrupoles and Horizontal Betatron Oscillations,” Tech. Rep. CERN-PBC-REPORT-2024-001, CERN, Geneva, 2024. <https://cds.cern.ch/record/2902257>.

[356] V. Cilento and C. Carli, “A systematic Effect in EDM Rings due to radial Offsets of electrostatic Bendings and longitudinal Magnetic Fields,” Tech. Rep. CERN-PBC-REPORT-2024-002, CERN, Geneva, 2024. <https://cds.cern.ch/record/2907231>.

[357] **JEDI** Collaboration, G. Guidoboni *et al.*, “How to Reach a Thousand-Second in-Plane Polarization Lifetime with 0.97-GeV/c Deuterons in a Storage Ring,” *Phys. Rev. Lett.* **117** (2016) no. 5, 054801.

[358] **JEDI** Collaboration, D. Eversmann *et al.*, “New method for a continuous determination of the spin tune in storage rings and implications for precision experiments,” *Phys. Rev. Lett.* **115** (2015) no. 9, 094801, [arXiv:1504.00635 \[physics.acc-ph\]](https://arxiv.org/abs/1504.00635).

[359] **JEDI** Collaboration, G. Guidoboni *et al.*, “Connection between zero chromaticity and long in-plane polarization lifetime in a magnetic storage ring,” *Phys. Rev. Accel. Beams* **21** (2018) no. 2, 024201, [arXiv:1710.09068 \[physics.acc-ph\]](https://arxiv.org/abs/1710.09068).

[360] **JEDI** Collaboration, S. Karanth *et al.*, “First Search for Axionlike Particles in a Storage Ring Using a Polarized Deuteron Beam,” *Phys. Rev. X* **13** (2023) no. 3, 031004, [arXiv:2208.07293 \[hep-ex\]](https://arxiv.org/abs/2208.07293).

[361] K. Zioutas *et al.*, “Search for anti-quark nuggets via their interaction with the LHC beam,” [arXiv:2403.05608 \[hep-ex\]](https://arxiv.org/abs/2403.05608).

[362] C. Pizzolotto *et al.*, “The FAMU experiment: muonic hydrogen high precision spectroscopy studies,” *Eur. Phys. J. A* **56** (2020) no. 7, 185.

[363] A. Ariga *et al.*, “Detecting LHC Neutrinos at Surface Level,” [arXiv:2501.06142 \[hep-ex\]](https://arxiv.org/abs/2501.06142).

[364] N. W. Kamp, C. A. Argüelles, A. Karle, J. Thomas, and T. Yuan, “Lake- and Surface-Based Detectors for Forward Neutrino Physics,” [arXiv:2501.08278 \[hep-ex\]](https://arxiv.org/abs/2501.08278).

[365] F. Spengler, D. Rätzel, and D. Braun, “Perspectives of measuring gravitational effects of laser light and particle beams,” *New J. Phys.* **24** (2022) no. 5, 053021, [arXiv:2104.09209 \[gr-qc\]](https://arxiv.org/abs/2104.09209).

[366] N. Paul, G. Bian, T. Azuma, S. Okada, and P. Indelicato, “Testing Quantum Electrodynamics with Exotic Atoms,” *Phys. Rev. Lett.* **126** (2021) no. 17, 173001, [arXiv:2011.09715 \[physics.atom-ph\]](https://arxiv.org/abs/2011.09715).

[367] J. Niedziela, “SHIFT@LHC: Searches for new physics with shifted interaction on a fixed target at the Large Hadron Collider,” *JHEP* **10** (2024) 204, [arXiv:2406.08557 \[hep-ph\]](https://arxiv.org/abs/2406.08557).

[368] **NA62** Collaboration, E. Cortina Gil *et al.*, “Search for hadronic decays of feebly-interacting particles at NA62,” [arXiv:2502.04241 \[hep-ex\]](https://arxiv.org/abs/2502.04241).

[369] J. Jerhot, B. Döbrich, F. Ertas, F. Kahlhoefer, and T. Spadaro, “ALPINIST: Axion-Like Particles In Numerous Interactions Simulated and Tabulated,” *JHEP* **07** (2022) 094, [arXiv:2201.05170 \[hep-ph\]](https://arxiv.org/abs/2201.05170).

[370] M. Ovchynnikov, J.-L. Tastet, O. Mikulenko, and K. Bondarenko, “Sensitivities to feebly interacting particles: Public and unified calculations,” *Phys. Rev. D* **108** (2023) no. 7, 075028, [arXiv:2305.13383 \[hep-ph\]](https://arxiv.org/abs/2305.13383).

[371] J. L. Feng, J. Li, X. Liao, J. Ni, and J. Pei, “Discovering quirks through timing at FASER and future forward experiments at the LHC,” *JHEP* **06** (2024) 197, [arXiv:2404.13814 \[hep-ph\]](https://arxiv.org/abs/2404.13814).

[372] T. Aoyama *et al.*, “The anomalous magnetic moment of the muon in the Standard Model,” *Phys. Rept.* **887** (2020) 1–166, [arXiv:2006.04822 \[hep-ph\]](https://arxiv.org/abs/2006.04822).

[373] **Muon g-2** Collaboration, G. W. Bennett *et al.*, “Final Report of the Muon E821 Anomalous Magnetic Moment Measurement at BNL,” *Phys. Rev. D* **73** (2006) 072003, [arXiv:hep-ex/0602035](https://arxiv.org/abs/hep-ex/0602035).

[374] **Muon g-2** Collaboration, D. P. Aguillard *et al.*, “Measurement of the Positive Muon Anomalous Magnetic Moment to 0.20 ppm,” *Phys. Rev. Lett.* **131** (2023) no. 16, 161802, [arXiv:2308.06230 \[hep-ex\]](https://arxiv.org/abs/2308.06230).

[375] **Muon g-2** Collaboration, D. P. Aguillard *et al.*, “Detailed report on the measurement of the positive muon anomalous magnetic moment to 0.20 ppm,” *Phys. Rev. D* **110** (2024) no. 3, 032009, [arXiv:2402.15410 \[hep-ex\]](https://arxiv.org/abs/2402.15410).

[376] M. Abe *et al.*, “A New Approach for Measuring the Muon Anomalous Magnetic Moment and Electric Dipole Moment,” *PTEP* **2019** (2019) no. 5, 053C02, [arXiv:1901.03047 \[physics.ins-det\]](https://arxiv.org/abs/1901.03047).

[377] A. Boccaletti *et al.*, “High precision calculation of the hadronic vacuum polarisation contribution to the muon anomaly,” [arXiv:2407.10913 \[hep-lat\]](https://arxiv.org/abs/2407.10913).

[378] **BaBar** Collaboration, B. Aubert *et al.*, “Precise Measurement of the  $e^+e^- \rightarrow \pi^+\pi^-(\gamma)$  Cross Section with the Initial State Radiation Method at BABAR,” *Phys. Rev. Lett.* **103** (2009) 231801, [arXiv:0908.3589 \[hep-ex\]](https://arxiv.org/abs/0908.3589).

[379] **BaBar** Collaboration, J. P. Lees *et al.*, “Precise measurement of the  $e^+e^- \rightarrow \pi^+\pi^-(\gamma)$  cross section with the initial-state radiation method at BABAR,” *Phys. Rev. D* **86** (2012) 032013, [arXiv:1205.2228 \[hep-ex\]](https://arxiv.org/abs/1205.2228).

[380] **CMD-3** Collaboration, F. V. Ignatov *et al.*, “Measurement of the  $e^+e^- \rightarrow \pi^+\pi^-$  cross section from threshold to 1.2 GeV with the CMD-3 detector,” *Phys. Rev. D* **109** (2024) no. 11, 112002, [arXiv:2302.08834 \[hep-ex\]](https://arxiv.org/abs/2302.08834).

[381] **CMD-3** Collaboration, F. V. Ignatov *et al.*, “Measurement of the Pion Form Factor with CMD-3 Detector and its Implication to the Hadronic Contribution to Muon (g-2),” *Phys. Rev. Lett.* **132** (2024) no. 23, 231903, [arXiv:2309.12910 \[hep-ex\]](https://arxiv.org/abs/2309.12910).

[382] **KLOE** Collaboration, F. Ambrosino *et al.*, “Measurement of  $\sigma(e^+e^- \rightarrow \pi^+\pi^-\gamma(\gamma))$  and the dipion contribution to the muon anomaly with the KLOE detector,” *Phys. Lett. B* **670** (2009) 285–291, [arXiv:0809.3950 \[hep-ex\]](https://arxiv.org/abs/0809.3950).

[383] **KLOE** Collaboration, F. Ambrosino *et al.*, “Measurement of  $\sigma(e^+e^- \rightarrow \pi^+\pi^-)$  from threshold to 0.85 GeV<sup>2</sup> using initial state radiation with the KLOE detector,” *Phys. Lett. B* **700** (2011) 102–110, [arXiv:1006.5313 \[hep-ex\]](https://arxiv.org/abs/1006.5313).

[384] **KLOE** Collaboration, D. Babusci *et al.*, “Precision measurement of  $\sigma(e^+e^- \rightarrow \pi^+\pi^-\gamma)/\sigma(e^+e^- \rightarrow \mu^+\mu^-\gamma)$  and determination of the  $\pi^+\pi^-$  contribution to the muon anomaly with the KLOE detector,” *Phys. Lett. B* **720** (2013) 336–343, [arXiv:1212.4524 \[hep-ex\]](https://arxiv.org/abs/1212.4524).

[385] **KLOE-2** Collaboration, A. Anastasi *et al.*, “Combination of KLOE  $\sigma(e^+e^- \rightarrow \pi^+\pi^-\gamma(\gamma))$  measurements and determination of  $a_\mu^{\pi^+\pi^-}$  in the energy range  $0.10 < s < 0.95$  GeV<sup>2</sup>,” *JHEP* **03** (2018) 173, [arXiv:1711.03085 \[hep-ex\]](https://arxiv.org/abs/1711.03085).

[386] M. Davier *et al.*, “The Discrepancy Between  $\tau$  and  $e^+e^-$  Spectral Functions Revisited and the Consequences for the Muon Magnetic Anomaly,” *Eur. Phys. J. C* **66** (2010) 127–136, [arXiv:0906.5443](https://arxiv.org/abs/0906.5443) [hep-ph].

[387] M. Davier, A. Höcker, B. Malaescu, C.-Z. Yuan, and Z. Zhang, “Update of the ALEPH non-strange spectral functions from hadronic  $\tau$  decays,” *Eur. Phys. J. C* **74** (2014) no. 3, 2803, [arXiv:1312.1501](https://arxiv.org/abs/1312.1501) [hep-ex].

[388] S. Borsanyi *et al.*, “Leading hadronic contribution to the muon magnetic moment from lattice QCD,” *Nature* **593** (2021) no. 7857, 51–55, [arXiv:2002.12347](https://arxiv.org/abs/2002.12347) [hep-lat].

[389] **ALICE** Collaboration, S. Acharya *et al.*, “Physics of the ALICE Forward Calorimeter upgrade,” Tech. Rep. ALICE-PUBLIC-2023-001, CERN, 2023. <https://inspirehep.net/files/e81d52c34a7f46998ce0ac101d2823ef>.

[390] S. Alekhin *et al.*, “A facility to Search for Hidden Particles at the CERN SPS: the SHiP physics case,” *Rept. Prog. Phys.* **79** (2016) no. 12, 124201, [arXiv:1504.04855](https://arxiv.org/abs/1504.04855) [hep-ph].

[391] R. D. Ball *et al.*, “Parton distributions with small-x resummation: evidence for BFKL dynamics in HERA data,” *Eur. Phys. J. C* **78** (2018) no. 4, 321, [arXiv:1710.05935](https://arxiv.org/abs/1710.05935) [hep-ph].

[392] A. Bhattacharya, F. Kling, I. Sarcevic, and A. M. Stasto, “Forward neutrinos from charm at the Large Hadron Collider,” *Phys. Rev. D* **109** (2024) no. 1, 014040, [arXiv:2306.01578](https://arxiv.org/abs/2306.01578) [hep-ph].

[393] Cruz-Martinez *et al.*, “The LHC as a Neutrino-Ion Collider,” *Eur. Phys. J. C* **84** (2024) no. 4, 369, [arXiv:2309.09581](https://arxiv.org/abs/2309.09581) [hep-ph].

[394] E. Hammou and M. Ubiali, “Unravelling New Physics Signals at the HL-LHC with Low-Energy Constraints,” [arXiv:2410.00963](https://arxiv.org/abs/2410.00963) [hep-ph].

[395] P. C. Barry, N. Sato, W. Melnitchouk, and C.-R. Ji, “First Monte Carlo Global QCD Analysis of Pion Parton Distributions,” *Phys. Rev. Lett.* **121** (2018) no. 15, 152001, [arXiv:1804.01965](https://arxiv.org/abs/1804.01965) [hep-ph].

[396] I. Novikov *et al.*, “Parton distribution functions of the charged pion within the xFitter framework,” *Phys. Rev. D* **102** (2020) no. 1, 014040, [arXiv:2002.02902](https://arxiv.org/abs/2002.02902) [hep-ph].

[397] **Jefferson Lab Angular Momentum (JAM)** Collaboration, P. C. Barry, C.-R. Ji, N. Sato, and W. Melnitchouk, “Global QCD Analysis of Pion Parton Distributions with Threshold Resummation,” *Phys. Rev. Lett.* **127** (2021) no. 23, 232001, [arXiv:2108.05822](https://arxiv.org/abs/2108.05822) [hep-ph].

[398] **Jefferson Lab Angular Momentum (JAM), HadStruc** Collaboration, P. C. Barry *et al.*, “Complementarity of experimental and lattice QCD data on pion parton distributions,” *Phys. Rev. D* **105** (2022) no. 11, 114051, [arXiv:2204.00543](https://arxiv.org/abs/2204.00543) [hep-ph].

[399] L. Kotz, A. Courtoy, P. Nadolsky, F. Olness, and M. Ponce-Chavez, “Analysis of parton distributions in a pion with Bézier parametrizations,” *Phys. Rev. D* **109** (2024) no. 7, 074027, [arXiv:2311.08447](https://arxiv.org/abs/2311.08447) [hep-ph].

[400] **Extended Twisted Mass** Collaboration, C. Alexandrou *et al.*, “Quark and Gluon Momentum Fractions in the Pion and in the Kaon,” *Phys. Rev. Lett.* **134** (2025) no. 13, 131902, [arXiv:2405.08529](https://arxiv.org/abs/2405.08529) [hep-lat].

[401] **ACCMOR** Collaboration, C. Daum *et al.*, “Diffractive Production of Strange Mesons at 63 GeV,” *Nucl. Phys. B* **187** (1981) 1–41.

[402] **KLF** Collaboration, M. Amaryan *et al.*, “Strange Hadron Spectroscopy with Secondary  $K_L$  Beam in Hall D,” [arXiv:2008.08215](https://arxiv.org/abs/2008.08215) [nucl-ex].

[403] H. Fujioka *et al.*, “Extension of the J-PARC Hadron Experimental Facility – summary report,” [arXiv:1706.07916 \[nucl-ex\]](https://arxiv.org/abs/1706.07916).

[404] T. Galatyuk, “[https://github.com/tgalatyuk/interaction\\_rate\\_facilities/blob/main/hist\\_rates\\_detectors\\_2022\\_jun.pdf](https://github.com/tgalatyuk/interaction_rate_facilities/blob/main/hist_rates_detectors_2022_jun.pdf)”,

[405] T. Galatyuk, “Future facilities for high  $\mu_B$  physics,” *Nucl. Phys. A* **982** (2019) 163–169.

[406] **CBM** Collaboration, T. Ablyazimov *et al.*, “Challenges in QCD matter physics –The scientific programme of the Compressed Baryonic Matter experiment at FAIR,” *Eur. Phys. J. A* **53** (2017) no. 3, 60, [arXiv:1607.01487 \[nucl-ex\]](https://arxiv.org/abs/1607.01487).

[407] M. Gazdzicki, D. Kikola, I. Pidhurskyi, and L. Tinti, “Production locality and spatial diffusion of heavy flavour at high energy densities,” [arXiv:2305.00212 \[hep-ph\]](https://arxiv.org/abs/2305.00212).

[408] **FASER** Collaboration, R. Mammen Abraham *et al.*, “Neutrino rate predictions for FASER,” *Phys. Rev. D* **110** (2024) no. 1, 012009, [arXiv:2402.13318 \[hep-ex\]](https://arxiv.org/abs/2402.13318).

[409] A. Ariga, J. Boyd, F. Kling, and A. De Roeck, “Neutrino Experiments at the Large Hadron Collider,” [arXiv:2501.10078 \[hep-ex\]](https://arxiv.org/abs/2501.10078).

[410] E. Worcester, “The Dawn of Collider Neutrino Physics,” *APS Physics* **16** (2023) 113.

[411] **FASER** Collaboration, R. Mammen Abraham *et al.*, “Prospects and Opportunities with an upgraded FASER Neutrino Detector during the HL-LHC era: Input to the EPPSU,” [arXiv:2503.19775 \[hep-ex\]](https://arxiv.org/abs/2503.19775).

[412] L. A. Anchordoqui, C. G. Canal, F. Kling, S. J. Sciutto, and J. F. Soriano, “An explanation of the muon puzzle of ultrahigh-energy cosmic rays and the role of the Forward Physics Facility for model improvement,” *JHEAp* **34** (2022) 19–32, [arXiv:2202.03095 \[hep-ph\]](https://arxiv.org/abs/2202.03095).

[413] R. Gauld, J. Rojo, L. Rottoli, S. Sarkar, and J. Talbert, “The prompt atmospheric neutrino flux in the light of LHCb,” *JHEP* **02** (2016) 130, [arXiv:1511.06346 \[hep-ph\]](https://arxiv.org/abs/1511.06346).

[414] J. Rojo, “Deep-inelastic scattering with collider neutrinos at the LHC and beyond,” *PoS DIS2024* (2025) 037, [arXiv:2407.06731 \[hep-ph\]](https://arxiv.org/abs/2407.06731).

[415] W. Bai *et al.*, “Forward production of prompt neutrinos from charm in the atmosphere and at high energy colliders,” *JHEP* **10** (2023) 142, [arXiv:2212.07865 \[hep-ph\]](https://arxiv.org/abs/2212.07865).

[416] **EAS-MSU, IceCube, KASCADE-Grande, NEVOD-DECOR, Pierre Auger, SUGAR, Telescope Array, Yakutsk EAS Array** Collaboration, D. Soldin, “Update on the Combined Analysis of Muon Measurements from Nine Air Shower Experiments,” *PoS ICRC2021* (2021) 349, [arXiv:2108.08341 \[astro-ph.HE\]](https://arxiv.org/abs/2108.08341).

[417] J. Albrecht *et al.*, “The Muon Puzzle in cosmic-ray induced air showers and its connection to the Large Hadron Collider,” *Astrophys. Space Sci.* **367** (2022) no. 3, 27, [arXiv:2105.06148 \[astro-ph.HE\]](https://arxiv.org/abs/2105.06148).

[418] P. Agrawal and K. Howe, “Factoring the Strong CP Problem,” *JHEP* **12** (2018) 029, [arXiv:1710.04213 \[hep-ph\]](https://arxiv.org/abs/1710.04213).

[419] A. Hook, S. Kumar, Z. Liu, and R. Sundrum, “High Quality QCD Axion and the LHC,” *Phys. Rev. Lett.* **124** (2020) no. 22, 221801, [arXiv:1911.12364 \[hep-ph\]](https://arxiv.org/abs/1911.12364).

[420] T. Flacke, C. Fruguele, E. Fuchs, R. S. Gupta, and G. Perez, “Phenomenology of relaxion-Higgs mixing,” *JHEP* **06** (2017) 050, [arXiv:1610.02025 \[hep-ph\]](https://arxiv.org/abs/1610.02025).

[421] A. Banerjee, H. Kim, O. Matsedonskyi, G. Perez, and M. S. Safronova, “Probing the Relaxed Relaxion at the Luminosity and Precision Frontiers,” *JHEP* **07** (2020) 153, [arXiv:2004.02899 \[hep-ph\]](https://arxiv.org/abs/2004.02899).

[422] T. Asaka and M. Shaposhnikov, “The vMSM, dark matter and baryon asymmetry of the universe,” *Phys. Lett. B* **620** (2005) 17–26, [arXiv:hep-ph/0505013](https://arxiv.org/abs/hep-ph/0505013).

[423] K. Bondarenko, A. Boyarsky, D. Gorbunov, and O. Ruchayskiy, “Phenomenology of GeV-scale Heavy Neutral Leptons,” *JHEP* **11** (2018) 032, [arXiv:1805.08567 \[hep-ph\]](https://arxiv.org/abs/1805.08567).

[424] J. L. Feng and J. Kumar, “The WIMPless Miracle: Dark-Matter Particles without Weak-Scale Masses or Weak Interactions,” *Phys. Rev. Lett.* **101** (2008) 231301, [arXiv:0803.4196 \[hep-ph\]](https://arxiv.org/abs/0803.4196).

[425] B. Batell, M. Pospelov, and A. Ritz, “Exploring pPortals to a hidden sector through fixed targets,” *Phys. Rev. D* **80** (2009) 095024, [arXiv:0906.5614 \[hep-ph\]](https://arxiv.org/abs/0906.5614).

[426] **ArgoNeuT** Collaboration, R. Acciarri *et al.*, “Improved Limits on Millicharged Particles Using the ArgoNeuT Experiment at Fermilab,” *Phys. Rev. Lett.* **124** (2020) no. 13, 131801, [arXiv:1911.07996 \[hep-ex\]](https://arxiv.org/abs/1911.07996).

[427] **milliQan** Collaboration, A. Ball *et al.*, “Sensitivity to millicharged particles in future proton-proton collisions at the LHC with the milliQan detector,” *Phys. Rev. D* **104** (2021) no. 3, 032002, [arXiv:2104.07151 \[hep-ex\]](https://arxiv.org/abs/2104.07151).

[428] A. A. Prinz *et al.*, “Search for Millicharged Particles at SLAC,” *Phys. Rev. Lett.* **81** (1998) 1175–1178, [arXiv:hep-ex/9804008](https://arxiv.org/abs/hep-ex/9804008).

[429] G. Magill, R. Plestid, M. Pospelov, and Y.-D. Tsai, “Millicharged Particles in Neutrino Experiments,” *Phys. Rev. Lett.* **122** (2019) no. 7, 071801, [arXiv:1806.03310 \[hep-ph\]](https://arxiv.org/abs/1806.03310).

[430] **LSND** Collaboration, L. B. Auerbach *et al.*, “Measurement of electron-neutrino electron elastic scattering,” *Phys. Rev. D* **63** (2001) 112001, [arXiv:hep-ex/0101039](https://arxiv.org/abs/hep-ex/0101039).

[431] H. Wu, E. Hardy, and N. Song, “Searching for heavy millicharged particles from the atmosphere,” *Phys. Rev. D* **110** (2024) no. 11, 115037, [arXiv:2406.01668 \[hep-ph\]](https://arxiv.org/abs/2406.01668).

[432] **SENSEI** Collaboration, L. Barak *et al.*, “Search by the SENSEI Experiment for Millicharged Particles Produced in the NuMI Beam,” *Phys. Rev. Lett.* **133** (2024) no. 7, 071801, [arXiv:2305.04964 \[hep-ex\]](https://arxiv.org/abs/2305.04964).

[433] **CMS** Collaboration, S. Chatrchyan *et al.*, “Search for Fractionally Charged Particles in  $pp$  Collisions at  $\sqrt{s} = 7$  TeV,” *Phys. Rev. D* **87** (2013) no. 9, 092008, [arXiv:1210.2311 \[hep-ex\]](https://arxiv.org/abs/1210.2311). [Erratum: *Phys. Rev. D* 106 (2022) 099903].

[434] G. Marocco and S. Sarkar, “Blast from the past: Constraints on the dark sector from the BEBC WA66 beam dump experiment,” *SciPost Phys.* **10** (2021) no. 2, 043, [arXiv:2011.08153 \[hep-ph\]](https://arxiv.org/abs/2011.08153).

[435] V. Gorkavenko, B. K. Jashal, V. Kholoimov, Y. Kyselov, D. Mendoza, M. Ovchynnikov, A. Oyanaguren, V. Svintozelskyi, and J. Zhuo, “LHCb potential to discover long-lived new physics particles with lifetimes above 100 ps,” *Eur. Phys. J. C* **84** (2024) no. 6, 608, [arXiv:2312.14016 \[hep-ph\]](https://arxiv.org/abs/2312.14016).

[436] **BNL-E949** Collaboration, A. V. Artamonov *et al.*, “Study of the decay  $K^+ \rightarrow \pi^+ v\bar{v}$  in the momentum region  $140 < P_\pi < 199$  MeV/c,” *Phys. Rev. D* **79** (2009) 092004, [arXiv:0903.0030 \[hep-ex\]](https://arxiv.org/abs/0903.0030).

[437] **NA62** Collaboration, E. Cortina Gil *et al.*, “Search for  $\pi^0$  decays to invisible particles,” *JHEP* **02** (2021) 201, [arXiv:2010.07644 \[hep-ex\]](https://arxiv.org/abs/2010.07644).

[438] **NA62** Collaboration, E. Cortina Gil *et al.*, “Measurement of the very rare  $K^+ \rightarrow \pi^+ v\bar{v}$  decay,” *JHEP* **06** (2021) 093, [arXiv:2103.15389 \[hep-ex\]](https://arxiv.org/abs/2103.15389).

[439] **MicroBooNE** Collaboration, P. Abratenko *et al.*, “Search for a Higgs Portal Scalar Decaying to Electron-Positron Pairs in the MicroBooNE Detector,” *Phys. Rev. Lett.* **127** (2021) no. 15, 151803, [arXiv:2106.00568](https://arxiv.org/abs/2106.00568) [hep-ex].

[440] **MicroBooNE** Collaboration, P. Abratenko *et al.*, “Search for long-lived heavy neutral leptons and Higgs portal scalars decaying in the MicroBooNE detector,” *Phys. Rev. D* **106** (2022) no. 9, 092006, [arXiv:2207.03840](https://arxiv.org/abs/2207.03840) [hep-ex].

[441] T. Ferber, A. Grohsjean, and F. Kahlhoefer, “Dark Higgs bosons at colliders,” *Prog. Part. Nucl. Phys.* **136** (2024) 104105, [arXiv:2305.16169](https://arxiv.org/abs/2305.16169) [hep-ph].

[442] **KOTO** Collaboration, J. K. Ahn *et al.*, “Study of the  $K_L \rightarrow \pi^0 \nu \bar{\nu}$  Decay at the J-PARC KOTO Experiment,” *Phys. Rev. Lett.* **126** (2021) no. 12, 121801, [arXiv:2012.07571](https://arxiv.org/abs/2012.07571) [hep-ex].

[443] **ICARUS** Collaboration, F. A. Alrahman *et al.*, “Search for a Hidden Sector Scalar from Kaon Decay in the Dimuon Final State at ICARUS,” *Phys. Rev. Lett.* **134** (2025) no. 15, 151801, [arXiv:2411.02727](https://arxiv.org/abs/2411.02727) [hep-ex].

[444] **LHCb** Collaboration, R. Aaij *et al.*, “Search for Hidden-Sector Bosons in  $B^0 \rightarrow K^{*0} \mu^+ \mu^-$  Decays,” *Phys. Rev. Lett.* **115** (2015) no. 16, 161802, [arXiv:1508.04094](https://arxiv.org/abs/1508.04094) [hep-ex].

[445] **LHCb** Collaboration, R. Aaij *et al.*, “Search for long-lived scalar particles in  $B^+ \rightarrow K^+ \chi(\mu^+ \mu^-)$  decays,” *Phys. Rev. D* **95** (2017) no. 7, 071101, [arXiv:1612.07818](https://arxiv.org/abs/1612.07818) [hep-ex].

[446] M. W. Winkler, “Decay and detection of a light scalar boson mixing with the Higgs boson,” *Phys. Rev. D* **99** (2019) no. 1, 015018, [arXiv:1809.01876](https://arxiv.org/abs/1809.01876) [hep-ph].

[447] **Belle II** Collaboration, I. Adachi *et al.*, “Search for a long-lived spin-0 mediator in  $b \rightarrow s$  transitions at the Belle II experiment,” *Phys. Rev. D* **108** (2023) no. 11, L111104, [arXiv:2306.02830](https://arxiv.org/abs/2306.02830) [hep-ex].

[448] D. Gorbunov, I. Krasnov, and S. Suvorov, “Constraints on light scalars from PS191 results,” *Phys. Lett. B* **820** (2021) 136524, [arXiv:2105.11102](https://arxiv.org/abs/2105.11102) [hep-ph].

[449] S. Foroughi-Abari and A. Ritz, “LSND constraints on the Higgs portal,” *Phys. Rev. D* **102** (2020) no. 3, 035015, [arXiv:2004.14515](https://arxiv.org/abs/2004.14515) [hep-ph].

[450] G. Dalla Valle Garcia and M. Ovchynnikov, “Di-decay signature of new physics particles at intensity frontier experiments,” [arXiv:2503.01760](https://arxiv.org/abs/2503.01760) [hep-ph].

[451] M. Drewes, J. Klarić, and J. López-Pavón, “New benchmark models for heavy neutral lepton searches,” *Eur. Phys. J. C* **82** (2022) no. 12, 1176, [arXiv:2207.02742](https://arxiv.org/abs/2207.02742) [hep-ph].

[452] J. L. Feng, A. Hewitt, F. Kling, and D. La Rocco, “Simulating heavy neutral leptons with general couplings at collider and fixed target experiments,” *Phys. Rev. D* **110** (2024) no. 3, 035029, [arXiv:2405.07330](https://arxiv.org/abs/2405.07330) [hep-ph].

[453] **NuTeV, E815** Collaboration, A. Vaitaitis *et al.*, “Search for Neutral Heavy Leptons in a High-Energy Neutrino Beam,” *Phys. Rev. Lett.* **83** (1999) 4943–4946, [arXiv:hep-ex/9908011](https://arxiv.org/abs/hep-ex/9908011).

[454] **WA66** Collaboration, A. M. Cooper-Sarkar *et al.*, “Search for heavy neutrino decays in the BEBC beam dump experiment,” *Phys. Lett. B* **160** (1985) 207–211.

[455] **T2K** Collaboration, K. Abe *et al.*, “Search for heavy neutrinos with the T2K near detector ND280,” *Phys. Rev. D* **100** (2019) no. 5, 052006, [arXiv:1902.07598](https://arxiv.org/abs/1902.07598) [hep-ex].

[456] **NA62** Collaboration, E. Cortina Gil *et al.*, “Search for  $K^+$  decays to a muon and invisible particles,” *Phys. Lett. B* **816** (2021) 136259, [arXiv:2101.12304](https://arxiv.org/abs/2101.12304) [hep-ex].

[457] **E949** Collaboration, A. V. Artamonov *et al.*, “Search for heavy neutrinos in  $K^+ \rightarrow \mu^+ \nu_H$  decays,” *Phys. Rev. D* **91** (2015) no. 5, 052001, [arXiv:1411.3963 \[hep-ex\]](https://arxiv.org/abs/1411.3963). [Erratum: *Phys. Rev. D* 91, 059903 (2015)].

[458] **MicroBooNE** Collaboration, P. Abratenko *et al.*, “Search for Heavy Neutral Leptons in Electron-Positron and Neutral-Pion Final States with the MicroBooNE Detector,” *Phys. Rev. Lett.* **132** (2024) no. 4, 041801, [arXiv:2310.07660 \[hep-ex\]](https://arxiv.org/abs/2310.07660).

[459] **CMS** Collaboration, A. Tumasyan *et al.*, “Search for long-lived heavy neutral leptons with displaced vertices in proton-proton collisions at  $\sqrt{s} = 13$  TeV,” *JHEP* **07** (2022) 081, [arXiv:2201.05578 \[hep-ex\]](https://arxiv.org/abs/2201.05578).

[460] **CMS** Collaboration, A. Hayrapetyan *et al.*, “Search for long-lived heavy neutral leptons decaying in the CMS muon detectors in proton-proton collisions at  $s=13$  TeV,” *Phys. Rev. D* **110** (2024) 012004, [arXiv:2402.18658 \[hep-ex\]](https://arxiv.org/abs/2402.18658).

[461] **CMS** Collaboration, A. Hayrapetyan *et al.*, “Search for heavy neutral leptons in final states with electrons, muons, and hadronically decaying tau leptons in proton-proton collisions at  $\sqrt{s} = 13$  TeV,” *JHEP* **06** (2024) 123, [arXiv:2403.00100 \[hep-ex\]](https://arxiv.org/abs/2403.00100).

[462] **ATLAS** Collaboration, G. Aad *et al.*, “Search for Heavy Neutral Leptons in Decays of W Bosons Using a Dilepton Displaced Vertex in  $s=13$  TeV pp Collisions with the ATLAS Detector,” *Phys. Rev. Lett.* **131** (2023) no. 6, 061803, [arXiv:2204.11988 \[hep-ex\]](https://arxiv.org/abs/2204.11988).

[463] **CHARM II** Collaboration, P. Vilain *et al.*, “Search for heavy isosinglet neutrinos,” *Phys. Lett. B* **343** (1995) 453–458.

[464] **DELPHI** Collaboration, P. Abreu *et al.*, “Search for neutral heavy leptons produced in Z decays,” *Z. Phys. C* **74** (1997) 57–71. [Erratum: *Z. Phys. C* 75 (1997) 580].

[465] **ATLAS** Collaboration, G. Aad *et al.*, “Search for events with a pair of displaced vertices from long-lived neutral particles decaying into hadronic jets in the ATLAS muon spectrometer in pp collisions at  $\sqrt{s}=13$  TeV,” *Phys. Rev. D* **106** (2022) no. 3, 032005, [arXiv:2203.00587 \[hep-ex\]](https://arxiv.org/abs/2203.00587).

[466] **CMS** Collaboration, A. Hayrapetyan *et al.*, “Search for long-lived particles decaying in the CMS muon detectors in proton-proton collisions at  $\sqrt{s} = 13$  TeV,” *Phys. Rev. D* **110** (2024) no. 3, 032007, [arXiv:2402.01898 \[hep-ex\]](https://arxiv.org/abs/2402.01898).

[467] **ATLAS** Collaboration, G. Aad *et al.*, “Combination of searches for invisible decays of the Higgs boson using  $139 \text{ fb}^{-1}$  of proton-proton collision data at  $\sqrt{s} = 13$  TeV collected with the ATLAS experiment,” *Phys. Lett. B* **842** (2023) 137963, [arXiv:2301.10731 \[hep-ex\]](https://arxiv.org/abs/2301.10731).

[468] A. Dainese, M. Mangano, A. B. Meyer, A. Nisati, G. Salam, and M. A. Vesterinen, eds., *Report on the Physics at the HL-LHC, and Perspectives for the HE-LHC*, vol. 7/2019 of *CERN Yellow Reports: Monographs*. CERN, Geneva, Switzerland, 2019.

[469] A. Coccaro, D. Curtin, H. J. Lubatti, H. Russell, and J. Shelton, “Data-driven model-independent searches for long-lived particles at the LHC,” *Phys. Rev. D* **94** (2016) no. 11, 113003, [arXiv:1605.02742 \[hep-ph\]](https://arxiv.org/abs/1605.02742).

[470] D. Curtin *et al.*, “Exotic decays of the 125 GeV Higgs boson,” *Phys. Rev. D* **90** (2014) no. 7, 075004, [arXiv:1312.4992 \[hep-ph\]](https://arxiv.org/abs/1312.4992).

[471] G. C. Branco, P. M. Ferreira, L. Lavoura, M. N. Rebelo, M. Sher, and J. P. Silva, “Theory and phenomenology of two-Higgs-doublet models,” *Phys. Rept.* **516** (2012) 1–102, [arXiv:1106.0034 \[hep-ph\]](https://arxiv.org/abs/1106.0034).

[472] **ATLAS** Collaboration, G. Aad *et al.*, “Search for light long-lived neutral particles that decay to collimated pairs of leptons or light hadrons in pp collisions at  $\sqrt{s} = 13$  TeV with the ATLAS detector,” *JHEP* **06** (2023) 153, [arXiv:2206.12181](https://arxiv.org/abs/2206.12181) [hep-ex].

[473] R. M. Schabinger and J. D. Wells, “A Minimal spontaneously broken hidden sector and its impact on Higgs boson physics at the large hadron collider,” *Phys. Rev. D* **72** (2005) 093007, [arXiv:hep-ph/0509209](https://arxiv.org/abs/hep-ph/0509209).

[474] B. Patt and F. Wilczek, “Higgs-field portal into hidden sectors,” [hep-ph/0605188](https://arxiv.org/abs/hep-ph/0605188).

[475] D. Curtin, R. Essig, S. Gori, and J. Shelton, “Illuminating dark photons with high-energy colliders,” *JHEP* **02** (2015) 157, [arXiv:1412.0018](https://arxiv.org/abs/1412.0018) [hep-ph].

[476] M. Fabbrichesi, E. Gabrielli, and G. Lanfranchi, “The Dark Photon,” [arXiv:2005.01515](https://arxiv.org/abs/2005.01515) [hep-ph].

[477] T. Ferber, C. Garcia-Cely, and K. Schmidt-Hoberg, “Belle II sensitivity to long-lived dark photons,” *Phys. Lett. B* **833** (2022) 137373, [arXiv:2202.03452](https://arxiv.org/abs/2202.03452) [hep-ph].

[478] E. Izaguirre, G. Krnjaic, and B. Shuve, “Discovering Inelastic Thermal-Relic Dark Matter at Colliders,” *Phys. Rev. D* **93** (2016) no. 6, 063523, [arXiv:1508.03050](https://arxiv.org/abs/1508.03050) [hep-ph].

[479] **OPAL** Collaboration, P. D. Acton *et al.*, “Search for anomalous production of high mass photon pairs in  $e^+e^-$  collisions at LEP,” *Phys. Lett. B* **311** (1993) 391–407.

[480] **BaBar** Collaboration, J. P. Lees *et al.*, “Search for Invisible Decays of a Dark Photon Produced in  $e^+e^-$  Collisions at BaBar,” *Phys. Rev. Lett.* **119** (2017) no. 13, 131804, [arXiv:1702.03327](https://arxiv.org/abs/1702.03327) [hep-ex].

[481] K. R. Dienes, J. L. Feng, M. Fieg, F. Huang, S. J. Lee, and B. Thomas, “Extending the discovery potential for inelastic-dipole dark matter with FASER,” *Phys. Rev. D* **107** (2023) no. 11, 115006, [arXiv:2301.05252](https://arxiv.org/abs/2301.05252) [hep-ph].

[482] M. Duerr, T. Ferber, C. Hearty, F. Kahlhoefer, K. Schmidt-Hoberg, and P. Tunney, “Invisible and displaced dark matter signatures at Belle II,” *JHEP* **02** (2020) 039, [arXiv:1911.03176](https://arxiv.org/abs/1911.03176) [hep-ph].

[483] A. Berlin and F. Kling, “Inelastic dark matter at the LHC lifetime frontier: ATLAS, CMS, LHCb, CODEX-b, FASER, and MATHUSLA,” *Phys. Rev. D* **99** (2019) no. 1, 015021, [arXiv:1810.01879](https://arxiv.org/abs/1810.01879) [hep-ph].

[484] **NA64** Collaboration, Y. M. Andreev *et al.*, “First Results in the Search for Dark Sectors at NA64 with the CERN SPS High Energy Muon Beam,” *Phys. Rev. Lett.* **132** (2024) no. 21, 211803, [arXiv:2401.01708](https://arxiv.org/abs/2401.01708) [hep-ex].

[485] **Belle II** Collaboration, I. Adachi *et al.*, “Search for an Invisible Z’ in a Final State with Two Muons and Missing Energy at Belle II,” *Phys. Rev. Lett.* **130** (2023) no. 23, 231801, [arXiv:2212.03066](https://arxiv.org/abs/2212.03066) [hep-ex].

[486] W. Altmannshofer, S. Gori, M. Pospelov, and I. Yavin, “Neutrino Trident Production: A Powerful Probe of New Physics with Neutrino Beams,” *Phys. Rev. Lett.* **113** (2014) 091801, [arXiv:1406.2332](https://arxiv.org/abs/1406.2332) [hep-ph].

[487] **CCFR** Collaboration, S. R. Mishra *et al.*, “Neutrino Tridents and W Z Interference,” *Phys. Rev. Lett.* **66** (1991) 3117–3120.

[488] P. Ilten, Y. Soreq, M. Williams, and W. Xue, “Serendipity in dark photon searches,” *JHEP* **06** (2018) 004, [arXiv:1801.04847](https://arxiv.org/abs/1801.04847) [hep-ph].

[489] M. Bauer, P. Foldenauer, and J. Jaeckel, “Hunting all the hidden photons,” *JHEP* **07** (2018) 094, [arXiv:1803.05466 \[hep-ph\]](https://arxiv.org/abs/1803.05466).

[490] C.-Y. Chen, M. Pospelov, and Y.-M. Zhong, “Muon beam experiments to probe the dark sector,” *Phys. Rev. D* **95** (2017) no. 11, 115005, [arXiv:1701.07437 \[hep-ph\]](https://arxiv.org/abs/1701.07437).

[491] A. Berlin, N. Blinov, G. Krnjaic, P. Schuster, and N. Toro, “Dark matter, millicharges, axion and scalar particles, gauge bosons, and other new physics with LDMX,” *Phys. Rev. D* **99** (2019) no. 7, 075001, [arXiv:1807.01730 \[hep-ph\]](https://arxiv.org/abs/1807.01730).

[492] Y. Kahn, G. Krnjaic, N. Tran, and A. Whitbeck, “M<sup>3</sup>: a new muon missing momentum experiment to probe  $(g - 2)_\mu$  and dark matter at Fermilab,” *JHEP* **09** (2018) 153, [arXiv:1804.03144 \[hep-ph\]](https://arxiv.org/abs/1804.03144).

[493] O. Salin *et al.*, “FASER2: Detector Design and Performance.” CERN-PBC-Notes-2025-005, 2025. <https://cds.cern.ch/record/2927003>.

[494] M. Vicenzi *et al.*, “Simulations and Performance Studies for the Forward Liquid Argon Experiment (FLArE) at the Forward Physics Facility.” CERN-PBC-Notes-2025-006, 2025. <https://cds.cern.ch/record/2927282>.

[495] J. Bian *et al.*, “Preliminary Design Considerations for the Forward Liquid Argon detector (FLArE) at the high luminosity LHC.” CERN-PBC-Notes-2025-007, 2025. <https://cds.cern.ch/record/2927376>.

[496] **NA64** Collaboration, D. Banerjee *et al.*, “Search for vector mediator of Dark Matter production in invisible decay mode,” *Phys. Rev. D* **97** (2018) no. 7, 072002, [arXiv:1710.00971 \[hep-ex\]](https://arxiv.org/abs/1710.00971).

[497] **SHiP/NA67** Collaboration, A. Golutvin and R. Jacobsson, “SHiP progress report 2024,” Tech. Rep. CERN-SPSC-2024-031, SPSC-SR-354, CERN, Geneva, 2024. <https://cds.cern.ch/record/2917226>.

[498] J. Pinfold, R. Soluk, and I. Ostrovskiy, “The MAPP-1 Outrigger Technical Proposal,” Tech. Rep. CERN-LHCC-2024-018, MoEDAL-TDR-002, CERN, Geneva, 2024. <https://cds.cern.ch/record/2918254>.

[499] **MoEDAL-MAPP** Collaboration, B. Acharya *et al.*, “MoEDAL-MAPP, an LHC Dedicated Detector Search Facility,” in *Snowmass 2021*. 9, 2022. [arXiv:2209.03988 \[hep-ph\]](https://arxiv.org/abs/2209.03988).

[500] S. Abel, S. Khalil, and O. Lebedev, “EDM constraints in supersymmetric theories,” *Nucl. Phys. B* **606** (2001) 151–182, [arXiv:hep-ph/0103320](https://arxiv.org/abs/hep-ph/0103320).

[501] M. Pospelov and A. Ritz, “Electric dipole moments as probes of new physics,” *Annals Phys.* **318** (2005) 119–169, [arXiv:hep-ph/0504231](https://arxiv.org/abs/hep-ph/0504231).

[502] S. Abel and O. Lebedev, “Neutron-electron EDM correlations in supersymmetry and prospects for EDM searches,” *JHEP* **01** (2006) 133, [arXiv:hep-ph/0508135](https://arxiv.org/abs/hep-ph/0508135).

[503] T. Chupp and M. Ramsey-Musolf, “Electric dipole moments: A global analysis,” *Phys. Rev. C* **91** (2015) no. 3, 035502, [arXiv:1407.1064 \[hep-ph\]](https://arxiv.org/abs/1407.1064).

[504] T. S. Roussy *et al.*, “An improved bound on the electron’s electric dipole moment,” *Science* **381** (2023) no. 6653, [adg4084, arXiv:2212.11841 \[physics.atom-ph\]](https://arxiv.org/abs/2212.11841).

[505] **Muon (g-2)** Collaboration, G. W. Bennett *et al.*, “Improved limit on the muon electric dipole moment,” *Phys. Rev. D* **80** (2009) 052008, [arXiv:0811.1207 \[hep-ex\]](https://arxiv.org/abs/0811.1207).

[506] **Belle** Collaboration, K. Inami *et al.*, “An improved search for the electric dipole moment of the  $\tau$  lepton,” *JHEP* **04** (2022) 110, [arXiv:2108.11543 \[hep-ex\]](https://arxiv.org/abs/2108.11543).

[507] C. Abel *et al.*, “Measurement of the Permanent Electric Dipole Moment of the Neutron,” *Phys. Rev. Lett.* **124** (2020) no. 8, 081803, [arXiv:2001.11966 \[hep-ex\]](https://arxiv.org/abs/2001.11966).

[508] **ACME** Collaboration, V. Andreev *et al.*, “Improved limit on the electric dipole moment of the electron,” *Nature* **562** (2018) no. 7727, 355–360.

[509] B. Graner, Y. Chen, E. G. Lindahl, and B. R. Heckel, “Reduced Limit on the Permanent Electric Dipole Moment of  $^{199}\text{Hg}$ ,” *Phys. Rev. Lett.* **116** (2016) no. 16, 161601, [arXiv:1601.04339 \[physics.atom-ph\]](https://arxiv.org/abs/1601.04339). [Erratum: *Phys. Rev. Lett.* 119 (2017) 119901].

[510] L. Pondrom, R. Handler, M. Sheaff, P. T. Cox, J. Dworkin, O. E. Overseth, T. Devlin, L. Schachinger, and K. J. Heller, “New limit on the electric dipole moment of the  $\lambda$  hyperon,” *Phys. Rev. D* **23** (1981) 814–816.

[511] J. Pretz, “Electric Dipole Moment (EDM) searches for leptons and hadrons,” *PoS HQL2023* (2024) 010.

[512] **CPEDM** Collaboration, F. Abusaif *et al.*, “Feasibility Study for an EDM Storage Ring,” [arXiv:1812.08535 \[physics.acc-ph\]](https://arxiv.org/abs/1812.08535).

[513] J. Aasi *et al.*, “Advanced LIGO,” *Class. Quantum Grav.* **32** (2015) 074001.

[514] **VIRGO** Collaboration, F. Acernese *et al.*, “Advanced Virgo: a second-generation interferometric gravitational wave detector,” *Class. Quant. Grav.* **32** (2015) no. 2, 024001, [arXiv:1408.3978 \[gr-qc\]](https://arxiv.org/abs/1408.3978).

[515] **KAGRA** Collaboration, Y. Aso *et al.*, “Interferometer design of the KAGRA gravitational wave detector,” *Phys. Rev. D* **88** (2013) no. 4, 043007, [arXiv:1306.6747 \[gr-qc\]](https://arxiv.org/abs/1306.6747).

[516] **ET** Collaboration, M. Maggiore *et al.*, “Science Case for the Einstein Telescope,” *JCAP* **03** (2020) 050, [arXiv:1912.02622 \[astro-ph.CO\]](https://arxiv.org/abs/1912.02622).

[517] **LISA** Collaboration, P. Amaro-Seoane *et al.*, “Laser Interferometer Space Antenna,” (2017) , [arXiv:1702.00786 \[astro-ph.IM\]](https://arxiv.org/abs/1702.00786).

[518] L. Badurina *et al.*, “Prospective sensitivities of atom interferometers to gravitational waves and ultralight dark matter,” *Phil. Trans. A. Math. Phys. Eng. Sci.* **380** (2021) no. 2216, 20210060, [arXiv:2108.02468 \[gr-qc\]](https://arxiv.org/abs/2108.02468).

[519] N. Aggarwal *et al.*, “Challenges and Opportunities of Gravitational Wave Searches above 10 kHz,” [arXiv:2501.11723 \[gr-qc\]](https://arxiv.org/abs/2501.11723).

[520] C. J. Moore, R. H. Cole, and C. P. L. Berry, “Gravitational-wave sensitivity curves,” *Class. Quant. Grav.* **32** (2015) no. 1, 015014, [arXiv:1408.0740 \[gr-qc\]](https://arxiv.org/abs/1408.0740).

## List of Acronyms

**c.m.** centre-of-mass. 13, 40, 44, 63

**ABS** Atomic Beam Source. 49

**AD** Antiproton Decelerator. 20, 21, 27, 28, 50, 58

**AI** Atom Interferometry. 51, 82, 83

**AION** Atom Interferometer Observatory and Network. 30, 51, 59

**aKWISP** advanced Kinetic Weakly interacting Sub-eV Particle experiment. 30

**ALADDIN** An Lhc Apparatus for Direct Dipole moments INvestigation. 48, 49, 59, 82

**ALICE** A Large Ion Collider Experiment. 22, 41, 66

**ALICE3** A Large Ion Collider Experiment Upgrade 3. 22, 66

**ALPs** Axion-Like Particles. 12, 14, 17, 39, 42, 45, 46, 57

**ALPS-II** Any Light Particle Search-II. 17, 18, 29

**ANUBIS** AN Underground Belayed In-Shaft search experiment. 44, 45, 59, 77, 80

**ASTAE** Advancing Science and Technology using Agile Experiments. 43

**ATLAS** A Toroidal LHC ApparatuS Experiment. 14, 39, 41–45, 47, 48, 72, 75–77, 80

**Auger** Pierre Auger Observatory. 41

**AWAKE** Advanced WAKEfield Experiment. 21, 25, 27, 32, 33, 55

**BabyIAXO** Baby International AXion Observatory. 18, 29, 53

**BASE** Baryon Antibaryon Symmetry Experiment. 50

**BC** Benchmark Case. 72–76

**BCs** Benchmark Cases. 72

**BD** Beam Dump. 11, 12, 35, 37, 55

**BDF** Beam Dump Facility. 25–27, 39, 80

**BDX** Beam Dump Experiment. 17

**Belle II** Belle II. 18, 65, 74, 77–79

**BES III** Beijing Spectrometer III. 65

**BMS** Beam Momentum Spectrometer. 40

**BNL** Brookhaven National Laboratory. 16, 61

**BSM** Beyond the Standard Model. 15–17, 29, 39, 41, 46, 47, 50, 58, 59, 68, 71, 80, 81

**CBM** Compressed Baryonic Matter experiment. 16, 66

**CBWG** Conventional Beams Working Group. 36

**CC** Charged-Current. 15, 30, 54, 68, 69

**CDR** Conceptual Design Report. 48

**CDS** Comprehensive Design Study. 25

**CERN** European Organization for Nuclear Research. 11, 12, 14, 18–20, 22, 26, 27, 29, 30, 33, 35, 36, 41, 46, 48, 50, 51, 54, 58, 82, 83

**CERN QTI** CERN Quantum Technology Initiative. 30, 51, 52

**CERN RB** CERN Research Board. 12, 25, 36

**CHARM** CERN High Energy Accelerator Mixed-field. 22

**CHARM Experiment** CERN HAmburg Rome Moscow Experiment. 39

**CKM** Cabibbo Kobayashi Maskawa. 39

**CLIC** Compact LInear Collider. 35

**CLOUD** Cosmics Leaving Outdoor Droplets experiment. 22

**CMS** Compact Muon Solenoid. 39, 41, 43, 44, 47, 48, 58, 72, 73, 75–77, 80

**CNGS** CERN Neutrino beam to Gran Sasso. 26, 27, 33

**CODEX- $\beta$**  Prototype of COmpact Detector for EXotics at LHCb. 59

**CODEX-**b**** COmpact Detector for EXotics at LHCb. 45, 46, 59, 76, 80

**COMPASS/NA58** Common Muon and Proton Apparatus for Structure and Spectroscopy. 64

**COSY** COoler SYnchrotron. 58

**CP** Charge Parity. 36, 38, 50, 55, 68, 81

**cpEDM** charged particle Electric Dipole Moment. 57, 58, 82

**CPV** Charge Parity violation. 13, 19

**CTF2** CLIC Test Facility 2. 33

**DarkSide-20k** DarkSide-20k. 29

**DESY** Deutsche Elektronen-Synchrotron. 17, 18, 29

**DICE/NA60+** Dilepton and Charm Experiment/NA60+ Collaboration. 22, 37, 41, 59, 65, 66

**DIS** Deep Inelastic Scattering. 39, 61, 63, 64

**DM** Dark Matter. 12, 14, 34, 51–53, 58, 65, 67, 71, 77–80

**DRD** Detector Research and Development programme. 30

**DS** Dark Sector. 11, 12, 35

**DUNE** Deep Underground Neutrino Experiment. 19, 30, 36, 68, 69

**DY** Drell-Yan. 13, 38, 49, 61, 62, 64

**E144** E144 Experiment. 55

**EA** East Area. 21–23

**EbyE** Event-by-Event. 36, 37

**ECFA** European Committee for Future Accelerators. 30

**ECN3** Experimental Cavern North 3. 16, 24–27, 39

**ECN4** Experimental Cavern North 4. 25, 26

**EDM** Electric Dipole Moment. 48–50, 57, 58, 81, 82

**EHN1** Experimental Hall North 1. 24, 27, 31, 59

**EHN2** Experimental Hall North 2. 24, 27, 31, 38, 59

**EIC** Electron Ion Collider. 16, 17, 61, 63

**ELENA** Extra Low Energy Antiproton ring. 21, 27, 28, 50

**EM** Electro-Magnetic. 50

**ENUBET** Enhanced NeUtrino BEams from kaon Tagging. 30, 53

**EoI** Expression of Interest. 25, 41, 45, 59

**EoT** Electrons on Target. 55

**EPPSU** European Particle Physics Strategy Update. 12, 16, 25, 30, 32

**ERC** European Research Council. 53

**ES** Electro-Static. 57, 58

**ET** Einstein Telescope. 82, 83

**EW** Electro-Weak. 44, 54

**FAIR** Facility for Antiproton and Ion Research. 16, 40, 66

**FASER** Forward Search Experiment. 14, 16, 42–44, 58, 69, 70

**FASERv** FASER Neutrino detector. 14, 42

**FASERv2** FASER Neutrino Detector 2. 42, 69, 70, 79, 80

**FASER2** Forward Search Experiment 2. 42, 78, 80

**FCC** Future Circular Collider. 50

**FCC-ee** Future electron-positron Circular Collider. 33, 34, 39, 55–57

**FCC-hh** Future hadron-hadron Circular Collider. 53

**Fermilab** Fermilab. 17, 19, 36, 51, 54

**FINUDA** FIIsica NUcleare a DA $\phi$ NE. 52

**FIPs** Feebly Interacting Particles. 12, 15, 16, 39, 44, 58, 72

**FLArE** Forward Liquid Argon Experiment. 42, 69, 71, 80

**FLASH** FINUDA magnet for Light Axion SearchH. 30, 52, 53, 82, 83

**FORMOSA** FORWARD MicrOcharge SeArch detector. 42, 80

**FPC** FIP Physics Centre. 16, 58, 59, 73–75

**FPP** Forward Physics Facility. 41–43, 59, 61, 63, 64, 69, 71, 80

**FT** Fixed-Target. 11–13, 20, 21, 23, 26, 35, 44, 56, 57, 67

**GF** Gamma Factory. 31, 32, 54, 59, 62, 63

**GF SPS PoP** Gamma Factory SPS Proof of Principle. 32

**GHG** Greenhouse Gas. 46

**GIF++** Gamma Irradiation Facility++. 24

**GPD** Generalized Parton Distribution. 62, 63

**GPS** General Purpose Separator. 22

**GrAHal** Grenoble Axion Haloscope. 30

**GTK** Giga-TracKer. 53

**GWs** Gravitational Waves. 51, 52, 82, 83

**HADES** High Acceptance Di-Electron Spectrometer. 66

**HEARTS** High Energy Accelerators for Radiation Testing and Shielding. 22

**HERA** Hadron-Elektron-Ringanlage. 17, 18

**HFGW** High Frequency Gravitational Waves. 52, 53, 83

**HI-ECN3** High Intensity ECN3. 25, 26

**HIE-ISOLDE** High Intensity and Energy ISOLDE. 23

**HIKE** High Intensity Kaon Experiment. 16, 18

**HiRadMat** High Radiation to Material. 25, 27, 31

**HL-LHC** High Luminosity LHC. 19, 22, 28, 29, 41, 43, 46–48, 54, 64, 69, 75–77, 80

**HNLs** Heavy Neutral Leptons. 39, 45, 46, 57, 72, 75

**HS** Hidden Sector. 11, 25, 46, 58

**HSDS** Hidden Sector Decay Spectrometer. 39

**HTS** High-Temperature Superconductors. 28, 29, 53

**HVP** Hadronic Vacuum Polarisation. 40, 60

**Hyper-K** Hyper-Kamiokande. 19, 30, 53, 54, 68

**IAXO** International AXion Observatory. 18, 53

**IceCube** IceCube Neutrino Observatory. 41

**IEFC** Injectors and Experimental Facilities Committee. 27

**IJCLab** Laboratory of the Physics of the two Infinities Irène Joliot-Curie. 32

**ILC** International Linear Collider. 35, 57

**INFN** Istituto Nazionale di Fisica Nucleare. 52, 53

**IP** Interaction Point. 13, 14, 28, 41, 42, 45–47

**IR** Insertion Region. 28, 48, 49

**ISOLDE** Isotope Separator On Line DEvice. 21–23, 50

**ITS3** Inner Tracking System 3. 41

**J-PARC** Japan Proton Accelerator Research Complex. 18, 19, 60, 65

**JLab** Jefferson Lab. 17, 64

**KAGRA** KAmioka GRAvitational wave detector. 82

**KM3NeT** Cubic Kilometre Neutrino Telescope. 41

**L1** Level 1. 48

**LAST** Large Acceptance Silicon Tracker. 36, 37, 67

**LC** Linear Collider. 35, 55, 57

**LDM** Light Dark Matter. 12, 17, 37, 39, 42, 56, 57

**LDMX** Light Dark Matter eXperiment. 17

**LEIR** Low Energy Ion Ring. 19

**LEP** Large Electron–Positron Collider. 73, 78

**LFU** Lepton Flavour Universality. 15, 39, 71

**LFV** Lepton Flavour Violation. 12

**LHC** Large Hadron Collider. 13–15, 19, 22, 27–29, 31, 32, 39–45, 47–52, 54, 55, 58, 59, 61–66, 69, 70, 72, 75, 76, 80, 82

**LHC-FT** PBC LHC Fixed-Target. 13, 16, 48, 65

**LHCb** Large Hadron Collider beauty Experiment. 13, 39, 44–46, 49, 61, 62, 65, 72, 74, 80

**LHCC** LHC Experiments Committee. 14, 47, 48, 59

**LHCspin** LHCSpin. 49, 59, 61, 62

**LIGO** Laser Interferometer Gravitational-Wave Observatory. 32, 82, 83

**Linac** Linear Accelerator. 17

**Linac 4** Linear Accelerator 4. 19, 21

**LISA** Laser Interferometer Space Antenna. 82, 83

**LIU** LHC Injectors Upgrade. 19, 20, 23, 28

**LLP** Long-Lived Particle. 76, 78, 80

**LLPs** Long-Lived Particles. 39, 44–47, 68, 76, 80

**LLRF** Low Level Radio Frequency. 19

**LNF** Laboratori Nazionali di Frascati. 53

**LoI** Letter of Intent. 14, 41, 47, 48, 53, 59

**LS2** Long Shutdown 2. 19–23, 27, 28

**LS3** Long Shutdown 3. 13, 21–23, 25, 26, 28, 32, 33, 36, 37, 40, 43, 45, 47, 49, 51, 67

**LS4** Long Shutdown 4. 23, 26, 31, 33, 39, 45

**LUXE** Laser Und XFEL Experiment. 18

**MAGIS** Matter-wave Atomic Gradiometer Interferometric Sensor. 51

**MAPP-2** MoEDAL Apparatus for Penetrating Particles, Phase-2. 46, 47, 59, 80

**MAPP-Outrigger** Outrigger Detector for the MoEDAL Apparatus for Penetrating Particles. 80

**MAPS** Monolithic Active Pixel Sensors. 41

**MATHUSLA40** MAssive Timing Hodoscope for Ultra-Stable neutralL pArticles,  $40 \times 40 \text{ m}^2$  area). 47, 48, 59, 74, 75, 77, 80

**MD** Machine Development. 21, 27, 49

**MDM** Magnetic Dipole Moment. 48, 49, 57, 58, 81, 82

**MilliQan** MilliQan Experiment. 42

**mQP** Milli-charged Particle. 80

**MTE** Multi Turn Extraction. 20, 21

**MUonE** Muon On Electron Elastic Scattering. 16, 40, 59, 60

**MWPC** Multi-Wire Proportional Chamber. 41

**NA** North Area. 11, 12, 16, 20–27, 31, 33

**NA-CONS** North Area Consolidation Project. 24, 26

**NA61/SHINE** SPS Heavy Ion and Neutrino Experiment. 11, 22, 24, 36, 37, 59, 65–67

**NA62** NA62 Experiment. 11, 18, 24, 25, 53, 54, 58, 59, 74, 75

**NA64** NA64 Experiment. 12, 24, 37, 56, 58, 59, 79, 80

**NA66/AMBER** Apparatus for Meson and Baryon Experimental Research. 12, 16, 24, 38, 39, 59, 61, 64, 65

**NBOA** Narrow-Band Off-Axis. 54, 68, 69

**NC** Neutral Current. 15, 68

**NP06** Neutrino Platform 06 Experiment. 53

**NSI** Non-Standard Interactions. 68

**nToF** neutron Time of Flight facility. 21, 23

**NuTag** Neutrino Tagging. 30

**P5** Particle Physics Project Prioritization Panel. 43

**PBC** Physics Beyond Colliders. 11, 12, 14–16, 18, 23, 25, 26, 29, 30, 34–36, 55–59, 61, 62, 65, 72, 73, 80

**PDF** Parton Distribution Function. 13, 43, 61, 63, 64, 71

**PDG** Particle Data Group. 38

**PID** Particle Identification. 37

**PoC** Proof of Concept. 32, 45

**PoT** Protons on Target. 27, 28, 30, 39, 49, 54, 68, 72

**ppb** particles per bunch. 34

**ppp** particles per pulse. 21–23, 27

**proANUBIS** ANUBIS prototype. 45, 59

**PS** Proton Synchrotron. 19–22, 27, 37

**PSB** Proton Synchrotron Booster. 19–21, 23

**PSI** Partially Stripped Ions. 31, 32

**PU** average event pile-up  $\langle \mu \rangle$ . 28

**PUMA** antiProton Unstable Matter Annihilation. 50

**QCD** Quantum Chromo-Dynamics. 13, 16–18, 40, 41, 52, 54, 60, 61, 64–67, 71, 81

**QED** Quantum Electro-Dynamics. 35, 54–57

**QGP** Quark-Gluon Plasma. 13, 22, 40, 65–67

**QRADES** Quantum Relic Axion DEtection Sensors. 53

**QUAX@LNF** QUaerere AXions experiment @ LNF. 53

**R&D** Research and Development. 31, 35, 37, 41, 43–46, 48, 51, 57

**RADES** Relic Axion Detector Exploratory Setup. 29, 30, 53

**RF** Radio Frequency. 19, 21, 29, 31, 33, 52, 53

**RHIC** Relativistic Heavy-Ion Collider. 37, 40, 66, 67

**RICH** Ring-Imaging Cherenkov. 48, 49

**RP** Radiation Protection. 22, 42

**RPC** Resistive Plate Chamber. 45, 46

**SBN** Short Baseline Neutrino. 30, 31, 53, 54, 59, 68, 69

**SBND** Short-Baseline Near Detector. 54

**SC** Superconducting. 29, 52

**SciFi** Scintillating Fibre. 15

**SHADOWS** Search for Hidden And Dark Objects With the SPS. 16

**SHiP/NA67** Search For Hidden Particles experiment. 16, 25–27, 30, 39, 44, 58, 63, 70–73, 77, 78, 80

**SiPM** Silicon Photo Multipliers. 46

**SLAC** Stanford Linear Accelerator Center. 17, 51, 52, 55

**SM** Standard Model. 17, 18, 29, 35, 46–48, 70–72, 74–76, 78, 79, 81

**SMBHs** supermassive black holes. 82

**SMOG** System to Measure the beam Overlap with Gas. 13

**SMOG2** System to Measure the beam Overlap with Gas 2. 13, 49, 61, 62, 65, 67

**SND** Scattering and Neutrino Detector. 39, 63, 78, 80

**SND@HL-LHC** Scattering and Neutrino Detector at the HL-LHC. 43, 44, 59, 80

**SND@LHC** Scattering and Neutrino Detector at the LHC. 14, 16, 43, 69, 70

**SPS** Super Proton Synchrotron. 11, 15, 19–27, 30–32, 37, 40, 41, 55, 56, 65–67, 80

**SPSC** SPS and PS Experiments Committee. 12, 25, 36, 41, 59

**SQMS** Superconducting Quantum Materials and Systems Center. 51

**SQUID** Superconducting QUantum Interference Device. 52

**STAR** Solenoidal Tracker at RHIC. 66

**STAX** Sub-THz Axion eXperiment. 30

**STEP** Symmetry Tests in Experiments with Portable antiprotons. 50

**TCC2** Tunnel Target Cavern 2. 24, 25, 30

**TCC4** Tunnel Target Cavern 4. 25

**TCC6** Tunnel Target Cavern 6. 31

**TCC8** Tunnel Target Cavern 8. 24

**TDR** Technical Design Report. 26, 27, 47

**TI** Tunnel Injection. 14, 43

**TMCI** Transverse Mode Coupling Instability. 21

**TMD** Transverse Momentum Distribution. 61–63

**TNC** Tunnel Neutrino Cavern. 25

**TPC** Time Projection Chamber. 54, 68

**TT61** Transfer Tunnel 61. 25

**TVLBAI** Terrestrial Very Long Baseline Atom Interferometry. 51

**TWOCRYST** Double Crystal set-up Proof of Principle Experiment. 48

**ULDM** Ultra-Light Dark Matter. 51

**US** United States. 19, 41, 43, 48, 51

**UX** Underground Experimental Cavern. 45

**VELO** Vertex Locator. 13, 49

**VHF** Very High Frequency. 52

**Virgo** Virgo interferometric gravitational-wave observatory. 82

**VMB@CERN** Vacuum Magnetic Birefringence experiment at CERN. 29

**WA** West Area. 31

**WG** Working Group. 13, 29, 30

**WLS** Wavelength Shifting. 46

**YETS** Year-End Technical Stop. 15